



Università degli Studi di Napoli Federico II

Scuola Politecnica e delle Scienze di Base
Corso di Laurea Magistrale in Ingegneria Aerospaziale

TESI DI LAUREA MAGISTRALE
IN
INGEGNERIA AEROSPAZIALE

Development of a Java-Based Framework for Aircraft Preliminary Design

Wing Aerodynamic Analysis Module,
Aircraft Longitudinal Static Stability Module

Relatori:

Prof. Ing. Fabrizio Nicolosi
Prof. Ing. Agostino De Marco

Candidato:

Manuela Ruocco
Matricola M53/408

ABSTRACT

The purpose of this Thesis work is to introduce the features and the potentialities of ADOpT (*Aircraft Design and Optimization Tool*), a java-based framework conceived as a fast and efficient tool useful as support in the preliminary design phases of an aircraft, and during its optimization process.

The **Aircraft Design and Optimization Tool (ADOpT)** development originates in the Department of Industrial Engineering of University of Naples “Federico II”, where is still in progress.

ADOpT is the software with the GUI that uses the functionality of the library **Java Program toolchain for Aircraft Design (JPAD)** that, at present, is capable to perform a multi-disciplinary analysis of an aircraft whose data can be entered by the user, with an XML, or loaded into memory. The ultimate goal of **JPAD** is to carry out an optimization process where the analyses are cyclically repeated in order to optimize some parameters while keeping others in fixed limits. Currently the software is able to estimate the aircraft weight breakdown, the center of gravity location, calculate some aerodynamic parameters and estimate the performance. All these types of estimates can be usually performed using several analysis methods, comparable and interchangeable. It is also provided a static longitudinal stability analysis, take-off and landing performances and the generation of Payload Range chart.

JPAD can be used from the command line or with a dedicated graphical user interface (**ADOpT**). The GUI allows the user to have an immediate feedback about the aircraft features when changing the input parameters, to manage simultaneously multiple aircrafts and to compare them side by side, and to view a 3D CAD model of the aircraft.

The **JPAD** potentialities, in the world of research or in industry, are remarkable and the software strengths are a considerable computing speed and flexibility, with an user-friendly GUI.

The structure of this thesis work has as ultimate goal to provide a comprehensive overview about **JPAD** and, at the same time, it is intended to be a developer’s manual. The first chapters provide a complete software overview paying particular attention at actual features and future goals. Following chapters introduce some case of study and the results achieved. The theoretical background is exposed at the beginning of each chapter , afterwards there is a description of the Java architecture and, at the end is reported the Test class used for the analysis and its results.

SOMMARIO

Lo scopo che il presente lavoro di Tesi auspica raggiungere è quello di presentare le capacità possedute e le potenzialità future di ADOpT, un software scritto in Java che si configura come uno strumento veloce ed efficiente per il supporto nella fase di progetto preliminare di un velivolo e per la sua ottimizzazione.

Lo sviluppo di ADOpT (*Aircraft Design and Optimization Tool*) nasce all' interno del Dipartimento di Ingegneria Industriale dell' Università degli Studi di Napoli Federico II, ove è tutt'ora in fase di progresso.

ADOpT rappresenta il software con interfaccia grafica le cui funzionalità sono implementate nella libreria **JPAD** il quale è attualmente in grado di svolgere una parziale analisi multidisciplinare di un velivolo i cui dati sono immessi dall' utente tramite XML o caricati in memoria. La linea guida dello sviluppo del software porta verso l'implementazione di un processo di ottimizzazione nel quale le analisi sono ciclicamente ripetute al fine di ottimizzare alcuni parametri mantenendone altri all' interno di limiti imposti.

Attualmente **JPAD** è in grado di effettuare una completa stima dei pesi, valutare la posizione del baricentro, calcolare un notevole numero di parametri aerodinamici e caratteristiche di performance. La stima di ciascun parametro può essere effettuata tramite diversi metodi implementati, tra di loro confrontabili ed intercambiabili. Inoltre è prevista un' analisi di stabilità statica, prestazioni di decollo ed atterraggio e la generazione del diagramma *Payload Range*.

JPAD può essere utilizzato sia in modalità *batch*, ossia da riga di comando, che tramite interfaccia grafica (**ADOpT**). Tale duplice scelta consente di ottenere le migliori prestazioni sia nei processi di analisi, ove la GUI consente di avere un immediato riscontro grafico, sia nei processi di ottimizzazione.

Dunque le potenzialità di **ADOpT** nel mondo della ricerca od anche in quello industriale sono senza dubbio notevoli e il software gioca i suoi punti di forza in un' elevata flessibilità e una notevole rapidità di calcolo, senza dimenticare una *user-friendly* interfaccia grafica.

L' organizzazione di questo lavoro di Tesi è stata studiata per cercare di fornire una completezza di esposizione, ma allo stesso tempo risultare un utile manuale per lo sviluppatore. I primi capitoli forniscono una visione globale del software con particolare attenzione alle funzionalità presenti e alle scelte effettuate. I capitoli che seguono presentano una panoramica su alcune funzionalità di ADOpT con i relativi casi di studio e i risultati ottenuti dalle analisi. Per ogni capitolo viene preliminarmente fornita una visione globale circa la teoria alla base dei metodi implementati, seguita dalla descrizione delle classi e dei metodi relativi in Java ed è, infine, riportato il codice della *Test Class* implementata per lo svolgimento delle analisi con i relativi risultati.

Acknowledgements

Ho avuto la fortuna di apprendere in questi mesi di tirocinio e tesi molto più di quanto avrei mai immaginato. Per questo desidero ringraziare chi mi ha trasmesso conoscenze e passione con una dedizione che va ben oltre il Loro lavoro.

Ringrazio il Professor Fabrizio Nicolosi per la sua immensa professionalità e disponibilità. La figura del Professore, per me, non potrebbe avere altro nome.

Ringrazio, altresì il professore Agostino De Marco per tutto ciò che mi ha insegnato. Ho ricevuto notifiche del suo lavoro ad ogni ora del giorno e della notte, la sua curiosità per ciò che è nuovo e la passione nel renderlo conosciuto, non ha eguali.

Ringrazio di cuore, per la loro disponibilità, Pierluigi, Salvatore, Danilo e Vincenzo. Grazie per averci fatto spazio quando spazio non c'era, grazie per averci aiutato ogni volta che ne avevamo bisogno e grazie anche per le finestre chiuse quando avevo sempre freddo.

Ho avuto la fortuna di lavorare per 6 mesi a questo splendido progetto. Tuttavia io non credo esista la fortuna. La fortuna è l'attimo in cui il talento incontra l'occasione. Io l'occasione l'ho avuta grandissima, spero di aver dimostrato a Voi un talento che ne sia stato almeno all'altezza.

Desidero ringraziare, infine, tutti quei Professori che durante questo percorso mi hanno trasmesso qualcosa. In fondo, credo sia facile trovare del buono quando lo si cerca. E del buono nell'università ce n'è davvero ancora.

Vorrei dedicare questo lavoro di Tesi a tutti quelli che mi sono stati vicini, quando starmi vicino non è mai facile.

A Francesco, il mio futuro. Un futuro così non ci sarebbe mai stato senza di te. Mi hai aiutato a diventare la donna che nemmeno sapevo di essere, ma che tu vedevi da sempre. E tu sei diventato sempre più l'uomo della mia vita. Hai capito anche quando non c'era da capire e hai cercato di pensarla come me, dove nemmeno io sapevo cosa cercavo. Perché l'amore è compromesso, ma noi siamo un incastro perfetto.

A mia Madre, per tutte le volte che io piangevo e lei con me. Per quando ero felice e

lei gioiva. A lei che ogni mia richiesta diventava lo scopo della sua giornata solo per avere un sorriso la sera. Gli abbracci che ti do ogni giorno, non sono mai abbastanza. A mia madre che é lo specchio della mia anima.

A mio fratello, che in questi due anni ha più vissuto all'estero che a casa. Ho dovuto prendere la difficile decisione di se era più fastidiosa la sua televisione accesa ogni giorno o l'assordante silenzio della sua assenza. Danilo, non sai che rumore faceva la tua stanza quando andavo da te dimenticandomi che eri via.

A mia zia Iaia. Perché tu sei la sicurezza di una casa e la dolcezza di una famiglia. Grazie per essere sempre presente anche quando non devi. Una vita senza di te non si può nemmeno immaginare. A mio zio Gianfranco, grazie anche a te.

A Giusi perché difficilmente incontrerò una persona dallo spirito puro come il tuo e difficilmente io sarei mai potuta legarmi a qualcuno come a te. Perché spero di non smettere mai di imparare da te come si fa ad essere puri. So che tu sei la parte più buona di me, per sempre.

Ad Antonetta e Giuseppe. Mi avete accolto da sempre come una figlia e non vi ringrazierò mai abbastanza per questo. Voi siete la mia seconda famiglia.

A Federica, la mia amica ritrovata. In fondo gli amici possono fare dei giri un po' più lunghi, ma ritornano sempre a casa.

A Marina e Martina. Ci siamo conosciute per caso, ma continueremo a stare vicine per scelta.

A Marta perché mi ha sempre perdonato per tutte le volte che non so essere una buona amica.

Ai miei compagni di questo viaggio: Giovanni, Nicola. Mal che vada, ci vediamo al ristorante.

E a me stessa, per tutte le notti passate sui libri, per tutti i denti stretti troppo e il coraggio di osare che non mi ha mai abbandonato. A me che quella notte prima dell'ultimo esame continuavo a ripetermi "ma chi me lo fa fare?" e che trovavo la motivazione di nuovo, ogni ora. A me, che sono quello che sono grazie a voi.

Contents

Acknowledgements	iii
I Aircraft Design Overview	1
1 Aircraft Design	2
1.1 Historical Overview	2
1.2 General Process of Aircraft Design	3
1.3 Design Requirements and Objectives of an Aircraft	4
1.4 Aircraft Design Optimization	6
2 Application overview	8
2.1 Software architecture	9
2.1.1 Aircraft package	10
2.1.2 MyOperatingConditions class	11
2.1.3 CAD package	11
2.1.4 Calculators package	12
2.1.5 Database package	12
2.1.6 Writers package	12
2.2 Graphical User Interface (GUI)	12
2.2.1 Typical work session	13
2.2.2 CAD modelling	16
2.2.3 Interface with external software	16
2.3 In Development	17
2.3.1 Input File	17
2.3.2 Calculation modules	20
2.3.3 Optimization Process	20
II Development of Application	21
3 Introduction to Java	22
3.1 The Java Language	22
3.2 Java choice	23
4 Work Object	25
4.1 Introduction	25
4.2 Input data from .XML file	25
4.3 Default Aircraft	26
4.3.1 How is made a default Aircraft	27

4.3.2	How is made a default Wing	30
4.4	Database in JPAD	31
4.4.1	Setup database	32
4.4.2	Assign database using an Aircraft object	32
4.4.3	Assign database using a Wing object	32
4.4.4	User's guide	33
III	Functionality Overview	35
5	Work Object Data	36
6	Wing Lift Characteristics	39
6.1	Theoretical background	39
6.1.1	Zero-Lift Angle and Lift Coefficient Slope	40
6.1.2	End of Linearity angle of attack	41
6.1.3	Maximum Lift Coefficient	41
6.1.4	Stall Angle of Attack	44
6.1.5	Construction of the curve	44
6.1.6	Mach number effects on Lift curve	45
6.1.7	High Lift devices	46
6.2	Java Class Architecture	47
6.3	Case Study	50
6.3.1	ATR-72	50
6.3.2	BOEING 747-100B	55
6.4	Modified Stall Path	58
6.5	Results Comparison	59
7	Wing Drag Characteristics	62
7.1	Theoretical background	62
7.1.1	Case 1: CD_0 and kCL	64
7.1.2	Case 2: Parasite Drag and Induced Drag	65
7.2	Java Class Architecture	66
7.3	Case Study	69
7.3.1	ATR-72	70
7.3.2	BOEING 747-100B	74
8	Downwash Estimation	79
8.1	Theoretical background	79
8.2	Java Class Architecture	81
8.2.1	Constant Downwash Gradient	83
8.2.2	Variable Downwash Gradient	83
8.3	Case Study	86
8.3.1	ATR-72	87
8.3.2	BOEING 747-100B	89
8.4	Results Comparison	91
8.4.1	Slingerland Method	91
8.4.2	NACA Modified Method	92
8.5	Roskam Method	94
8.5.1	Results	94

9 Aircraft Longitudinal Static Stability	96
9.1 Aerodynamic Lift	98
9.1.1 Wing	99
9.1.2 Fuselage	99
9.1.3 Horizontal Tail	101
9.1.4 Complete Aircraft	104
9.2 Aerodynamic Drag	104
9.2.1 Drag of a lifting surface	105
9.2.2 Additional drag due to elevator	105
9.3 Pitching Moments	106
9.3.1 Lifting surface	107
9.3.2 Additional moment due to elevator	108
9.3.3 Fuselage	110
9.4 Propulsors	115
9.4.1 Direct Effects	115
9.5 Stability Calculation	116
9.5.1 Neutral Point and Static Margin	117
9.5.2 Pendular Stability	117
9.6 Java Class Architecture	118
9.6.1 Focus on the class methods	120
9.7 Case Study	121
9.7.1 ATR 72	122
9.7.2 Boeing 747-100B	130
10 Induced Angle of Attack	132
10.1 Induced Angle of Attack	132
10.2 Case Study	134
A HDF dataset and database reader creation	136
A.1 Chart Digitization	136
A.2 Creation of an HDF file with Matlab	137
B Java Reference	140
B.1 Object and Class in Java	140
B.2 Packages	140
B.3 Documentation	141
Glossary	143
Acronyms	145
List of symbols	146
Bibliography	148

Part I

Aircraft Design Overview

Chapter 1

Aircraft Design

*Scientists discover that which exists,
engineers creates that which never was.*

– T. Von Karman

Engineering design is a non-unique iterative process, the aim of which is to reach the best compromise of a number of conflicting requirements. Whether the need is for a totally new item or for a development of an existing one the design procedure commences with an interpretation of the requirements into a first concept.

The conceptual and preliminary design phases play a key role for the best development of future transport aircraft. A software framework that could help in finding a configuration which satisfies several basic requirements and eventually a constrained optimum is an essential tool for academic and industrial aircraft design activity. Since in the conceptual and preliminary design phases a lot of different configurations have to be analyzed, the software has been conceived to provide results in a relatively short computational time. For these reasons the aircraft design is projected to the utilization of new analysis tools who hold a main role in the design and optimization process.

Some new software have recently followed innovative approaches considering concepts like KBE (knowledge Based Engineering) and **Multi-disciplinary Design Optimization (MDO)** (Multi-Disciplinary Optimization) and have highlighted the necessity of an efficient graphical user interface and the importance of making the application results easily exploitable with external software.

In this scenery ranks **ADOpT** and its reference library **JPAD** that is a Java-based desktop application developed at the University of Naples Federico II, conceived as a fast, reliable and user friendly computational aid for aircraft designers in the conceptual and preliminary design phases.

1.1 Historical Overview

During the last century, three design methods have been developed in the aerodynamic design process. Until the early 1960s, only two methods were available: empirical and mathematical methods. Since the 1960s, a third method has been developed: computational fluid dynamics, which can be considered as a combination of the two earlier methods. These three methods and their history will be discussed briefly in this chapter.

The empirical method is the oldest method of aerodynamic design; until about 1940, it was the only practical tool available. Based on either theory or experiments or a combination

of both, the empirical methods consist of handbooks which are essentially a collection of graphs and equations. They are meant to give a relation between elementary parameters of the geometry of the aircraft and the desired characteristics of the aircraft.

Through the mathematical methods the aerodynamic characteristics of the detailed geometry are obtained by physical insight, in other words, through pressure distributions. This approach uses mathematical modelling of flow physics.

With the development of computers, more and more powerful numerical methods became available to aircraft designers. These numerical methods are known as computational fluid dynamics. It allows them to obtain the intended characteristics of the aircraft (or one of its major components) by directly determining the required detailed aerodynamic shape through the use of fluid dynamics and the associated pressure distribution.[34]

Modern aerospace design begins with the desire of mankind to achieve powered, heavier-than-air flight. Early aerospace designs were characterized not only by a great deal of trial and error but also by a not inconsiderable amount of analysis.

At the beginning of the aviation history the entire design process occurred in six months. Some companies produced more than ten aircraft in only 20 years. Today in order to develop a new transport aircraft it takes more than 10 years. The current aircraft design strategy is linked to industrial growth, which in turn depends on national infrastructure, governmental policies, workforce capabilities, and natural resources; these are generally related to global economic-political circumstances. More than any other industry, the aerospace sector is linked to global trends. It is possible to view the first 75 years of aerospace design as a series of stages: first came the early pioneers, working at a time when many were skeptical about the benefits of flight or even if it was possible at all. Next came the phase where outstanding individuals dominated aeronautical science and design during the interwar and early postwar years. This was followed in the 1950s and 1960s by a greater emphasis on design teams and the massive expansion of the great aerospace companies that we recognize today, such as Lockheed Martin and Rolls-Royce. Following these stages, the advent of CAE, design and manufacture in the mid-1970s transformed activities in aerospace with an increasing focus on faster design cycles, more accurate predictive capabilities and the rise of computer science. At the same time, the great drawing offices of the 1950s declined and fewer people were involved in the design of each individual component.[17]

Recent developments in information technology have had a major impact upon the aeronautical design process. The emphasis has become one where the whole design procedure from concept to the derivation of manufacturing data is covered by an integrated information technology system. Computer aided design techniques are used to produce digital data. While these procedures are particularly relevant to the detail phases of the design process their application commences as soon as a requirement is defined and numerical data are derived from it.[22]

1.2 General Process of Aircraft Design

The design process is usually divided into the following phases:

1. **Requirements phase.**
2. **Conceptual design phase.** This phase determines the feasibility of meeting the requirements with a credible aircraft design. The concept definition phase can be characterized

as the highly creative and imaginative idea stage during which the component geometry, placement and connectivity of a future aircraft designed to fulfill the needs of a specific market are defined. Conceptual design also entails the development of a novel aircraft concept at an overall system level in competition with a more traditional layout. The objective is to explore a preferred configuration to determine a layout which is technically superior and economically viable.

3. **Preliminary design phase.** This phase aims at defining subsystems and making component trade-offs. Specialists from different functional groups contribute to this process of refining the initial vehicle concept. This team will (re)design the delivered baseline vehicle in sufficient detail to carry out supporting analysis and specify peripheral testing programmes but not with enough detail to specify each sub-assembly.
4. **Detail design phase.** In the detail design phase, the configuration is “frozen” and the decision has been made to build the aircraft. Detailed structural design is completed. All of the detail design and shop drawings of the mechanisms, joints, fittings, and attachments are accomplished. Interior layout is detailed with respect to location and mounting of equipment, hydraulic lines, ducting, control cables, and wiring bundles. This development phase is entered soon after the aircraft is committed to production and lasts between two and three years.
5. **Testing phase.**

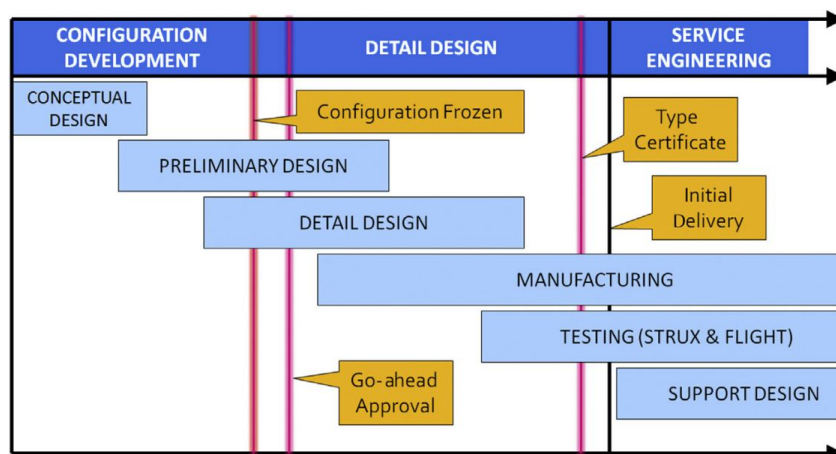


Figure 1.1: Aircraft design process for Torenbeek (1986).

1.3 Design Requirements and Objectives of an Aircraft

The general design objective of a transport aircraft is to transport a payload over a distance between airports against minimum costs (i.e. at an optimum speed). So, in the design of an aircraft there is never a right answer only a best answer at a point in time. The reason is that the design of an aircraft is a balance between the following competing requirements:

- **Technical.** Performance, survivability
- **Signature.** Survivability, appearance
- **Economic.** Cost, LCC

- **Political.** Policy, payback, risk, and so on
- **Schedule.** When needed? The need to be first to market
- **Environmental.** Limited energy source, noise, hydrocarbon emissions

Also, the priorities of these requirements change with time. An aircraft might be designed to certain technical and economic requirements, but if the government administration changes, then the priority requirement becomes political or environmental. The advice to the designer is to remain flexible and develop as robust a design as possible so that it will survive as the requirements change over time. The watchwords are compromise, balance, and flexibility.

Significant characteristics of the various classes of aircraft	
Private aircraft	"Poor people" / Flying clubs Costs are dominant
	"Rich people" / business men Costs / performance
Business aircraft	Balance between costs, comfort and performance
Agricultural aircraft	Very specialized, good balance between costs and revenue with probably accent on costs
Aerobatic aircraft	Very specialized, performance (manoeuvrability) is dominant, often very expensive
Civil transport aircraft	Costs may be high if, given a certain fare structure, revenues are higher
Military aircraft (non-transport types)	Costs may be high, military capabilities and operational readiness are dominant
	Most military aircraft have apart from load-carrying requirements high demands on both manoeuvrability ("dog-fighting") and stability ("aiming platform")

Figure 1.2: Main design requirements of various aircraft categories.[34]

An aircraft comprised of several major components. It mainly includes wing, horizontal tail, vertical tail, fuselage, propulsion system, landing gear and control surfaces. In order to make a decision about the configuration of each aircraft component, the designer must be fully aware of the function of each component. Each aircraft component has inter-relationships with other components and interferes with the functions of other components.

No	Component	Primary function	Major areas of influence
1	Fuselage	Payload accommodations	Aircraft performance, longitudinal stability, lateral stability, cost
2	Wing	Generation of lift	Aircraft performance, lateral stability
3	Horizontal tail	Longitudinal stability	Longitudinal trim and control
4	Vertical tail	Directional stability	Directional trim and control, stealth,
5	Engine	Generation of thrust	Aircraft performance, stealth, cost, control
6	Landing gear	Facilitate take-off and landing	Aircraft performance, stealth, cost
7	Control surfaces	Control	Maneuverability, cost

Figure 1.3: Aircraft major components and their functions.[30]

1.4 Aircraft Design Optimization

At the beginning of the aircraft design history, optimization was limited to relatively superficial investigations to study the effects of varying a few major design parameters. Since the 1970s, there has been a tremendous expansion of optimization strategies and algorithms supporting advanced designers. The introduction of automated optimization has enabled designers to go into much greater in depth and fidelity of analysis than before. Synthesis programs effectively connecting the inputs and outputs of the functional group disciplines by means of an automatic control logic have been developed at aircraft manufacturers, research establishments and academia. Sophisticated computer assisted design (**Computer-Aided Design (CAD)**) systems for defining three-dimensional body geometries and computer graphics tools for rapidly preparing parametric surveys are available at a modest cost.

There are several options available to an aerodynamicist to obtain the best possible solution for a design problem. In general the optimization is an iterative process control system which interprets numerical results and then iteratively assesses variables to seek the global optimum of an objective function. In the aircraft design context, the objective function is used to decide which configuration is considered the best combination of design variables.[47]

It is emphasized frequently that optimization of individual goals through separate design considerations may prove counterproductive and usually prevents the overall (i.e., global) optimization of ownership cost. **MDO** offers good potential but it is not easy to obtain global optimization; it is still evolving. In a way, global **MDO** involving many variables is still an academic pursuit. Industries are in a position to use sophisticated algorithms in some proven areas. An example is reducing manufacturing costs by reshaping component geometry as a compromise – such as minimizing complex component curvature. The compromises are evident in offering a family of variant aircraft because none of the individuals in the family is optimized, whereas together, they offer the best value.

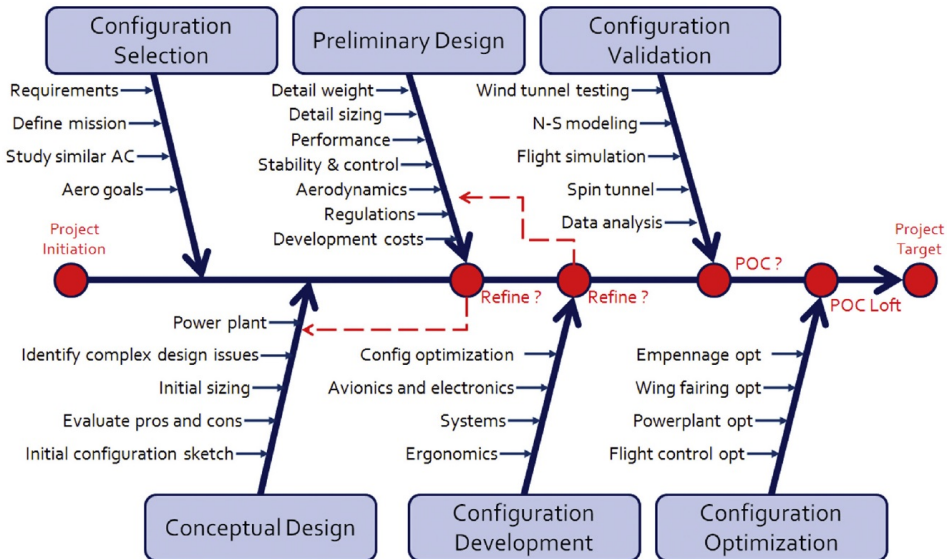


Figure 1.4: A typical fishbone diagram.

According to [22], the optimization of the configuration of the aircraft within the constraints imposed by the specification is an essential feature of the project definition process. Optimization implies that the proposed design concept not only meets the specification, but does so when a target criterion has been imposed, usually the minimisation of mass or some aspect of costs. The basis of optimisation is a comparison of different design concepts and

configuration variations within a given concept to determine the one which best meets the specification. Broadly the process is undertaken at two levels.

- **Concept/configuration studies** At this level alternative concepts and configurations are investigated to establish the one which would seem best suited to meet the requirements. For example a military combat requirement might possibly be met by aircraft of conventional tail, foreplane or tailless layout. Mostly the configuration of transport aircraft is well established. This phase of the study may be included at the feasibility level.
- **Parametric studies within a given configuration** At this level the dominant parameters are varied to ascertain the best combination of them. These parameters include such items as wing geometry determined by aspect ratio, sweep, taper and thickness as well as variations in fuselage layout, powerplant installation and so on. The benefits of selecting near optimum values of certain parameters are "traded-off" against the implied penalties imposed upon other parameters. The parametric studies may be commenced during feasibility investigations and certainly form a major part of the project definition phase. The two fundamental design characteristics which drive the parametric studies are:
 - Wing loading, that is wing area as a function of take-off mass or weight
 - Thrust or power loading, defined as the ratio of the basic powerplant to the aircraft mass or weight

Chapter 2

Application overview

*I do not fear computers.
I fear the lack of them.*
— Isaac Asimov

In this Chapter an overview of the **ADOpt** software, and its reference library **JPAD** will be presented. **ADOpt** is a Java-based desktop application developed at the University of Naples Federico II, conceived as a fast, reliable and user friendly computational aid for aircraft designers in the conceptual and preliminary design phases. The ultimate goal of such a tool is to perform a parametric, multi-disciplinary analysis of an aircraft and then search for an optimized configuration. The search domain boundaries are usually defined by the user through a set of specified parameters. An important design requirement of **ADOpt** is related to its interoperability with other engineering analysis tools. In fact, the application can be easily integrated into a comprehensive aircraft optimization cycle. This is made possible because **ADOpt** can be launched both in **Graphical User Interface (GUI)** and command line mode. Much care has been given to input/output and configuration files to increase the possible uses of the software.

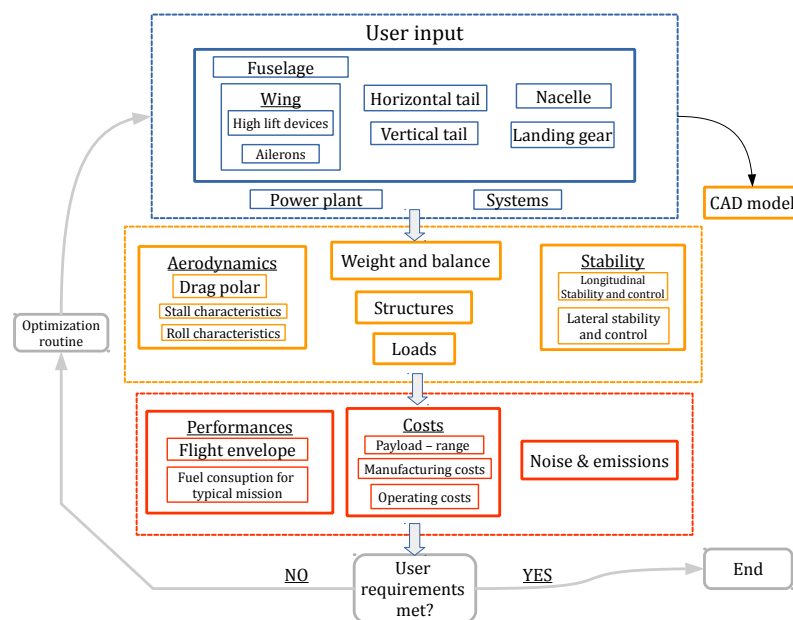


Figure 2.1: Software calculation modules.

2.1 Software architecture

JPAD library is actually divided into three package: JPADConfigs, JPADCore and JPADSandbox. Each package is organized in several classes or more package in order to have a clear and simple classification. The possibility to place similar classes in the same package has been extensively exploited for the same reasons, see section A.2. The source code has been extensively commented following Javadoc practices. This enabled us to automatically generate documentation using Doxygen [50]

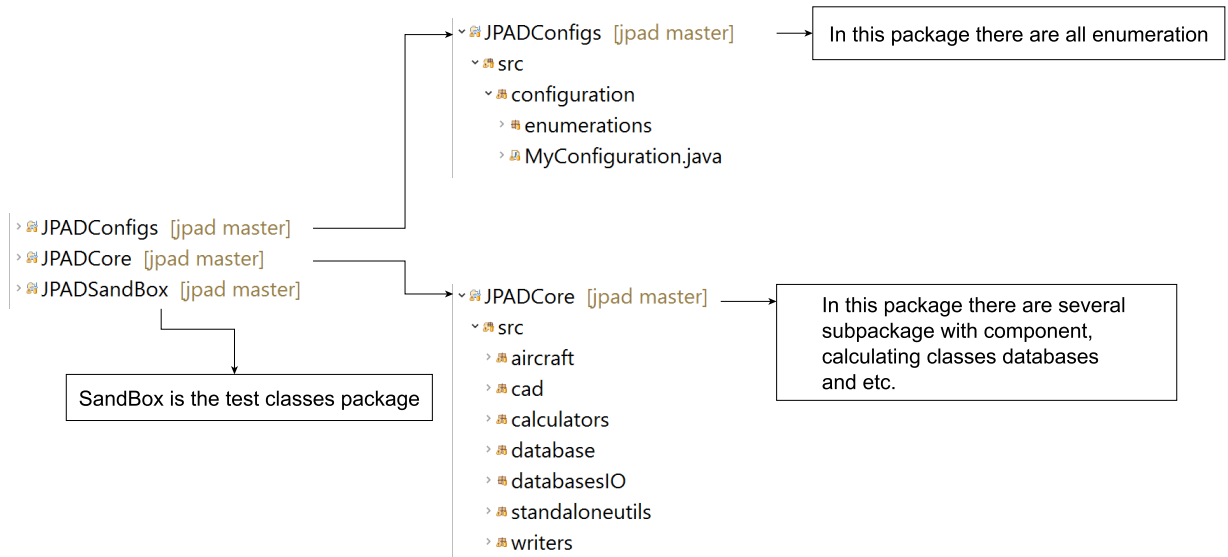


Figure 2.2: Software package division.

The main package of **JPAD** library is JPADCore where there are all aircraft component, the managers of calculator and its computers classes. In the following subsection will explained the main features of JPADCore.

JPADCore contains the following sub-packages:

1. `aircraft` → This package contains all aircraft's component classes, their calculators and the related managers and also the operating condition's class.
2. `cad` → This package contains everything concerning the creation of CAD model.
3. `calculators` → In this package there are the classes, divided in package by type of analysis, whose methods implement the calculation formulas.
4. `database` → This package contains the classes that manage the database .h5 whose data are useful for the analysis.
5. `standaloneutils` → In this package there are several calculation classes with mathematical tools to support the analysis.
6. `writers` → this class is in charge of writing files.

Following will be explained the main features of the fundamental packages.

2.1.1 Aircraft package

Each component (e.g., the fuselage, the wing, the engine) is therefore defined in its own class. In the aircraft package there are other sub-package for components. In each of these there are a class for the object definition and a manager for the analysis. These manager classes uses the utilities located in the calculator package.

The sub-package in the `aircraft` package are the following:

- `Auxiliary` that manages the airfoils
- Component that contains the `aircraft` class, the aircraft components packages (fuselage, lifting surfaces, nacelles, power plant, fuel tank, landing gear, systems) and, inside them, their manager analysis classes used to call related analysis methods.
- `OperatingConditions`

The main aircraft components are organized as follows:

Basic data for describing the **fuselage** are contained in the `fuselage` class. This holds all the fuselage overall properties, such as the length, maximum width and maximum height, length ratios between the nose and the tail parts length to the constant section part length, number of decks and so on. Other classes in the package manage the shape of fuselage sections and outlines (which define the fuselage shape in the xz and xy planes) and aerodynamics calculations (Aerodynamics class).

The data relating to the **lifting surfaces** are contained in the `liftingSurface` class. Since the lifting surfaces of an aircraft share several characteristics, a single class has been created to manage the wing, the horizontal and vertical tail and, eventually, the canard. The lifting surface specific category (that is, wing, horizontal tail etc.) is acknowledged through a `MyComponentEnum` variable which has to be specified when creating the lifting surface object. By default, a lifting surface has three primary span stations: root ($\eta = 0$), middle and tip ($\eta = 1$). The middle station location is user-defined and is used to represent a change in chord.y/ law; such a change can be due to a lifting surface kink or to the beginning of a tapered part. If the wing is simple tapered the middle station can also be omitted.

The data relating to the **airfoils** are handled by `Airfoil` class, that creates for each lifting surface three airfoils, located respectively at $\eta = 0$, $\eta = 1$ and at middle station. An airfoil object holds:

1. the position along the semispan, η ;
2. twist value relative to root, ϵ_g ;
3. zero lift angle of attack, $\alpha_{0\ell}$;
4. angle of attack value at the end of the linear part of $C_l(\alpha)$ curve, α^* ;
5. stall angle of attack, α_{stall} ;
6. lift gradient of the linear part of $C_l(\alpha)$ curve, C_{ℓ_α} ;
7. minimum drag coefficient, $C_{d,min}$;

8. lift coefficient at $C_{d,min}$, $C_l @ C_{d,min}$;
9. lift coefficient at the end of linear part;
10. maximum lift coefficient, $C_{\ell_{max}}$
11. drag polar K factor;
12. aerodynamic moment coefficient gradient, C_{m_α} ;
13. aerodynamic center x coordinate, x_{ac} ;
14. aerodynamic moment coefficient with respect to the aerodynamic center, $C_{m_{ac}}$ or C_{m_0} ;
15. aerodynamic moment coefficient with respect to the aerodynamic center at stall, $C_{m_{ac,stall}}$;
16. maximum thickness to chord ratio, t/c_{max} ;
17. x,z non dimensional coordinates.

At the time of writing all these quantities have to be entered by the user. The `Airfoil` class provides the `populateCoordinateList()` method which transforms the non dimensional coordinates provided by the user in order to obtain their actual coordinates, which takes into account of actual chord length, ACRF position, sweep, twist and dihedral.

The **power plant** is defined in the package `PowerPlant` in `components`. In this package there is the `engine` class that initializes the data related to the single engine. An other class in the same package, `powerPlant` creates the parametric model of the power plant using a list of objects creates by `engine`.

2.1.2 MyOperatingConditions class

As the name suggests, this class contains all the data related to atmosphere conditions (which are currently derived from altitude value using the 1976 ISA model), current speed (Mach number), gravitational acceleration ($9.806\,65\text{ m/s}^2$) and sea level pressure (101 325 Pa).

A `MyOperatingConditions` object can be created regardless of the aircraft configuration as the class is entirely self contained: the aircraft could also be undefined at the time of the object creation. If the user wants to run several analysis at different operating conditions, a `MyOperatingConditions` instance has to be created for each one.

2.1.3 CAD package

Throughout the development of the application, great care has been given to the making of the CAD model for several reasons:

- it enables the user and the user developer to have an immediate feedback about the data provided to the application: if some geometrical parameter is wrong, the CAD model makes it impossible not noticing it;
- it allows the user to run a CFD analysis with an external program. The CAD model has been in fact built so that it is ready to be meshed by an external mesher without any further adjustment;

- it provides an accurate estimate of the wetted surface of each component.

The creation of the CAD model was made possible by the occjava library, whose classes and methods have been used to build each component's model.

2.1.4 Calculators package

This package includes all the calculators classes. Calculator classes have been created to evaluate quantities related with more than one component. The calculator classes are the following:

- aerodynamics package
- cost package
- geometry package
- performance package
- stability package

Each of these package contains calculators classes and concerning methods that implement all mathematical equations. These methods are called by the analysis manager classes that are in the package of relatives components (such as fuselage, lifting surfaces etc.).

2.1.5 Database package

In order to manage a large quantity of data, it has been necessary to read data from graphs available in literature; for such a reason an extensive database has been built over the years by several of my colleagues to digitalize this data in order to exploit it in a computer program. The data has been stored in an hdf5 file.

In the database package there are all the classes that manage and reads the .h5 files. To obtain the useful data in JPAD, interpolating functions are used. These functions can be of one, two or three dimensions and read data from graphics that have been digitized previously.

2.1.6 Writers package

This class is based on the Apache POI library and provides methods which enable the user developer to easily add a sheet to an XLS file, to set the styles of the XLS file and to compare different XLS files. The last function permits to create an XLS file which contains a different aircraft data for each column; in such a way the comparison between two or more aircraft (or, simply, between slightly different configurations of the same aircraft) is easier and effective.

2.2 Graphical User Interface (GUI)

An extensive work has been done to set up an effective Graphical User interface (GUI) to reduce the time the user has to spend to obtain relevant results. The result presented in this section is the early step of graphical interface, which is currently in development.

The Java programming language greatly helped to build the GUI: several open source libraries (SWT, JFace) allowed us to build a functional yet pleasant GUI which allows the

user to easily change the aircraft's parameters, to view a 3D model of the defined geometry, to launch a new analysis and view the corresponding results. The current GUI appearance is shown in fig. 2.3. It is composed of several items:

1. a menu bar (on top), which holds all the available actions divided in sub-categories;
2. a toolbar (below the menu bar), which holds the most important actions needed to interact with the application. The toolbar, as the menu bar, is always visible to the user;
3. a project tree (on the left), a key component of the GUI since it provides access to all the components of the aircraft and the analysis results any time during the execution of the application. The project tree appears once an aircraft is created and can be eventually hidden;
4. a 3D view, which shows the CAD model of the aircraft selected by the user. The CAD model can be updated each time the user wants to check the changes made to the aircraft geometry;
5. a log message window, placed at the bottom, that tells the user the status of pending operations. This window can be hidden;
6. a tab folder, which contains all the windows opened using the project tree; these windows can be closed and reopened any time.

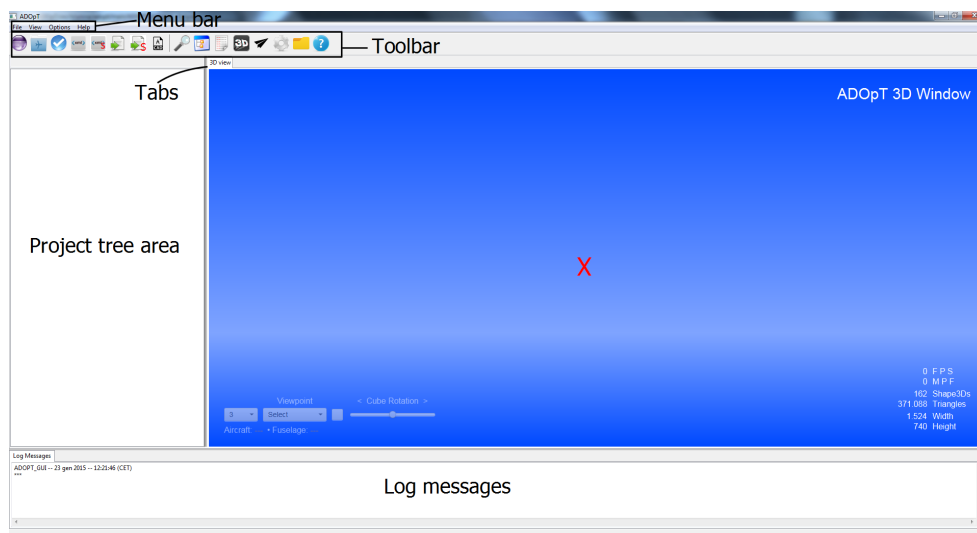


Figure 2.3: The GUI when the application is started.

2.2.1 Typical work session

In developing the application we focused on making the user's typical work session as simple as possible. Few basics steps are required for running an analysis:

1. create a new aircraft, which we will call A. This can be done using the corresponding button (.addButton) in the toolbar, which instantiates the default aircraft
2. set the parameters that define the aircraft model using the corresponding window opened using the tree

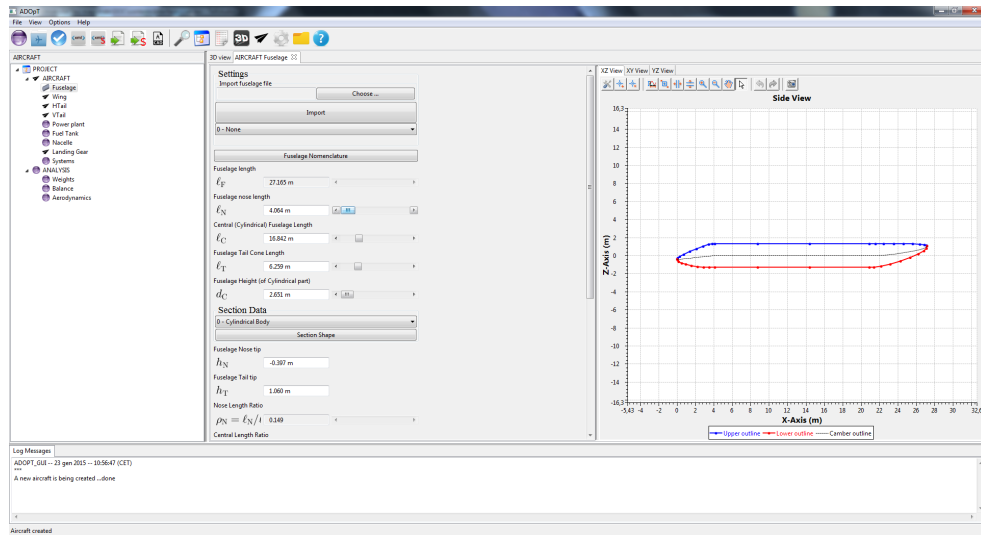


Figure 2.4: The window for changing the fuselage parameters.

3. explore the 3D model (3D) of the aircraft and eventually change some parameters if there is some error

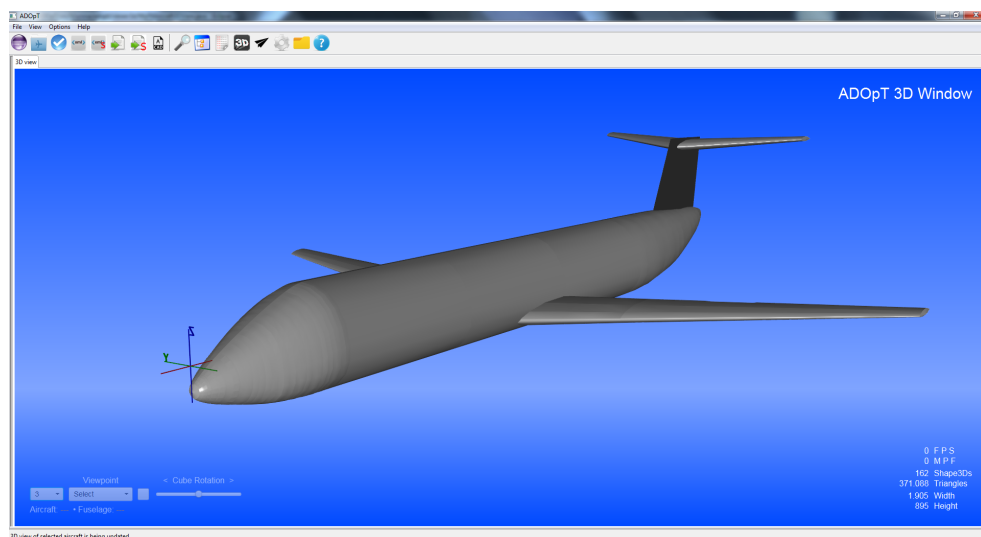


Figure 2.5: The aircraft 3D view (log window and project tree hidden).

4. execute a complete analysis (🔍) of the aircraft previously defined;
5. export the analysis results to an XML and/or an XLS file (📄);
6. eventually export the CAD model of the aircraft (CAD);
7. save the current aircraft to an XML file (XML).

At this point the user could simply change the current configuration until the analysis results are satisfactory. The application can however help the user in finding such a configuration, since it can hold multiple configurations simultaneously, analyse all of them and compare them side by side. To accomplish this task, once the first aircraft has been created, the user should:

1. import the aircraft previously saved or create an entirely new aircraft, which we will call B;
2. change B parameters and run a new analysis on it;
3. study the results and eventually change some of the parameters;
4. save every configuration and the corresponding results to file;
5. export both aircraft and the corresponding results to an XLS file.

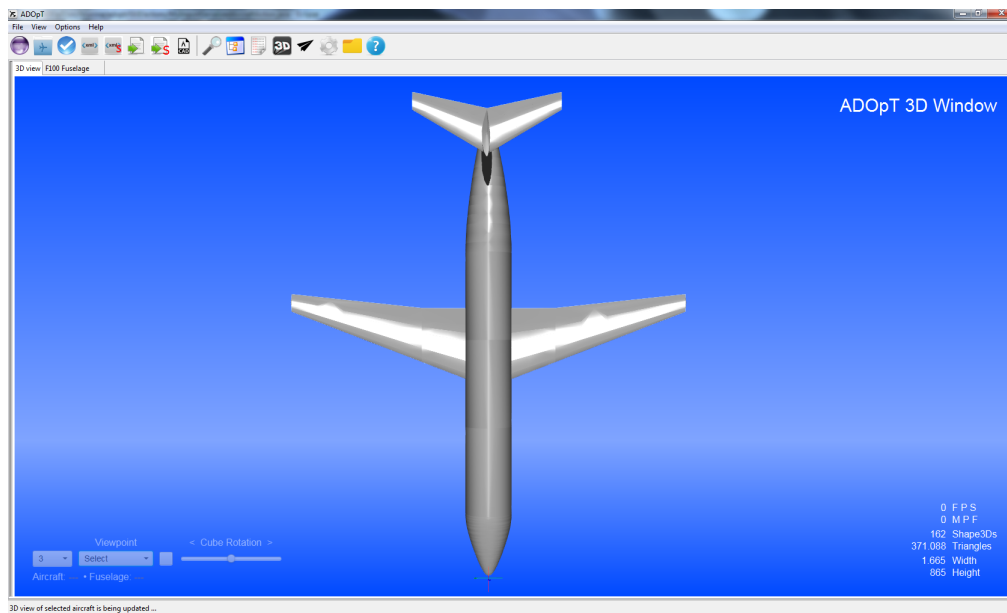


Figure 2.6: The aircraft 3D view.

There is no limit to the number of aircraft the application can handle; each aircraft is added to the project tree as shown in fig. 2.7 providing access to the corresponding components and analysis.

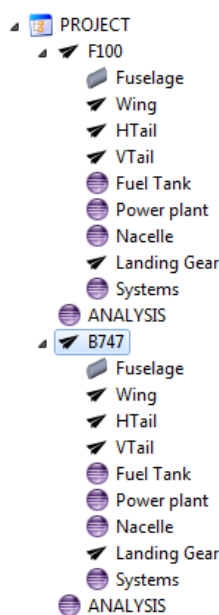


Figure 2.7: The project tree holding two different aircraft

3D view F100 Fuselage A320 Fuselage

Figure 2.8: Same component tab belonging to different aircraft

2.2.2 CAD modelling

The application can also be used as a basic parametric **CAD** modeler. The capability to change the aircraft parameters using the corresponding controls in the **GUI**, coupled with the 3D view, allows the user to change each component shape and dimension, view the updated **CAD** model and eventually export it to file once some satisfactory results have been obtained. The creation of the **CAD** model was made possible by the occjava library, whose classes and methods have been used to build each component's model. The **CAD** model can be saved in two different file formats: STEP and BREP; they have proven to take both little memory and to give the best results in terms of geometry representation. The IGES format gave instead mixed results so we preferred to use only the first two.

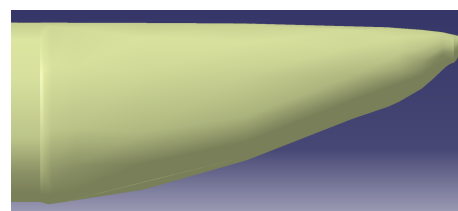


Figure 2.9: A detail of the tail of the fuselage obtained as a unique loft.

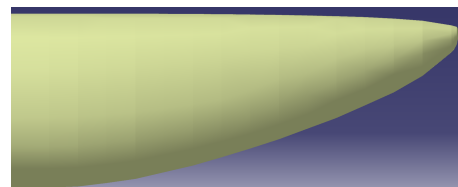


Figure 2.10: A detail of the tail of the fuselage obtained sewing together its parts.

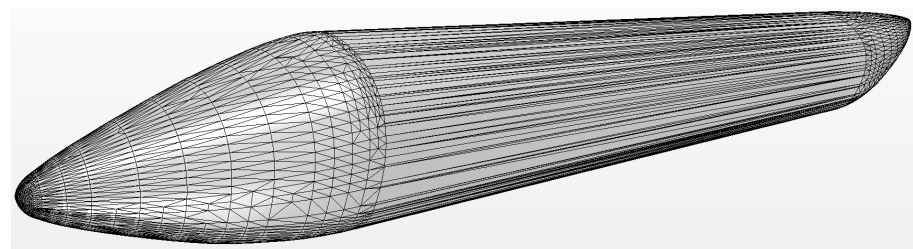


Figure 2.11: External fuselage shape exported as STEP file.

2.2.3 Interface with external software

With ADOpt it's also possible to execute some high-fidelity analyses using external tools (i.e. CFD Navier-Stokes solver, panel method, FEM for structural static and dynamic analysis, etc.) by importing the dedicated output (such as a **CAD** model) produced by the software. The higher-fidelity tools could improve the results obtained and give therefore some useful clues in order to start a new design loop with different requirements and/or different constraints. The possibility to interface the software with drawings and graphical representation (i.e. **CAD** or Catia) of the designed aircraft is also very important.

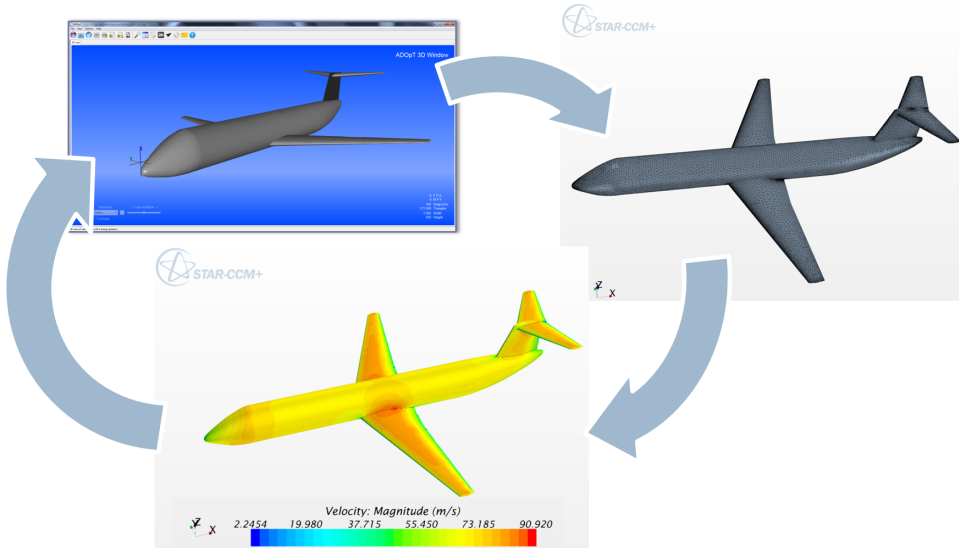


Figure 2.12: Interface with external CFD tools.

2.3 In Development

JPAD library is currently being developed in order to achieve a complete analysis of an aircraft and its optimization. The development is actually moving on a complete reorganization of the input file, and the implementation of other methods of analysis. Anyway, to date, it was reached an advanced level of implemented methods and a full functionality of some modules.

2.3.1 Input File

In order to obtain an useful and intuitive input structure a new data arrangement is in development. The JPAD input files are actually in XML data format. This extension will not change, but the purpose of the new structure is to allow the user to easily manage the input data in order to execute the desired analyzes.

The structure is inspired by that proposed by SUAVE. SUAVE is an open source suite constructed as a modular set of analysis tools written in Python and it is currently being developed in the Aerospace Design Lab at Stanford University. [9]

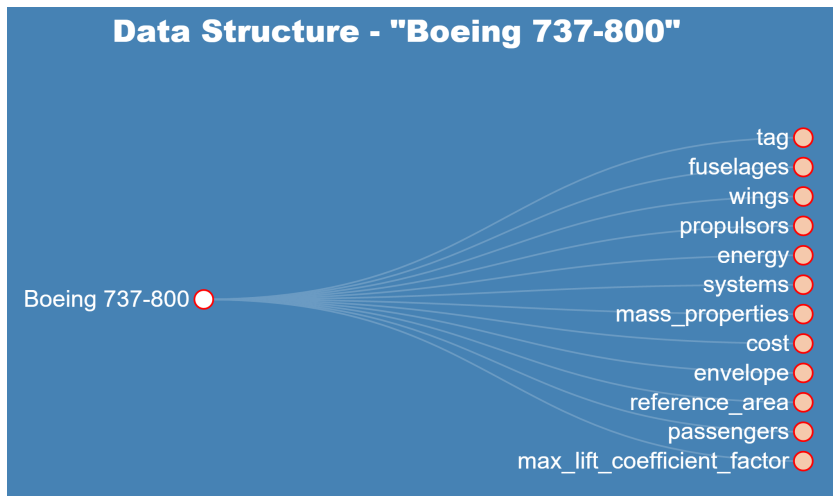


Figure 2.13: Data Structure used by SUAVE.

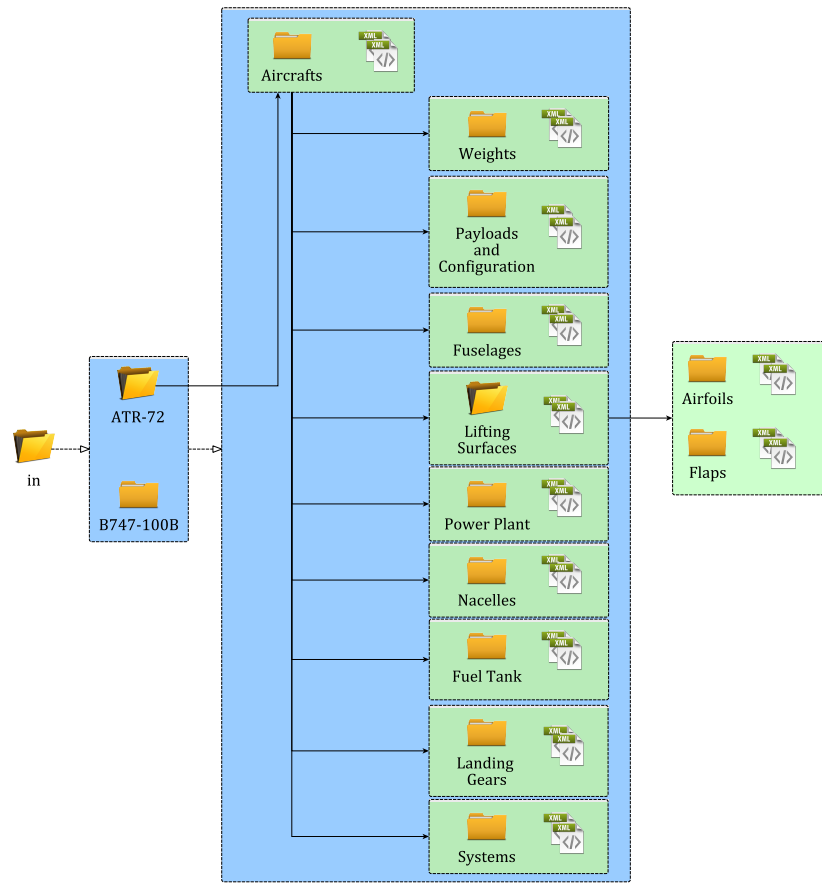


Figure 2.14: Folder Structure in development.

The fundamental criteria on which the construction is based are expressed following. In the input file folder, there are many sub-folder for different aircraft. In each of these there are several folders for component in which may be more XML file that corresponding to a different configuration. In fact, there is an XML file for each configuration of each aircraft component (fuselage, lifting surfaces etc.).In this way it's possible to choose different configuration for the same aircraft simply changing one or more XML input file. For the analysis the useful data will be explained in a user guide. User could make a complete analysis on a new aircraft, simply defining the required data and organize them in separated xml file.

The main XML file is “aircraft.xml” which calls the other XML of the aircraft components. A typical file structure is in the following listings.

Listing 2.1 XML input file for an aircraft.

```

<?xml version="1.0" encoding="utf-8"?>
<jpad_config>
  <aircraft>
    <wings>
      <wing type="WING" file="wing.xml">
        <position>
          <x unit="m">12.0</x>
          <y unit="m"> 0.0</y>
          <z unit="m"> 2.0</z>
        </position>
        <rigging_angle unit="deg">2.0</rigging_angle>
      </wing>
      <wing type="HTAIL" file="htail.xml">
        <position>
          <x unit="m">30.0</x>
          <y unit="m"> 0.0</y>
          <z unit="m"> 4.0</z>
        </position>
      </wing>
    </wings>
  </aircraft>
</jpad_config>
  
```

```

        <rigging_angle unit="deg">0.0</rigging_angle>
    </wing>
    <wing type="VTAIL" file="vtail.xml">
        <position>
            <x unit="m">30.0</x>
            <y unit="m"> 0.0</y>
            <z unit="m"> 5.0</z>
        </position>
        <rigging_angle unit="deg">0.0</rigging_angle>
    </wing>
</wings>
<fuselages>
    <fuselage file="fuselage.xml">
        <position>
            <x unit="m">0.0</x>
            <y unit="m">0.0</y>
            <z unit="m">0.0</z>
        </position>
    </fuselage>
</fuselages>
<propulsors>
    <propulsor file="propulsor.xml">
        <position>
            <x unit="m">12.0</x>
            <y unit="m"> 5.0</y>
            <z unit="m"> 0.0</z>
        </position>
        <tilting_angle unit="deg">2.0</tilting_angle>
        <yawing_angle unit="deg">0.0</yawing_angle>
    </propulsor>
    <propulsor file="propulsor.xml">
        <position>
            <x unit="m">12.0</x>
            <y unit="m">-5.0</y>
            <z unit="m"> 0.0</z>
        </position>
        <tilting_angle unit="deg">2.0</tilting_angle>
        <yawing_angle unit="deg">0.0</yawing_angle>
    </propulsor>
</propulsors>
</aircraft>
</jpad_config>

```

Listing 2.2 XML input file for an aircraft.

```

<?xml version="1.0" encoding="utf-8"?>
<jpad_config>
    <wing mirrored="TRUE">
        <panels>
            <panel id="Inner_Panel">
                <semispan unit="m">4.0</semispan>
                <dihedral unit="deg">1.5</dihedral>
                <inner_section>
                    <airfoil file="naca63209.xml"/>
                    <geometric_twist unit="deg">0.0</geometric_twist>
                </inner_section>
                <outer_section>
                    <airfoil file="naca63209.xml"/>
                    <geometric_twist unit="deg">0.0</geometric_twist>
                </outer_section>
            </panel>
            <panel id="Outer_Panel" linked_to="Inner_Panel">
                <semispan unit="m">7.0</semispan>
                <dihedral unit="deg">3.5</dihedral>
                <outer_section>
                    <airfoil file="naca63209.xml"/>
                    <geometric_twist unit="deg">-2.5</geometric_twist>
                </outer_section>
            </panel>
        </panels>
        <symmetric_flaps>
            <symmetric_flap id="Inner_flap" type="SINGLE_SLOTTED">
                <inner_station_spanwise_position type="PERCENT_SEMISPA
                <value>0.15</value>

```

```

</inner_station_spanwise_position>
<outer_station_spanwise_position type="PERCENT_SEMISPAN" ref_to=
"FULL_SEMISPAN">
    <value>0.45</value>
</outer_station_spanwise_position>
<percent_chord value="40"/>
<angle_range unit="deg">[0.0,40.0]</angle_range>
</symmetric_flap>
</symmetric_flaps>
<slats>
    <slat linked_to="Inner_flap" type="SINGLE">
        <percent_chord value="10"/>
        <angle_range unit="deg">[0.0,10.0]</angle_range>
    </slat>
</slats>
<asymmetric_flaps>
    <asymmetric_flap id="Aileron" type="PLAIN">
        <inner_station_spanwise_position type="PERCENT_SEMISPAN" ref_to=
"FULL_SEMISPAN">
            <value>0.75</value>
        </inner_station_spanwise_position>
        <outer_station_spanwise_position type="PERCENT_SEMISPAN" ref_to=
"FULL_SEMISPAN">
            <value>0.97</value>
        </outer_station_spanwise_position>
        <percent_chord value="20"/>
        <angle_range unit="deg">[-5.0,10.0]</angle_range>
        <differential_deflection_factor value="1.0"/>
    </asymmetric_flap>
</asymmetric_flaps>
</wing>
</jpad_config>

```

2.3.2 Calculation modules

Currently the software is able to estimate the aircraft weight breakdown, the center of gravity location, calculate some aerodynamic parameters and estimate the performance. All these types of estimates can be usually performed using several analysis methods, comparable and interchangeable. It is also provided a static longitudinal stability analysis, take-off performances and the generation of Payload Range chart.

Future targets for the software are the implementation of landing performances, ultimate the directional static stability

2.3.3 Optimization Process

It has always been the engineer's dream to have all aspects of analysis done in a relatively short time period so that many different configurations can be examined and the best suitable product can be delivered on time. Although this may still be a dream, actual design turn-around time has become shorter due to the use of mathematical optimization techniques which have been introduced into the design process.[47] As all analysis modules inside the JPADCore package will be completed and tested, the final purpose of the code will be to allow users to define a certain numbers of macroscopical geometrical parameters, along with a given objective function, and to receive as output the best set of the previous parameters which suits the wanted objective.

Part II

Development of Application

Chapter 3

Introduction to Java

*Language is only the instrument of science,
and words are but the signs of ideas.*

— Samuel Johnson

3.1 The Java Language

The term Java refers both to a programming language with the higher number of developers in the worldwide and to a technology that has several sub-technologies that have emerged in different fields of use of the software. Java was developed by Sun Microsystems, a company that was incorporated in Oracle from a few years. In 1996, James Gosling, Bill Joy, and Guy Steele wrote for the First Edition of The Java Language Specification: “*We believe that the Java programming language is a mature language, ready for widespread use. Nevertheless, we expect some evolution of the language in the years to come. We intend to manage this evolution in a way that is completely compatible with existing applications.*”

This programming language is a general-purpose, concurrent, class-based, object-oriented language. It is designed to be simple enough that many programmers can achieve fluency in the language.[45] One design goal of Java is portability, which means that programs written for the Java platform must run similarly on any combination of hardware and operating system with adequate runtime support. This is achieved by compiling the Java language code to an intermediate representation called Java bytecode, instead of directly to architecture-specific machine code. Java bytecode instructions are analogous to machine code, but they are intended to be executed by a virtual machine (VM) written specifically for the host hardware. End users commonly use a Java Runtime Environment (JRE) installed on their own machine for standalone Java applications, or in a web browser for Java applets.[7] Standard libraries provide a generic way to access host-specific features such as graphics, threading, and networking.

There were five primary goals in the creation of the Java language:[35]

1. It must be “simple, object-oriented, and familiar”.
2. It must be “robust and secure”.
3. It must be “architecture-neutral and portable”.
4. It must execute with “high performance”.
5. It must be “interpreted, threaded, and dynamic”.

Java SE 8 represents the single largest evolution of the Java language in its history. A relatively small number of features - lambda expressions, method references, and functional interfaces - combine to offer a programming model that fuses the object-oriented and functional styles. Under the leadership of Brian Goetz, this fusion has been accomplished in a way that encourages best practices - immutability, statelessness, compositionality - while preserving “the feel of Java” - readability, simplicity, universality.

Actually Java is the most used programming language according to TIOBE. The TIOBE Programming Community index is an indicator of the popularity of programming languages. The ratings are based on the number of skilled engineers world-wide, courses and third party vendors.

3.2 Java choice

The software presented in this thesis work is completely written in Java. The choice of the programming language was driven by several considerations. These include the following:

- The language should be widely supported; this to avoid the case of many valid aircraft design applications and libraries that became obsolete due to the aging of the programming language used to build them;
- The language is object oriented;
- The language should promote the use of open source libraries, especially for I/O tasks and for complex mathematical operations;
- The language and the companion **Integrated Development Environment (IDE)** should provide a widely supported **Graphical User Interface (GUI)** framework and a **GUI visual builder**;
- The language should support and promote modularity.

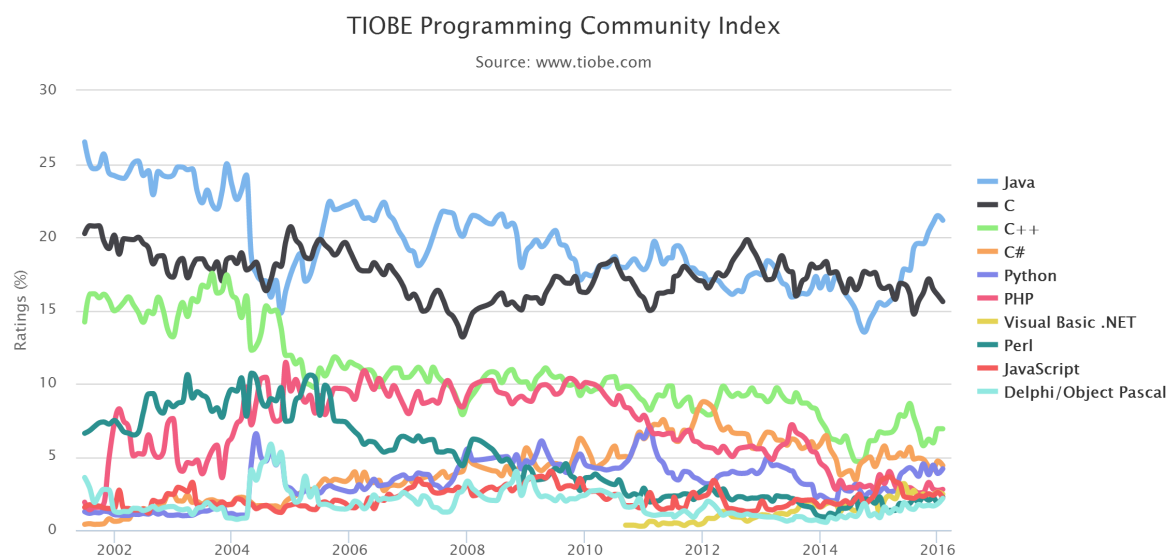


Figure 3.1: Programming Language popularity trade.

The Java programming language meets all these requirements: it is backed by Oracle and by a huge community of developers so it is continuously updated. Also, advanced and

free IDEs (such as Eclipse) allow programmers to streamline and simplify the development process. In particular, the Eclipse IDE and the SWT/JFace libraries have been chosen to develop JPAD and its GUI. Being Java a pure object oriented programming language, it greatly encourages and simplifies modularization. Each module (package) can be programmed quite independently so that it is relatively easy to divide the work among several programmers. This is essential since the amount of classes and calculations needed to abstract, manage and analyze the entire aircraft is very large (presently the whole project counts more than 56000 lines of code). For such a reason the establishment of common practices and the adherence to fundamental principle of software development (Don't Repeat Yourself, Separation of Concerns, Agile software development) are equally important. An important design requirement of ADOpt is related to its interoperability with other engineering analysis tools. In fact, the application can be easily integrated into a comprehensive aircraft optimization cycle. This is made possible because ADOpt can be launched both in GUI and command line mode. Much care has been given to input/output and configuration files to increase the possible uses of the software.[28]

Chapter 4

Work Object

*If the facts don't fit the theory,
change the facts.*
– Albert Einstein

4.1 Introduction

In JPAD it is possible to read an .XML file as input or generate an object whose data are written in the code. Both in the first and in the second case all needed variables are initialized with data relating the chosen aircraft. The difference between these two methods is that using an .XML file, user can define its own aircraft having a clear view about the needed data useful for the analysis.

Contrariwise in order to perform a test of program functionality, to use a default aircraft is the most simple way to generate a work object.

4.2 Input data from .XML file

XML is a file extension for an *Extensible Markup Language (XML)* file format which is a markup language that defines a set of rules for encoding documents in a format which is both human-readable and machine-readable. Although the design of XML focuses on documents, it is widely used for the representation of arbitrary data structures such as those used in web services. It is defined “Markup Language” due to the use of tags that describes the content. XML is considered extensible because the markup symbols are unlimited and self-defining. So it is possible to use a personal tag for each data. In this way to read an .XML file results relatively simple.[5]

The key concepts of an .XML File Format are the followings:

- markup symbol (tag)
- attribute
- tree structure

As mentioned, each part of the test is contained between an opening **markup symbol** and an end markup symbol that expressed the meaning of the text.

```
<name>Test XML</name>
```

Figure 4.1: Use of markup symbols in XML language.

In addition to tag name, the markup symbols may contain also some **attributes** that introduce more informations such as the unit of measure.

```
<tag attribute1='value' attribute2='value'> text </tag>
```

Figure 4.2: Use of attributes in XML language.

An .XML file has a tree structure in which external knots that branch into internal knots.

In order to read an XML file it is necessary, first of all, to give the file path. The class JPADXMLReader opens the file and the methods of the class MyXMLReaderUtils read the useful data from the XML having the tag path as input. It is possible to read data as Amount, namely with units of measurement or as double. The unit of measurement is written in the attributes of data in XML file.

Likewise it is possible to write output data on XML file using JPADDatWriter class. First of all it is necessary to define and build the xml tree structure. After each variable is associated with a name that is the markup symbol of the XML file.

4.3 Default Aircraft

At the moment it is possible to define two different aircrafts in order to test the functionality of the application: **ATR-72** and **B747-100B**.

The **ATR 72** is a twin-engine turboprop made by the French-Italian aircraft manufacturer ATR entered service in 1989. It was developed as a variant of the ATR 42 with a 4.5 m stretched fuselage. The ATR 72 was developed from the ATR 42 in order to increase the seating capacity (48 to 66 in standard configuration) by stretching the fuselage, increasing the wingspan, adding more powerful engines, and increasing fuel capacity by approximately 10 percent. It has been typically employed as a regional airliner, although other roles have been performed by the type such as corporate transport, cargo aircraft and maritime patrol aircraft. [3]

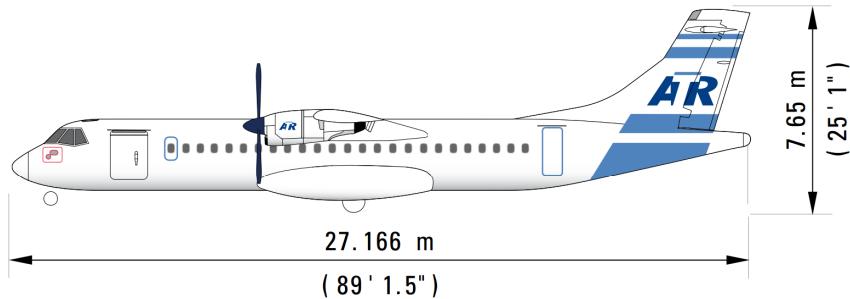


Figure 4.3: ATR 72. Side view.

The **Boeing 747-100B** is a four-engined long-range widebody commercial jet airliner and cargo aircraft produced by the American manufacturer Boeing Commercial Airplanes. It has

a capacity of maximum 480 passengers in a partial double deck configuration. The Boeing 747 is also known as Jumbo Jet. The basic B747-100 entered service with Pan American On January 15, 1970.

One of the reasons to create the 747 was reductions in airfares with a consequent increase of passenger traffic[4]. The original version of the 747 had two and a half times greater capacity than the Boeing 707, one of the common large commercial aircraft of the 1960s and it was the largest passenger carrier from 1970 until the introduction of Airbus A380. The Boeing 747 has two aisles and four wing-mounted engines. The upper deck is its distinctive "hump" along the forward part of the aircraft. It provides space for a lounge or extra seating. The raised cockpit allows front loading of cargo on freight variants.

The 747-100B model was developed from the 747-100SR. This configuration has a typical 452 passengers and unlike the original 747-100, the 747-100B was offered with Pratt & Whitney JT9D-7A, General Electric CF6-50, or Rolls-Royce RB211-524 turbofan engines.

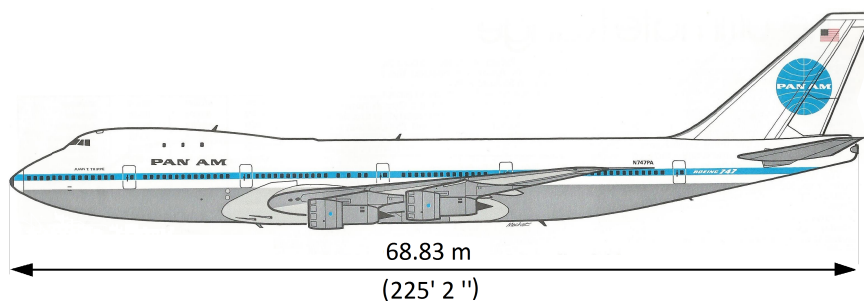


Figure 4.4: Boeing 747-100B. Side view.

4.3.1 How is made a default Aircraft

In order to define a Default Aircraft in a test class, and use it to check the functionalities of the application, it is necessary to follow some steps. First of all it is necessary to initialize the working directory tree using the method `initWorkingDirectoryTree` of `MyConfiguration` class located in `JPADConfigs` package that initializes the working directory tree and fills the map of folders. This step is required in order to create the following default folders that are necessary for the right behavior of the code:

- Database directory
- Input directory
- Output directory

Using `MyConfiguration` class is possible to point at a specific folder, like the input or output directory, with the static method `getDir`. This is a crucial step that must be executed at the beginning of every test. To set the working directory with the useful folders, is necessary to call the function `initWorkingDirectoryTree()` at the beginning of each test. The function creates all necessary folders. Moreover the function has been overloaded and it can be even called with a variable number of arguments (`initWorkingDirectoryTree(String...str)`). These strings are the directory strings in `MyConfiguration` class. The second step is the creation of an `Aircraft` object choosing between the ones grouped into a dedicated `Enum`, named `AircraftEnum`. After it is possible to create an `Aircraft` using the method `createDefaultAircraft` from `Aircraft` class. This method defines a new `Aircraft` object and invokes another `Aircraft`'s method that creates the components using default data. In the method `createDefaultAircraft` there is a calling to the

builder of Aircraft class that initializes the objects of the classes that perform calculations. At this step all the components of the aircraft are created. It is possible also to define new airfoils for the aircraft or change some data from the existing.

Afterwards it is necessary to set the operating conditions such as the number of Mach of analysis or altitude. Each default aircraft has a set of default conditions but the user could change them.

In order to manage all the aircraft related analyses it is necessary to define an object of the class ACAnalysisManager. Similarly to the aircraft, an analysis manager exists also for the wing that is an object of the LSAerodynamicManager class.

The next step is to define and assign the needed databases. This will be explained in detail in the next section. Finally it is possible to do analysis.

Listing 4.1 Generation of default aircraft

```
public static void main(String[] args) {

    // -----
    // Define directory
    // -----
    MyConfiguration.initWorkingDirectoryTree();

    // -----
    // Generate default Aircraft
    // -----
    Aircraft aircraft = Aircraft.createDefaultAircraft(AircraftEnum..B747_100B);
    LiftingSurface theWing = aircraft.get_wing();

    // Default operating conditions
    OperatingConditions theConditions = new OperatingConditions();

    // -----
    // Define an ACAnalysisManager Object
    // -----
    ACAnalysisManager theAnalysis = new ACAnalysisManager(theConditions);
    theAnalysis.updateGeometry(aircraft);

    // -----
    // Define an LSAerodynamicsManager Object
    // -----
    LSAerodynamicsManager theLSAnalysis = new LSAerodynamicsManager (
        theConditions,
        theWing,
        aircraft
    );

    // -----
    // Setup database(s)
    // -----

    theLSAnalysis.setDatabaseReaders(
        new Pair(DatabaseReaderEnum.AERODYNAMIC,
            "Aerodynamic_Database_Ultimate.h5"),
        new Pair(DatabaseReaderEnum.HIGHLIFT,
            "HighLiftDatabase.h5")
    );

    // -----
    // Do analysis
    // -----

    theAnalysis.doAnalysis(aircraft,
        AnalysisTypeEnum.AERODYNAMIC);
}
```

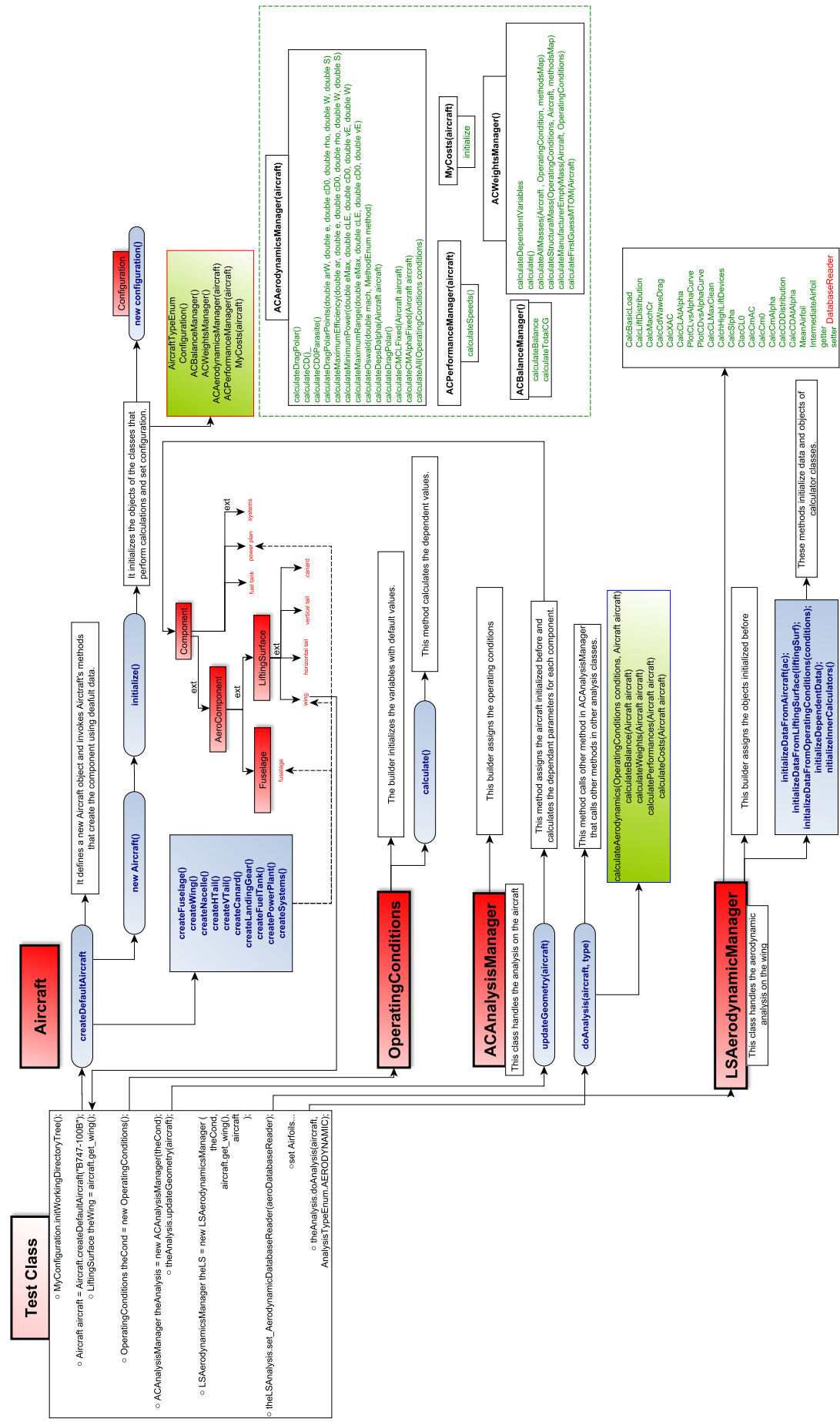


Figure 4.5: Flow chart of the creation of default Aircraft.

4.3.2 How is made a default Wing

Similary to the default aircraft it is possible to define a default wing. This is very useful if the user wants to make an analysis only on a wing. In this case it is necessary to define the origin of the **Local Reference Frame (LRF)** in **Body Reference Frame (BRF)** and the coordinates of the **Gravity Center (GC)**.

Contrary to the case of the aircraft, for an isolated wing it is not necessary to define a fuselage in order to create a **Lifting Surface** object, but there is an overload of the builder that does not need a fuselage as input. In this case the exposed surface is calculated as the surface of the wing.

Listing 4.2 Generation of an isolated Wing

```
public static void main(String[] args) {

    // Assign all default folders
    MyConfiguration.initWorkingDirectoryTree();

    // -----
    // Coordinates of LRF
    // -----

    double xAw = 11.0; //meter
    double yAw = 0.0;
    double zAw = 1.6;
    double iw = 0.0;

    // -----
    // Generate default Wing
    // -----

    LiftingSurface theWing = new LiftingSurface(
        "Wing", // name
        "Data_from_AC_ATR_72_REV05.pdf",
        xAw, yAw, zAw, iw,
        ComponentEnum.WING
    );

    theWing.calculateGeometry();
    theWing.getGeometry().calculateAll();

    // -----
    // Center of Gravity
    // -----

    double xCgLocal= 1.5; // meter
    double yCgLocal= 0;
    double zCgLocal= 0;

    CenterOfGravity cg = new CenterOfGravity(
        Amount.valueOf(xCgLocal, SI.METER), // coordinates in LRF
        Amount.valueOf(yCgLocal, SI.METER),
        Amount.valueOf(zCgLocal, SI.METER),
        Amount.valueOf(xAw, SI.METER), // origin of LRF in BRF
        Amount.valueOf(yAw, SI.METER),
        Amount.valueOf(zAw, SI.METER),
        Amount.valueOf(0.0, SI.METER), // origin of BRF
        Amount.valueOf(0.0, SI.METER),
        Amount.valueOf(0.0, SI.METER)
    );

    cg.calculateCGinBRF();
    theWing.set_cg(cg);
    theWing.set_aspectRatio(6.0);

    // Default operating conditions
    OperatingConditions theOperatingConditions = new OperatingConditions();
    theOperatingConditions.set_alphaCurrent(Amount.valueOf(2.0, NonSI.DEGREE_ANGLE)
```

```

// -----
// Define an LSAerodynamicsManager Object
// -----

LSAerodynamicsManager theLSSimulation = new LSAerodynamicsManager (
    theOperatingConditions,
    theWing
);

// -----
// Setup database(s)
// -----

theLSSimulation.setDatabaseReaders(
    new Pair(DatabaseReaderEnum.AERODYNAMIC,
        "Aerodynamic_Database_Ultimate.h5"),
    new Pair(DatabaseReaderEnum.HIGHLIFT, "HighLiftDatabase.h5")
);

// -----
// Assign Airfoil(s) ...
// -----

// Define airfoilRoot...

// -----
// Set Airfoil(s)
// -----

List<MyAirfoil> myAirfoilList = new ArrayList<MyAirfoil>();
myAirfoilList.add(0, airfoilRoot);
myAirfoilList.add(1, airfoilKink);
myAirfoilList.add(2, airfoilTip);
theWing.set_theAirfoilsList(myAirfoilList);
theWing.updateAirfoilsGeometry();
theLSSimulation.initializeDependentData();

}

```

4.4 Database in JPAD

In JPAD it is possible to consult external databases in .h5 format. **HDF 5** (Hierarchical Data Format Release 5) is a data file format designed by the *National Center for Supercomputing Applications* (NCSA) to assist users in the storage and manipulation of scientific data across different operating systems and machines.

To obtain the useful data in JPAD interpolating functions are used. These functions can be of one, two or three dimensions and read data from graphics that have been digitized previously. Starting from these digitalizations, databases in .h5 format are built. Reading data from databases is entrusted to methods of classes in the `database` package.

In order to read these databases, and obtain the useful data, it is necessary to define an object of the database reading class and associate it with the object of analysis.

This is a crucial step to read correctly the external data. In fact JPAD allows to work with an aircraft object or only with an isolated lifting surface object. Aircraft is usually composed of a fuselage, lifting surfaces, nacelle and power plant. Furthermore, Aircraft and Wing are associated with classes of calculation like `LSAerodynamicManager` or `ACAnalysisManager`. So it is necessary that these databases are also visible from these classes.

So because both in the aircraft and in the wing there is a lifting surface object, databases relative to wing are associated to `LSAerodynamicManager`.

4.4.1 Setup database

Here the database path is created and associated to object that interpolates the required data from the .h5 file using a MyInterpolatingFunction object. After this it is possible to access the double value of the interpolating function using the standaloneutils method called value.

Now the procedure to assign the database is different if is used an Aircraft object or a Wing object.

4.4.2 Assign database using an Aircraft object

In order to assign correctly the database and associate it to all analysis management is necessary to practise the following order.

1. Define an Aircraft Object.

This command associates to the Aircraft an object that defines the aerodynamic. Defining an Aircraft object is defined the Wing, that is a LiftingSurface object.

2. Define an ACAnalysisManager object.

All the aircraft computations are managed by this class.

3. Define an LSAerodynamicManager object.

All the lifting surfaces computations are managed by this class.

4. Associate database to LSAerodynamicManager.

5. Eventually do analysis.

4.4.3 Assign database using a Wing object

Using a Wing object it is not necessary to define a manager for Aircraft aerodynamic analysis. So the step to follow are the same of aircraft starting from the third.

1. Define a Wing Object.

2. Define an LSAerodynamicManager object.

3. Associate database to LSAerodynamicManager.

The definition of an isolated Wing is explained in the relative section.

Listing 4.3 Assign database using an Aircraft object

```
// -----
// Setup database(s)
// -----
theLSAnalysis.setDatabaseReaders(
    new Pair(DatabaseReaderEnum.AERODYNAMIC,
        "Aerodynamic_Database_Ultimate.h5"),
    new Pair(DatabaseReaderEnum.HIGHLIFT,
        "HighLiftDatabase.h5")
);
```

The databases are assigned to LSAerodynamic using a method of this class. This method accept as input a variable number of Pair objects. Using Pair objects it is possible to assign, for each database, both name and type.

Listing 4.4 setDatabaseReaders method

```
public void setDatabaseReaders(Pair... args) {
    String databaseFolderPath = MyConfiguration.getDir(FoldersEnum.DATABASE_DIR);

    for (Pair a : args) {
        DatabaseReaderEnum key = (DatabaseReaderEnum)a.getKey();
        String databaseFileName = (String)a.getValue();

        switch (key) {
            case AERODYNAMIC:
                _aerodynamicDatabaseReader =
                    new AerodynamicDatabaseReader(
                        databaseFolderPath,
                        databaseFileName);
                listDatabaseReaders.add(_aerodynamicDatabaseReader);
                break;

            case HIGHLIFT:
                _highLiftDatabaseReader =
                    new HighLiftDatabaseReader(
                        databaseFolderPath,
                        databaseFileName);
                listDatabaseReaders.add(_highLiftDatabaseReader);
                break;
        }
    }
}
```

4.4.4 User's guide

In order to execute some analysis in JPAD it is necessary, first of all, to define an analysis object in the Test class. The method `createDefaultAircraft` creates a new aircraft and the object that composes it. This method also populates the data of aircraft with default value corresponding to ATR-72 or Boieng 747-100B. Moreover the method `createDefaultAircraft` calls another method in Aircraft class: `initialize` that initializes the objects of the classes that perform calculations.

The purpose of this structure is to have only a way to assign the databases at an aircraft. Inasmuch as the wing is always present, the chosen strategy is to assign the database to the aerodynamic manager of the wing.

In order to bring to use the database also for the aircraft calculation, it is assigned at the aerodynamic manager of the aircraft in the method called `doAnalysis`.

At the same time `LSAerodynamicManager` sets itself as aerodynamic in the wing object. So it is possible to call the database using equally the following codes:

- `theWingObject.getAerodynamics.get_Database;`
- `theAircraftObject.get_theAerodynamic.get_Database;`
- `theLSManagerObject.get_Database;`
- `theACManagerObject.get_Database;`

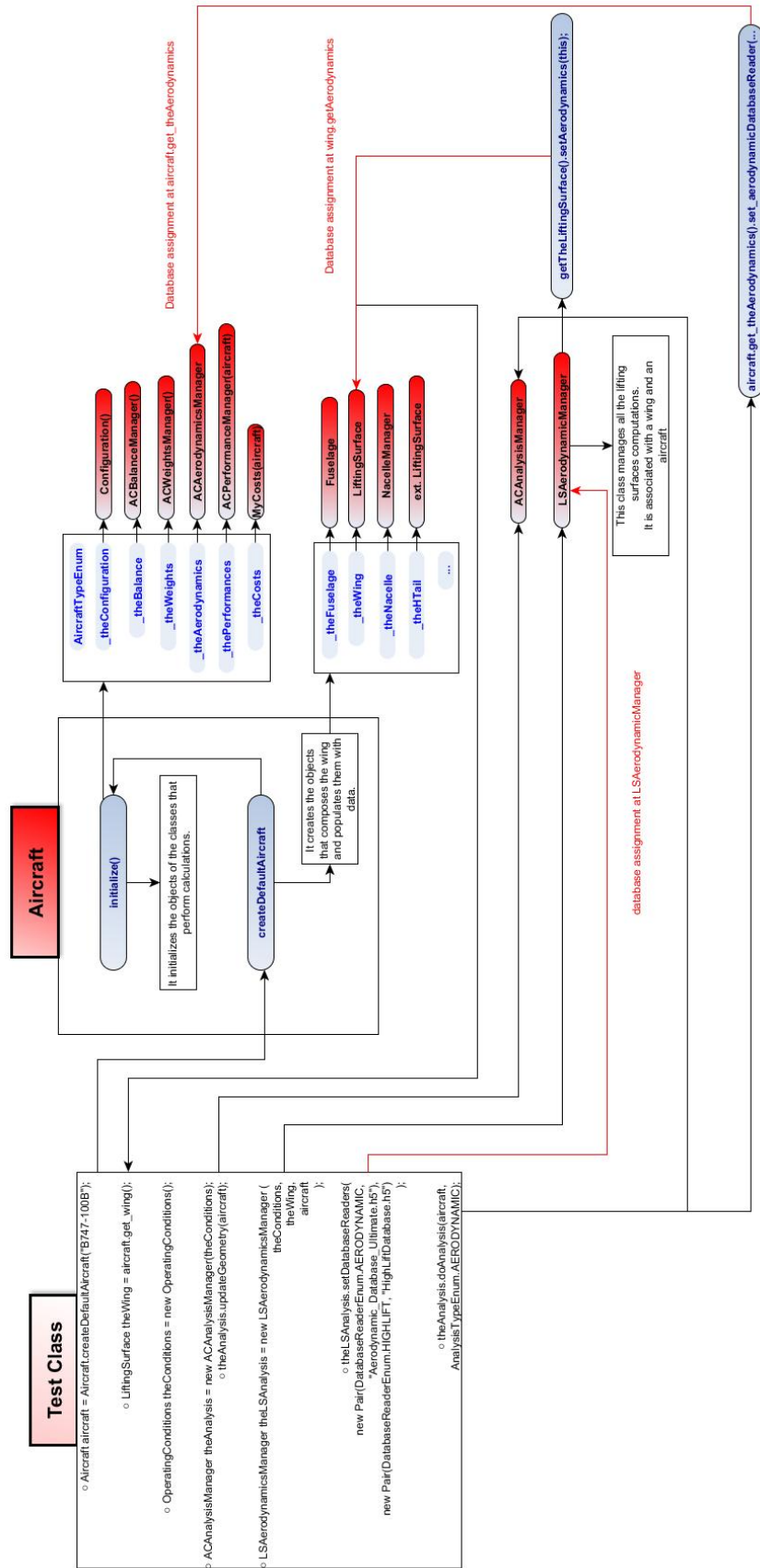


Figure 4.6: Flow chart of database assignment.

Part III

Functionality Overview

Chapter 5

Work Object Data

*It is not certain
that everything is uncertain*
– Blaise Pascal

All the following analysis will be carried out using a default aircraft. This choice is made in order to avoid the collection and validation data phase for each analysis and make focus on the results. As mentioned, there are two default aircraft in the code: ATR-72 and Boeing 747-100B whose data are shown in the table below.

All the analyses that follow, refer to the data presented in this chapter and those derived from them .

	ATR-72	B747-100B
Operating Conditions		
Altitude	6000.0000 m	10 000.0000 m
Cruising Mach number	0.4300	0.8300
Weights		
Maximum Take-Off Mass	23 063.5790 kg	354 991.5060 kg
Operating Empty Mass	12 935.5790 kg	153 131.9860 kg
Maximum Fuel Mass	5000.0000 kg	147 409.5200 kg
Maximum number of passengers	72	550
Fuselage		
Length	27.1660 m	68.6300 m
Diameter	2.7561 m	6.7934 m
Fineness Ratio	9.8566	10.1025
Wing		
Surface	61.0000 m ²	511.0000 m ²
\mathcal{R}	12.0000	6.9000
Span	27.055 49 m	59.3792 m
Taper Ratio	0.5450	0.2840
Root Chord	2.9186 m	14.6152 m
Mean Aerodynamic Chord	2.3198 m	9.6913 m
Sweep _{LE}	2.8390°	38.4290°

continued on next page

(continued from previous page)

	ATR-72	B747-100B
Sweep _{C/4}	1.3997°	35.4999°
t/c_{\max}	0.1675	0.1292
C_{D0}	0.03170	0.01820
Oswald Factor	0.7585	0.6277
Airfoil type	Conventional	Modern Supercritical
Horizontal Tail		
Surface	11.7300 m ²	136.6000 m ²
\mathcal{R}	4.5550	3.5700
Span	7.3095 m	22.083 07 m
Taper Ratio	0.5700	0.2650
Root Chord	2.044 30 m	9.7798 m
Mean Aerodynamic Chord	1.6450 m	6.8835 m
Sweep _{LE}	3.4410°	38.2250°
Sweep _{C/4}	0.0000°	32.0003°
t/c_{\max}	0.1500	0.1500
Vertical Tail		
Surface	12.4800 m ²	77.1000 m ²
\mathcal{R}	1.6600	1.3400
Span	4.5515 m	10.1643 m
Taper Ratio	0.3200	0.3300
Root Chord	4.1544 m	11.4065 m
Mean Aerodynamic Chord	2.9323 m	8.2285 m
Sweep _{LE}	40.5485°	53.9913°
Sweep _{C/4}	28.5998°	45.0001°
t/c_{\max}	0.2227	0.2245
Power Plant		
Static Thrust (per engine)	7700.0000 N	204 000.0000 N
Engines Number	2	4
Engines type	Turboprop	Turbofan
BRR	0.0000	5.0000
η_p	0.85	0.00

Table 5.1: ATR-72 and B747-100B input data

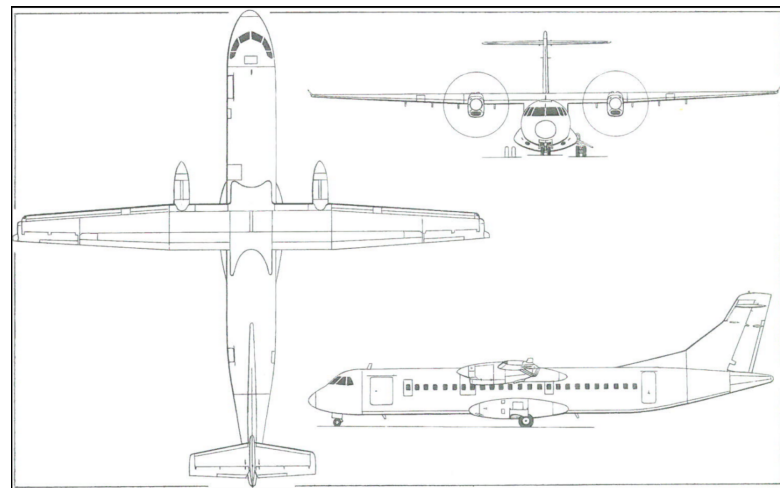


Figure 5.1: ATR-72 views – Jane's All the World's Aircraft 2004-2005.

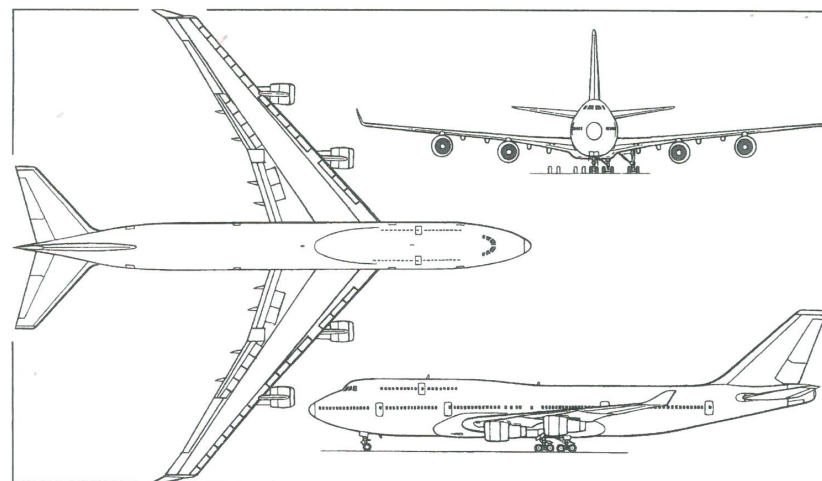


Figure 5.2: B747-100B views – Jane's All the World's Aircraft 2004-2005.

Chapter 6

Wing Lift Characteristics

*C'è qualcuno che può rompere il muro del suono,
mentre tutto il mondo si commenta da solo.*

– L. Ligabue

Any body in motion in a fluid presents a result of force acting on it, which can be decomposed in two components:

- A **Lift** acting normal to the Velocity direction and is positive upward.
- A **Drag** acting in the opposite direction to the airspeed vector.

The lifting surfaces of an airplane are designed to generate lift exceeding their drag, in order to obtain a positive efficiency.

In this chapter it will be explained how it is possible to evaluate the complete lift coefficient curve of a wing, both in its linear trait and non linear.

The lift coefficient is a dimensionless number used to model all of the complex dependencies of shape, inclination, and some flow conditions on lift. The lift coefficient also contains the effects of air viscosity and compressibility that are molded respectively with the Reynolds and Mach number.

6.1 Theoretical background

In order to achieve the complete curve of coefficient list it is necessary to obtain the following parameters:

1. Zero-Lift Angle
2. Lift Coefficient slope
3. End of Linearity Angle
4. Maximum Lift Coefficient
5. Stall Angle of attack

Following it will be explained the theory behind how these contributions have been made.

6.1.1 Zero-Lift Angle and Lift Coefficient Slope

In order to evaluate the linear trait of the wing lift curve, it is been used the Nasa-Blackwell method.

The **Nasa-Blackwell** is a numerical method for calculating the subsonic load distribution for arbitrary lifting surface arrangements at a fixed angle of attack. The method is suitable for swept wings, non-planar wings, wing with pylons and/or end-plates; it can be also used to study the aerodynamic interaction of the wing and the horizontal tail. The method has been implemented because its results, as shown in the report, were in good agreement with the experimental results. The lifting surfaces are divided in several rectangular horse-shoe vortices along the span; one horseshoe vortex along the chord is used, that is, the midpoints of the vortices are placed only at points along the quarter-chord lines. An equal number of control points are located along the three-quarter-chord lines. The velocity from the total vortex system is equated to the component of free-stream velocity normal to the lifting surface chord at each control point. Application of this tangent-flow boundary condition for a symmetrical loading provides a set of N simultaneous equations in the N unknown circulation strengths. Solution of this set of equations provides the loading distributions over the lifting surfaces. Mach number effect is introduced through a Prandtl-Glauert correction. Further details can be found in [12].

In this way the Zero Lift angle it is calculated using the integral of the load distribution and the linear trait slope starting from the value of CL at $\alpha = 0^\circ$ and $\alpha = 2^\circ$.

$$CL_\alpha = \frac{CL|_2 - CL|_0}{\Delta\alpha} \quad (6.1)$$

In JPAD it is possible also evaluating these two contributes using different methods. For the evaluation of the α_{0L} it is possible to use a method of the class `CalcAlpha0L`, a nested class in `LSAerodynamicManager`. Using these method, the zero-lift angle is calculated with the following formula, where ϵ_T is the twist angle:

$$\alpha_{0L} = \frac{1}{S} \int_{-\frac{b}{2}}^{\frac{b}{2}} c(y)[\alpha_0(y) - \epsilon_T(y)] dy \quad (6.2)$$

This formula is applied to the exposed wing. When a default aircraft is defined, during the creation of components, is calculated the exposed wing. This is the wing outside of the fuselage. It starts at semi-diameter of fuselage and its root airfoil is the airfoil of wing at this station calculated by the method `calculateIntermediateAirfoil`.

In order to evaluate the lift coefficient linear slope it is possible to use different method belonging to `CalcCLAlpha` class. The first one use the Polhamus formula which is valid for arbitrary aspect ratios and sweep angles in subsonic flow:

$$CL_\alpha = \frac{2\pi AR}{\left\{ 2 + \sqrt{\frac{AR^2\beta^2}{k^2} \left(1 + \frac{\tan^2(\Lambda_{\frac{c}{2}})}{\beta^2} \right)} + 4 \right\}} \quad (6.3)$$

Thus CL_α is a function of wing aspect ratio, mid-chord sweep angle $\Lambda_{\frac{c}{2}}$, Mach number, and airfoil section (defined parallel to the free stream) lift curve slope. The factor K in the equation is the ratio of the experimental two-dimensional lift curve slope.

Alternately it is possible to use the Anderson formula for swept wing, compressible and

subsonic flow:

$$CL_\alpha = \frac{Cl_\alpha \cos \Lambda_{\frac{c}{2}}}{\sqrt{1 - M^2 \cos^2 \Lambda_{\frac{c}{2}} + \left[\frac{Cl_\alpha \cos \Lambda_{\frac{c}{2}}}{\pi R} \right]^2 + \frac{Cl_\alpha \cos \Lambda_{\frac{c}{2}}}{\pi R}}} \quad (6.4)$$

6.1.2 End of Linearity angle of attack

The angle of end linearity is calculated using the characteristics of the mean airfoil of the wing. This is obtained through the influence area of the airfoils as shown in fig. 6.1.

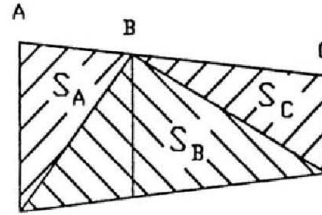


Figure 6.1: Influence area of the sections for finite wing.

Then is possible to calculate the influence coefficients.

$$K_i = \frac{2S_i}{S} \quad (6.5)$$

The mean parameters can be obtained from:

$$\bar{x} = x_1 K_1 + x_2 k_2 + x_3 k_3 \dots \quad (6.6)$$

In particular, for a wing defined by three airfoils, the end of linearity angle of attack is obtained from the following equation:

$$\alpha^* = \alpha_1^* K_1 + \alpha_2^* k_2 + \alpha_3^* k_3 \quad (6.7)$$

6.1.3 Maximum Lift Coefficient

In order to evaluate the maximum lift coefficient the Stall Path Method has been used. The load distribution is calculated using Nasa-Blackwell method.

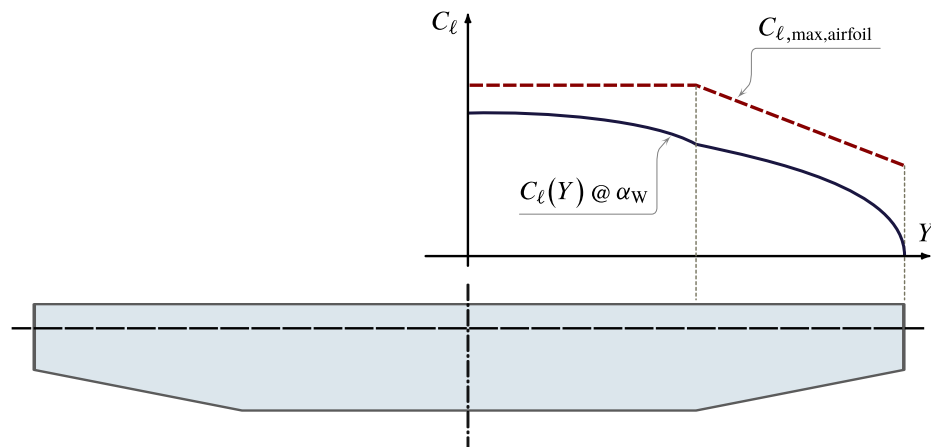


Figure 6.2: Determination of wing lift distribution and Cl distribution of airfoils.

The practiced procedure is the following:

1. For each value of an Alpha array the load distribution is calculated using the NasaBlack method. The distribution of Cl_{max} is known. fig. 6.3.
2. At $\alpha = \alpha_j$ the load distribution curve intersects for the first time the Cl_{max} curve of the airfoils. fig. 6.3.
3. For each $y > y_1$, along y axis (where y_1 is the station of first intersection) is evaluated the difference between CL_{wing} and Cl_{max} . fig. 6.4.
4. $\Delta\alpha$ is evaluated until the maximum difference between CL_{wing} and Cl_{max} is smaller than the required accuracy. Actually the accuracy is 0.0001.

The evauation of $\Delta\alpha$ is not simple.

After finding the first value of intersection between CL_{wing} and Cl_{max} a new α is evaluated. The first value used for the optimization is

$$\Delta\alpha = \alpha_j - \alpha_{j-1}$$

$$\alpha_{new} = \alpha_j - \frac{\Delta\alpha}{2}$$

$$\alpha_{old} = \alpha_j$$

For the following step if there isn't a point of intersection at α_{new} the new value of α is, for the step $j + 1$:

$$\Delta\alpha = |\alpha_{j-1} - \alpha_j|$$

$$\alpha_{new} = \alpha_j + \frac{\Delta\alpha}{2}$$

$$\alpha_{old} = \alpha_j$$

Instead, if there is a point of intersection at α_{new} the new value of α is, for the step $j + 1$:

$$\Delta\alpha = |\alpha_{j-1} - \alpha_j|$$

$$\alpha_{new} = \alpha_j - \frac{\Delta\alpha}{2}$$

$$\alpha_{old} = \alpha_j$$

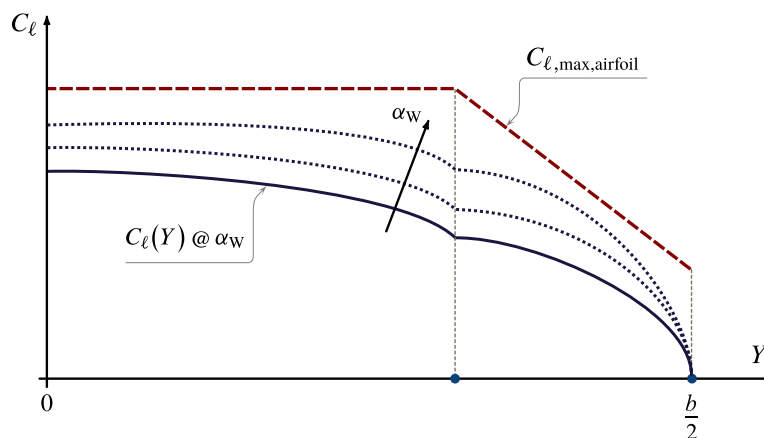


Figure 6.3: Determination of wing lift distribution and Cl distribution of airfoils.

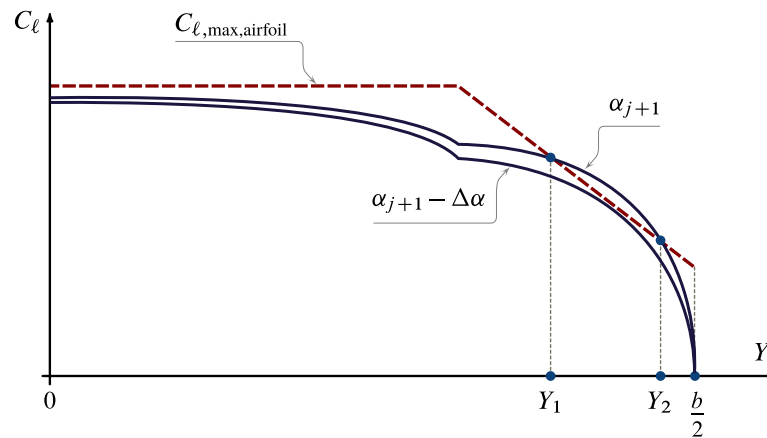
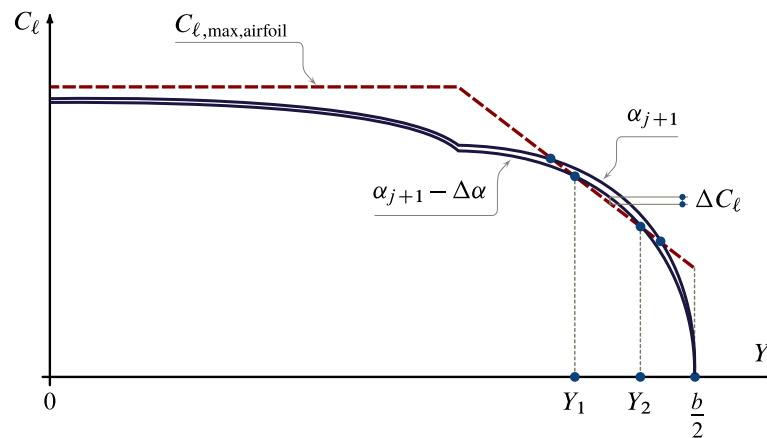
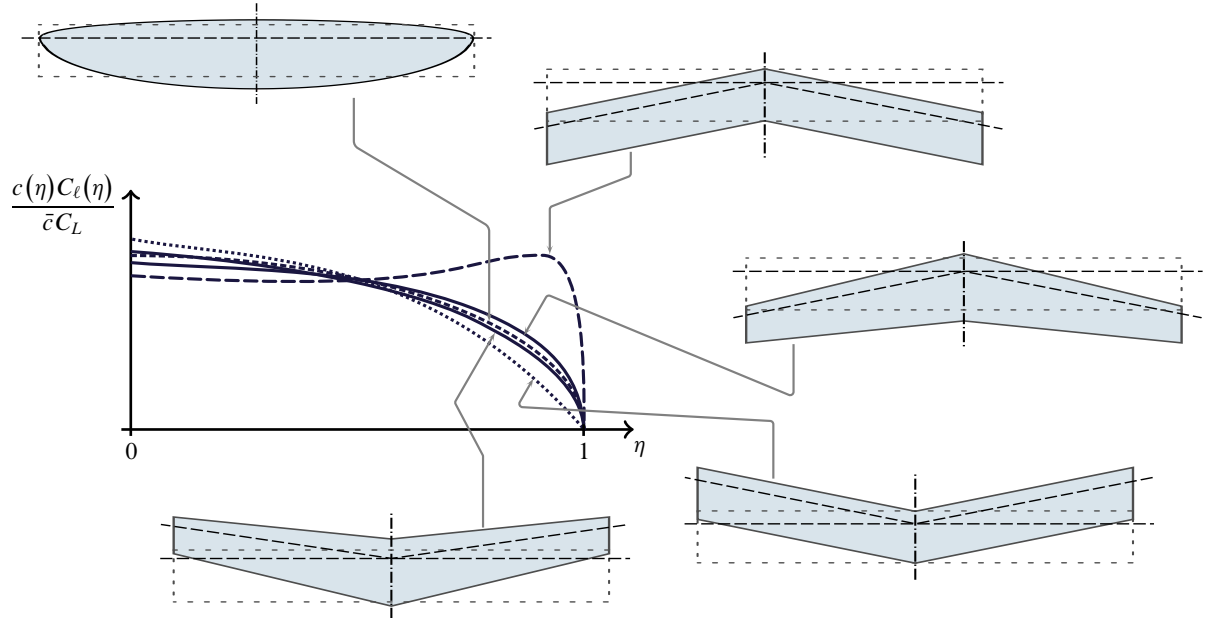
Figure 6.4: Intersection between CL_{wing} and $C_{l,max}$ curves.Figure 6.5: Determination of $\Delta\alpha$.

Figure 6.6: Wing Loading distribution.

6.1.4 Stall Angle of Attack

Nasa-Blackwell is an inviscid method for calculating the subsonic aerodynamic load distributions for arbitrary lifting-surface arrangements. This means that it does not see the non linear trait of the lift curve. So in correspondence of the value of $C_{L_{MAX}}$ calculated, the angle of attack obtained from the Nasa-Blackwell method is not correct because it is the maximum angle of attack that you would get if you reach the max C_L linearly.

So first it is evaluated the angle of attack at maximum lift coefficient through the linear trend of the lift line, then it's added to this angle the increment evaluated by the diagram in fig. 6.7, this is valid strictly for wing with high taper ratio without twist, with unique airfoil type and Mach number included between 0.2 and 0.6.

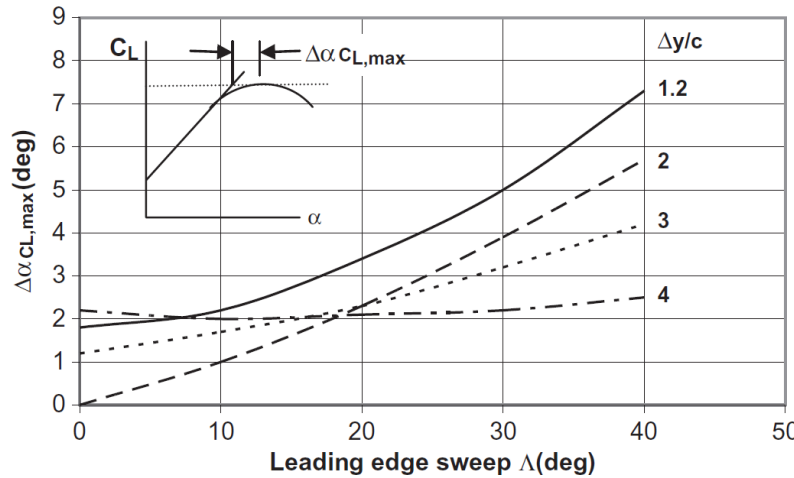


Figure 6.7: Diagram useful for evaluation of $\Delta\alpha$.

6.1.5 Construction of the curve

At this point all elements are available in order to draft the CL vs α curve. The linear trait is evaluated using the equation of straight line.

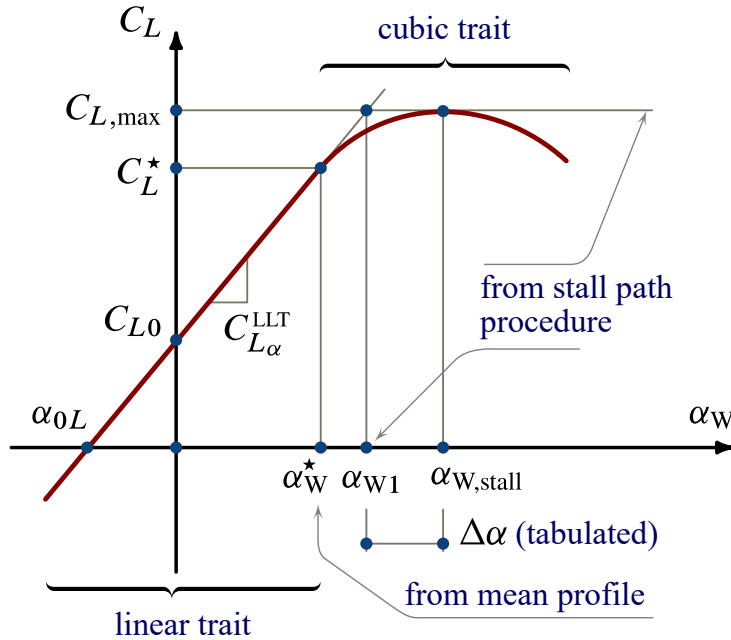
$$C_L = C_{L_\alpha} \alpha + C_{L_0} \quad (6.8)$$

In order to plot the non linear trait is used a cubic function. In fact in this zone we have four conditions:

- Pass to α^* , C_L^*
- The derivative in α^* , C_L^* is C_{L_α} for continuity
- Pass to α_{stall} , $C_{L_{MAX}}$
- The derivative in α_{stall} , $C_{L_{MAX}}$ is 0. Here there is the maximum of the curve.

So the system of equations is :

$$\begin{cases} C_L^* = a\alpha^{*3} + b\alpha^{*2} + c\alpha^* + d \\ C_{L_\alpha} = 3a\alpha^{*2} + 2b\alpha^* + c \\ C_{L_{MAX}} = a\alpha_{stall}^3 + b\alpha_{stall}^2 + c\alpha_{stall} + d \\ 0 = 3a\alpha_{stall}^2 + 2b\alpha_{stall} + c \end{cases} \quad (6.9)$$

Figure 6.8: Wing C_L vs α curve.

6.1.6 Mach number effects on Lift curve

The features of airflow depend heavily from the Mach number. These changes in airflow have a significant effect on the airplane lift. For airplanes that operate entirely within the subsonic speed range, there are no significant effects of compressibility of the air on the airplane lift. For airplanes that operate at high subsonic speeds in the transonic speed region, the airplane lift and drag curves will vary as the flight Mach number is increased due to the compressible nature of the air, so there is a family of lift curves one for each flight Mach number of interest.

The family of lift curves is characterized by an increase in the slope of the curve and decrease in maximum lift coefficient as the Mach number increased in the high subsonic region as shown in the fig. 6.9. The explanation of these Mach number effects on the lift curve has been derived from the theory of compressible flow, and confirmed by experimental data obtained in wind tunnels and from flight tests. It can be shown that, for an airplane at given angle of attack, the lift coefficient will increase with Mach number because the suction on the wing upper surface, and the pressures on the wing lower surface tend to grow with Mach number. [25]

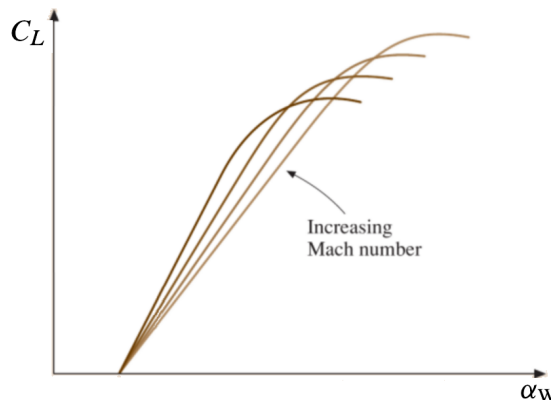


Figure 6.9: Mach number effects on Lift curve.

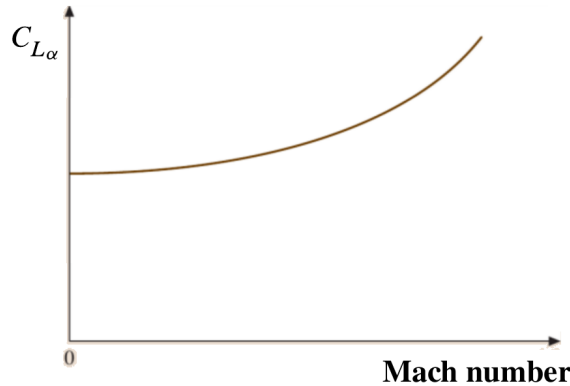


Figure 6.10: Mach number effects on Lift linear slope.

6.1.7 High Lift devices

The aircraft's performances at low speed are very important for their mission, in fact good high lift devices allow to land or take off on many airports, with their various runways.[16] To assure high lift in take-off and landing without varying weight and wing surface, it is varied the airfoil shape, for this reasons high-lift systems are used. High-lift systems are commonly defined as the devices that allow to increase the maximum lift coefficient of the aircraft and consequently to decrease the stalling speeds. A great variety of high lift devices exists, many of which are mechanically complex. The most simple systems change only the camber of the aerofoil. More complex concepts not only change camber but also extend the chord, opening up slots as they do so. [22]

High-lift devices can be classified in two main categories: trailing edge devices, or leading edge devices. TE devices are small aerofoil-like elements that are fitted at the trailing edge of the wing that are called flap, while at the LE as a slat.

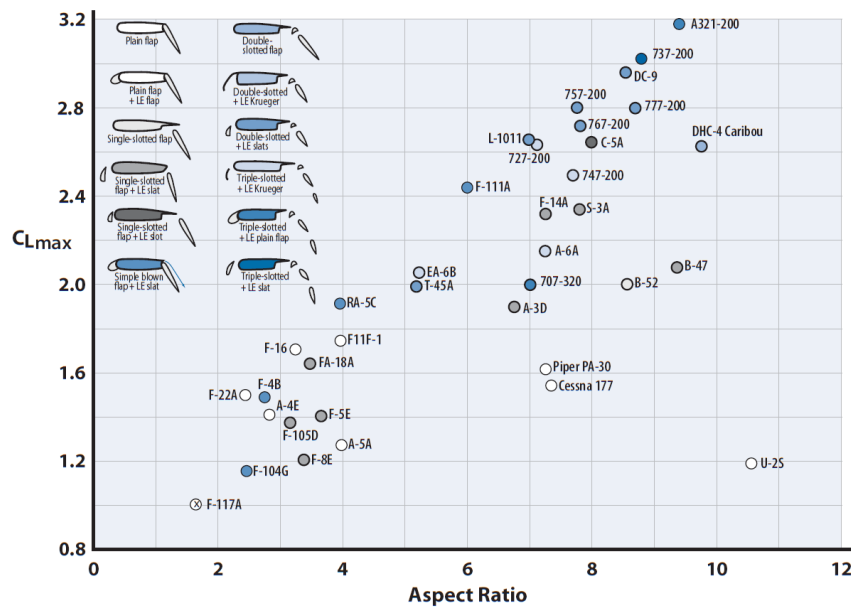


Figure 6.11: Different kind of High Lift devices and their effects.

In order to evaluate the new wing lift curve with flap and slat it is necessary to evaluate the contribution due to these devices starting from the clean C_L vs α curve. In particular these contributions on the lift curve are the following:

- ΔC_{L_0} flap
- $\Delta C_{L_{MAX}}$ flap
- CL_α flap
- $\Delta\alpha_{MAX}$ flap
- $\Delta C_{L_{MAX}}$ slat
- $\Delta\alpha_{MAX}$ slat

All of these parameters are calculated using formulas or graphs. For further details see [32]

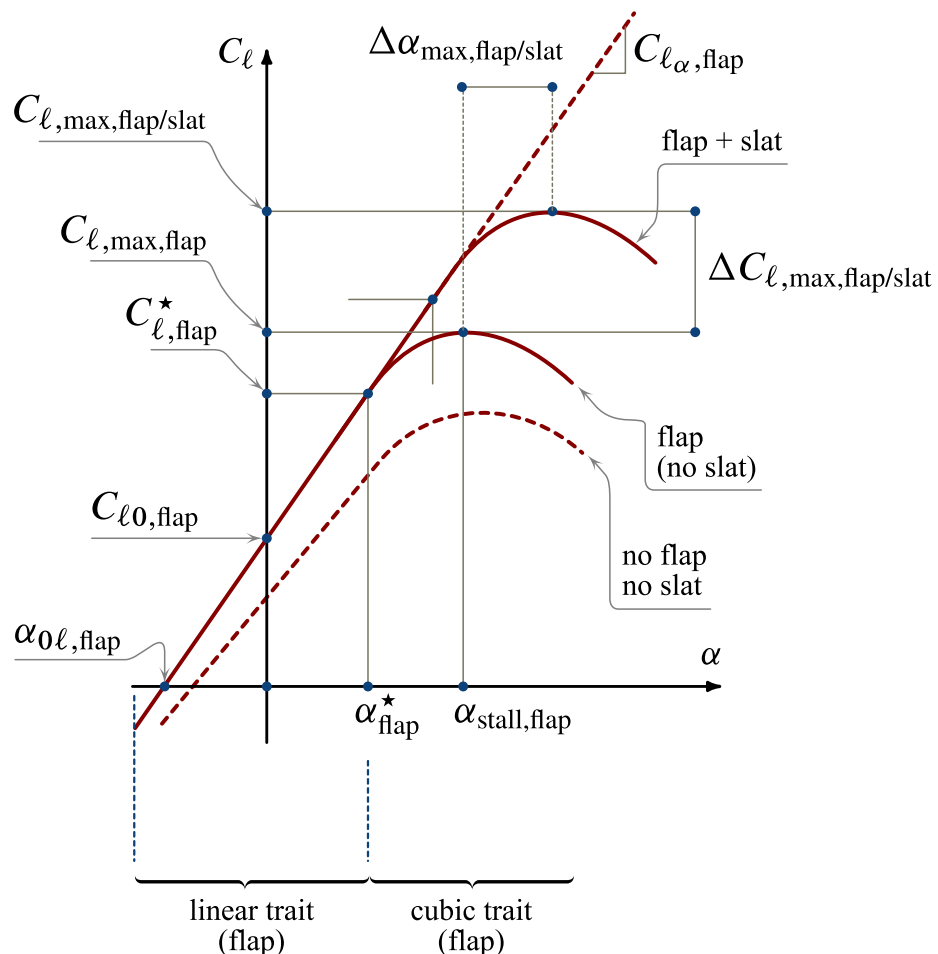


Figure 6.12: Wing C_L vs α curve for clean wing and with high lift devices.

6.2 Java Class Architecture

In this paragraph the implementation inside the JPAD library of the calculation of the wing lift characteristics will be described. In JPAD there are several methods relating to the calculation of lift or wing load, which are summarized in the table below, all contained in LSAerodynamicManager class. In order to have a clear organization of the class, the methods relating to the calculations of the same items are organized in nested classes.

CalcBasicLoad	This nested class contains a method that evaluate the basic load semi-spanwise using the Schrenk method.
CalcLiftDistribution	This nested class contains some methods that calculates the lift distribution semi-spanwise. It is possible to choose Schrenk method, the Nasa-Blackwell method and it is also possible to evaluate the lift distibution using 50 airfoil and evaluating for each of them the lift coefficient from the 2D lift curves.
CalcCLAtAlpha	Using a method of this class it is possible to evaluate the lift coefficient of a lifting surface at a given angle of attack. It is possible to use the following formulas: DLR equation, Anderson compressible subsonic equation and Nasa-Blackwell method. With the last method it is calculated both linear trait and non linear trait. In order to builds the non-linear trait a cubic interpolation is used.
CalcCLMaxClean	This class contains some method that evaluatex the maximum lift coefficient of a lifting surface without hig-lift devices. It' possible to use Phillips and Alley method or stall path method in which the load distribution in evaluated with Nasa-Blackwell method.
plotCLvsAlphaCurve()	This function plot CL vs Alpha curve of an isolated wing using 30 value of alpha between $\alpha = -10.0^\circ$ deg and $\alpha = \alpha + 2^\circ$.
CalcCLvsAlphaCurve	The methods of this class, calculate CL at alpha given as input. It uses values of field filled before. So in order to evaluate the lift coefficient with this class it is necessary to call other method before.
calcAlphaAndCLMax	This method calls all the needed method in order to evaluate the maximum lift coefficient and the stall angle.
CalcHighLiftDevices	This method calculates the effects of high-lift devices on the lift characteristics.
CalcCLAlpha	This class calculates the lift coefficient gradient of the whole lifting surface. It is possible to choose Polhamus formula, Anderson equation, or Nasa-Blackwell method where the lift coefficient gradient is evaluated from two value of lift coefficient.
CalcCL0	This class calculates C_{L_0} using Anderson formula.

Table 6.1: Methods for lift characteristcs of a lifting surface.

In order to evaluate the lift coefficient of a lifting surface and to obtain the lift curve it is

necessary, first of all, to define an object of `LSAerodynamicManager` class. This class holds all aerodynamic analysis methods available for a generic lifting surface. There are different constructors of this class depending on the presence of the aircraft. In fact in JPAD it is possible to analyze a complete aircraft or an isolated wing. In both cases it is necessary to give an object of `OperatingConditions` class as input parameter. After it is possible to define an object of the nested class `CalcCLAtAlpha` and then it is possible to use a method of this class in order to evaluate the lift coefficient. The process is shown in Fig.6.19.

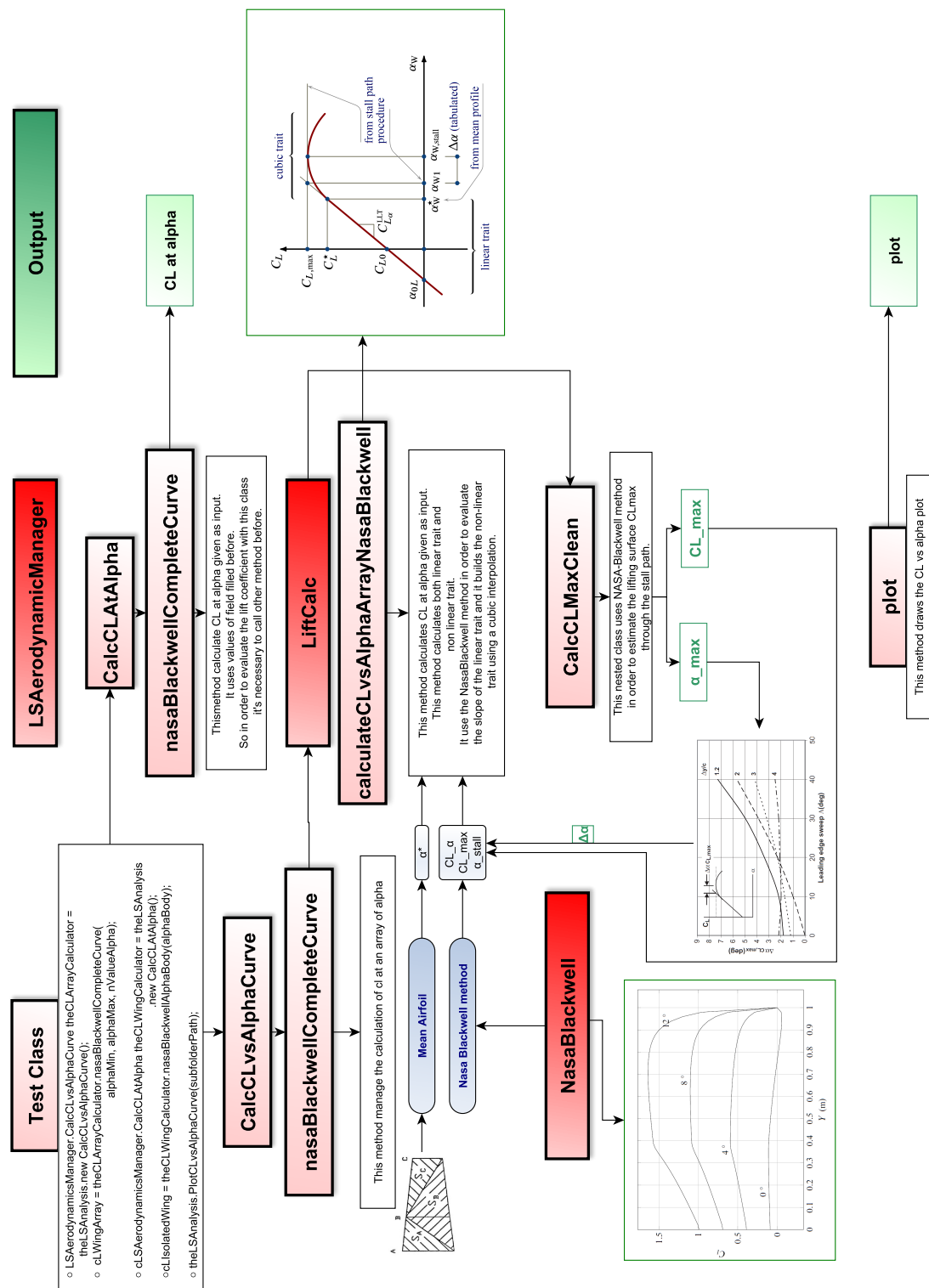


Figure 6.13: Flow chart of lift estimation classes.

6.3 Case Study

The last task to be done is to show an application of the calculation of lift characteristics of a lifting surface in order to validate the calculation performed as well as to give a useful example of use. In previous chapters two aircraft were introduced: ATR-72 and B747-100B. On these two aircrafts analyses were made, the results of which are shown below.

6.3.1 ATR-72

In order to correctly use the lift modulus of JPAD it is necessary to set the correct Reynolds number of airfoils and, consequently, the correct value of CL_{MAX} . Referring to [1] the value for ATR 72 are the following

Table 6.2: Airfoils CL_{MAX} for ATR-72. Mach number = 0.4

Station	Airfoil	Reynolds Number	CL_{max}
Root	NACA 23018	$6.28 \cdot 10^6$	1.65
Kink	NACA 23018	$6.28 \cdot 10^6$	1.65
Tip	NACA 23015	$4.41 \cdot 10^6$	1.7

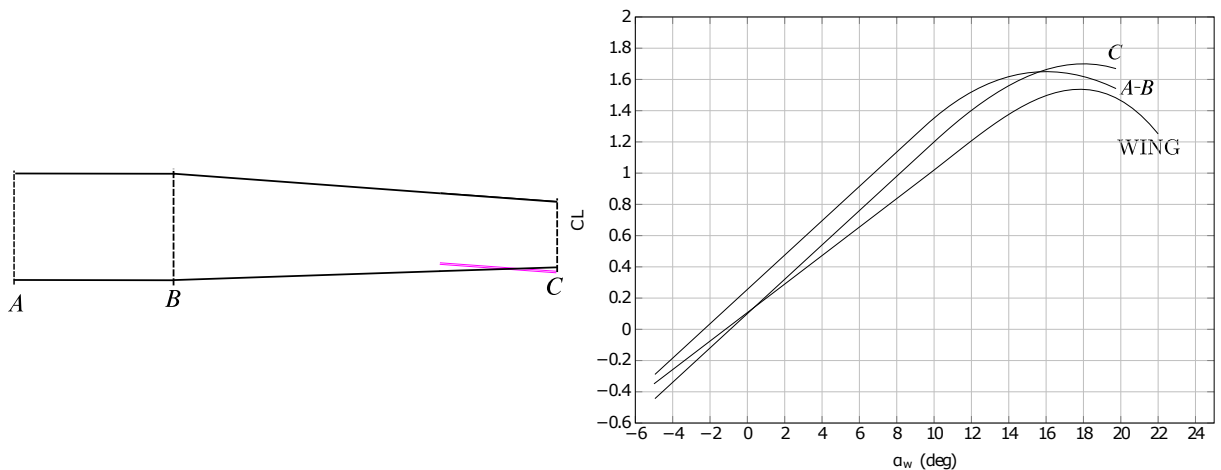


Figure 6.14: Lift curve for ATR-72 airfoils and wing for $M=0.2$.

Listing 6.1 Lift Characteristics of a Lifting Surface - Test Class

```

System.out.println("\n-----");
System.out.println("\n_LIFT_CHARACTERISTICS_");
System.out.println("\n-----");

System.out.println("\n-----");
System.out.println("|\t\t\tWING\t\t\t|");
System.out.println("-----\n\n");

System.out.println("\n\tData:");

System.out.println("Angle_of_attack_alpha_body_(deg) = "
+ "" + Math.ceil(alphaBody.to(NONSI.DEGREE_ANGLE)
.getEstimatedValue())));
System.out.println("Angle_of_incidence_of_wing_(deg) = "

```

```

+ " " + Math.ceil(theWing.get_iw())
    .to(NonSI.DEGREE_ANGLE)
    .getEstimatedValue()));

System.out.println("\n-----");
System.out.println("Starting evaluate_stall_path_of_wing");
System.out.println("-----");

LSAerodynamicsManager theLSSAnalysis = new LSAerodynamicsManager(
    theConditions,
    theWing,
    aircraft
);

LSAerodynamicsManager.CalcCLAtAlpha theCLWingCalculator =
    theLSSAnalysis
    .new CalcCLAtAlpha();
cLIsoletedWing = theCLWingCalculator.nasaBlackwell(alphaBody);

theLSSAnalysis.PlotCLVsAlphaCurve(subFolderPath);
System.out.println("-----");
System.out.println("CL_of_Isolated_wing_at_alpha_body=" + cLIsoletedWing);
System.out.println("\n\t\ttDONE_PLOTTING_CL_VS_ALPHA_CURVE");

// -----
// Using NASA-Blackwell method in order to estimate the lifting surface CLmax
// -----


LSAerodynamicsManager.CalcCLMaxClean theCLmaxAnalysis =
    theLSSAnalysis
    .new CalcCLMaxClean(); //is nested
LSAerodynamicsManager.CalcCLvsAlphaCurve theCLAnalysis
    = theLSSAnalysis.new CalcCLvsAlphaCurve();
theCLAnalysis.nasaBlackwell();
theCLmaxAnalysis.nasaBlackwell();
Amount<Angle> alphaAtCLMax = theLSSAnalysis.get_alphaStall();
double clMax = theCLWingCalculator.nasaBlackwell(alphaAtCLMax);

// PLOT

System.out.println("\n\tWRITING_CHART_TO_FILE.Stall_path.");
// interpolation of CL MAX_airfoil
MyArray clMaxAirfoil = theCLmaxAnalysis.getClAirfoils();

MyArray clAlphaThird = theLSSAnalysis.getCLMap()
    .getCxyVsAlphaTable()
    .get(MethodEnum.NASA_BLACKWELL ,alphaAtCLMax);

double [][] semiSpanAd = {
    theLSSAnalysis.get_yStationsND(),
    theLSSAnalysis.get_yStationsND()};

double [][] clDistribution = {
    clMaxAirfoil.getRealVector().toArray(),
    clAlphaThird.getRealVector().toArray()};
String [] legend = new String [4];
legend[0] = "CL_max_airfoil";
legend[1] = "CL_distribution_at_alpha_"
+ Math.toDegrees( alphaAtCLMax.getEstimatedValue());

MyChartToFileUtils.plot(
    semiSpanAd,      clDistribution, // array to plot
    0.0, 1.0, 0.0, 2.0,
    "eta", "CL", "", "",           // label with unit
    legend,          ""           // legend
    subFolderPath, "Stall_Path_of_Wing");

System.out.println("-----");
System.out.println("\t DONE ");

```

Listing 6.2 Lift Characteristics of a Lifting Surface - Results for M=0.2. ATR-72

```

LIFT CHARACTERISTICS
-----
| WING |
-----
Data:
Angle of attack alpha body (deg) = 2.0
Angle of incidence of wing (deg) = 2.0

-----
Starting evaluate stall path of wing
-----
-----CLEAN-----
alpha max 15.229385456031025 (deg)
alpha star 10.918671750781748 (deg)
cL max 1.4880884199886235
cL star 1.1785803287397512
cL alpha 5.582578511036018 (1/rad)
-----
CL of Isolated wing at alpha body = 0.5045422247468523
      DONE PLOTTING CL VS ALPHA CURVE

      WRITING CHART TO FILE. Stall path.
-----
      DONE
-----
```

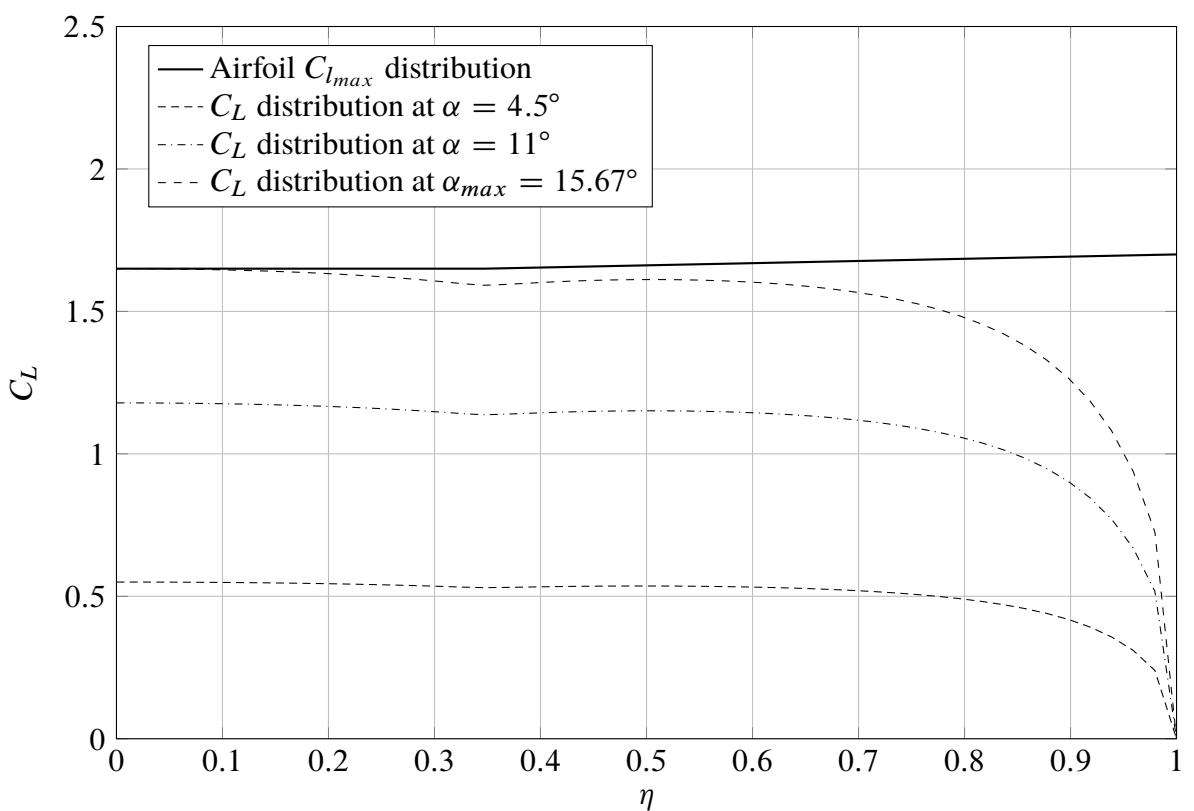


Figure 6.15: ATR 72 Stall Path of wing at Mach 0.2.

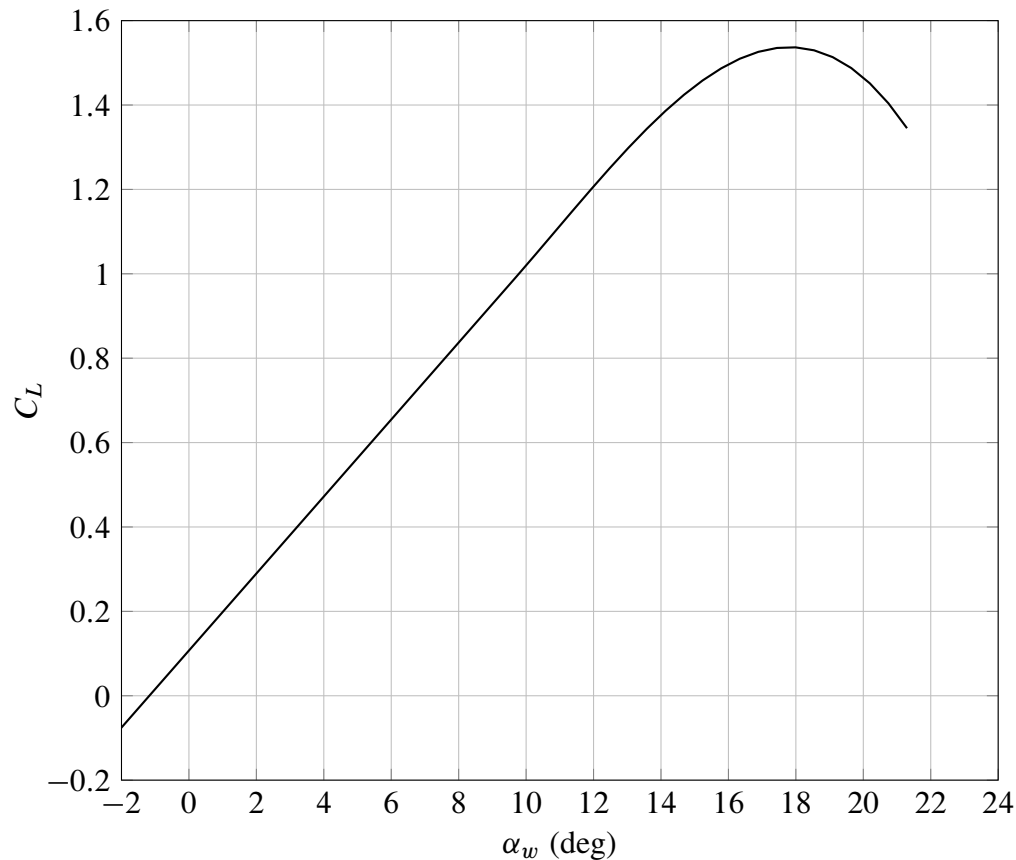


Figure 6.16: ATR 72 CL vs Alpha_w at Mach 0.2.

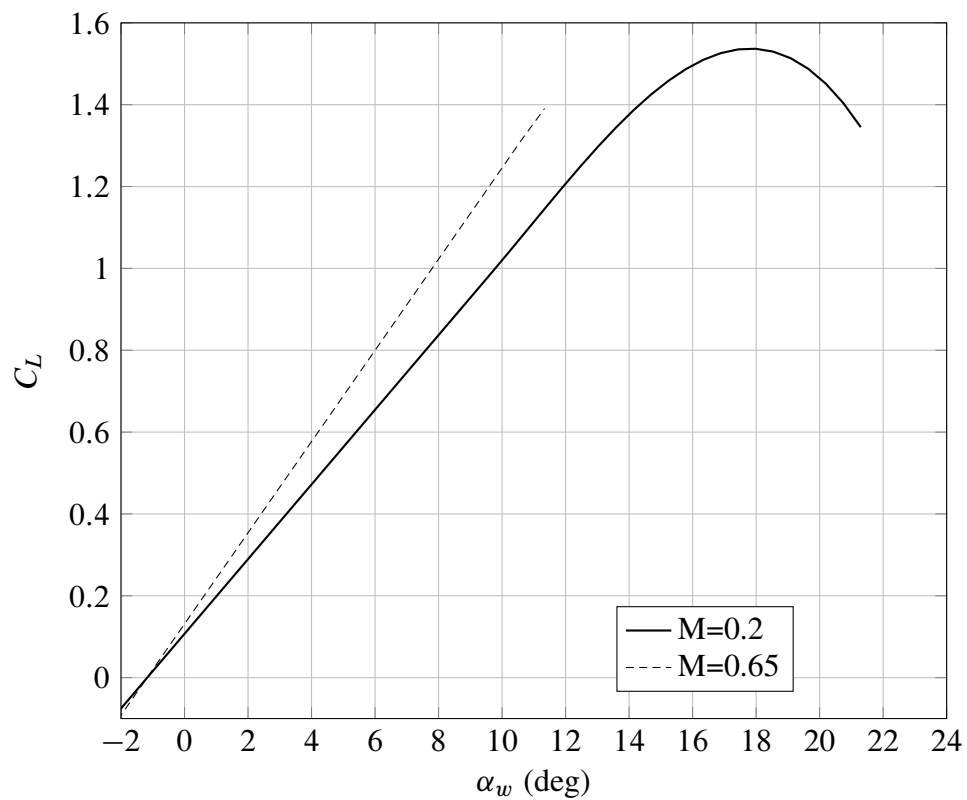


Figure 6.17: ATR-72 lift curve. Variation with Mach number.

Table 6.3: High-lift devices geometrical data for ATR72

Number of Flap	Type	η in	η out	$\frac{c_f}{c}$
1	Single Slotted	0.08	0.35	0.38
2	Single Slotted	0.35	0.8	0.38

Table 6.4: High-lift devices data for ATR72

Configuration	δ_{f_1}	δ_{f_2}
Take off	22°	22°
Landing	40°	40°

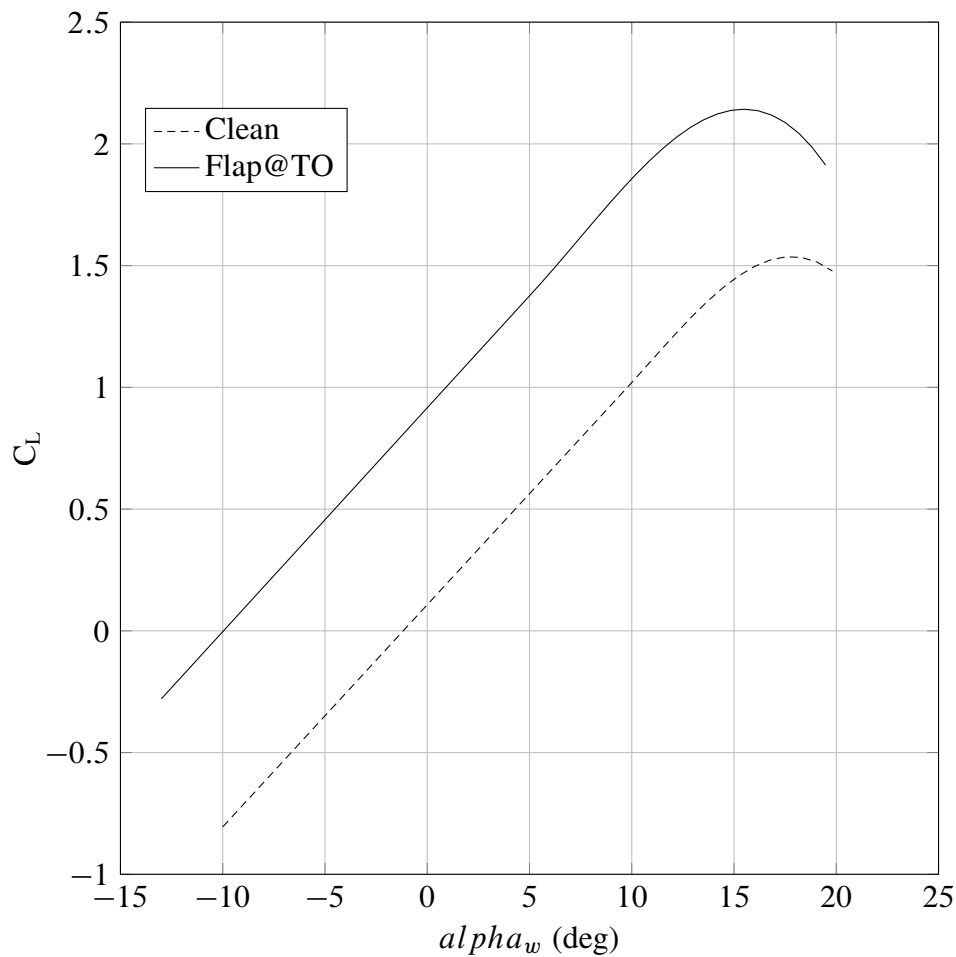


Figure 6.18: ATR-72 lift curve with and without flaps in take-off configuration.

Listing 6.3 Wing Lift characteristic results for TAKE-OFF. ATR-72, M=0.2

```

-----CLEAN-----
alpha max 17.8116610484647 (deg)
alpha star 9.6267723716381 (deg)
cl max 1.5370911540497318
cl star 0.9854862505109439
cl alpha 5.227776418346189 (1/rad)

----- DELTA HIGH LIFT TAKE_OFF -----
deltaCL0_flap = 0.80887111935885
deltaCLmax_flap = 0.6053024400694088
deltaCLmax_slat = 0.0
cLalpha_new = (1/rad) 5.26834311032201

```

```

deltaAlphaMax = (deg) 2.139367521679026
deltaCD = 0.022631019249350154
deltaCMc_4 = -0.14067311296011697

-----HIGH LIFT-----
alpha max 15.47805767446944 (deg)
alpha star 5.191658954896691 (deg)
cl max 2.1423935941191408
cl star 1.393329795148776
cl alpha 5.26834311032201 (1/rad)

CL wing TAKE_OFF Array [0.594167494459124, 0.6448337842917097, 0.6955000741242955...]
CL of wing at TAKE_OFF at alpha body = 1.2378170282582692

```

6.3.2 BOEING 747-100B

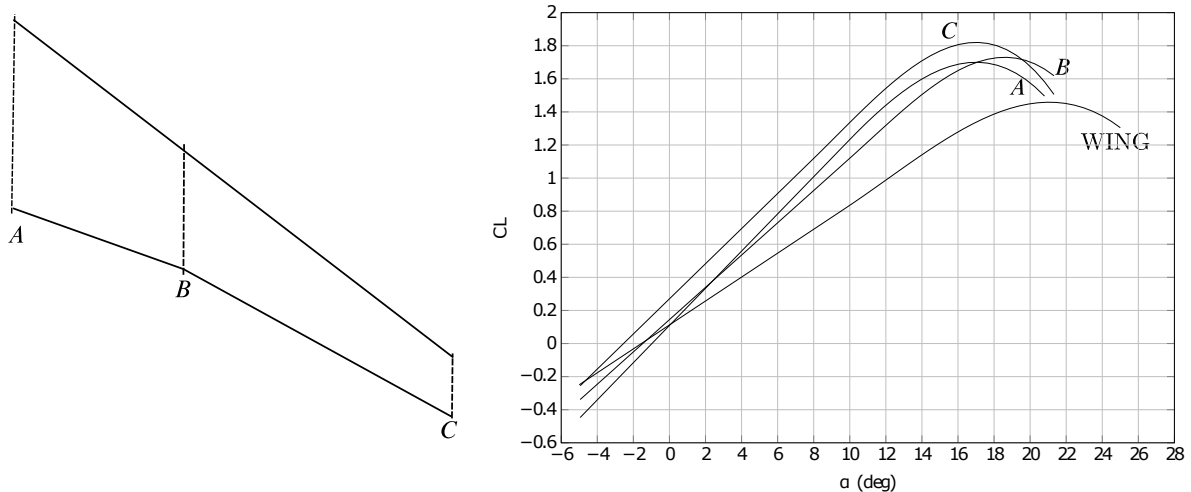


Figure 6.19: Lift curve for BOEING 747-100B similar airfoils and wing.

Table 6.5: Airfoils CL_{MAX} for BOEING 747-100B. Mach number = 0.84

Station	Airfoil	Reynolds Number	CL_{max}
Root	similar to BAC root 747	$3.67 \cdot 10^7$	1.7
Kink	similar to BAC kink 747	$2.18 \cdot 10^7$	1.73
Tip	similar to BAC tip 747	$9.53 \cdot 10^6$	1.82

Listing 6.4 Lift Characteristics of a Lifting Surface - Results. BOEING 747-100B for M=0.84

```

-----
LIFT CHARACTERISTICS
-----
|       WING      |
-----
Data:
Angle of incidence of wing (deg) = 1.500110492089126
Angle of attack alpha body (deg) = 2.000147322785501
Angle of attack alpha Wing (deg) = 3.4999999999999996

```

```

-----CLEAN-----
alpha max 15.632268822248909 (deg)
alpha star 9.749010907718121 (deg)
cL max 1.3961111386040277
cL star 1.0698441603187268
cL alpha 5.4275479968166955 (1/rad)

CL wing Clean Array [-0.18514784517157623, -0.12715075362802075, ...]

CL of Isolated wing at alpha body = 0.4779522348097419

-----
WRITING CL vs ALPHA CHART TO FILE
DONE

-----
WRITING STALL PATH CHART TO FILE
DONE

```

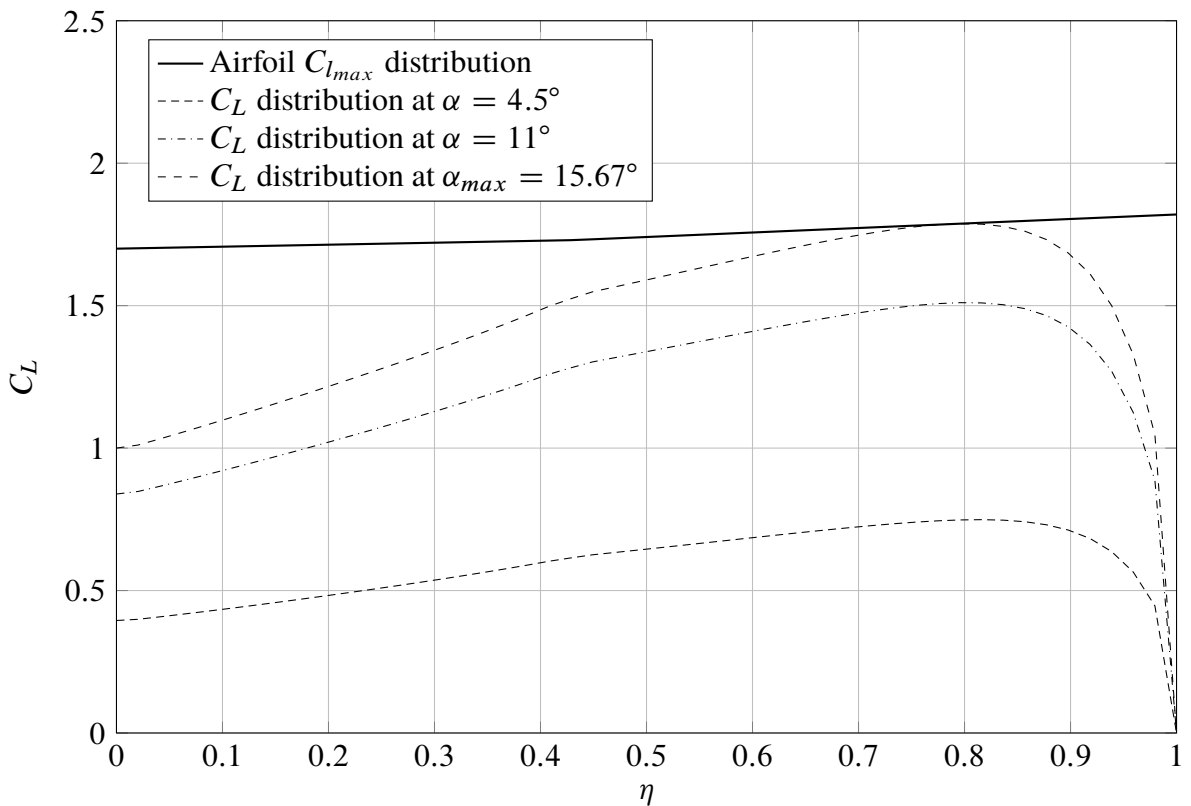


Figure 6.20: BOEING 747-100B Stall Path at Mach 0.84.

Table 6.6: High-lift devices geometrical data for BOEING 747-100B. Flap.

Number of Flap	Type	η in	η out	$\frac{c_f}{c}$
1	Triple Slotted	0.104	0.357	0.18
2	Triple Slotted	0.411	0.636	0.18

Table 6.7: High-lift devices geometrical data for BOEING 747-100B. Slat.

Number of Slat	η in	η out	$\frac{c_{ext}}{c}$	$\frac{c_s}{c}$
1	0.192	0.364	1.1	0.09
2	0.414	0.648	1.1	0.136
3	0.692	0.961	1.1	0.187

Table 6.8: High-lift devices data for BOEING 747-100B

Configuration	δ_{f_1}	δ_{f_2}	δ_{s_1}	δ_{s_2}	δ_{s_3}
Take off	5°, 3°, 2°	5°, 3°, 2°	10°	10°	10°
Landing	10°, 10°, 10°	10°, 10°, 10°	20°	20°	20°

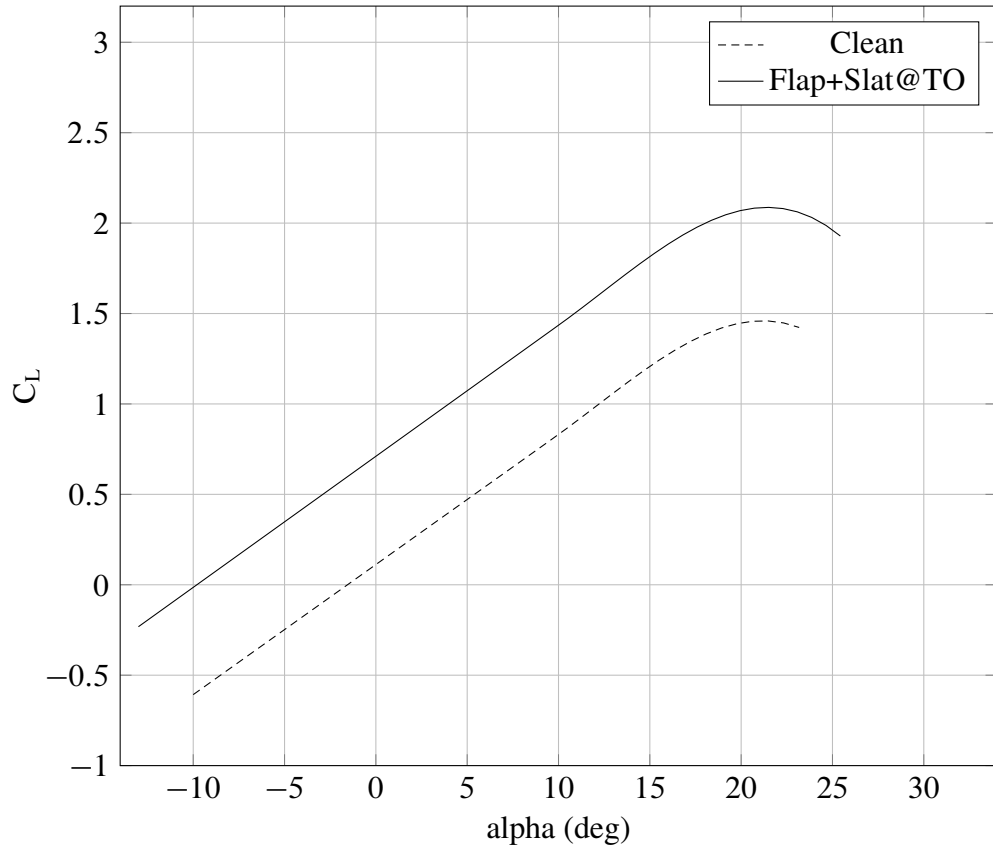


Figure 6.21: BOEING 747-100B lift curve with and without flaps in take-off configuration.

Listing 6.5 Wing Lift characteristic results for TAKE-OFF. BOEING 747-100B, M=0.2

```

-----CLEAN-----
alpha max 21.1765973230843 (deg)
alpha star 9.7482928348910 (deg)
cl max 1.4597134105954703
cl star 0.8130642471456172
cl alpha 4.121408852511737 (1/rad)

----- DELTA HIGH LIFT TAKE_OFF -----
deltaCL0_flap = 0.5985742466275841
deltaCLmax_flap = 0.6272563565428977
deltaCLmax_slat = 0.0
cLalpha_new = (1/rad) 4.153009870215378
deltaAlphaMax = (deg) 2.4385950909414857
deltaACD = 0.023580578759700432
deltaCMc_4 = -0.12074049808439227

-----HIGH LIFT-----
alpha max 21.431119618227623 (deg)
alpha star 10.003551951328152 (deg)
cl max 2.086969767138368

```

```

cl_star 1.4354638015005163
cl_alpha 4.153009870215378 (1/rad)

CL of wing at TAKE_OFF at alpha_body 2 (deg) = 0.9641157258005986

```

6.4 Modified Stall Path

In order to evaluate the lift curve of a wing another method has been implemented. This is a modification of Stall Path Method that uses the Nasa-Blackwell lift distribution also for the non linear trait. As known NB method does not see the viscous phenomena. The modified stall path method is based on the consideration that the lift distribution obtained from Nasa-Blackwell is the distribution that you would get if the airfoil's lift moved along the linear lift curve.

The process is the following.

1. For each angle of attack the lift distribution using Nasa-Blackwell method has been evaluated
2. For each of n point along the semi-span the local value of C_L is obtained
3. Each of these n points corresponds to an intermediate airfoil with its own lift curve
4. With the local value of C_L it is possible to enter in the linear lift chart obtaining the angle of attack of the airfoil
5. Using this angle of attack it is possible to enter in the lift curve of the airfoil and derive the local C_L
6. In this way a new lift distribution is obtained that considers the bidimensional non linearity.
7. The wing C_L is obtained integrating the new lift distribution.

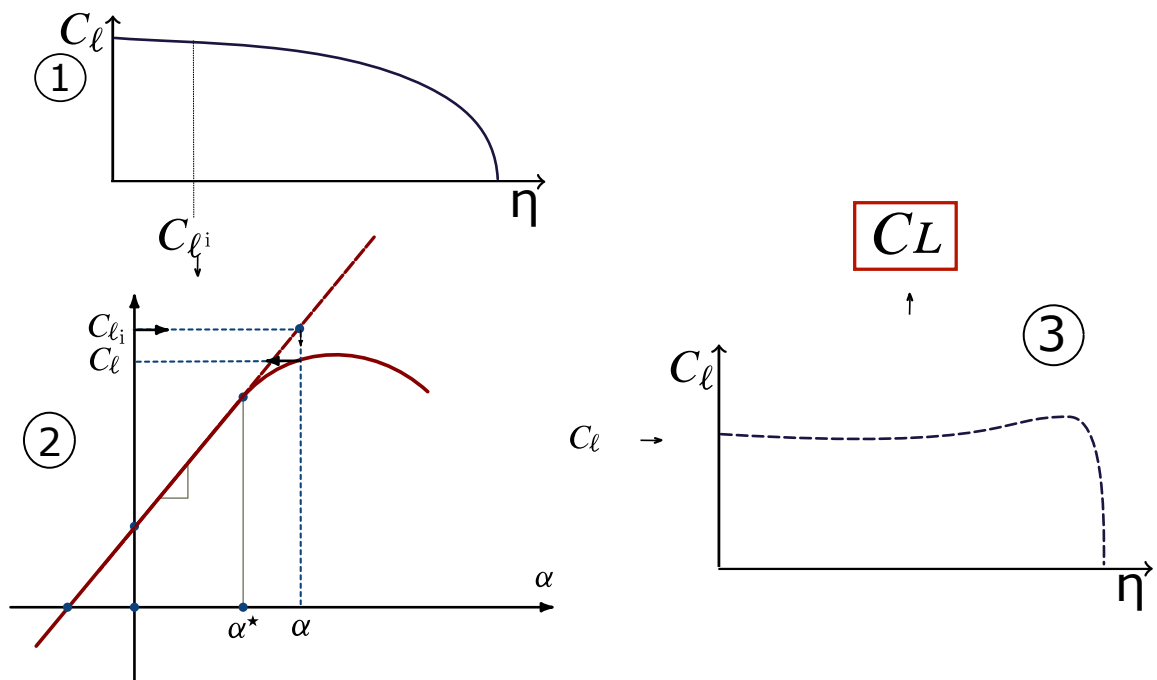


Figure 6.22: Flow chart of the modified stall path method.

6.5 Results Comparison

In order to compare and validate the results an analysis on a wing has been done with different method.

Table 6.9: Airfoils Data

Station	t/c	$C_{l_{max}}$	C_{l_α}	α_{stall}
Root	0.18	1.90	6.48(1/rad)	18°
Kink	0.18	1.90	6.48(1/rad)	18°
Tip	0.18	2.1	6.72(1/rad)	17.5°

Table 6.10: Wing Data

Span	Aspect Ratio	Cr	Ck	Cr	Ad. station kink
31 m	12	2.9 m	2.9 m	1.65 m	0.33

Table 6.11: Mission Data

Reynolds Number	Mach Number
$13 \cdot 10^6$	0.2

The analysis has been done with the following methods :

- Stall Path
- Modified Stall Path
- Philipps and Alley
- CFD

Phillips and Alley present a method for estimating the maximum wing lift that is based on the classical lifting line theory discussed in Appendix C. Their approach involves providing correction factors for the effects of twist and sweep-back on the span loading of unswept, untwisted, tapered wings. The correction factors are developed with the aid of CFD panel method computations for a variety of conventional wing planforms. Curves for the correction factors are presented for a number of specific taper and aspect ratio as long with the general method for calculating these effects for other wing geometry. [42]

$$C_{L_{max}} = \left(\frac{C_L}{c_{l_{max}}} \right)_{\Gamma=0, \epsilon=0} K_{LS} K_{LR} c_{l_{max}} \left(1 - \frac{K_{L\epsilon} C_{L,\alpha\epsilon}}{c_{l_{max}}} \right) \quad (6.10)$$

Where K_{LS} is a stall factor

$$K_{LS} = 1 + (0.0042 \mathcal{A}R - 0.066) \left(1 + 2.3 \frac{C_{L_\alpha}}{c_{l_{max}}} \right) \quad (6.11)$$

Computational Fluid Dynamics (CFD) is a methodology that allows engineers to predict the performance of their designs when exposed to fluid flow, either internal flow (such as the flow of air and gasoline through an engine manifold) or external flow (such as the aerodynamic flow past an automobile or the hydrodynamic flow past a boat). CFD software programs can simulate problems involving gases, liquids and solids and multi-phase problems that depend

on the interaction of any number of the above. CFD is used in the design of almost every major product, reducing uncertainty in the design process, and resulting in higher quality products and designs, with greater robustness that better meet customer requirements. CD-adapco is the world's largest independent CFD focused provider of engineering simulation software, support and services. [11]

Considering the reduction of CL_{max} due to flow separation and other tridimensional effects, an additional modification has been implemented starting from the Stall Path method and the Modified Stall Path Method. The used value for CL_{max} is obtained from the traditional Stall Path method, while the value of α_{max} is obtained from the modified Stall Path Method. In this way a small percentual error has been obtained.

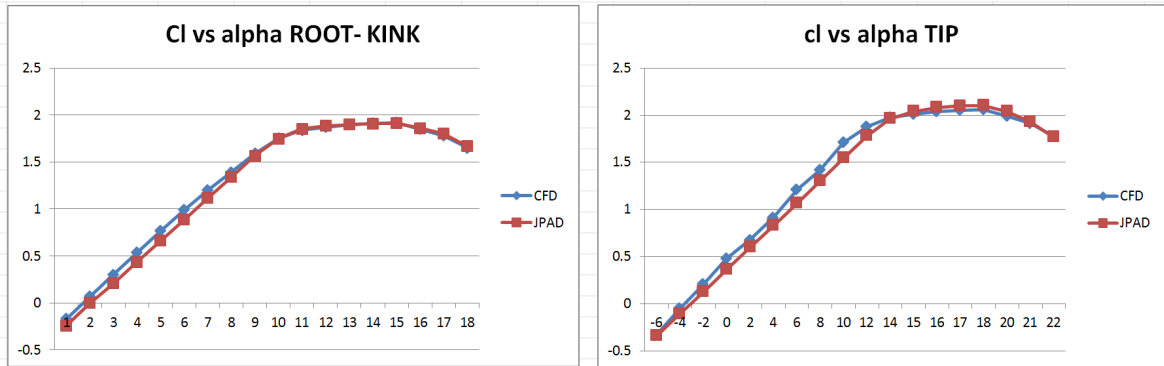


Figure 6.23: Comparison of wing lift curve of airfoils.

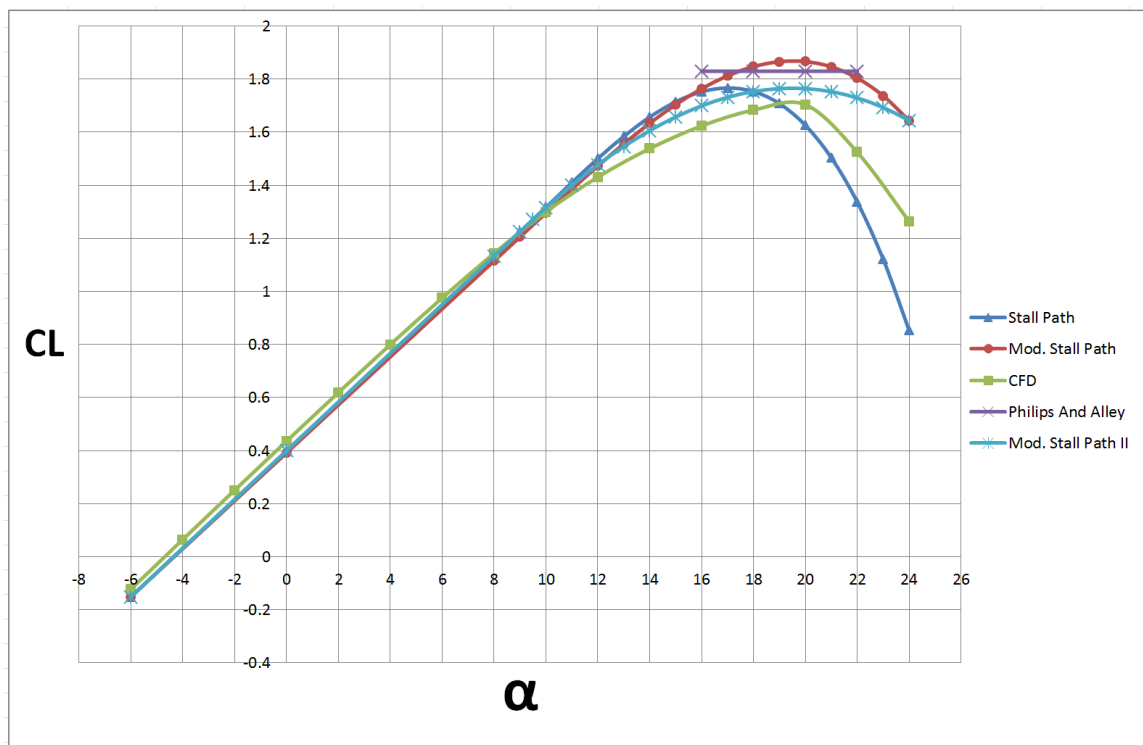


Figure 6.24: Comparison of wing lift curve of wing.

Table 6.12: Lift results comparison

Method	$C_{L_{MAX}}$	α_{stall}
Stall Path	1.766	17.1°
Modified Stall Path	1.86	19.5°
Modified Stall Path II	1.766	19.5°
Phillips And Alley	1.83	n.e.
CFD	1.699	19.6°

	Method					Reference Values (CFD)
	Stall Path	Mod. Stall Path	Mod. Stall Path II	Philips and Alley		
α_{stall}	17	19.5	19.5			19.6
CL_{max}	1.766	1.867	1.766	1.83		1.699
α_{stall} Error (%)	13.27	0.51	0.51			
CL_{max} Error (%)	3.94	9.89	3.94	7.71		

Figure 6.25: Percentage Error.

Chapter 7

Wing Drag Characteristics

*Le avversità
possono essere delle formidabili occasioni*
– Thomas Mann

As mentioned in the previous chapter, the drag is the force component acting in the opposite direction to the airspeed vector.

7.1 Theoretical background

There is not a single classification of the drag but, dependent on the purpose of the work, the drag may be broken down in different way. Following will be explained the two main classifications.

- The drag is subdivided using a causal breakdown. In this way the drag contributes are in accordance with the physical mechanism such as the viscosity of the flow.
- The drag is subdivided using a component breakdown. Every component of aircraft added an own drag contribute.

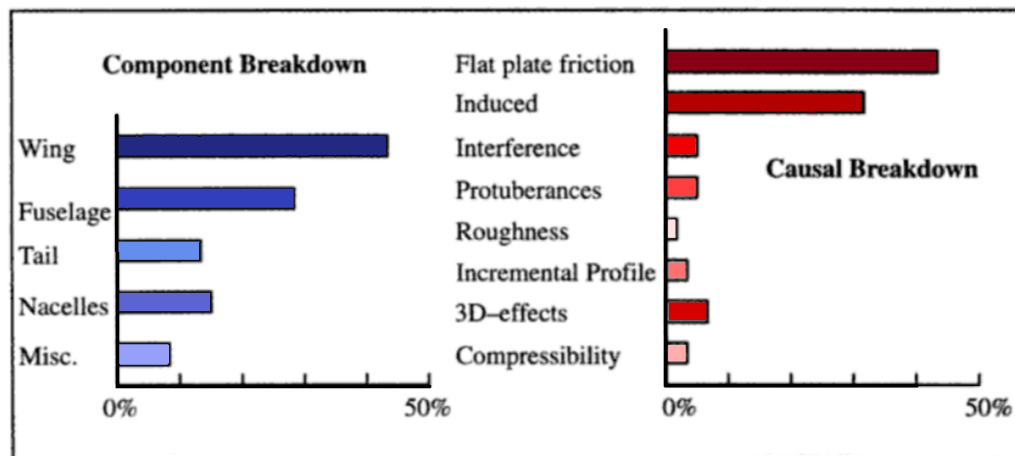


Figure 7.1: Drag breakdown for a business jet in cruise.

According to the causal breakdown it is possible to make a preliminary division considering normal and tangential stress. The tangential forces produce the **friction drag**. While it is possible to divide the drag due of the normal component in viscous, that generates **form drag**, and inviscid. A further division can be made for the last one, in **induced drag** and **wave drag**.

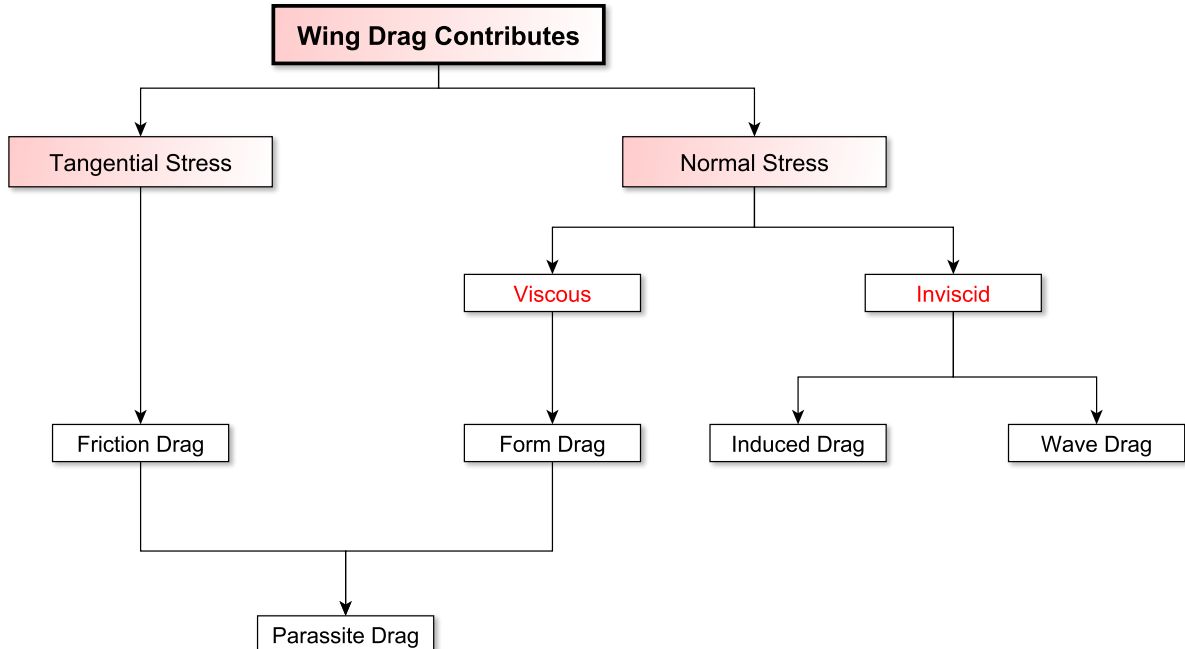


Figure 7.2: Causal breakdown of airplane drags.

Friction drag is caused by the air closest to the body's surface that is dragged along with it. Due to this interaction shearing stresses are born within the thin layer of air (boundary layer) adjacent to the skin. The magnitude of this drag depends on the kind of boundary layer what can be laminar or turbulent in dependence on the Raynolds number. Usually it is accustomed to assume, at the flight speed and altitudes at which aircraft fly, a fully turbulent flow over the entire airplane. In this way a conservative result is obtained.

Form drag is caused by the air that is flowing over the body. The separation of air creates turbulence and results in pockets of low and high pressure that leave a wake behind the airplane. The departure of the boundary layer alters the pressure field from its inviscid distribution resulting in an additional drag component. The general size and shape of the body are the most important factors in form drag; bodies with a larger presented cross-section will have a higher drag than thinner bodies.

Induced drag is the drag due to lift. It is the drag created by the vortices at the tip of an aircraft's wing. The high pressure underneath the wing causes the airflow at the tips of the wings to curl around from bottom to top in a circular motion. So it is depend on the spanwise distribution of lift.

Wave drag is a component of the drag due to the presence of shock waves. Wave drag is independent of viscous effects, and tends to present itself as a sudden and dramatic increase in drag as the vehicle increases speed.

In this work the drag will be classified using a component breakdown and for each component of the aircraft is used a causal breakdown. In this way it is possible to evaluate separately the wing drag and tail drag, considering the aerodynamic centers of these lifting surfaces as application point.

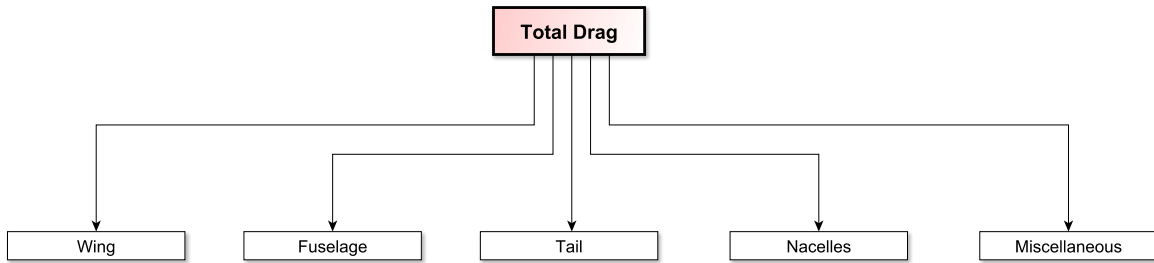


Figure 7.3: Components breakdown of airplane drags.

In JPAD is possible to use different methods in order to evaluate the drag coefficient of a wing and of the entire aircraft. In particular in this section will be explained two approaches and in the next chapter will be shown the results.

In order to evaluate the drag coefficient you can divide it into different contributes as shown in the fig. 7.4

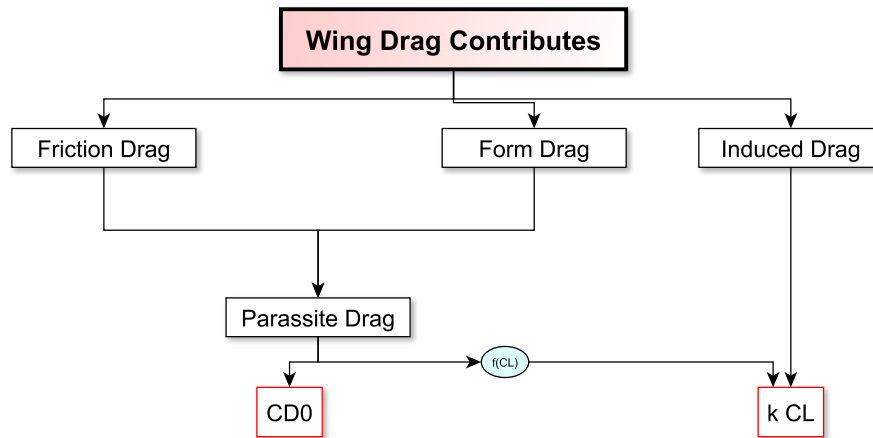


Figure 7.4: Used breakdown for the wing drag.

It is possible to evaluate the contributes using different methods.

7.1.1 Case 1: CD_0 and $k CL$

Part of the parasite drag depends on the angle of attack and, consequently, on the CL ; while part is constant and it is called CD_0 . So the contributes of CD which varies with the CL consist of the induced drag (due to vortex) and a part of parasite drag, not considering wave effects. It is possible to approximate the drag polar of a wing as a parabola where the CD_0 is the origin. It is important to note that using the parabolic approximation the CD_0 is the coefficient drag value at $CL = 0$ but this is not properly correct.

$$CD = CD_0 + KCL^2 = CD_0 + \frac{CL^2}{\pi AR}(1 + \delta) \quad (7.1)$$

In order to evaluate the zero lift drag coefficient it is possible to introduce the concept of equivalent parasite area f . This is the area of a thin plate that has the same drag of the wing.

$$f = CD_0 S \quad (7.2)$$

Introducing the equivalent friction coefficient, it is possible to express the equivalent parasite area as follows

$$f = S_{wet} C_{f_e} \quad (7.3)$$

Therefore it is possible to obtain the zero lift drag coefficient by eq. 7.2 and 7.3.

$$CD_0 = C_{f_e} \left(\frac{S_{wet}}{S} \right) \quad (7.4)$$

In order to evaluate the induced drag it is possible to use the following chart entering in it with the equivalent wing. This δ parameter is the correction factor for non elliptical wings

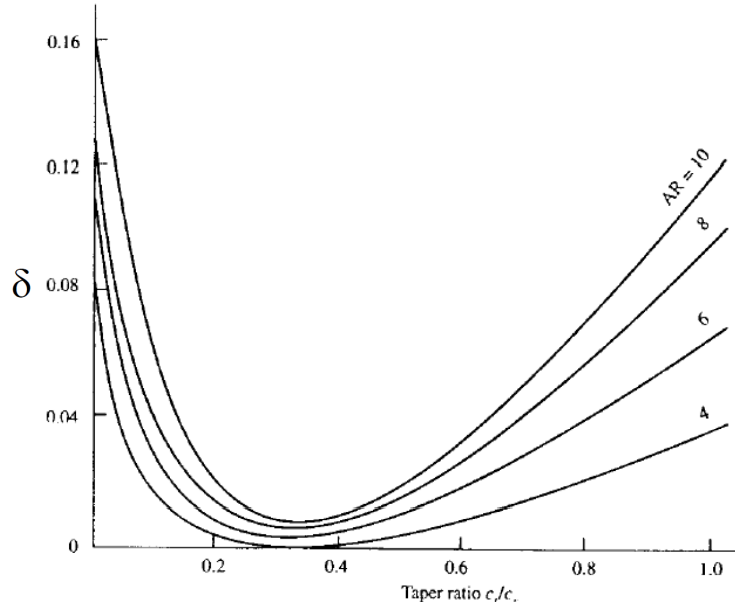


Figure 7.5: Delta factor for induced drag.

7.1.2 Case 2: Parasite Drag and Induced Drag

It is possible to evaluate the parasite drag starting from the airfoils while the contribution that varies with the CL is calculated from the induced angle of attack.

Parasite Drag

1. First of all the load distribution at a given angle of attack is calculated.
2. Fifty points are defined along the semi-span.
3. An intermediate profile is calculated for each point.
4. The lift coefficient at each station corresponds to a profile.
5. Starting from the Cl and using a parabolic approximation for the drag polar, the Cd is calculated with the following equation

$$Cd = Cd_{min} + (Cl - Cl_{(Cd_{min})})^2 \cdot k \quad (7.5)$$

6. Known the drag distribution it is possible to calculate the drag coefficient of the lifting surface integrating

In the tool it is possible to choose the method used to calculate the load distribution. In particular it is possible to use Shrenk or Nasa-Blackwell method.

Schrenk Method is based on an elliptical lifting coefficient distribution span wise hypothesis on the wing. This method also assumes that the pressure distribution is proportional to the wing area. The **Nasa-Blackwell**, as mentioned, is a numerical method for calculating the subsonic load distribution for arbitrary lifting surface arrangements at a fixed angle of attack. (CAP . 6)

Induced Drag

The induced drag introduces tridimensional effects on the drag estimation.

$$CD_i = CL\alpha_i \quad (7.6)$$

So it is necessary to evaluate the induced angle of attack along the semi-span(CHAP. 10).

1. The load distribution at a given angle of attack is calculated.
2. The distribution of induced angle at a given angle of attack is calculated.
3. Fifty points are defined along the semi-span.
4. The lift coefficient at each station corresponds to local profile and it's possible to evaluate the drag coefficient.

$$Cd = Cl\alpha_i \quad (7.7)$$

5. Known the drag distribution it is possible to calculate the drag coefficient of the lifting surface integrating.

7.2 Java Class Architecture

In this paragraph the implementation inside the JPAD library of the calculation of the wing drag characteristics will be described. In this library there are several methods relating to the calculation of drag, which are summarized in the table below, all contained in LSAerodynamicManager class. As mentioned the drag may be broken down in different ways: using a causal breakdown or a component breakdown, so there are various methods that evaluate the different contributions. In order to have a clear organization of the class, the methods relating to the calculations of the same items are organized in nested classes in LSAerodynamicManager.

As mentioned it is possible to evaluate the drag coefficient in JPAD using different methods. The first method is to evaluate the zero lift drag coefficient using the nested class `calculateCD0Total`. In order to evaluate the induced drag it is possible to evaluate the CL of the wing and the oswald factor from an aerodynamic analysis.

The second method is to evaluate th CD0 as the zero lift defining an object of the class `CalcCDAtAlpha`. This class evaluates the drag coefficient of a lifting surface. This method calls a method of an other class `CalcCdDistribution` in order to evaluate the Cd distribution at alpha. The drag coefficient distribution is calculated starting from the lift distribution and using a parabolic approximation for the lifting surface polar by the class `CalculateCd`. In order to evaluate the induced drag it is necessary to use the method `calculateCDInduced` that calculate the wing lift distribution using NasaBlackwell method and the induced angle of attack using the methods of the class `AlphaEffective`.

calculateCD0Total	This class contains methods that calculates CD0
CalcCdWaveDrag	This method calculates a lifting surface wave drag
CalcCDAtAlpha	This method calculates the drag coefficient of the lifting surface using an integral and calling other method that fills the needed field.
calculateCDParasiteFromAirfoil	This method calculates drag distribution starting from the load distribution calculated with Nasa-Blackwell method or Schrenk method using a parabolic approximation for the drag polar.
CalculateCdAirfoil	This nested class has some methods that evaluates the cd of an airfoil corresponding to an alpha that is the input value of the method. The difference between the methods is the way to calculate cl from alpha.
PlotCDvsAlphaCurve	This method draws CD vs Alpha curve and CD vs CL curve of a wing, using 30 value of alpha between $\alpha = -2^\circ$ and $\alpha = 18^\circ$.
calculateCDInduced	This method calculates the cd induced from cl distribution and induced angle of attack.

Table 7.1: Methods for drag coefficient calculator of a lifting surface.

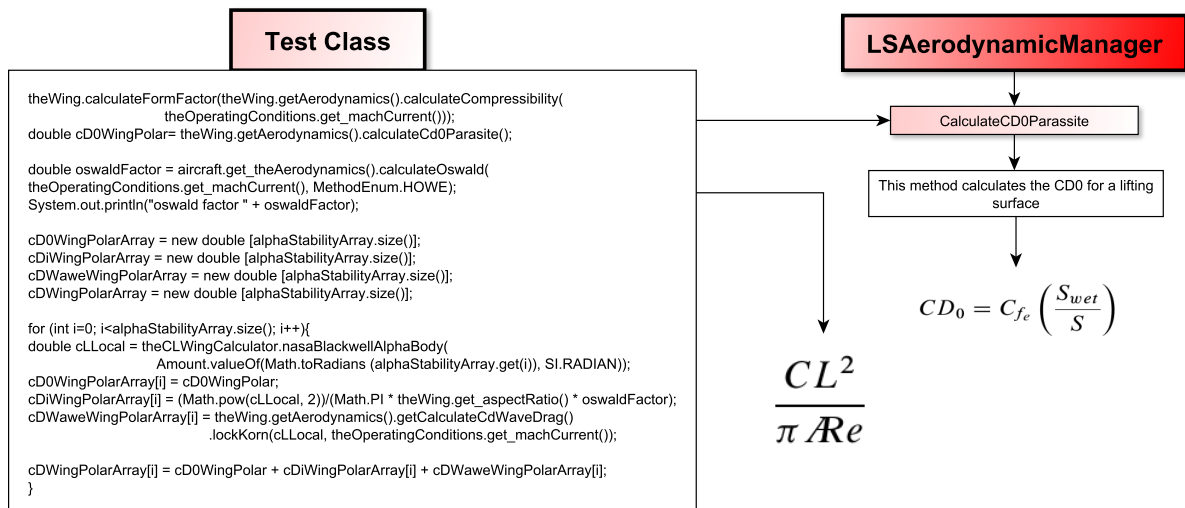


Figure 7.6: Flow chart of drag estimation classes. Case 1.

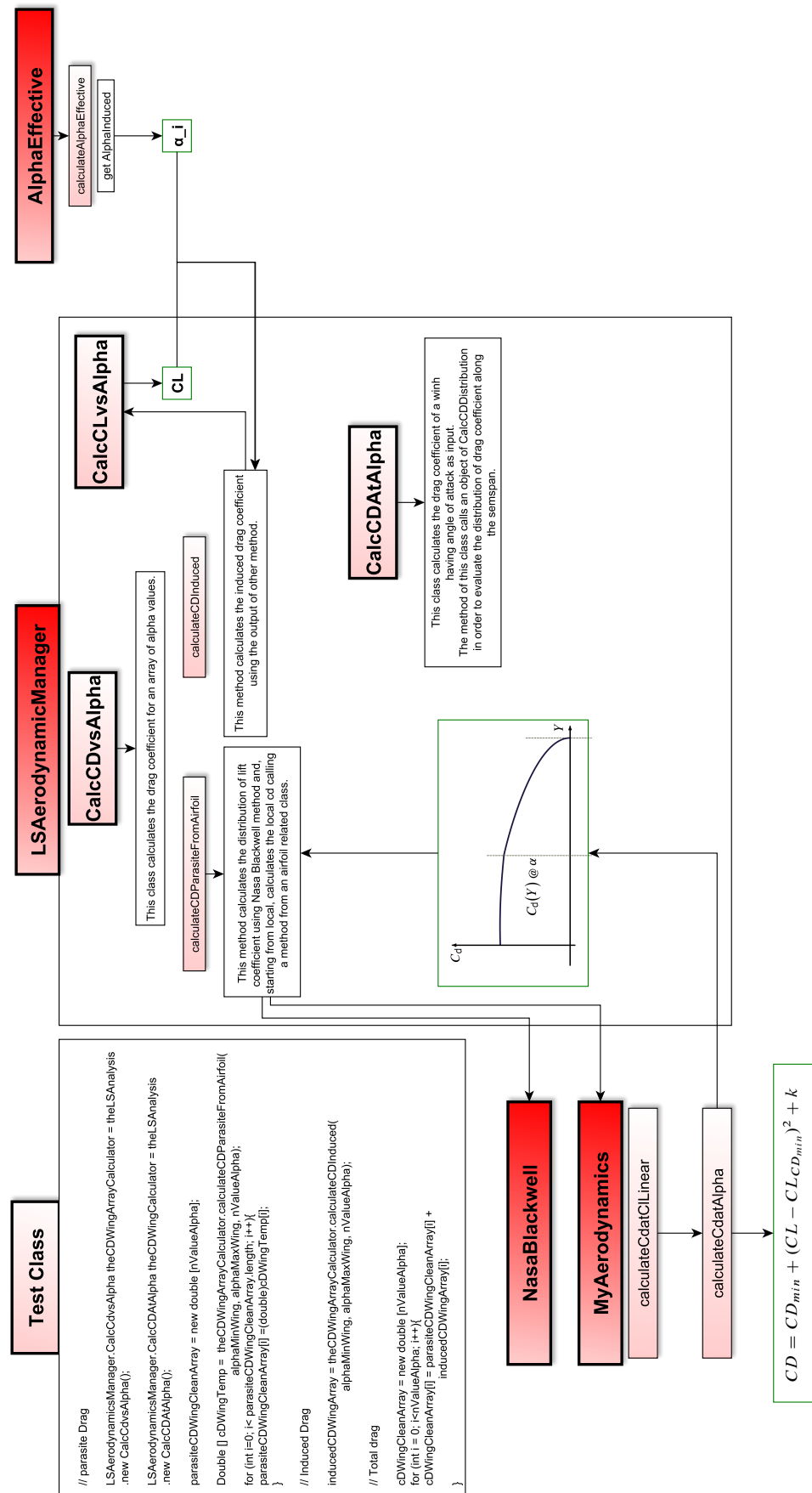


Figure 7.7: Flow chart of drag estimation classes. Case 2.

7.3 Case Study

In this section there will be present the results of the application of the previously introduced method on two aircraft: ATR-72 and B747-100B. After initializing the Test class and defining the work object, it is possible to define an object of the class `CalcCDAtAlpha` that calculates the drag coefficient of a wing at a given angle of attack. This method accepts as input three parameters: the angle of attack of the wing, the method used in order to calculate of lift distribution and an object of the lifting surface aerodynamic manager.

Listing 7.1 Use of Drag Calculator class

```

// -----
// DRAG CHARACTERISTICS
// -----



System.out.println("\n\n-----");
System.out.println("\n_DRAG_CHARACTERISTICS_");
System.out.println("\n-----");

System.out.println("\n-----");
System.out.println(" | WING | ");
System.out.println("-----\n\n");



//-----CDairfoil+ CL*alpha_i


// parasite Drag

LSAerodynamicsManager.CalcCdVsAlpha theCDWingArrayCalculator = theLSAnalysis
        .new CalcCdVsAlpha();

LSAerodynamicsManager.CalcCdAtAlpha theCDWingCalculator = theLSAnalysis
        .new CalcCdAtAlpha();

parasiteCDWingCleanArray = new double [nValueAlpha];

Double [] cDWingTemp = theCDWingArrayCalculator
.calculateCDParasiteFromAirfoil(alphaMinWing, alphaMaxWing, nValueAlpha);

for (int i=0; i< parasiteCDWingCleanArray.length; i++){
    parasiteCDWingCleanArray[i] =(double)cDWingTemp[i];
}

// Induced Drag

inducedCDWingArray = theCDWingArrayCalculator
.calculateCDInduced(alphaMinWing, alphaMaxWing, nValueAlpha);



// Total drag

cDWingCleanArray = new double [nValueAlpha];

for (int i = 0; i<nValueAlpha; i++){
    cDWingCleanArray[i] = parasiteCDWingCleanArray[i]+
        inducedCDWingArray[i];
}






// Total Drag with Parabolic interpolation

theWing.calculateFormFactor(theWing.getAerodynamics()
        .calculateCompressibility(
            theOperatingConditions.get_machCurrent())));

```

```

        double cD0WingPolar= theWing.getAerodynamics().calculateCd0Parasite();

        double oswaldFactor = aircraft.get_theAerodynamics().calculateOswald(
            theOperatingConditions.get_machCurrent(), MethodEnum.HOWE);
        System.out.println("oswald_factor_" + oswaldFactor);

        cD0WingPolarArray = new double [alphaStabilityArray.size()];
        cDiWingPolarArray = new double [alphaStabilityArray.size()];
        cDWaveWingPolarArray = new double [alphaStabilityArray.size()];
        cDWingPolarArray = new double [alphaStabilityArray.size()];

        for (int i=0; i<alphaStabilityArray.size(); i++){

            double cLLocal = theCLWingCalculator.nasaBlackwellAlphaBody(
                Amount.valueOf(Math.toRadians
                    (alphaStabilityArray.get(i)), SI.RADIAN));

            cD0WingPolarArray[i] = cD0WingPolar;
            cDiWingPolarArray[i] = (Math.pow(cLLocal, 2))/
                (Math.PI * theWing.get_aspectRatio() * oswaldFactor);

            cDWaveWingPolarArray[i] = theWing.getAerodynamics()
                .getCalculateCdWaveDrag().lockKorn(
                    cLLocal, theOperatingConditions.get_machCurrent());

            cDWingPolarArray[i] = cD0WingPolar + cDiWingPolarArray[i]
                + cDWaveWingPolarArray[i];
        }
    }
}

```

7.3.1 ATR-72

Following there are the summary diagrams of the results obtained for the ATR 72. In case 2, at the moment, there are not contemplated the not linear effects due to induced drag.

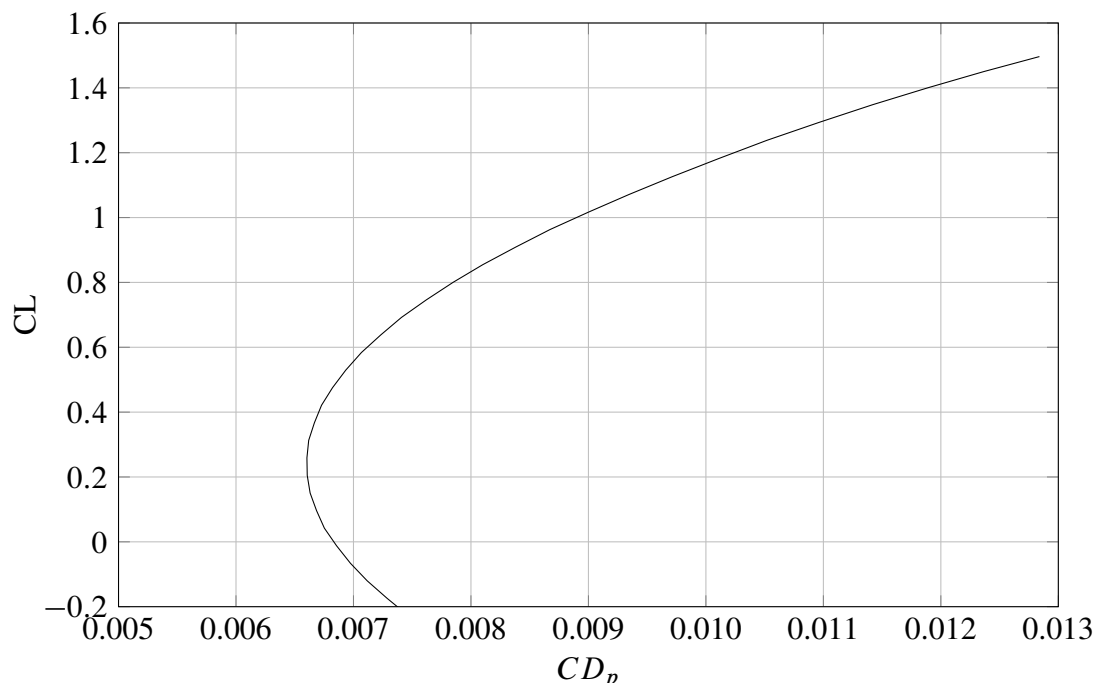
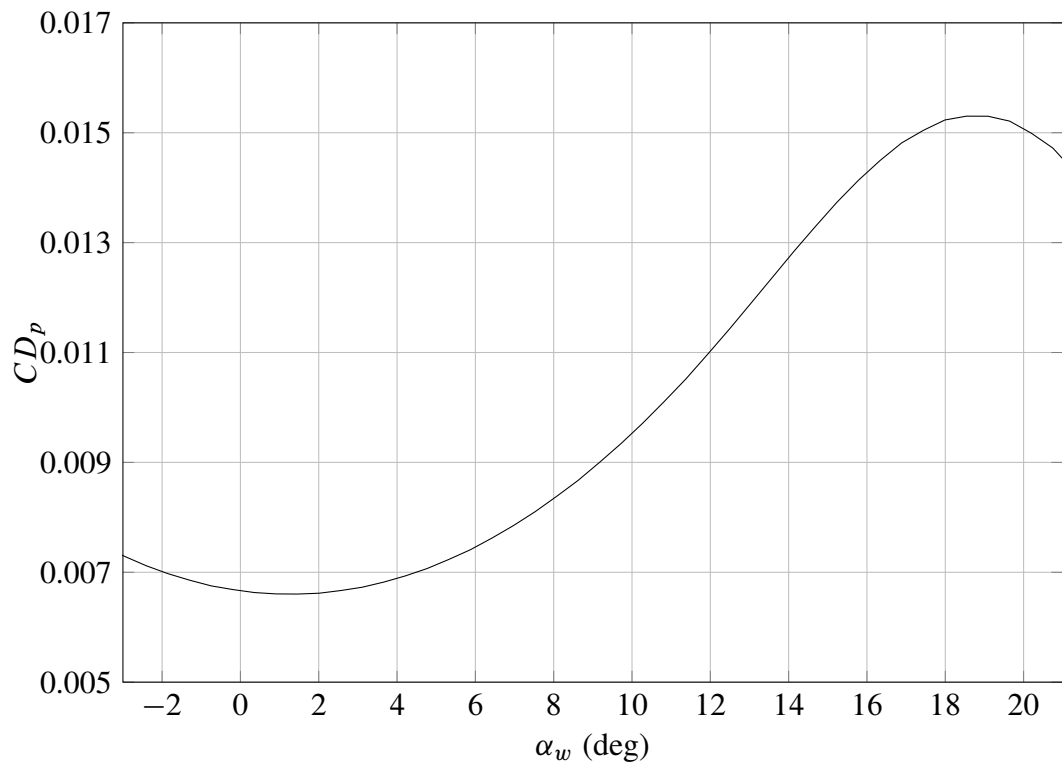
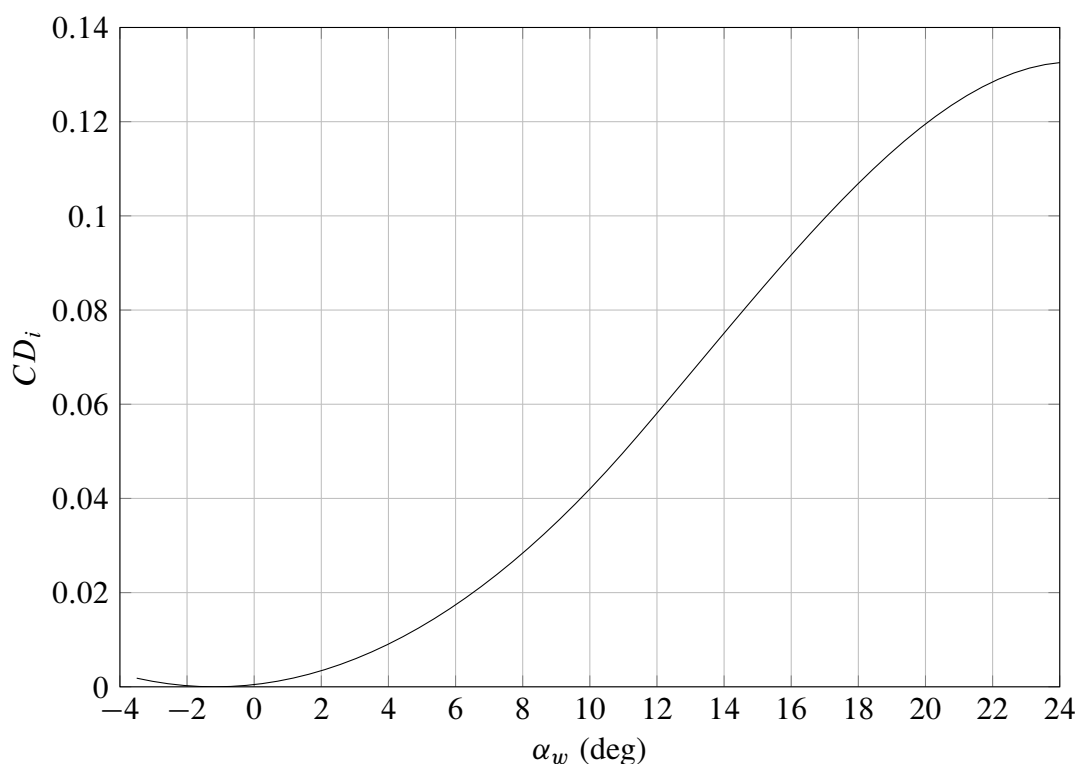
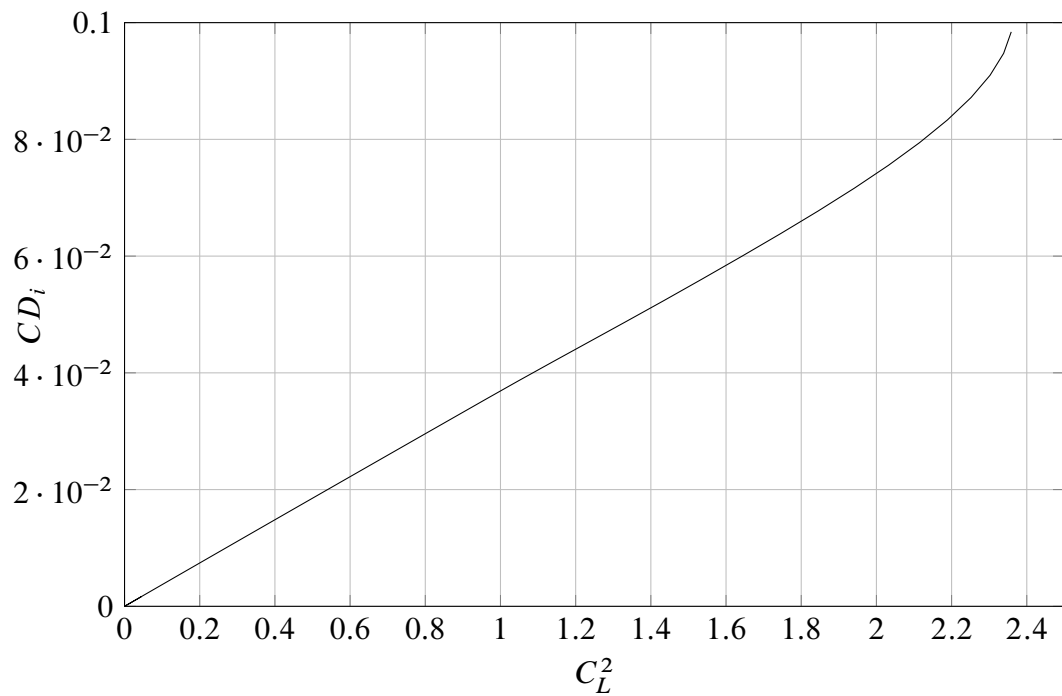
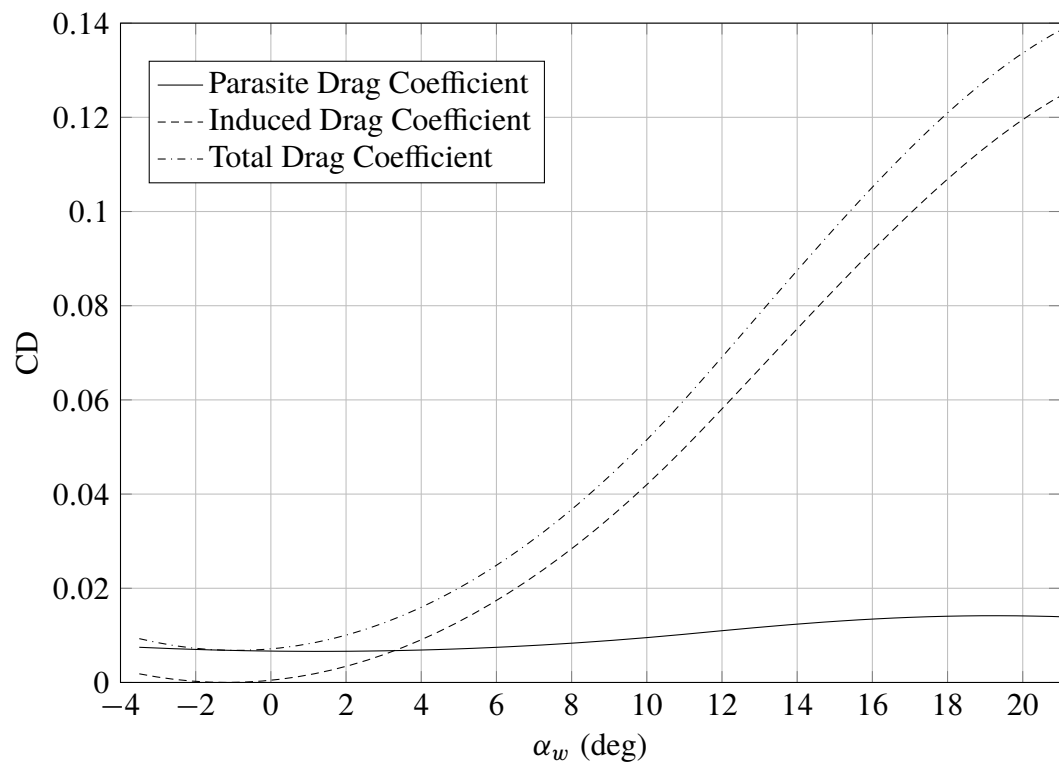


Figure 7.8: ATR 72 CD vs CL at Mach 0.4. Parasite Drag.

Figure 7.9: ATR 72 CD vs α_w at Mach 0.4. Parasite Drag.Figure 7.10: ATR 72 CD vs α_w at Mach 0.4. Induced Drag.

Figure 7.11: ATR 72 CD_i vs C_L^2 at Mach 0.4.Figure 7.12: ATR 72 CD vs α_w at Mach 0.4. Drag Coefficients calculated as case 2.

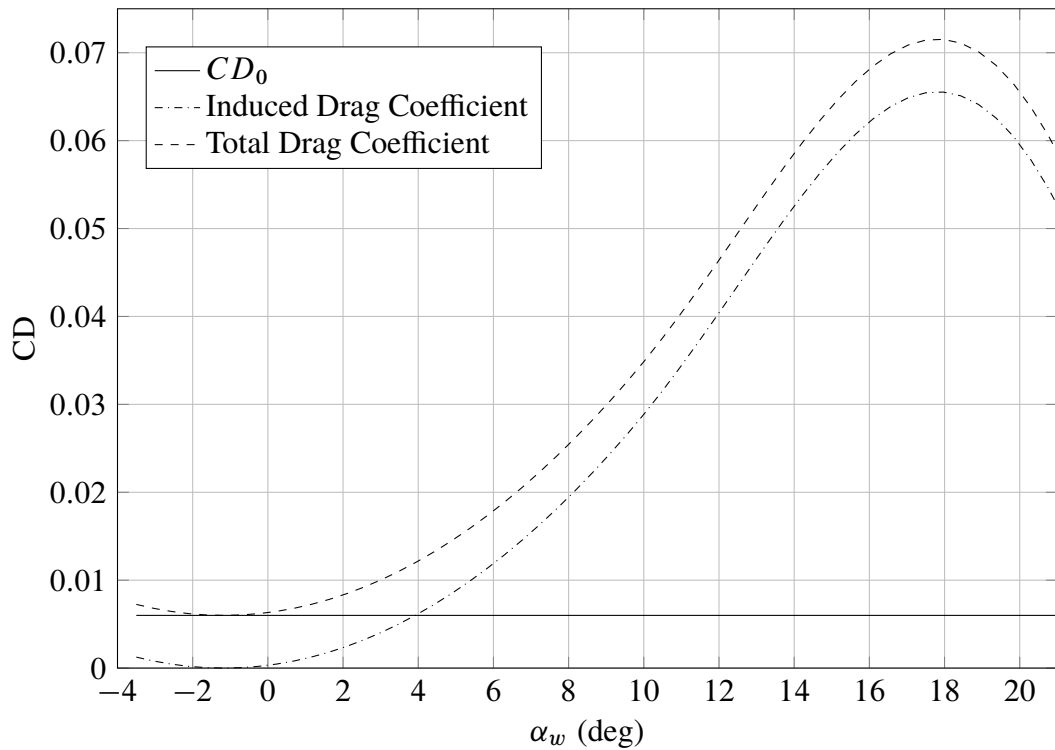


Figure 7.13: ATR 72 CD vs α_w at Mach 0.4. Drag Coefficients calculated as case 1.

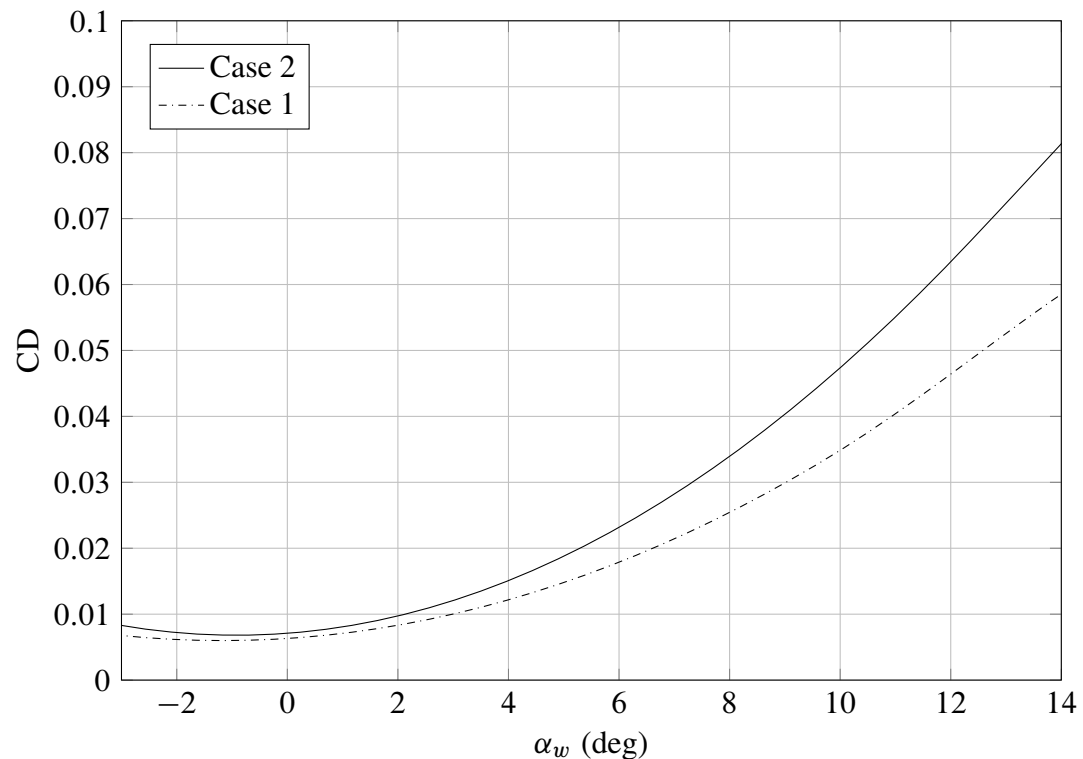


Figure 7.14: ATR 72 CD vs α_w at Mach 0.4. Method comparison.

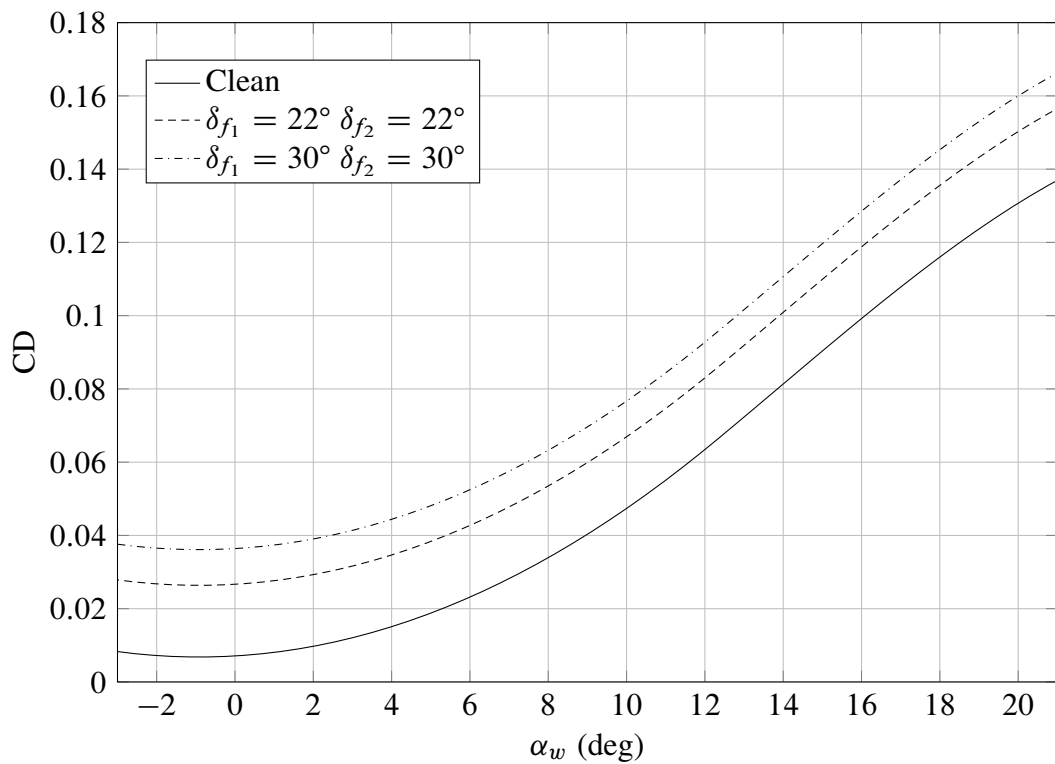


Figure 7.15: ATR 72 CD vs α_w at Mach 0.2. Clean and Flapped wing.

7.3.2 BOEING 747-100B

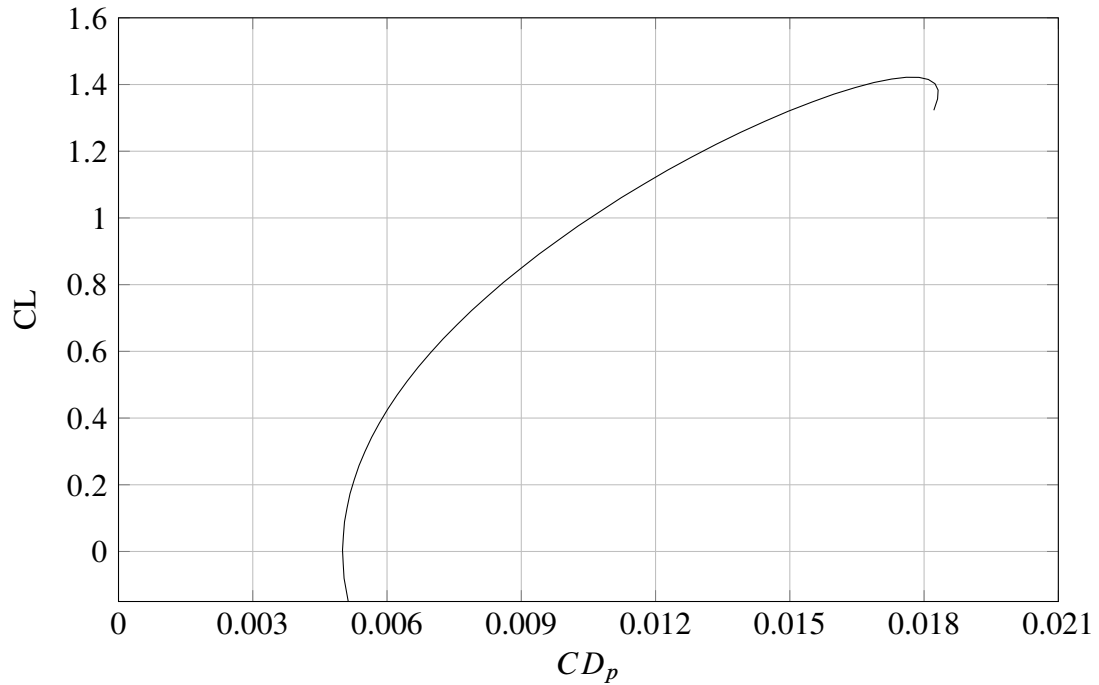


Figure 7.16: BOEING 747-100B CD vs CL at Mach 0.75. Parasite Drag.

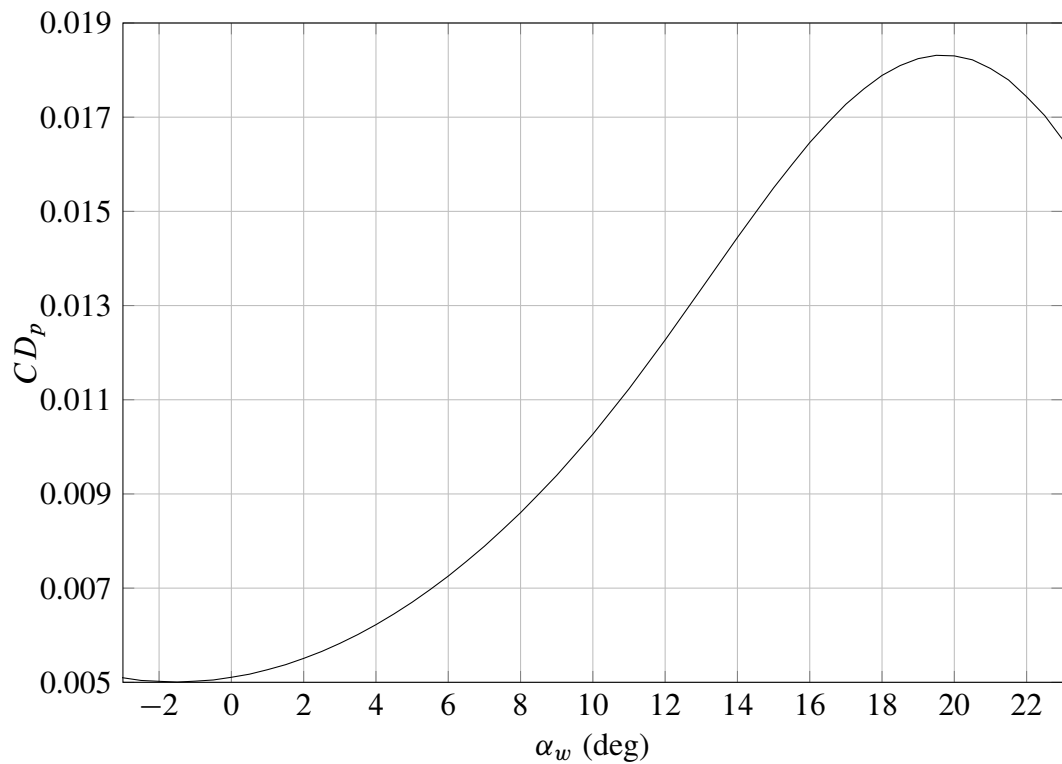


Figure 7.17: BOEING 747-100B CD vs α_w at Mach 0.75. Parasite Drag.

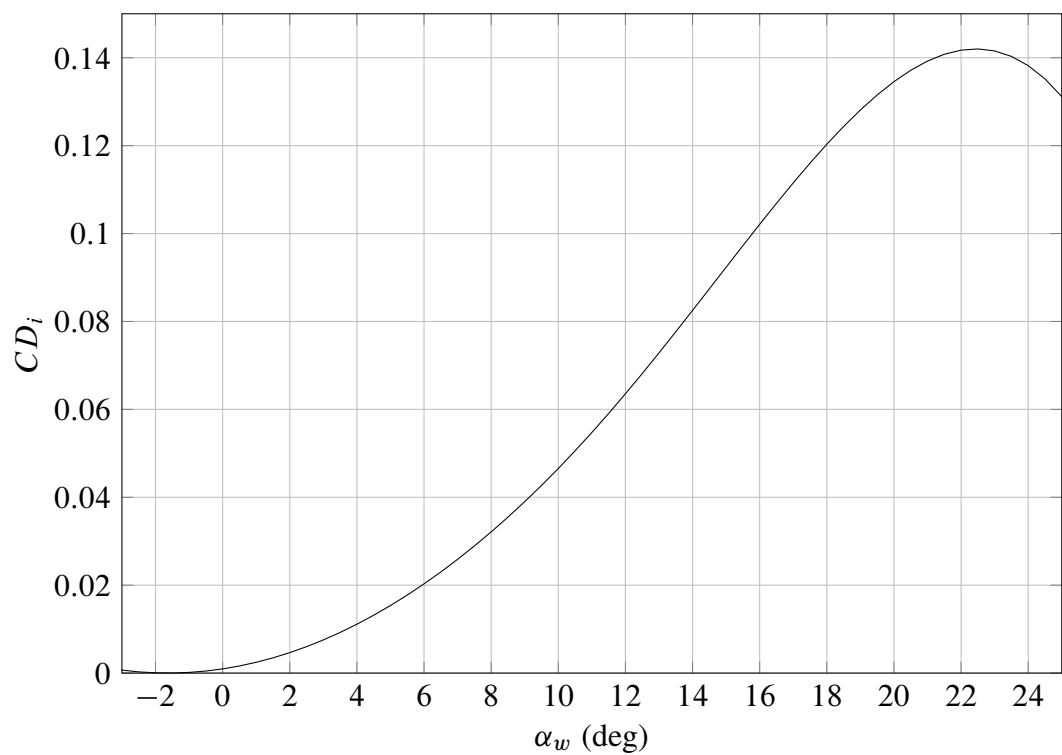


Figure 7.18: BOEING 747-100B CD vs α_w at Mach 0.75. Induced Drag.

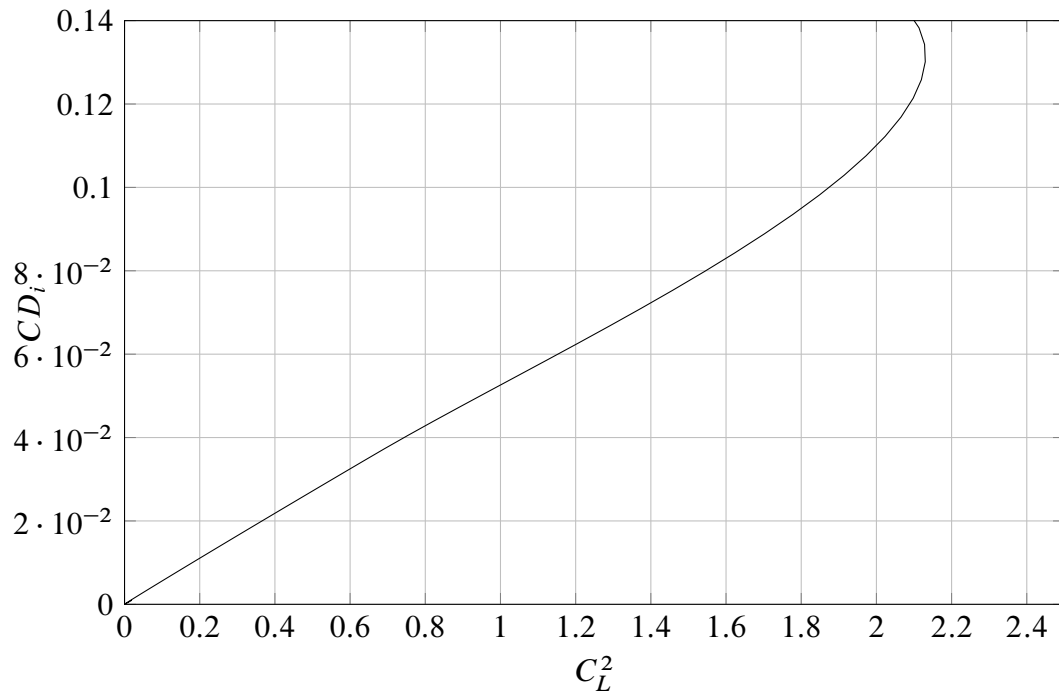


Figure 7.19: BOEING 747-100B CD_i vs C_L^2 at Mach 0.75.

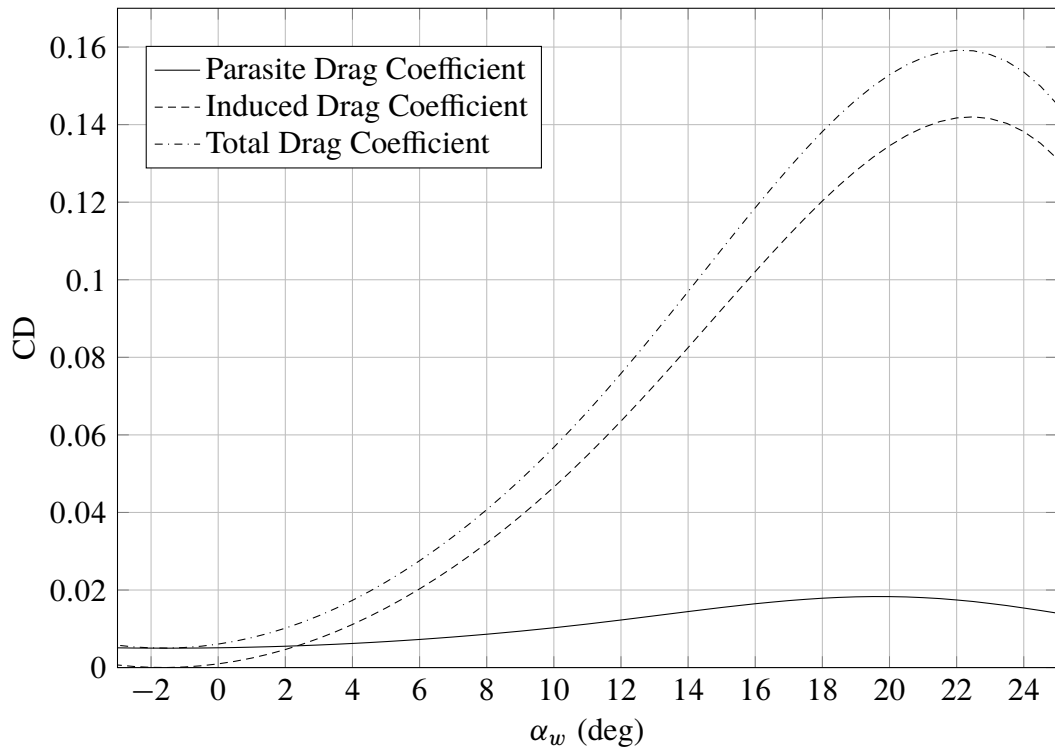


Figure 7.20: BOEING 747-100B CD vs α_w at Mach 0.75. Drag Coefficients calculated as case 2.

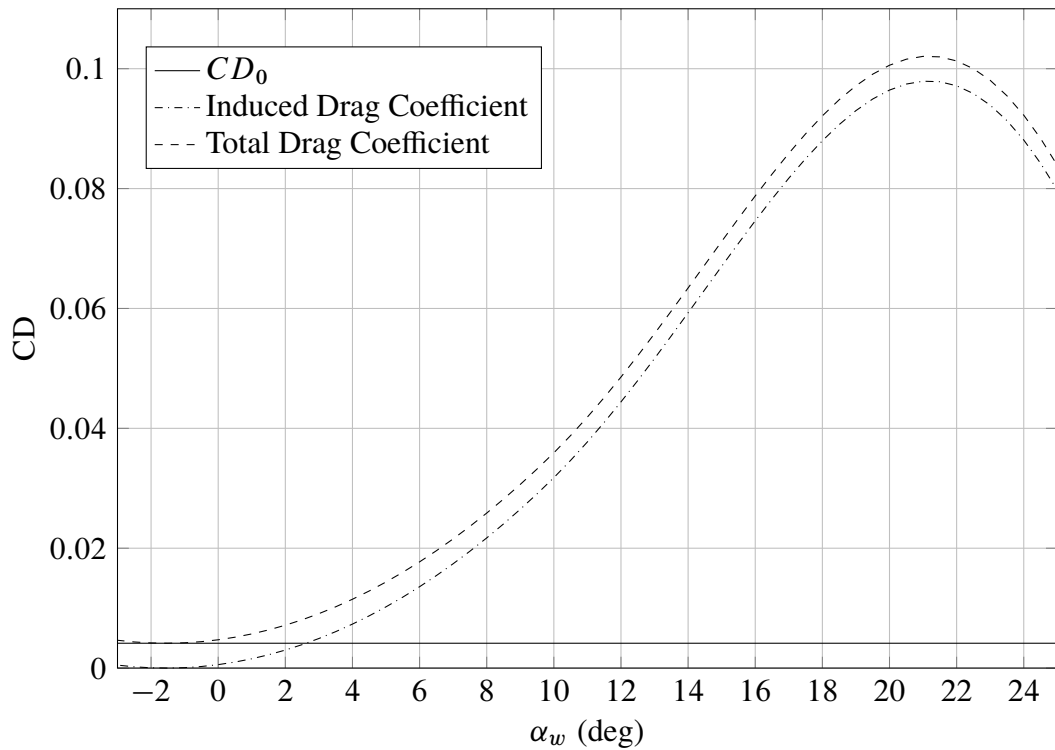


Figure 7.21: BOEING 747-100B CD vs α_w at Mach 0.75. Drag Coefficients calculated as case 1.

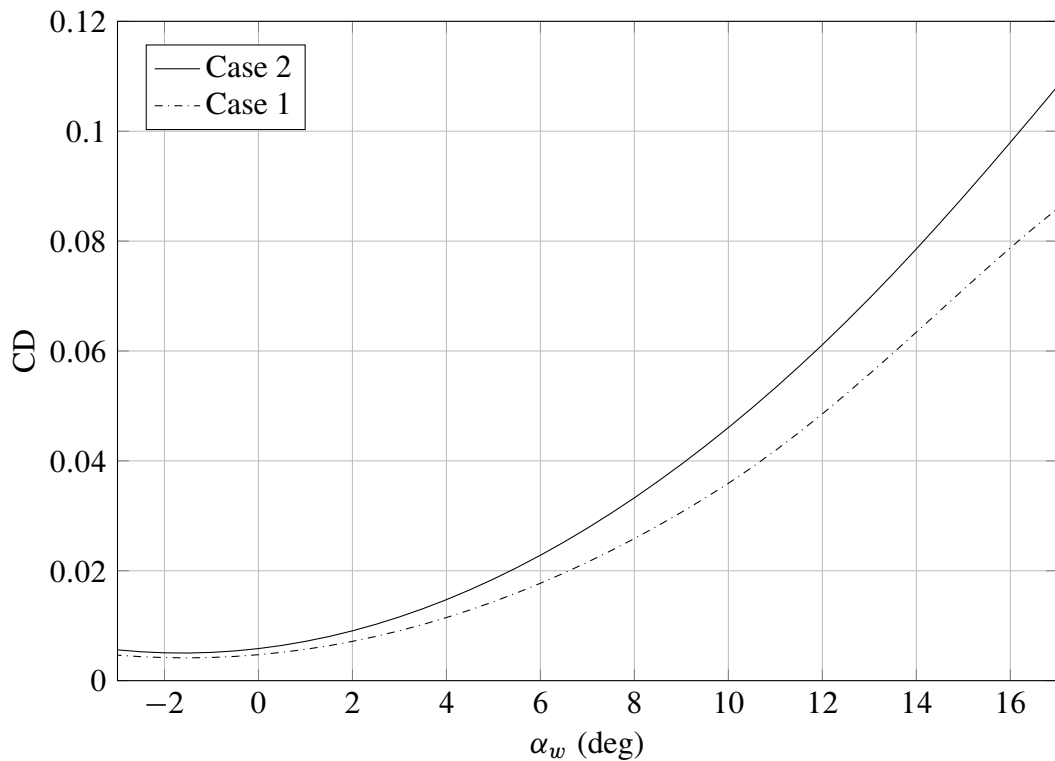


Figure 7.22: BOEING 747-100B CD vs α_w at Mach 0.75. Method comparison.

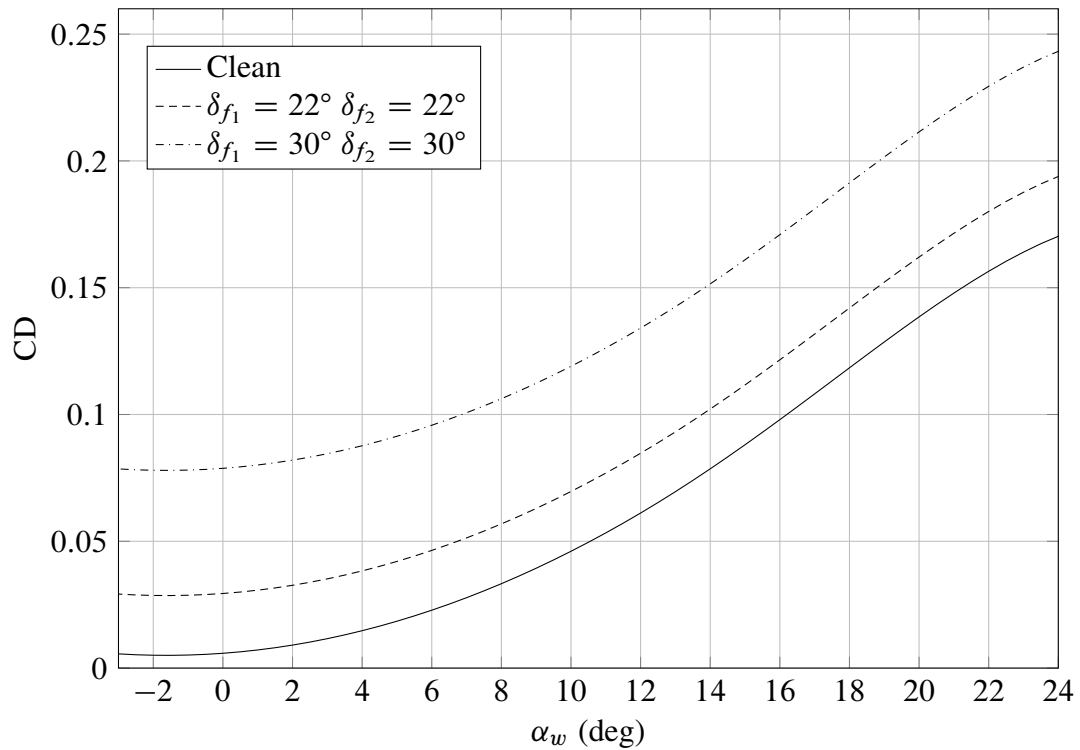


Figure 7.23: BOEING 747-100B CD vs α_w at Mach 0.2. Clean and Flapped wing.

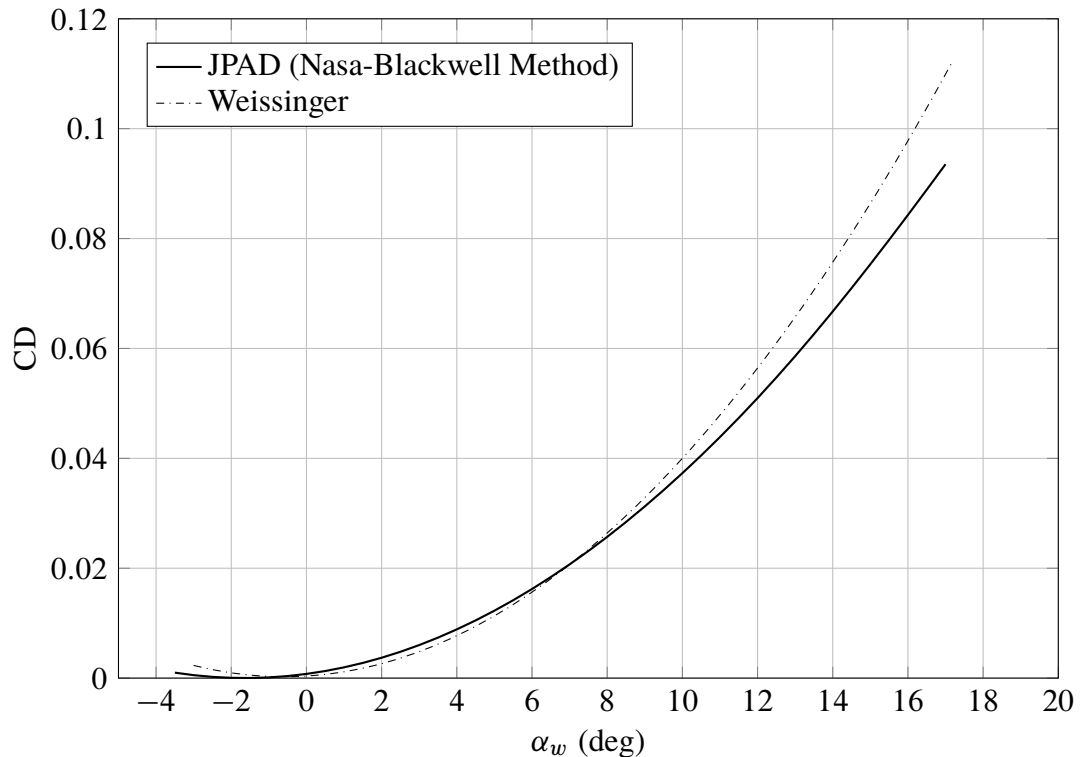


Figure 7.24: BOEING 747-100B CD_i vs α_w at Mach 0.75. Method comparison.

Chapter 8

Downwash Estimation

*The important thing is not to stop questioning.
Curiosity has its own reason for existing.*
– Albert Einstein

In order to evaluate the characteristics of longitudinal stability of an aircraft it's necessary to assess the flow direction aft of the wing. The contribution of horizontal tail surface to the airplane equilibrium and stability, in fact, strongly depends on the flow direction. The purpose of this chapter is to introduce and evaluate the downwash gradient due from the wing's vortex system, considering a dependence of the downwash angle from the absolute angle of attack.

8.1 Theoretical background

Due to the finite extension of the wing the lift distribution in span is not uniform. For this reason the difference of pressure between upper and lower surfaces generates a movement of air around the wingtips. The tendency is for particles of air to move from the region of high pressure around the wing tip to the region of low pressure (from positive lift from the lower wing surface to the upper surface). This made the wing's vortex system that consists of the bound vortex, located at the wing quarter chord and a vortex sheet which rolling up, at the wing tip, in two trailing vortex.[36] [43]

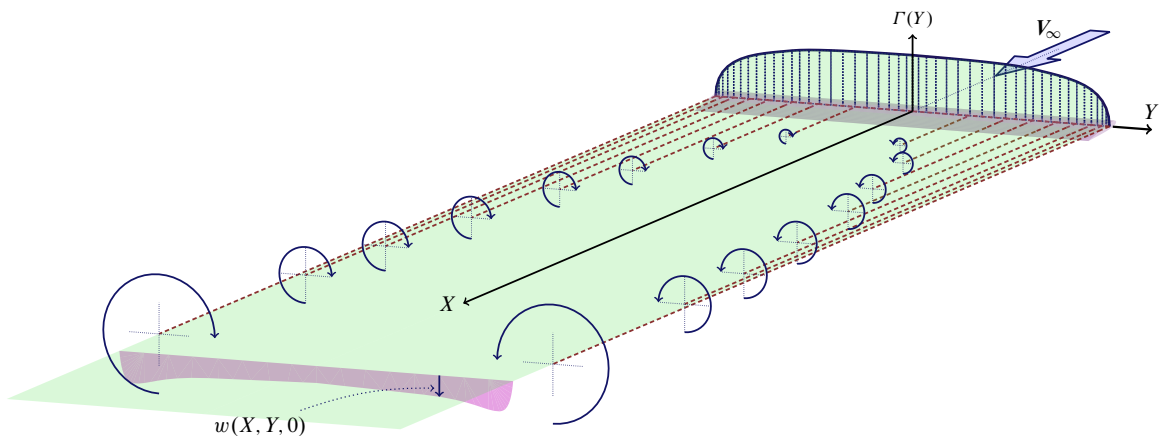


Figure 8.1: The wing vortex sheet.

The main effect of this vortex system is to deflect the airflow behind the wing downward relative to the direction of freestream flow. This angle of deviation is known as *Downwash Angle* ϵ . This phenomenon occurs for every lifting surface, but in subsonic flow a lifting surface also affects the flow forward of itself. In this region the vortex creates an itshape upwash, that is an upward flow deflection.

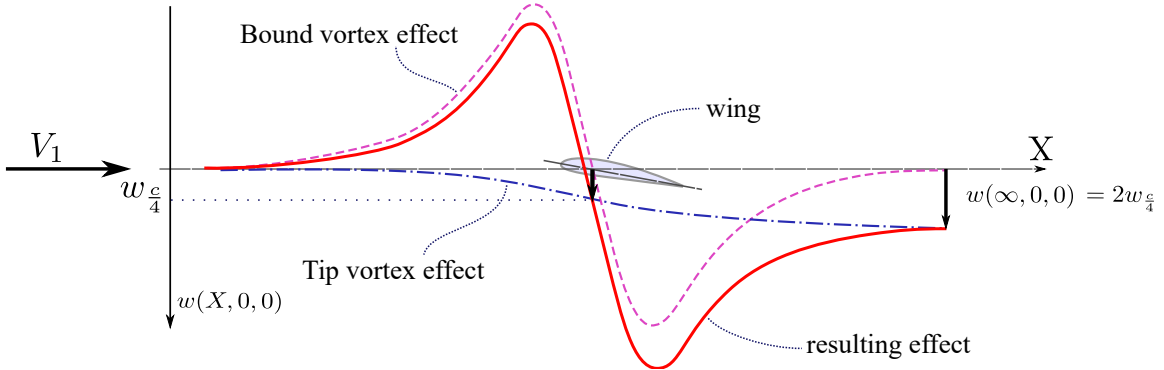


Figure 8.2: Upwash and Downwash in a finite wing.

As consequence of the downwash behind the wing, the local angle of attack on the horizontal tail is reduced by ϵ . In order to evaluate the flow direction behind the wing, an other important parameter is the change in downwash angle with angle of attack, that is the *Downwash Gradient* $\frac{d\epsilon}{d\alpha}$.

This parameter depends principally on the location of the horizontal tail respect to the wing and the vortex plane. As first approximation this value could be considered constant in alpha, but more accurately it's possible to evaluate this dependence considering the reference variable for the calculation of the distances. If the vertical distance is considered constant, starting from the downwash gradient, the downwash angle is :

$$\epsilon = \frac{d\epsilon}{d\alpha_w} (\alpha_w - \alpha_{0,w}) \quad (8.1)$$

In order to evaluate the downwash gradient we refer to fig. 8.3, where “ $r\frac{b}{2}$ ” is the distance between the aerodynamic center of wing and the aerodynamic center of the horizontal tail. In order to have a greater accuracy it is possible to measure this distance along the direction of local flow and, consequently, consider it as variable with the angle of attack. The parameter “ $m\frac{b}{2}$ ”, properly, is the distance between the horizontal tail and the vortex shed plane, but it is possible to approximate it with the distance between the horizontal tail and the wing root chord.[41]

Referring to [44] the equation used in order to evaluate the downwash gradient is the following:

$$\frac{d\epsilon}{d\alpha} = \frac{K_{\epsilon A}}{K_{\epsilon A=0}} \left(\frac{r}{r^2 + m_{tv}^2} \frac{0.4876}{\sqrt{r^2 + 0.6319 + m_{tv}^2}} + \left[1 + \left(\frac{r^2}{r^2 + 0.7915 + 5.0734m_{tv}^2} \right)^{0.3113} \right] \left\{ 1 - \sqrt{\frac{m_{tv}^2}{1 + m_{tv}^2}} \right\} \right) \frac{C_{L\alpha_w}}{\pi AR} \quad (8.2)$$

Considering a variable downwash gradient the changing parameters are “ $r \frac{b}{2}$ ”, $m \frac{b}{2}$ and the slope of the CL vs α curve.

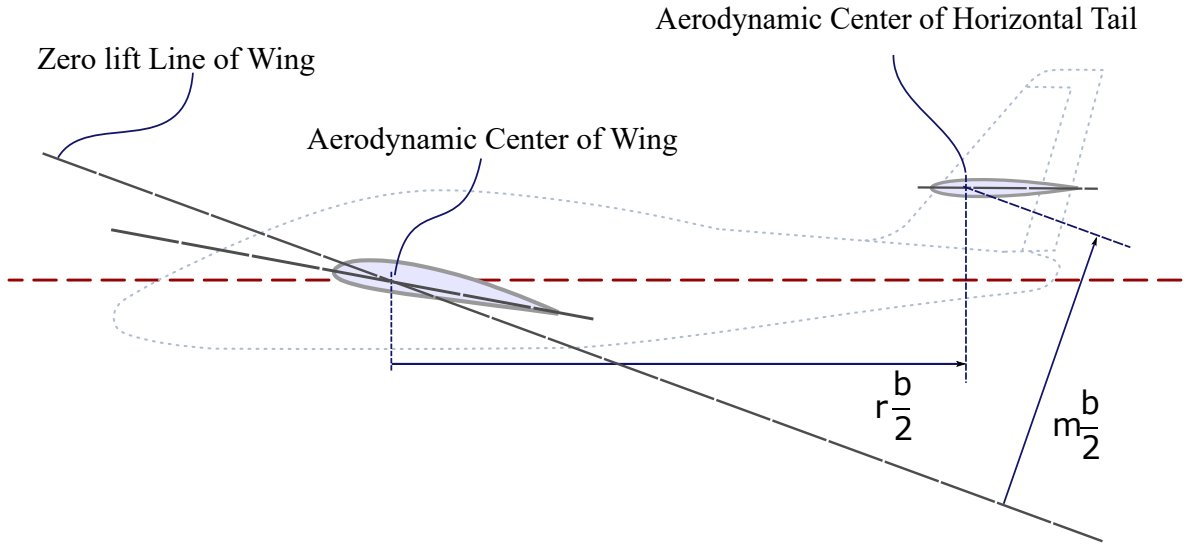


Figure 8.3: Dimensions for determination of Downwash Gradient, considering constant distances.

The two K_ϵ terms in the eq 8.2 accounting for the wing sweep angle effect are defined as follow (where Λ expressed in radians):

$$K_{\epsilon \Lambda} = \frac{0.1124 + 0.1265\Lambda + 0.1766\Lambda^2}{r^2} + \frac{0.1024}{r} + 2 \quad (8.3)$$

$$K_{\epsilon \Lambda=0} = \frac{0.1124}{r^2} + \frac{0.1024}{r} + 2 \quad (8.4)$$

These two terms are constant with α because it does not appear the variable parameter in them.

8.2 Java Class Architecture

In order to simplify the calculation of downwash, as mentioned, it is possible to assume the downwash gradient constant with the angle of attack. In this case the reference line to calculate the distance along z axis is the plane from the wing root chord or else the zero-lift line of the wing.

To obtain a more accurate analysis it is possible to consider the variation in alpha of the downwash gradient. So the reference line of wing it is not costant, but is the vortex sheed plane. The location of this plane depends from the value of downwash, but this location is itself necessary to evaluate the downwash. So it is necessary an iterative process in which the position of the vortex reference line at alpha is calculated from the value of downwash gradient at previous step.

In this process the reference angle of attack is the absolute angle α_a , that is the angle between the flow direction and the zero lift line of the wing. This choice is necessary because for $\alpha_a = 0$ it is possible to assume the downwash zero, but the downwash gradient is not null. In this way it is possible to assume the downwash value in the first step of the iteration

and to continue for each step with the previous value as first attempt. In view of stability, however, the reference angle of attack is the α_B . There two angles they are related by the relation: $\alpha_B = \alpha_{0L} - i_w + \alpha_a$.

The relation between the angles is in the fig 8.4.

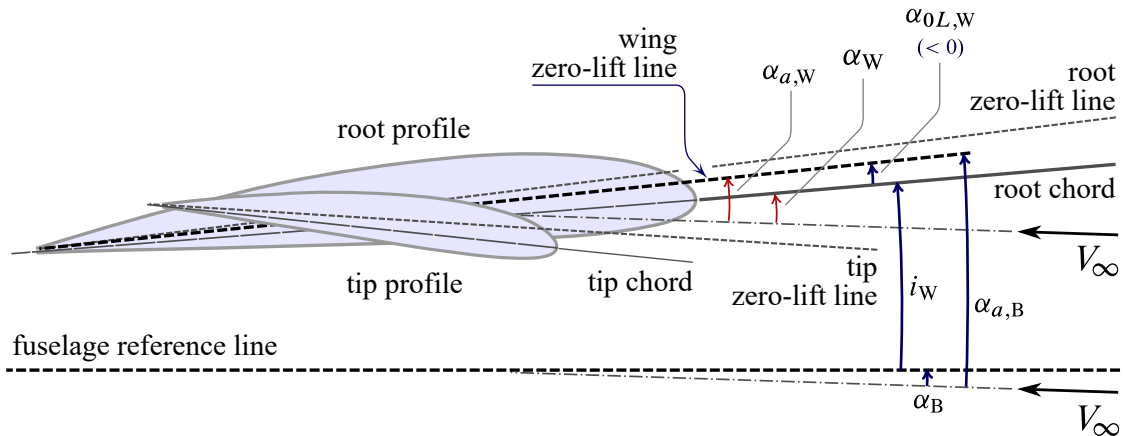


Figure 8.4: Definition of wing angles.

The downwash angle is calculated by a class named `DownwashCalculator`. The builder of this class defines and assigns all the geometrical variables, necessary to implement the calculation and defines an array of $C_{L\alpha}$. The `DownwashCalculator` class has seven methods and some overloads. The methods are explained in the table 8.1. The methods will be explained more in detail below.

`calculateDownwashGradientConstantDelft`

This method calculates the downwash gradient considering the vertical distance geometrical and constant

`calculateDownwashNonLinearDelft`

This method calculates the downwash considering a non constant downwash gradient.

`getDownwashAtAlphaBody`

This method returns the value of downwash angle, interpolating data filled before.

`calculateZDistanceZeroLift`

This method calculates the distance between the aerodynamic centre of horizontal tail and the zero lift line of the wing.

`Plot Methods ...`

Using these methods it is possible to plot the downwash angle, the downwash gradient and the distance in function of α_B

Table 8.1: Methods of `DownwashCalculator` class.

8.2.1 Constant Downwash Gradient

In order to evaluate the downwash angle case of constant downwash gradient it is necessary only to call the method `calculateDownwashGradientConstantDelft` using the distance from aerodynamic center of horizontal tail and the alpha zero lift line as input. It is possible to calculate this distance geometrically using the method `calculateZDistanceZeroLift` of the same class. The choice to calculate separately the distance and the downwash gradient is made to reuse the method to calculate downwash gradient simply varying the input distance.

This method has the downwash gradient as output. To obtain the angle of downwash it simply need to multiply the output value and the absolute angle of attack.

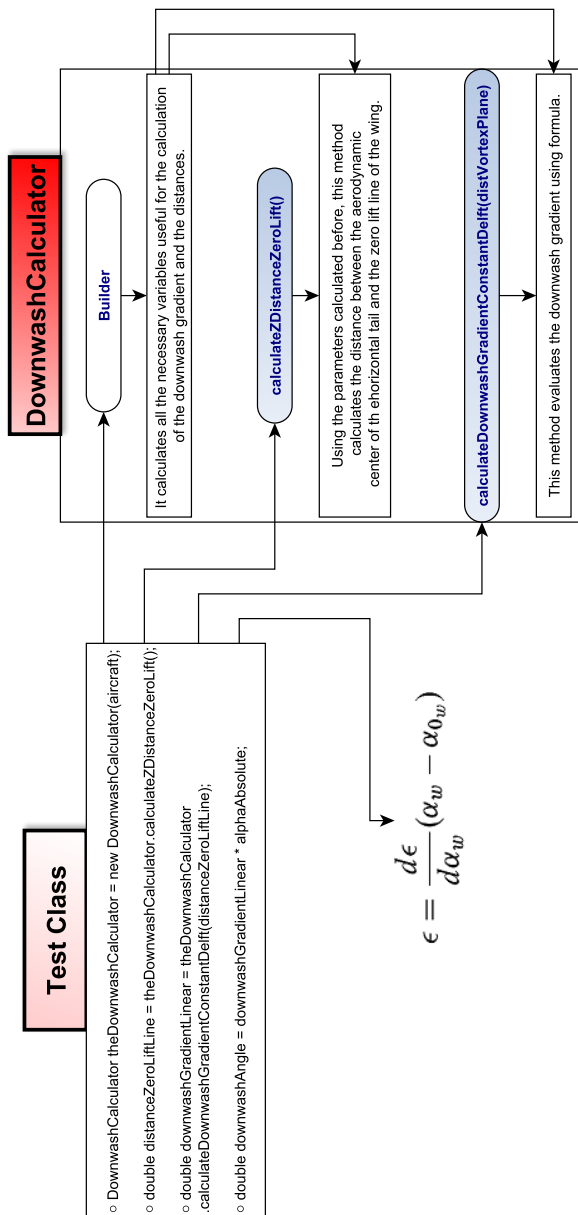


Figure 8.5: Flow chart of the calculation of linear downwash angle.

8.2.2 Variable Downwash Gradient

In order to evaluate the non-constant downwash gradient it is necessary to use the method `calculateDownwashNonLinearDelft`. This method calculates the downwash gra-

dient using Slingerland formula. The downwash gradient is considered variable with alpha absolute.

The distances considered in the formula are variable and they are measured from the vortex shed plane. These distances have been calculated referring to the geometrical construction proposed by [19].

First of all it is necessary to evaluate the geometrical distances m_0 and x_0 , then it is possible to evaluate step-by-step the other distances which, fixed geometry, only depend with alpha. Starting from a value of $\alpha_a = 0^\circ$ and proceeding with an increase of angle of attack equal to $\Delta\alpha$, the distances are the following (see fig. 8.6).

- $x_0 \rightarrow$ distance between the aerodynamic center of the wing and the aerodynamic center of the horizontal tail calculated along the x axis.
- $m_0 \rightarrow$ distance between the aerodynamic center of the horizontal tail and the horizontal line passing through the trailing edge of the airfoil root of the wing.
- $d \rightarrow$ distance between the trailing edge of the wing and the aerodynamic center of the horizontal tail. Considering the triangle $B\hat{C}D$ it is possible evaluate the hypotenuse as follows:

$$d = \sqrt{CD^2 + BD^2} \quad (8.5)$$

where CD is the distance m_0 defined before and it is possible to evaluate the distance BD geometrically:

$$BD = x_0 - \frac{3}{4}c_r \cos(i_w) \quad (8.6)$$

- $\psi \rightarrow$ This is the angle between the distance d and the horizontal reference line.

$$\psi = \arctan\left(\frac{m_0}{BD}\right) \quad (8.7)$$

Starting from these geometrical values it is possible to evaluate the distances m and r for each angle of attack.

- $m|_i = d \sin(\psi + i_w - \alpha_{0L} - i \Delta\alpha + \epsilon)$
- $x|_i = d \cos(\psi + i_w - \alpha_{0L} - i \Delta\alpha + \epsilon) + \frac{3}{4}c_r \cos(-\alpha_{0L} - i \Delta\alpha + \epsilon)$

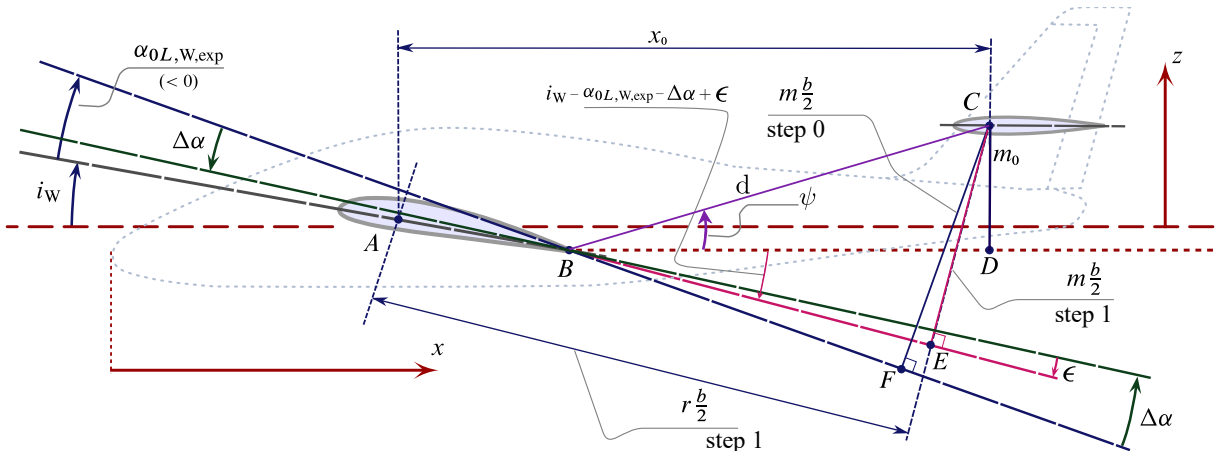


Figure 8.6: Arm definitions for downwash gradient evaluation.

The `calculateDownwashNonLinearDelft` method works uses these distances and through the following steps:

1. First of all this method creates an array of absolute angle of attack starting from $\alpha = 0^\circ$ to $\alpha = 20^\circ$ with a step of 0.25° .
2. The results array are initialized ($\alpha_a, \alpha_B, \frac{d\epsilon}{d\alpha}, \epsilon, m \frac{b}{2}$).
3. For the first step the state is the following:
 - $\alpha_a = 0^\circ$
 - $\alpha_B = \alpha_{0L} - i_w$
 - $\frac{d\epsilon}{d\alpha}$ is the constant value
 - $m = d \sin(\phi + i_w - \alpha_{0L})$
 - $r = d \cos(\phi + i_w - \alpha_{0L}) + 0.75c_r \cos(-\alpha_{0L})$
 - $\epsilon = 0$
4. Starting from the second step the process is iterative. Starting from $\alpha_a = 0^\circ$ the absolute angle of attack increase of $\Delta\alpha$. For the step i :
 - $\alpha_a|_i = i \Delta\alpha$
 - $\epsilon_{temp} = \epsilon_{i-1} + \frac{d\epsilon}{d\alpha}|_{i-1} * \Delta\alpha|_i$
 - $m \frac{b}{2}|_{temp}$ is calculated considering the temporary value of downwash angle.
 - $r \frac{b}{2}|_{temp}$ is calculated considering the temporary value of downwash angle.
 - $\frac{d\epsilon}{d\alpha}|_{temp}$ is calculated using the formula and the temporary value of distance.
 - $\epsilon_i = \epsilon_{i-1} + \frac{d\epsilon}{d\alpha}_{temp} * \Delta\alpha|_i$
 - $m \frac{b}{2}|_i$ is calculated considering the new value of downwash angle.
 - $r \frac{b}{2}|_i$ is calculated considering the new value of downwash angle.
 - $\frac{d\epsilon}{d\alpha}|_i$ is updated.
 - $\alpha_B = \alpha_{0L} - i_w + \alpha_a$

In order to relieve the calculations, the evaluation of downwash angle and downwash gradient should be done only one time. To obtain the value of epsilon at alpha body it is possible to call the method `getDownwashAtAlphaBody` that interpolates the value of downwash angle and angle of attack which field must be filled before.

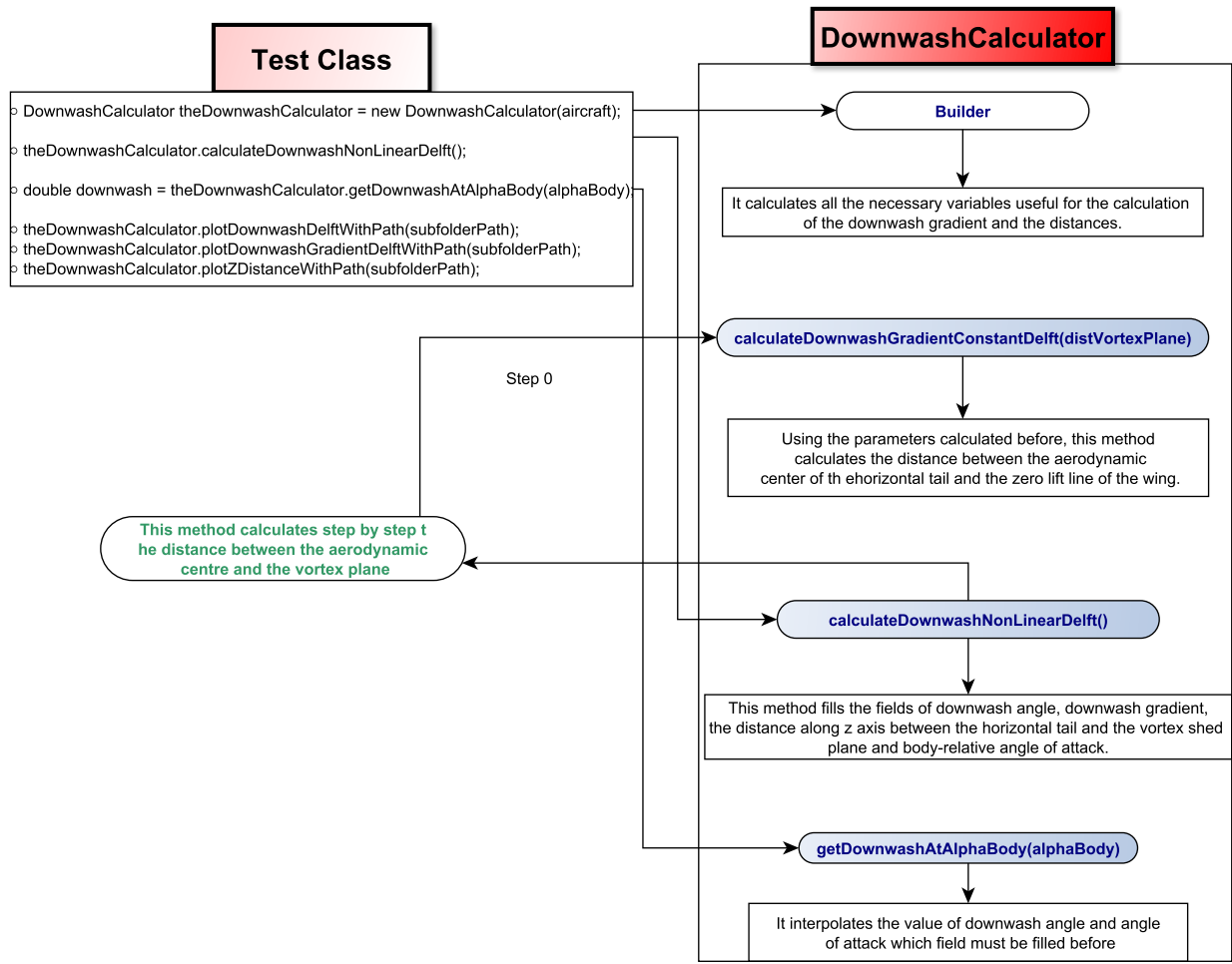


Figure 8.7: Flow chart of the calculation of non-linear downwash angle.

8.3 Case Study

Listing 8.1 Downwash Test Class

```

// -----
// INITIALIZE TEST CLASS ...
// -----

// -----Downwash-----

System.out.println("\n-----Start_of_downwash_calculation-----\n" );
DownwashCalculator theDownwashCalculator = new DownwashCalculator(aircraft);

theDownwashCalculator.calculateDownwashNonLinearDelft();

theDownwashCalculator.plotDownwashDelftWithPath(subFolderPath);
theDownwashCalculator.plotDownwashGradientDelftWithPath(subFolderPath);
theDownwashCalculator.plotZDistanceWithPath(subFolderPath);
theDownwashCalculator.plotXDistanceWithPath(subFolderPath);
System.out.println("_DONE_PLOTTING_DOWNWASH_ANGLE_vs_ALPHA_BODY");

double downwash = theDownwashCalculator.getDownwashAtAlphaBody(alphaBody);
Amount<Angle> downwashAmountRadian = Amount
    .valueOf(Math.toRadians(downwash), SI.RADIAN);
System.out.println( "At_alpha_" + alphaBody
    .to(NonSI.DEGREE_ANGLE)
    .getEstimatedValue() + "_(deg)_the_downwash_angle_is_(deg)_=" + downwash );
}
}

```

In the previous listing is reported the Test Class used in order to evaluate the variability of the downwash gradient with α_B . First of all the test class is initialized, after an Aircraft object is defined with the related analysis classes.

Below are the charts representing the results obtained by applying the method described at ATR 72 and BOEING 747-100B.

8.3.1 ATR-72

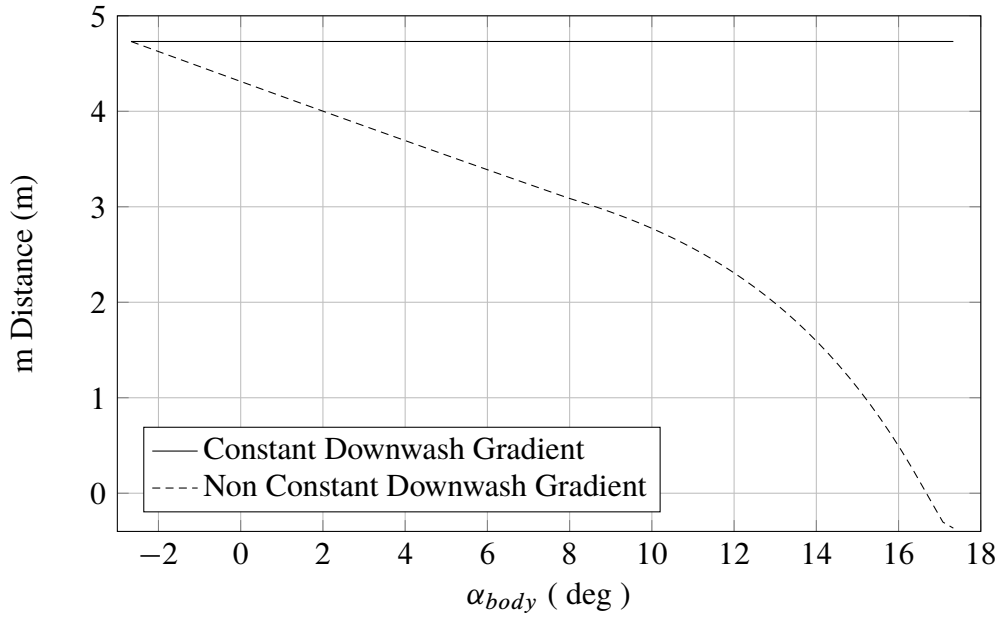


Figure 8.8: ATR 72 Distance between AC horizontal tail and vortex plane vs α_B .

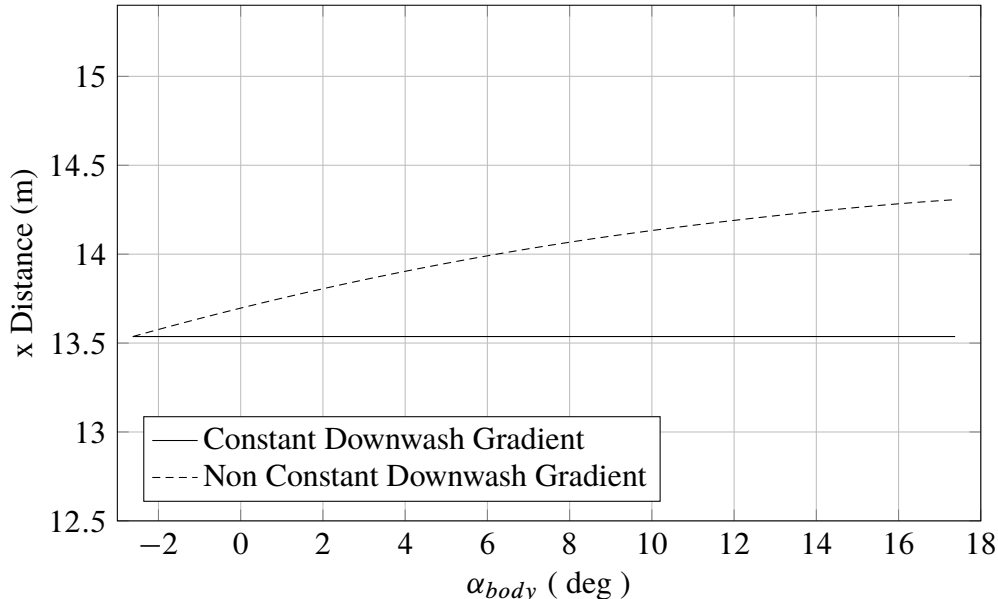
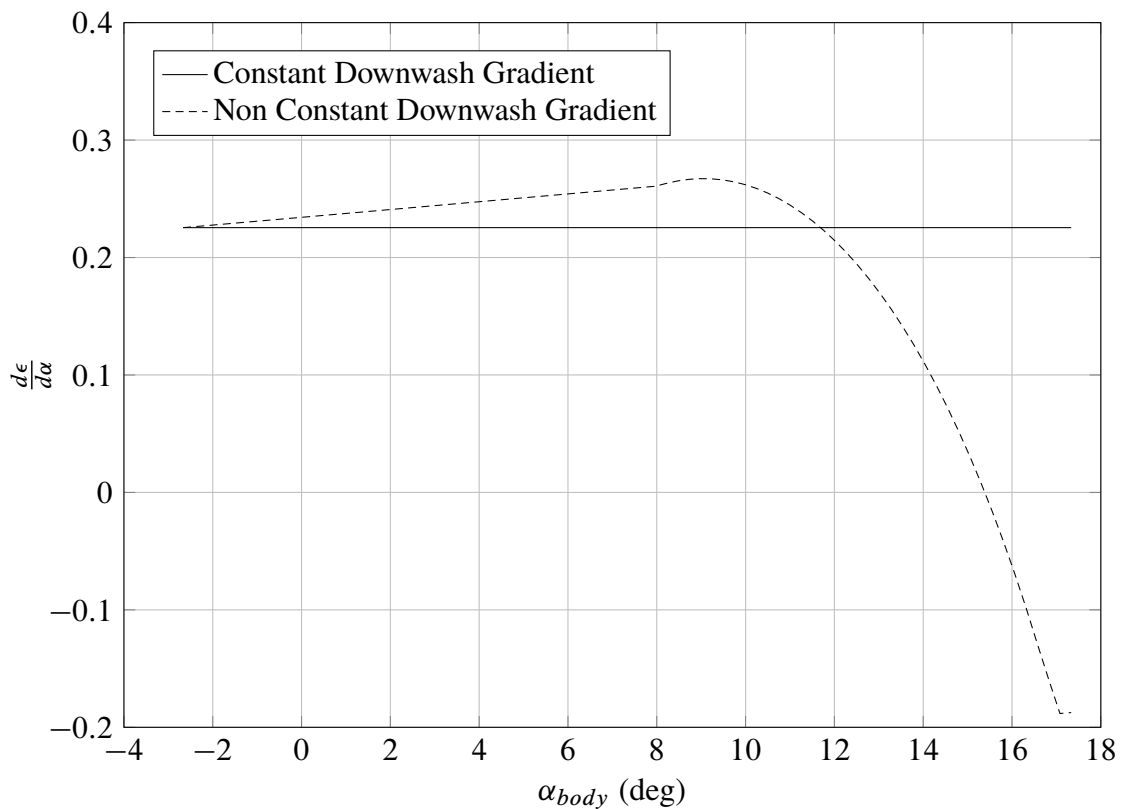
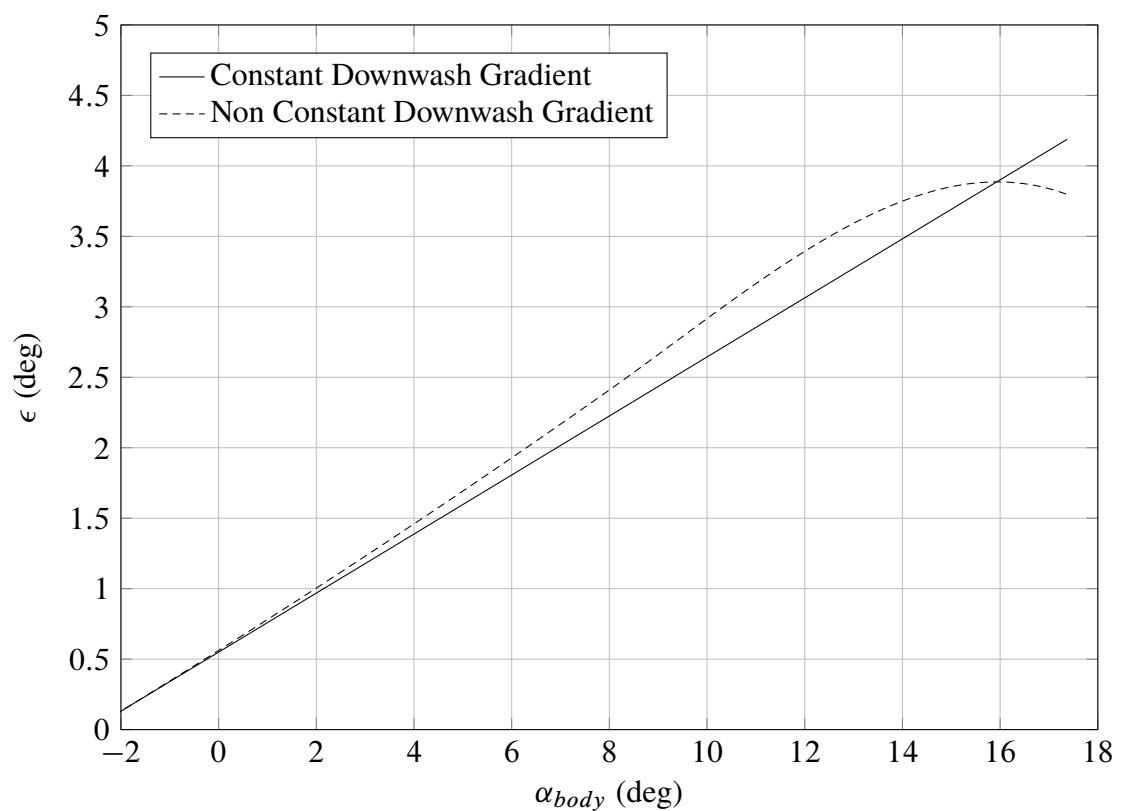


Figure 8.9: ATR 72 distance between AC horizontal tail and AC of wing along the m direction vs α_B .

Figure 8.10: ATR 72 Downwash gradient vs α_B . M=0.4Figure 8.11: ATR 72 Downwash angle vs α_B . M=0.4.

Listing 8.2 Downwash estimation - Results. ATR 72

```
-----Start of downwash calculation-----
DONE PLOTTING DOWNWASH ANGLE vs ALPHA BODY

At alpha 1.999999999999999 (deg) the downwash angle is (deg) = 1.1242568216721218
-----angles-----
Angle of attack alpha body (deg) = 2.0
Angle of incidence of horizontal tail (deg) 0.0
Downwash Angle at Alpha Body (deg) 1.1242568216721218
Angle of Attack of Horizontal Tail (deg) 0.8757431783278777
```

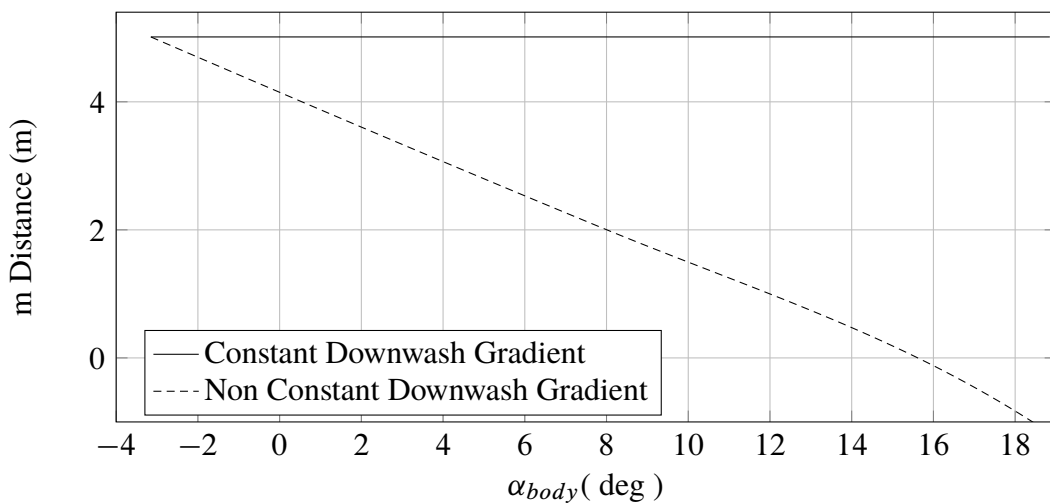
8.3.2 BOEING 747-100B

Figure 8.12: BOEING 747-100B Distance between AC horizontal tail and vortex plane vs α_B .

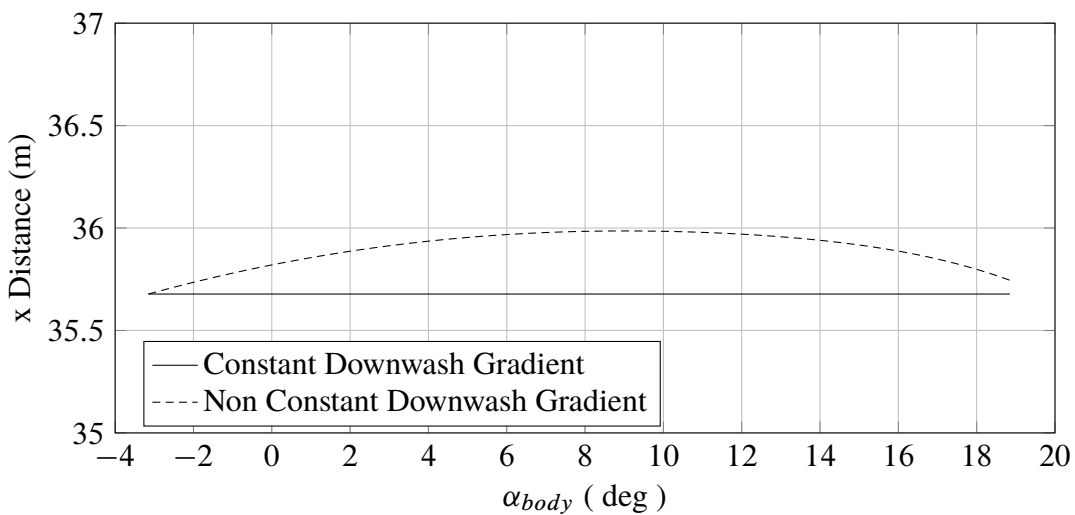


Figure 8.13: BOEING 747-100B distance between AC horizontal tail and AC of wing along the m direction vs α_B .

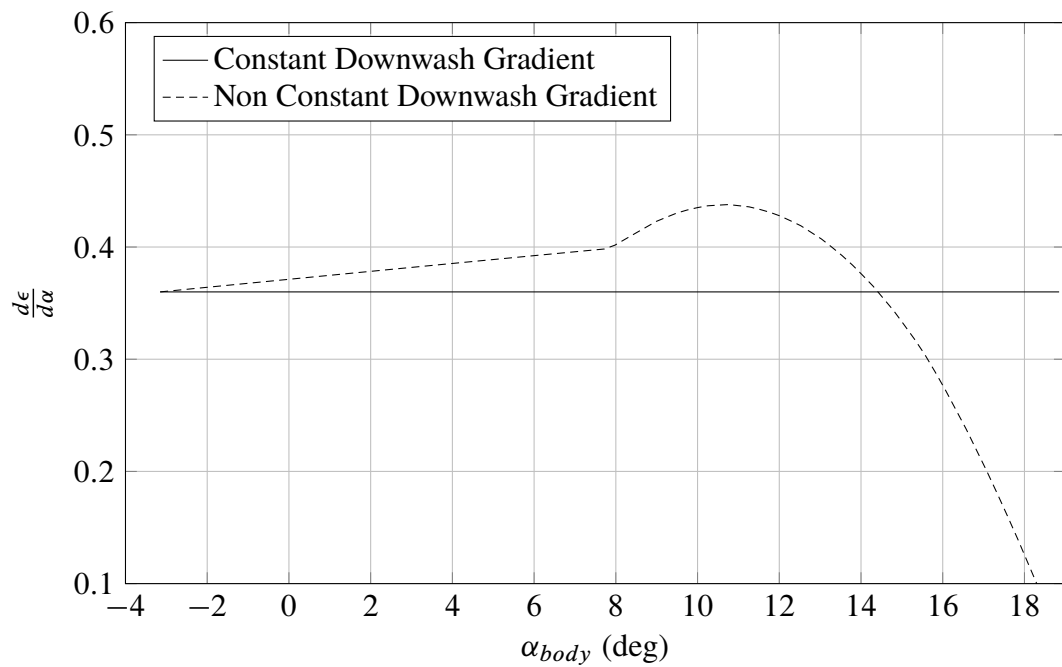


Figure 8.14: BOEING 747-100B Downwash gradient vs α_B .

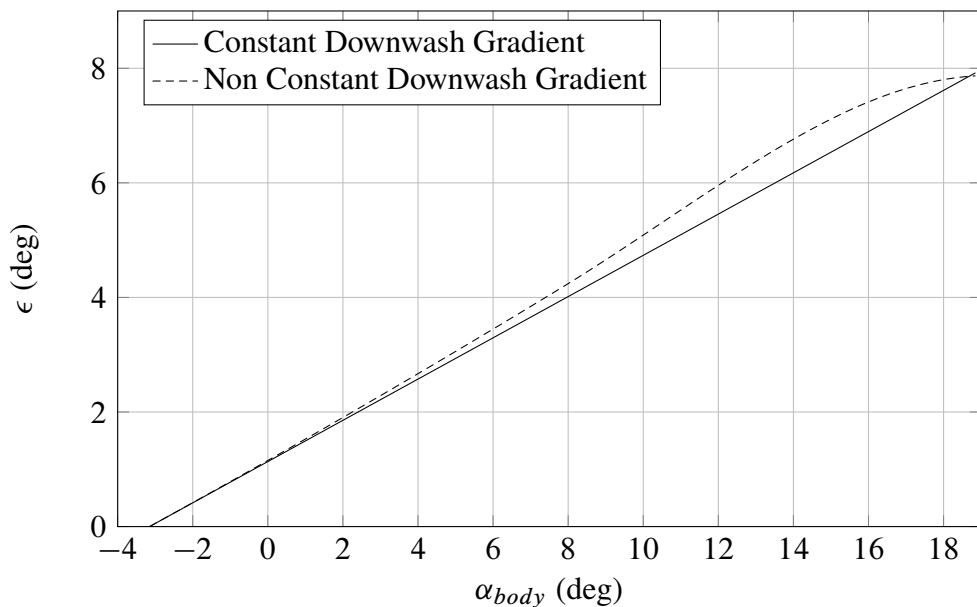


Figure 8.15: BOEING 747-100B Downwash angle vs α_B .

Listing 8.3 Downwash estimation - Results. BOEING 747-100B

```
-----Start of downwash calculation-----

DONE PLOTTING DOWNWASH ANGLE vs ALPHA BODY

At alpha 1.999999999999996 (deg) the downwash angle is (deg) = 2.540913931771228

-----angles-----
Angle of attack alpha body (deg) = 2.0
Angle of incidence of horizontal tail (deg) -0.999999999999998
Downwash Angle at Alpha Body (deg) 1.3810738944458758
Angle of Attack of Horizontal Tail (deg) -0.381073894445876
```

8.4 Results Comparison

In order to compare the achieved results three methods of downwash estimation have been implemented in Microsoft Excel using ATR 72 data. The distances are obtained using the explained method, while the equation are expressed in the following sections.

	A	B	C	D	E	F	G	H	I	J	K	L
1	AR	Cr	b/2	Λ_c/4	α₀_w	lw	λ	r = 1/λ	x₀	m₀	d	ϕ
2	12	2.497	13.53	0.0244	-0.02037	0.0262	0.636	1.57	13.74	4.09	12.55228	0.331897151

Figure 8.16: Useful data for the downwash estimation.

8.4.1 Slingerland Method

This is the method explained in the previous sections and this is the method that has been implemented in JPAD. This method has been presented in a master thesis by Mr. R. Slingerland, in TU Delft University. In order to evaluate the downwash, a model has been developed that computes the lift, drag and pitching moment in ground effect, utilizing Prandtl's lifting-line theory. As a by-product also the downwash in free air at the tail is determined. This model is innovative in the sense that it uses closed form expressions to include the vortex sheet relaxation, wing sweep and dihedral, the interaction of the wing-and flap vortices and the contribution of the rear fuselage-mounted nacelles. The equation presented in the relative section is valid also for swept wing.

α_abs	α_b	α_w	CL_α	CL	X	m	r (X/b/2)	m (m/b/2)
0	-2.66846	-1.1672	0.098283	0.115403	13.69173	4.3125	1.0119535	0.31873614
1	-1.66846	-0.1672	0.098283	0.213685	13.74589	4.156638	1.0159563	0.30721641
2	-0.66846	0.832799	0.098283	0.311968	13.79722	4.001444	1.0197504	0.29574603
3	0.331539	1.832799	0.098283	0.410251	13.84578	3.846964	1.0233396	0.28432844
4	1.331539	2.832799	0.098283	0.508534	13.89163	3.693241	1.0267279	0.27296684
5	2.331539	3.832799	0.098283	0.606817	13.93481	3.540316	1.0299196	0.26166415
6	3.331539	4.832799	0.098283	0.7051	13.97539	3.388223	1.0329185	0.25042302
7	4.331539	5.832799	0.098283	0.803382	14.01341	3.236996	1.035729	0.23924585
8	5.331539	6.832799	0.098283	0.901665	14.04883	3.087177	1.0383466	0.22817274
9	6.331539	7.832799	0.098283	0.999948	14.08041	2.944824	1.0406811	0.21765147
10	7.331539	8.832799	0.098279	1.098435	14.1157	2.773978	1.0432886	0.20502421
11	8.331539	9.832799	0.099188	1.197844	14.155	2.564952	1.0461934	0.18957518
12	9.331539	10.8328	0.098887	1.2945	14.19764	2.307337	1.0493449	0.1705349
13	10.33154	11.8328	0.094048	1.383858	14.24162	1.988892	1.052596	0.14699868
14	11.33154	12.8328	0.084661	1.461369	14.28292	1.594331	1.0556485	0.1178367
15	12.33154	13.8328	0.070728	1.522487	14.31415	1.104207	1.0579568	0.08161176
16	13.33154	14.8328	0.052247	1.562665	14.32233	0.49357	1.0585611	0.03647967
17	14.33154	15.8328	0.02922	1.577357	14.28729	-0.24306	1.0559711	-0.0179648
18	15.33154	16.8328	0.001646	1.562016	14.27707	-0.36564	1.0552155	-0.02702438
19	16.33154	17.8328	-0.03048	1.523058	14.27707	-0.36564	1.0552155	-0.02702438

K _e _Λ	K _e _Λ0	dε/dα_k	dε/dα_1	dε/dα_2	dε/dα_3	dε/dα	ε
2.214067	2.210951	1.001409702	0.330651716	1.77409674	0.696316791	0.23438014	0
2.212781	2.209689	1.001399415	0.331606975	1.77897598	0.706329751	0.23769521	0.21143035
2.211574	2.208505	1.001389765	0.332530655	1.78369771	0.716396797	0.24101781	0.4259958
2.210444	2.207396	1.001380727	0.333423753	1.7882588	0.726511501	0.24434544	0.64372387
2.209386	2.206358	1.001372274	0.334287221	1.79265637	0.736667486	0.24767557	0.8646402
2.208399	2.20539	1.001364381	0.335121968	1.79688781	0.74685845	0.2510057	1.08876841
2.207478	2.204486	1.001357026	0.335928864	1.80095076	0.757078187	0.25433332	1.31612997
2.206622	2.203647	1.001350185	0.33670874	1.80484314	0.767320617	0.25765594	1.54674412
2.20583	2.20287	1.00134386	0.337459789	1.80855073	0.777544614	0.26095978	1.78062772
2.205128	2.202181	1.001338256	0.338154161	1.81193321	0.787327624	0.26410867	2.01779519
2.20435	2.201417	1.001332037	0.338963094	1.81580788	0.79915362	0.26788807	2.25825843
2.203488	2.200572	1.001325159	0.339917461	1.82026673	0.813742218	0.27505695	2.50332385
2.202561	2.199662	1.001317756	0.341041995	1.82532198	0.831892053	0.27999848	2.75756077
2.201612	2.198731	1.001310183	0.342354632	1.83087507	0.854564259	0.27308717	3.01114473
2.200728	2.197864	1.001303131	0.343865032	1.83664419	0.882972991	0.25338621	3.25322266
2.200064	2.197213	1.001297836	0.345565418	1.84202134	0.918658676	0.21945666	3.47250301
2.199891	2.197043	1.001296454	0.347411702	1.84852539	0.963544576	0.16913088	3.65718809
2.200635	2.197773	1.001302389	0.349222757	1.84599277	0.9820381	0.09619569	3.79512403
2.200853	2.197987	1.001304128	0.349463614	1.84555061	0.972985486	0.00537498	3.87352941
2.200853	2.197987	1.001304128	0.349463614	1.84555061	0.972985486	-0.099561	3.87884407

Figure 8.17: Data used for the calculation of downwash using Delft method.

8.4.2 NACA Modified Method

This method has been explained by Prof. Vincenzo Giordano[19] based on the results obtained in NACA Report -648 [43]. The downwash behind a wing is mainly a function of the wing loading and is a manifestation of the associated vortex system. A first approximation to the downwash is obtained by assuming the sheet to originate at the quarter-chord line and to extend unchanged indefinitely downstream, the vortex system thereby consisting of elementary U-vortices (or horseshoe vorticcs). The actual sheet, however, does not extend unaltered from the lifting line to infinity because, as a result of the air motions that the vortex system itself creates, it is rapidly displaced downward and deformed. Inasmuch as the downwash depends to a predominant extent on the trailing vortex sheet, a vertical displacement of the sheet causes a vertical displacement of the entire downwash pattern by the same amount.

This method introduces a function Φ useful in order to evaluate the downwash gradient and the downwash angle.

$$\Phi = \Phi(\mathcal{R}, \lambda, \alpha) \quad (8.8)$$

Starting from this function it is possible to evaluate the downwash gradient as follows:

$$\frac{d\epsilon}{d\alpha} = C_{L_\alpha} \Phi + C_L \frac{d\Phi}{d\alpha} \quad (8.9)$$

The value of Φ is obtained from charts fixed the \mathcal{R} and λ . The process is explained following.

1. An array of absolute angle of attack is defined
2. Each value of α_a corresponds to an angle α_b and to an angle α_w
3. For each α is calculated the value of the lift coefficient curve slope
4. The relative value of C_L is calculated
5. Using the geometrical construction introduced before the distances “m” and “x” is calculated
6. Consequently the percentages distances “ $\frac{m}{2} 100$ ” and “ $\frac{x}{2} 100$ ” is calculated

7. With the obtained value of “x” it is possible to enter in a chart that are parametrized for “x”, “m” and λ value. There are three charts for $x = 70$, $x = 80$, $x = 90$. If the obtained value is not between these it is possible to do a linear interpolation
8. For each value of \mathcal{R} and “x” there are four curves in a chart that corresponding to different values of “m”. The first curve represents the value of “m” for which the plan is in the slipstream. The other curves differ from the first one for $m \pm 10$. It’s necessary to obtain the value of Φ corresponding to the real value of “m”.

Known the value of the dowhwash gradient for each angle of attack it’s possible to evaluate the angle of downwash

$$\epsilon = \frac{d\epsilon}{d\alpha} \alpha_a \quad (8.10)$$

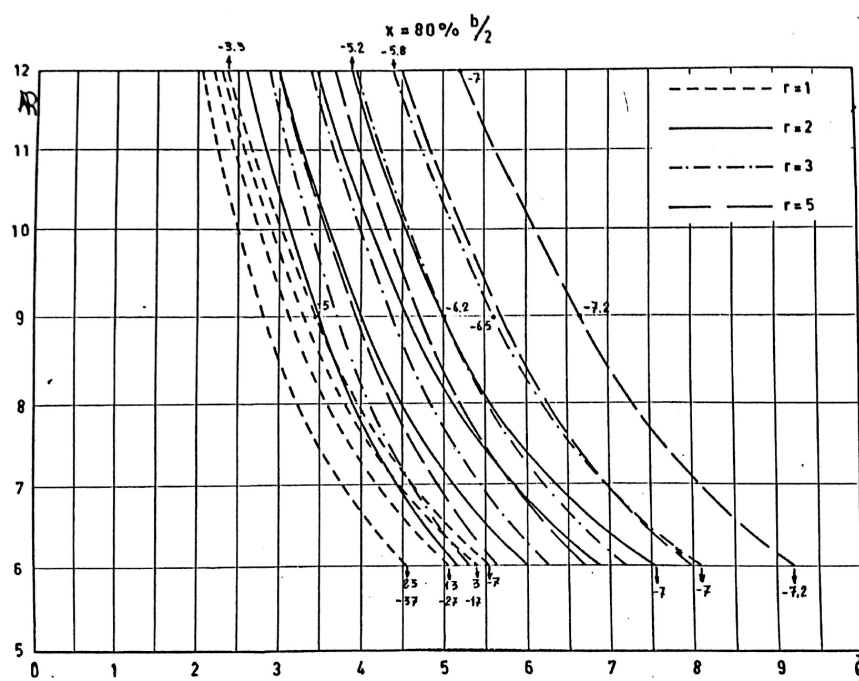


Figure 8.18: Chart for the evaluation of Φ for $x = 80$

α_{abs}	α_b	α_w	CL_α	CL	x	X_p	m	m_p	Φ	ϵ	$d\Phi/d\alpha$	$d\epsilon/d\alpha$
0	-2.668461	-1.167201	0.0982828	6.23E-04	13.615251	100.63009	4.4337679	32.769903	2.09240143	0.0013046	0.0209253	0.20566019
1	-1.668461	-0.167201	0.0982828	0.0918654	13.689696	101.18031	4.2281617	31.250271	2.11332673	0.19414161	0.02109714	0.20964184
2	-0.668461	0.832799	0.0982828	0.1831073	13.759971	101.69971	4.0212678	29.721122	2.13442387	0.39082862	0.02128544	0.21367475
3	0.331539	1.832799	0.0982828	0.2743492	13.826055	102.18814	3.8131491	28.18292	2.15570931	0.59141718	0.02149098	0.21776525
4	1.331539	2.832799	0.0982828	0.3655911	13.887929	102.64545	3.603869	26.636135	2.17720029	0.79596513	0.02171451	0.22192005
5	2.331539	3.832799	0.0982828	0.456833	13.945573	103.07149	3.3934914	25.081237	2.1989148	1.004553695	0.02195672	0.22614614
6	3.331539	4.832799	0.0982828	0.548075	13.998969	103.46614	3.1820802	23.5187	2.22087153	2.12720407	0.02221826	0.23045082
7	4.331539	5.832799	0.0982828	0.6393169	14.048102	103.82928	2.9696998	21.949001	2.24308978	1.43404514	0.0224997	0.23484166
8	5.331539	6.832799	0.0982828	0.7305588	14.092956	104.1608	2.756415	20.372617	2.26558948	1.65514629	0.02280159	0.23932646
9	6.331539	7.832799	0.0982828	0.8218007	14.133519	104.4606	2.5422907	18.790027	2.28839108	1.88060137	0.02312441	0.24391317
10	7.331539	8.832799	0.098279	0.9130426	14.169776	104.72857	2.3273921	17.201715	2.31151549	2.11051211	0.02344899	0.24858345
11	8.331539	9.832799	0.099188	1.0044864	14.201718	104.96466	2.1117846	15.608164	2.33496448	2.34544014	0.02362494	0.2553314
12	9.331539	10.832799	0.0988874	1.0978944	14.229335	105.16877	1.895534	14.00986	2.35858942	2.58948217	0.02399902	0.25958311
13	10.331539	11.832799	0.0940478	1.1914556	14.252617	105.34085	1.6787061	12.407288	2.38258845	2.83874838	0.02476592	0.25358462
14	11.331539	12.832799	0.0846612	1.2813236	14.271559	105.48085	1.4613669	10.800938	2.40735436	3.0845999	0.02595775	0.2370699
15	12.331539	13.832799	0.0707278	1.3632983	14.286155	105.58873	1.2435826	9.1912976	2.43331211	3.3173303	0.02752867	0.20963252
16	13.331539	14.832799	0.0522473	1.4336509	14.296399	105.66444	1.0254195	7.5788582	2.46084078	3.52798668	0.02949132	0.17085263
17	14.331539	15.832799	0.0292199	1.4885331	14.302289	105.70798	0.8069442	5.9641106	2.4903321	3.70694178	0.03184852	0.12017492
18	15.331539	16.832799	0.0016455	1.5240946	14.303823	105.71931	0.588223	4.3475465	2.52218062	3.84404187	0.03460436	0.05689066
19	16.331539	17.832799	-0.03048	1.5364852	14.301001	105.69845	0.3693228	2.7296583	2.55678498	3.92846221	0.044544	-0.0094906
20	17.331539	18.832799	-0.057431	1.5218546	13.406425	99.086656	4.6380238	34.279555	-1.8566011	-2.825477	-0.1071227	-0.0563987

Figure 8.19: Input and output values of NACA method.

8.5 Roskam Method

For the evaluation of downwash ratio at the horizontal tail the following equation at low speed is suggested:

$$\frac{d\epsilon}{d\alpha} = 4.44 \left[K_A K_\lambda K_H \sqrt{\cos \Gamma_{\frac{c}{4}}} \right]^{1.19} \quad (8.11)$$

Where the K parameters are:

$$K_A = \frac{1}{A} - \frac{1}{1 + AR^{1.7}} \quad (8.12)$$

$$K_\lambda = \frac{10 - 3\lambda}{7} \quad (8.13)$$

$$K_H = \frac{1 - \frac{h_H}{b}}{\sqrt[3]{\frac{2l_H}{b}}} \quad (8.14)$$

α_{abs}	α_b	α_w	CL_α	CL	X	m	K_A	K_λ	K_H	$d\epsilon/d\alpha$	ϵ
0	-2.66846	-1.1672	0.098283	0.115403	13.69173	4.3125	0.08	1.156	0.837309	0.211416	0
1	-1.66846	-0.1672	0.098283	0.213685	13.74589	4.156638	0.08	1.156	0.841937	0.212807	0.212807
2	-0.66846	0.832799	0.098283	0.311968	13.79722	4.001444	0.08	1.156	0.84659	0.214207	0.428414
3	0.331539	1.832799	0.098283	0.410251	13.84578	3.846964	0.08	1.156	0.851264	0.215615	0.646846
4	1.331539	2.832799	0.098283	0.508534	13.89163	3.693241	0.08	1.156	0.855958	0.217031	0.868123
5	2.331539	3.832799	0.098283	0.606817	13.93481	3.540316	0.08	1.156	0.860669	0.218453	1.092264
6	3.331539	4.832799	0.098283	0.7051	13.97539	3.388223	0.08	1.156	0.865395	0.219881	1.319287
7	4.331539	5.832799	0.098283	0.803382	14.01341	3.236996	0.08	1.156	0.870135	0.222135	1.549206
8	5.331539	6.832799	0.098283	0.901665	14.04883	3.087177	0.08	1.156	0.874871	0.222749	1.781994
9	6.331539	7.832799	0.098283	0.999948	14.08041	2.944824	0.08	1.156	0.879407	0.224124	2.01712
10	7.331539	8.832799	0.098279	1.098435	14.1157	2.773978	0.08	1.156	0.884899	0.225791	2.25791
11	8.331539	9.832799	0.099188	1.197844	14.155	2.564952	0.08	1.156	0.891689	0.227854	2.506394
12	9.331539	10.8328	0.098887	1.2945	14.19764	2.307337	0.08	1.156	0.900163	0.230433	2.765201
13	10.33154	11.8328	0.094048	1.383858	14.24162	1.988892	0.08	1.156	0.910804	0.233679	3.037821
14	11.33154	12.8328	0.084661	1.461369	14.28292	1.594331	0.08	1.156	0.924246	0.237788	3.329033
15	12.33154	13.8328	0.070728	1.522487	14.31415	1.104207	0.08	1.156	0.941349	0.243033	3.645502
16	13.33154	14.8328	0.052247	1.562665	14.32233	0.49357	0.08	1.156	0.963312	0.249796	3.996735
17	14.33154	15.8328	0.02922	1.577357	14.28729	-0.24306	0.08	1.156	0.990831	0.258311	4.391282
18	15.33154	16.8328	0.001646	1.562016	14.27707	-0.36564	0.08	1.156	0.995517	0.259765	4.675771
19	16.33154	17.8328	-0.03048	1.523058	14.27707	-0.36564	0.08	1.156	0.995517	0.259765	4.935536
20	17.33154	18.8328	-0.05743	1.523058	14.27707	-0.36564	0.08	1.156	0.995517	0.259765	5.195302

Figure 8.20: Input and output values of Roskam method.

This method does not consider a variation of distances with α . But the values of h_H and l_H are considered as variable.

It's important to note that in this equation there isn't the $C_{L\alpha}$ contributor so this non linear effect is not considerate.

8.5.1 Results

As it is possible to see in the following charts the obtained values and the trend are confrontable for low angles of attack. At elevate angles the Roskam method does not see the effect of the reduction of $C_{L\alpha}$.

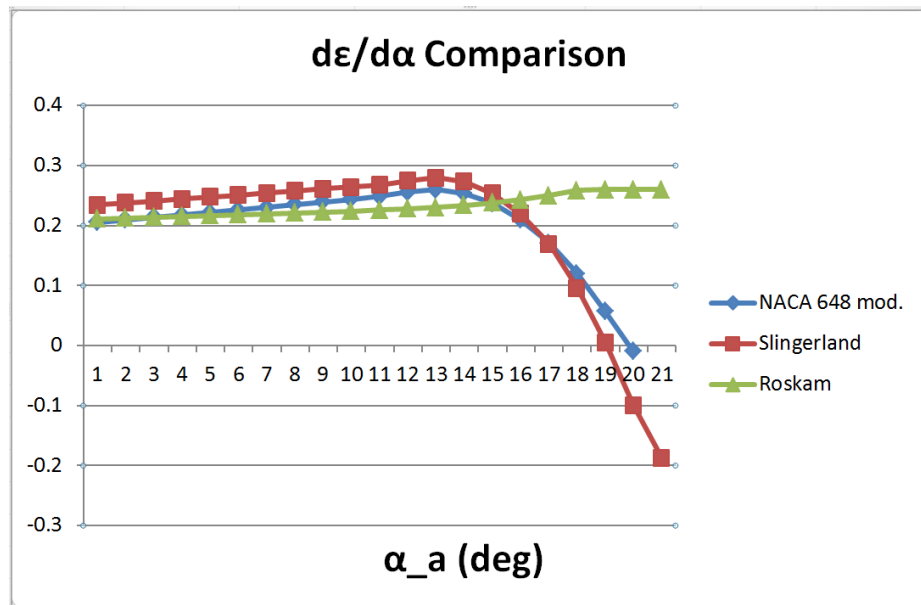


Figure 8.21: Results comparison of downwash gradient.

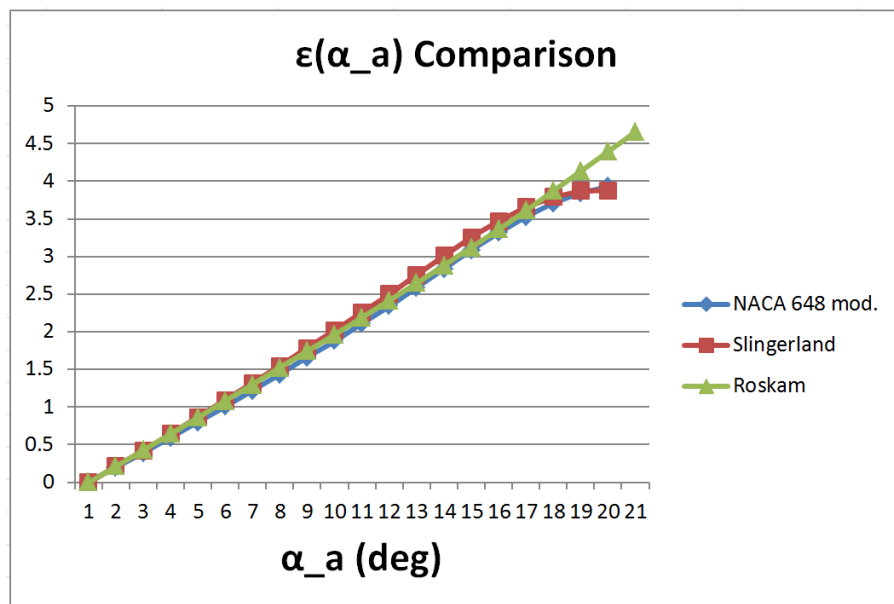


Figure 8.22: Results comparison of downwash angle.

Chapter 9

Aircraft Longitudinal Static Stability

*For every bad thing in life,
there are more good things to tip the balance.*
– Richelle Mead

Static stability is the reaction of a body to a disturbance from equilibrium. To determine the static stability of a body, the body must be initially disturbed from its equilibrium state. If, when disturbed from equilibrium, the initial tendency of the body is to return to its original equilibrium position, the body displays positive static stability or is stable. If the initial tendency of the body is to remain in the disturbed position, the body is said to be neutrally stable. However, should the body, when disturbed, initially tend to continue to displace from equilibrium, the body has negative static stability or is unstable. [14]

In addition to the static stability it's possible to analyze the dynamical stability that is the time history of an aircraft response after it has been disturbed. A statically stable aircraft may not be dynamically stable, as explained in subsequent discussions. However, it is clear that a statically unstable aircraft also is dynamically unstable.

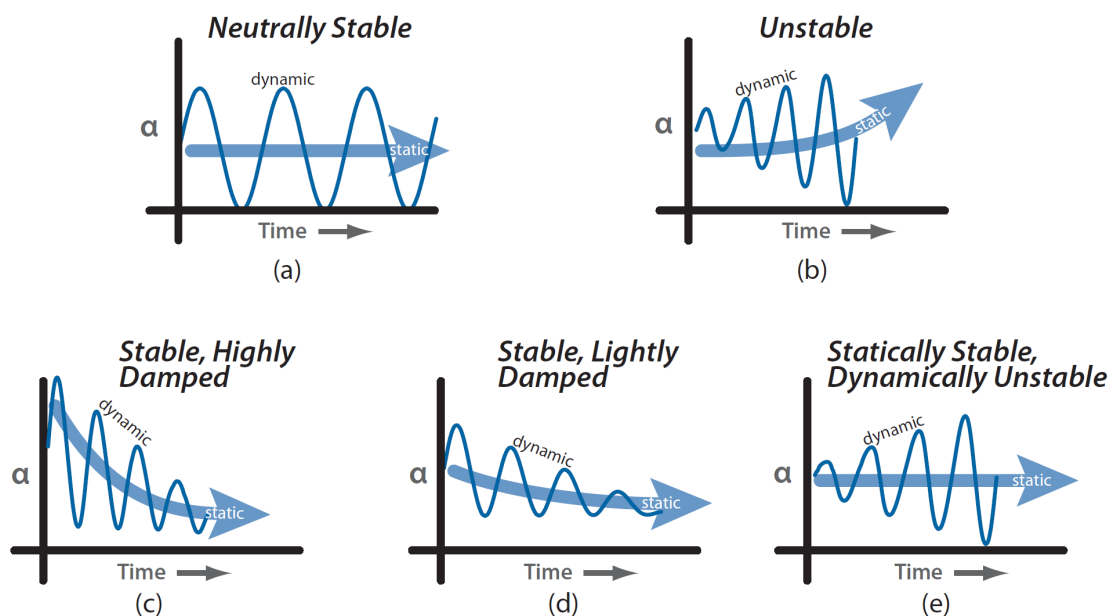


Figure 9.1: Static and dynamic stability about the pitch axis.

It is important to note that there is a substantial difference between the concepts of “Stability” and “Equilibrium”. In fact, stability is a characteristic of an aircraft, while equilibrium is a state in which airplane can be, that means the equilibrium of the forces and the moments acting on it.

“Longitudinal static stability” is the stability of an aircraft in the longitudinal, or pitching, plane under steady-flight conditions. This characteristic is important because an airplane must have the tendency to return to the equilibrium position if perturbed. The pitch plane is the XZ plane of aircraft symmetry. The linear velocities are along the X-axis and w along the Z-axis. Angular velocity is about the Y-axis, known as pitching (positive if nose up). Pilot-induced activation of the elevator changes the aircraft pitch. In the plane of symmetry, the aircraft motion is uncoupled; that is, motion is limited only to the pitch plane.[27]

In order to evaluate the characteristics of longitudinal stability of an aircraft it's necessary to express all the forces and the moments acting on it and evaluate the resultant pitching moment about the center of gravity.

The lift and drag are by definition always perpendicular and parallel to V_∞ . It is, therefore, inconvenient to use these forces to obtain moments because their moment arms relative to the center of gravity vary with angle-of-attack. For this reason, all forces are resolved into normal, N, and chord-wise, C, forces whose axes remain fixed with the aircraft and whose arms are, therefore, constant. [32]

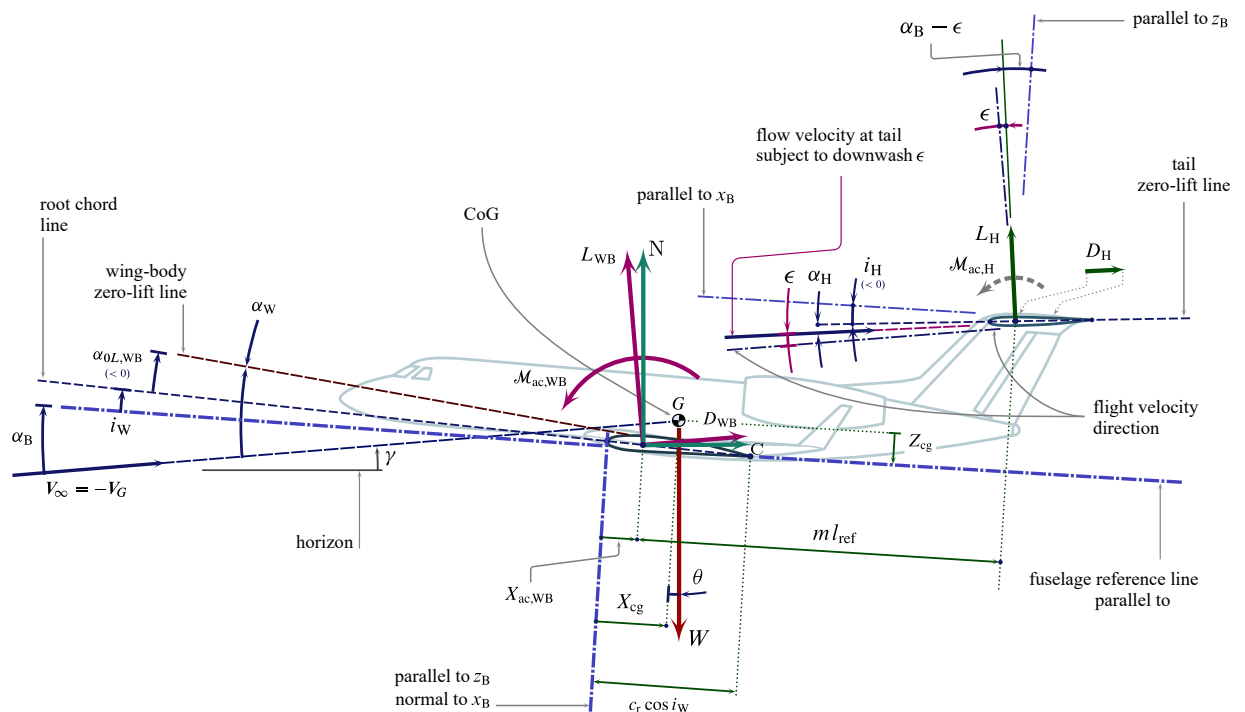


Figure 9.2: Forces and moments acting on an aircraft..

The relation between the lift, the drag and the normal and chord-wise forces are the following:

$$N = L \cos(\alpha) + D \sin(\alpha) \quad (9.1)$$

$$C = D \cos(\alpha) - L \sin(\alpha) \quad (9.2)$$

According to what said, the aircraft can, in general, be trimmed, that is, put into an

equilibrium state where the combined lift of the wing and the tail balances the weight while the moment about the center of gravity is zero. It's necessary that this equilibrium point corresponds to positive lift. As regards the stability it is necessary that the response of the aircraft to a disturbance in angle of attack is to tend to return to the original equilibrium position. Thus, if flying in equilibrium at one angle of attack and a disturbance increases the angle of attack, the moment produced at this angle of attack must act to reduce it, that is, tend back toward the original equilibrium state. Conversely, if a disturbance decreases the angle of attack, the moment at the new, lower, angle of attack must serve to increase that angle. This means that the rate of change of the moment about the center of gravity must be negative for static stability: an increase in α should reduce $C_{M_{cg}}$ and a decrease in α should increase $C_{M_{cg}}$.[42] As higher is the slope of the curve, greater is the restoring moment. Thus the slope of the curve is called *Static Margin*. Static margin is a concept used to characterize the static longitudinal stability and controllability of aircraft. In aircraft analysis, static margin is defined as the distance between the center of gravity and the neutral point of the aircraft, expressed as a percentage of the mean aerodynamic chord of the wing. In order to have static stability, thus, is necessary that the neutral point is behind the center of gravity.

In conclusion the requirements for static stability are the following:

- The pitching-moment curve exhibits a negative slope
- At a zero angle of attack there is positive nose-up moment

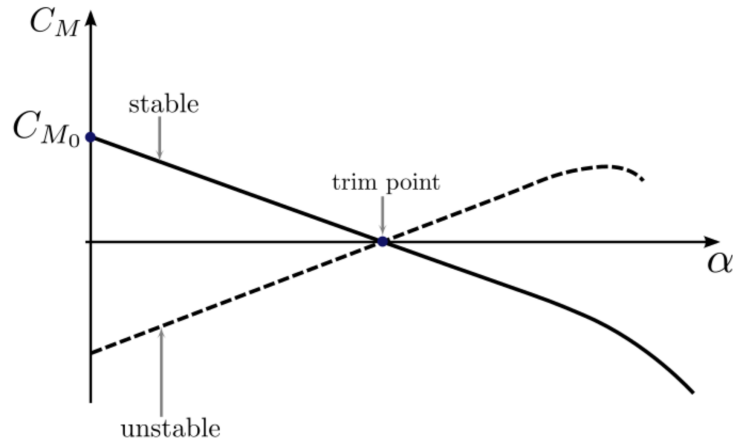


Figure 9.3: Qualitative representation of the moment coefficient vs α .

Below will be calculated all the contributions in order to evaluate the pitching moment coefficient about the center of gravity.

9.1 Aerodynamic Lift

Considering a reference angle of attack α_B , the aircraft components generates lift. So it is necessary to evaluate these contributes. In particular, first of all, is wanted to evaluate the C_L of isolated wing. This value will be correct with fuselage influence. Afterwards it is necessary to evaluate the contribute of horizontal tail. It is important to note that each component works at a different angle of attack in dependence of angles of incidence and downwash , meanwhile for longitudinal stability the reference angle of attack is α_B .

9.1.1 Wing

The wing may be considered as the most important component of an aircraft. Its main purpose is to generate sufficient lift force. However, the wing has two other productions, namely drag force or drag and pitching moment. While a wing designer is looking to maximize the lift, the other two (drag and pitching moment) must be minimized. The theoretical background and the followed process are shown in the CHAPT 6.

9.1.2 Fuselage

The fuselage is that portion of the aircraft wherein the payload is carried. In jet transports the payload consists of the passengers and their baggage and/or cargo. It is important that the fuselage has some features as a low aerodynamic drag; a minimum aerodynamic instability; comfort and attractiveness in terms of seat design, placement, and storage space; safety during emergencies; minimization of noise and ease of cargo handling in loading and unloading.[42]

The lift distribution on a wing is affected by the presence of the fuselage as a result of the following effects:

- The presence of the fuselage disturbs the longitudinal velocity field near the wing.
- At an angle of attack relative to the free stream, the fuselage also perturbs the flow about the wing in planes normal to the free stream.
- The fuselage has a blocking effect on the flow.

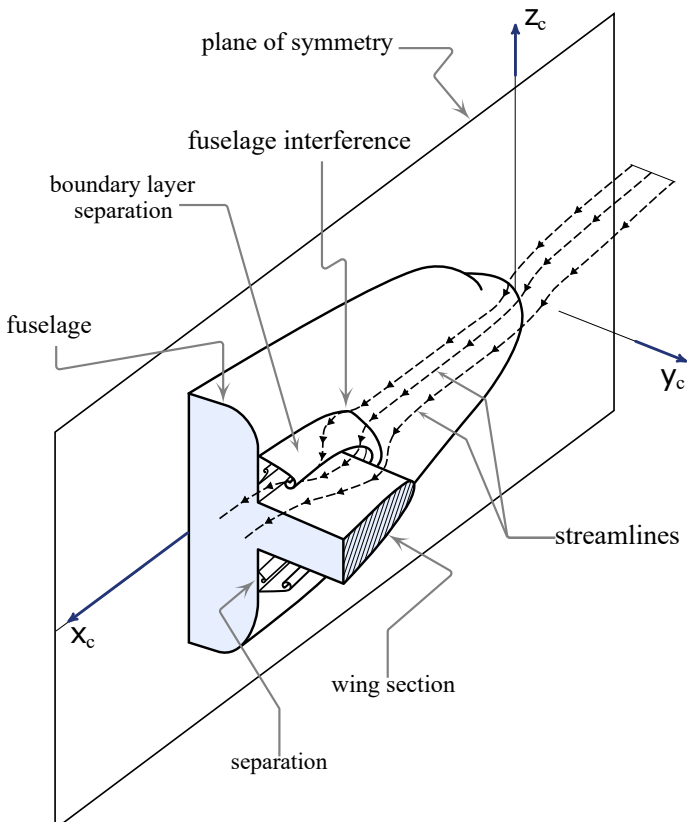


Figure 9.4: Wing fuselage junction flow.

These effects are not large for a slender fuselage but may be important when the fuselage is relatively bulky, so that a substantial alteration to the local longitudinal velocity may result. The cross-flow caused by the fuselage at angle of attack changes the component of free stream velocity normal to the fuselage axis and affects the downwash flow produced by the wing. The blocking effect of the fuselage is always present even if the fuselage is an infinite cylinder aligned with the free stream, in which case the other two effects are not present. [42]

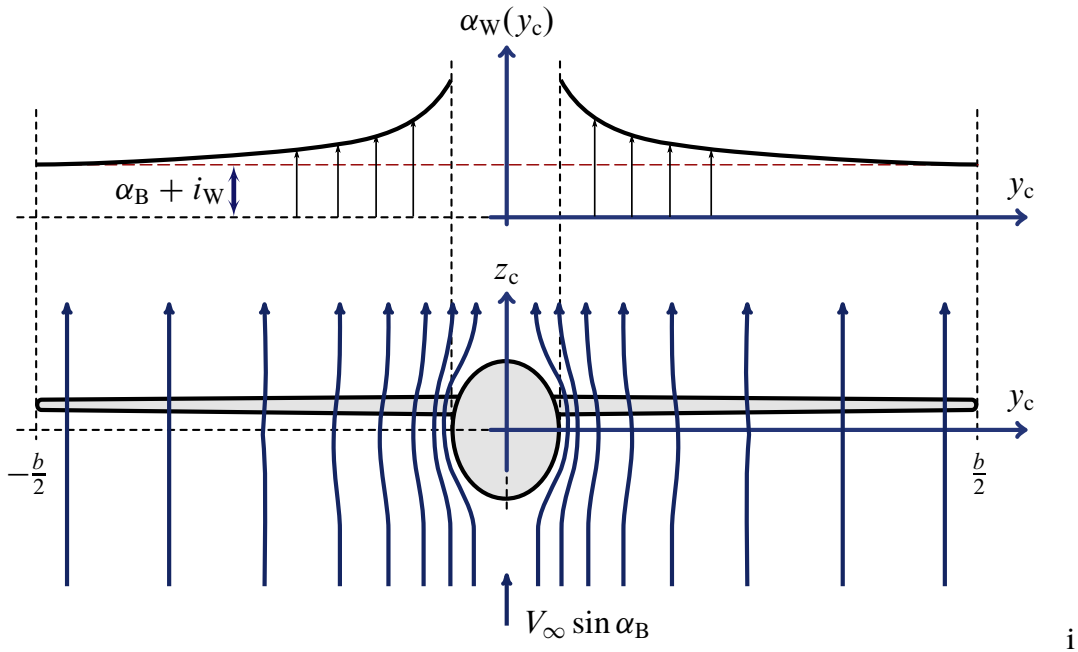


Figure 9.5: Wing fuselage front view interference.

However, theoretical analysis showed that the presence of a slender fuselage does not have an important effect on the lift distribution on an unswept wing of moderate aspect ratio, but a larger change in the lift distribution on a wing in the presence of a fuselage may be anticipated if the wing is swept.[46] For greater accuracy of the calculation, the value of lift linear slope has been corrected using the following equation from [40]:

$$\left(\frac{dC_L}{d\alpha} \right)_{wb} = \left[1 + \frac{1}{4} \left(\frac{d}{b} \right) - \frac{1}{40} \left(\frac{d}{b} \right)^2 \right] \left(\frac{dC_L}{d\alpha} \right)_w \quad (9.3)$$

Note that for typical airliners $\frac{d}{b} \approx 0.1$ and therefore the lift curve slope of the wing-body is approximately equal to that of the wing alone.

In addition to the calculation of the linear slope of the wing body group, it is necessary to calculate the intersection point between the lift curve of wing and the lift curve of wing-body. This point is the α_{0L} of the exposed wing. The exposed wing is the part of wing outside of the fuselage that generates lift in a complete aircraft. This value has been calculated with the following integral formula.

$$\alpha_{0L}|_{EW} = \frac{2}{S_E} \int_{y_{0E}}^{\frac{b}{2}} c(y) [\alpha_0(y_E) - \epsilon_T(y_E)] dy \quad (9.4)$$

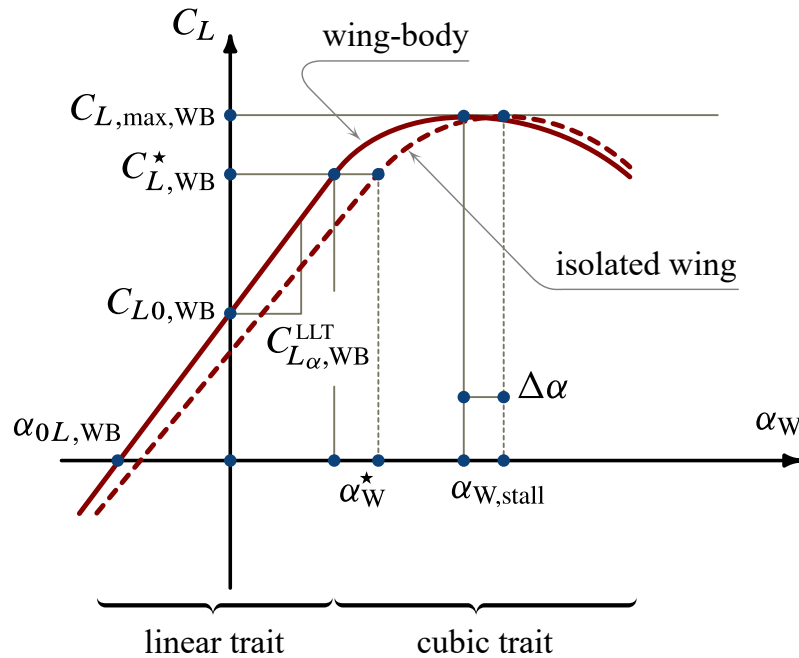


Figure 9.6: Lift curve of isolated wing and of wing-body group.

9.1.3 Horizontal Tail

The horizontal tail is an aerodynamic surface, typically including one or more movable control surfaces, that provides longitudinal stability and control. A stabilizer can feature a fixed or adjustable structure on which any movable control surfaces are hinged, or it can itself be a fully movable surface. In the first case the horizontal tail consists of the *stabilizer* and the *elevator* (moving) for handling the pitch degree of freedom. In case of a fully movable surface it is called *stabilator*.

The H-tail can be positioned low through the fuselage, in the middle cutting through the V-tail, or at the top of the V-tail to form a T-tail. [27] The horizontal tail provides longitudinal stability and control. It may be sized by one or more of the following conditions[34]:

- Provide static and dynamic stability. Provide a state of equilibrium in each flight condition.
- Enable aircraft control.
- Provide a state of equilibrium in each flight condition.

The stabilizer is a fixed wing section whose job is to provide stability for the aircraft, to keep it flying straight. The horizontal stabilizer prevents up-and-down, or pitching, motion of the aircraft nose. The elevator is the small moving section at the rear of the stabilizer that is attached to the fixed sections by hinges. Because the elevator moves, it varies the amount of force generated by the tail surface and is used to generate and control the pitching motion of the aircraft. There is an elevator attached to each side of the fuselage. The elevators work in pairs; when the right elevator goes up, the left elevator also goes up.

Considering an horizontal tail formed by stabilizer and elevator, in order to evaluate the lift coefficient of this lifting surface it is necessary to consider the deflection of control surface. The elevator, in fact, can be considered as a *plain flap*.

Elevator index of effectiveness

In order to evaluate the contribution to the longitudinal stability of horizontal tail it's necessary to consider the deflection of the elevator.

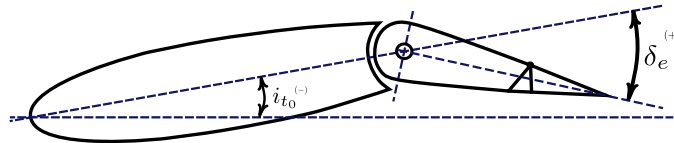


Figure 9.7: Characteristic angles of the horizontal tail.

The variation of zero lift angle is not constant with the angle of deflection. So it's necessary to evaluate the tau factor which is defined as follows:

$$\tau_e = \frac{d\alpha_{0l}}{d\delta_e} \quad (9.5)$$

Introducing this parameter the lift coefficient of the horizontal tail can be rated as follows:

$$C_{L_H} = C_{L_0} + C_{L_{\alpha_H}} \alpha_H + C_{L_{\alpha_H}} \tau_e \delta_e \quad (9.6)$$

Considering a symmetrical horizontal tail, the term C_{L_0} is zero, so it's possible to express the lift coefficient in the following form:

$$C_{L_H} = C_{L_{\alpha_H}} (\alpha_H + \tau_e \delta_e) \quad (9.7)$$

In general the value of τ is constant until about 15 deg; after this value, due to the flow separation, the effectiveness of elevator decrease and consequently the product $\tau_e \delta_e$ that appears in the equation of lift coefficient.

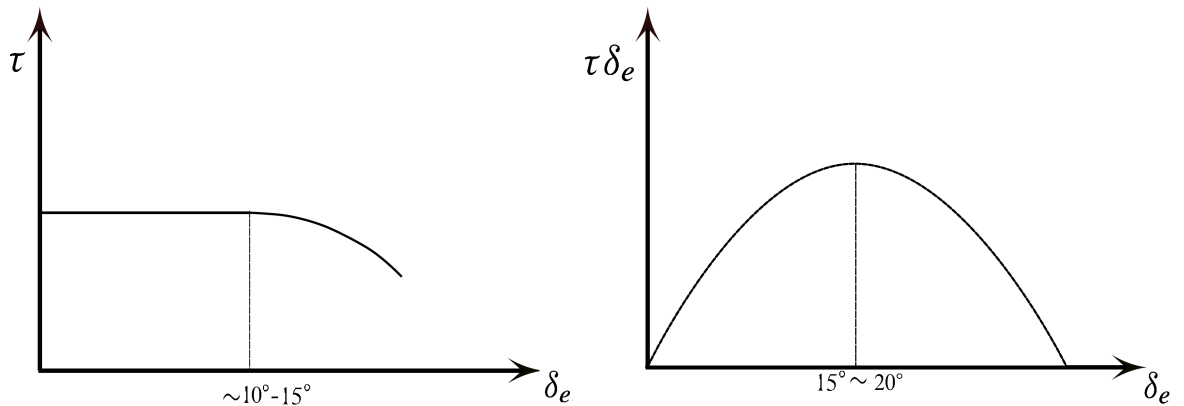


Figure 9.8: Qualitative trend of τ with the deflection of elevator.

Figure 9.9: Qualitative trend of the term $\tau \cdot \delta_e$ with the deflection of elevator.

The evaluation of tau is made by reading of external database, considering the following graphs.

$$\tau = \alpha_\delta \eta_\delta = \frac{\alpha_{\delta_{cL}}}{\alpha_{\delta_{cL}}} \alpha_{\delta_{cL}} \eta_\delta \quad (9.8)$$

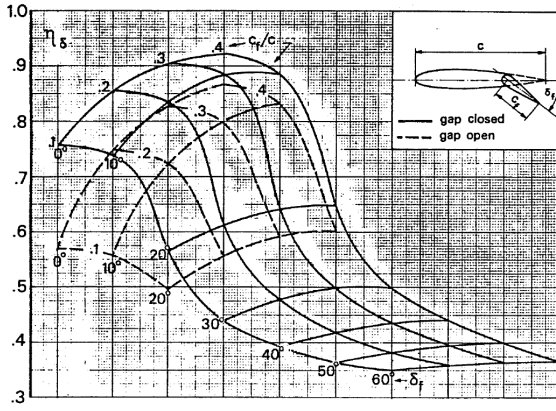


Figure 9.10: 2D efficiency correction for elevator.

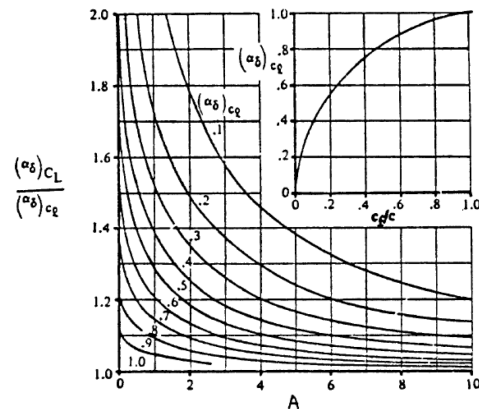


Figure 9.11: $\frac{d\alpha_{0L}}{d\delta_e}$ 2D and 3D correction.

The construction of the C_L vs α curve is made as follows for each value of elevator deflection.

1. It's necessary to know the value of C_{L_α} and α_{0L} clean
2. The $\alpha_{0L_{\delta_e}}$ is obtained starting from the τ value

$$\alpha_{0L_{\delta_e}} = \alpha_{0L_{clean}} - (\tau \delta_e) \quad (9.9)$$

3. In order to evaluate the variation in C_{L_α} due to elevator deflection, references to [49] have been made. In particular, Torenbeek provides the following equation which approximates the results of the exact theory fairly accurately and is in qualitative agreement with experimental data.

$$C_{l\alpha_{(flap\ down)}} = C_{l\alpha} \left[\frac{c'}{c} \left(1 - \frac{c_f}{c'} \sin^2 \delta_f \right) \right] \quad (9.10)$$

This equation is then corrected for the three-dimensional wing as follows.

$$C_{L\alpha_{(flap\ down)}} = C_{L\alpha} \left\{ 1 + \frac{\Delta C_{L0}}{\Delta C_{l0}} \left[\left(\frac{c'}{c} \left(1 - \frac{c_f}{c'} \sin^2 \delta_f \right) - 1 \right) \right] \right\} \quad (9.11)$$

4. The new value of C_{L0} is obtained from the following equation

$$C_{L0} = -C_{L\alpha_{\delta_e}} \alpha_{0L_{\delta_e}} \quad (9.12)$$

5. The Δ is obtained from High Lift modulus. An empirical method for predicting airfoil maximum lift increments for plain and slotted flaps is presented in DATCOM and will be followed from [42]. The maximum lift increment provided to an airfoil by the deflection of a trailing edge flap is given by the (9.13).

$$\Delta C_{l\max} = k_1 k_2 k_3 (\Delta C_{l\max})_{base} \quad (9.13)$$

Here $(\Delta C_{l\max})_{base}$ is the section maximum lift increment for 25 percent-chord flaps at the reference flap-deflection angle. The quantity k_1 is a factor accounting for flap-chord-to-airfoil-chord ratios, $\frac{c_f}{c}$, other than 0.25. The quantity k_2 is a factor accounting for flap deflections other than the reference value. Finally, k_3 is a factor accounting for flap motion as a function of flap deflection.

6. The value of α_{stall} is obtained considering the same Δ of clean lifting surface between the linear α_{max} and non linear α_{stall} .

9.1.4 Complete Aircraft

In order to evaluate the lift coefficient of the entire airplane it's possible to consider it as consisting of the following parts[39]:

- Wing and Fuselage
- Horizontal Tail
- Canard

It's important to consider the effective angles of attack in which the surfaces work. This is made considering the angles of incidence of the lifting surfaces and the downwash angle aft of the wing. An horizontal tail and a canard may be equipped with a trailing edge control surface. So in order to evaluate these contributes it's important to know the angle of deflection δ of these control surfaces.

The calculation of the individual contributions is reported in the relevant sections. In this section will be shown the method to evaluate the aircraft lift coefficient, known the single contributes.

For an aircraft with no canard, the formula is the following:

$$C_L = C_{L_{wb}} + \frac{S_t}{S_w} \eta_t C_{L_t} \quad (9.14)$$

Where η_t is the ratio of dynamic pressure, called *tail efficiency factor*. In fact the dynamic pressure seen by horizontal tail differs from the free stream dynamic pressure due to two main reasons: the combination wing-fuselage and the presence of the propeller. The dynamic pressure of the tail depends on the location of the tail. If the tail is in the wake of the wing-body, the local dynamic pressure will be less than the free-stream because the flow gradually loses its kinetic energy. While if the tail is in the slipstream of propeller, the local dynamic pressure may increase due to the power absorbed by the propeller.

9.2 Aerodynamic Drag

The drag of an aircraft depends on its shape and speed, which are design-dependent, as well as on the properties of air, which are nature-dependent. Drag is a complex phenomenon arising from several sources, such as the viscous effects that result in skin friction and pressure differences as well as the induced flow field of the lifting surfaces and compressibility effects. The aircraft drag estimate starts with the isolated aircraft components. Each component of the aircraft generates drag largely dictated by its shape. Total aircraft drag is obtained by summing the drag of all components plus their interference effects when the components are combined. It is important to note that the drag of two isolated bodies increases when they are brought together due to the interference of their flow fields.[27]

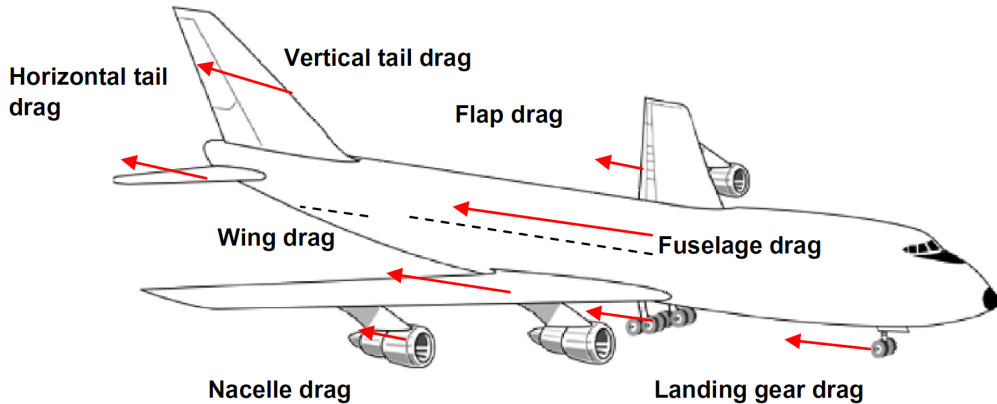


Figure 9.12: Drag components making up the total commercial airplane drag.[42]

In this thesis work, in order to evaluate the pitching moment coefficient of an aircraft has been considered the drag forces due to wing and horizontal tail.

9.2.1 Drag of a lifting surface

As widely expressed in the CHAPT 7, the drag coefficient of a lifting surface is calculated starting from the drag coefficient of the airfoils, expressed by the following equation:

$$CD = CD_{min} + (CL - CL_{CD_{min}})^2 \cdot k \quad (9.15)$$

For each station, known the semi-spanwise lift distribution, it is possible to calculate the local lift coefficient of the intermediate airfoil and, consequently, the drag parasite coefficient. The induced drag is calculated starting from induced angle of attack. After the drag coefficient of the entire lifting surface is calculated with an integral.

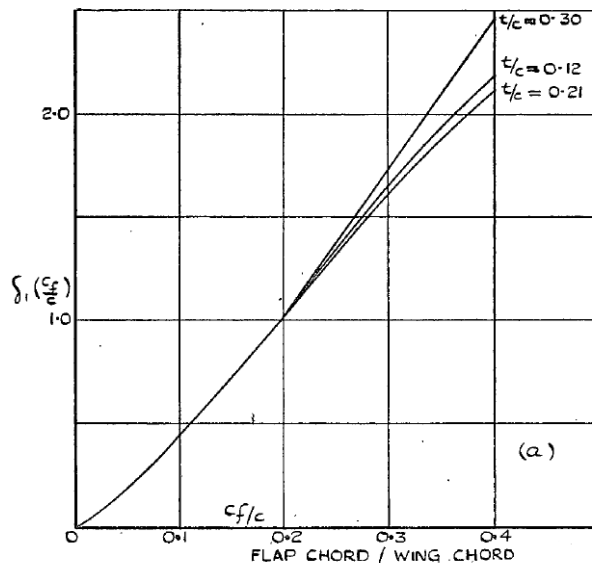
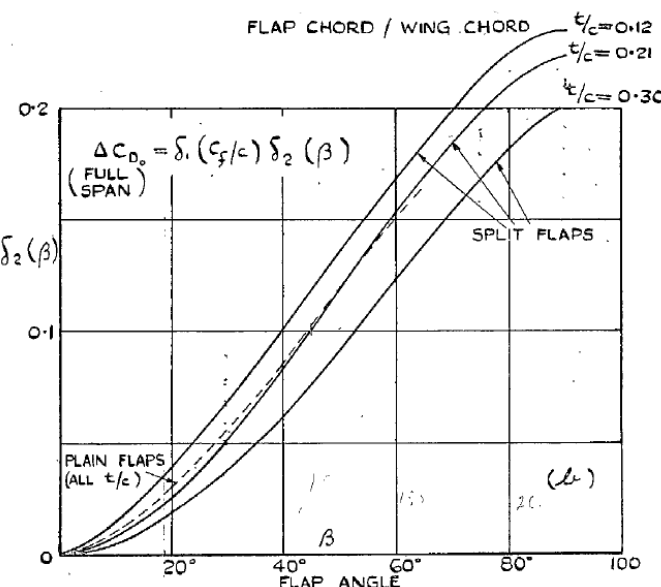
9.2.2 Additional drag due to elevator

For the horizontal tail it is necessary to consider the additional drag due to the elevator deflection. It is possible to consider the elevator as a *plain flap* and use the concerning methods.

A plain flap is a high lift devices where a portion of the rear of a wing is simply hinged. The effectiveness of the flap derives from the fact that on rotation it changes the camber of the section and so permits of a change of circulation and therefore, of lift at a given incidence. The increment in profile drag coefficient due to a flap at a given incidence is rather more influenced by test conditions than is the lift coefficient increment. Nevertheless, the influence of test conditions and wing incidence is still sufficiently small over a wide range of incidence for us to accept the increment at a standard incidence as a reliable measure of the profile drag characteristics of a flap. [51] The increment of drag is a ΔCD_0 Young and Hufton assumed that ΔCD_0 can be calculated as follow for a full-span flap:

$$\Delta CD_0 = \delta_1 (c_f/c) \cdot \delta_2 (\delta_f) \quad (9.16)$$

where δ_1 and δ_2 are functions that were determined from experimental data. Their related curves are shown in figure 9.13 and 9.14 for plain flap.

Figure 9.13: The functions $\delta_1 (c_f/c)$ for split and plain flapsFigure 9.14: The functions $\delta_2 (\beta)$ for plain flaps

9.3 Pitching Moments

The purpose of this section is to explain the followed procedure used to evaluate the pitching coefficient moments of the aircraft components.

Due to the interaction between the body and the flow a pressure distribution is generated whose result is the aerodynamic force acting at the center of pressure. In consequence of what there is a pitching moment that is a moment acting on the pitch axis of a moving body. As the angle of attack changes on a cambered airfoil, there is a movement of the center of pressure forward and aft. One of the remarkable properties of a cambered airfoil is that, even though the center of pressure moves forward and aft, there is a point, called Aerodynamic Center, with respect to which the moment coefficient is constant. The aerodynamic center is the most convenient place to locate the lift, drag, and moment of an aircraft wing or airfoil

section.

So, for each component of the aircraft, it will be calculated the pitching moment coefficient respect to its aerodynamic center.

9.3.1 Lifting surface

In order to evaluate the pitching moment coefficient of a lifting surface, at a given angle of attack, the implemented process is the following.

First it is calculated the pitching moment coefficient respect to the point at a quarter of the mean aerodynamic chord. Starting from these values, to vary the angle of attack, it's possible to evaluate the position of aerodynamic center.

1. Fifty points are defined along the semi-span.
2. An intermediate airfoil is calculated for each point.
3. The lift coefficient is calculated with the local C_l vs α curve for each airfoil at a given station. In this way it's possible to consider both the linear trait and the non linear one.
4. The position of the center of pressure is calculated for each airfoil using the following equation

$$\frac{x_{CP}}{c} = \frac{x_{AC}}{c} - \frac{C_{M_{ac}}}{C_l} \quad (9.17)$$

5. The arm between the local center of pressure and the point at a quarter of lifting surface's MAC is calculated for each airfoil. The equations that define the MAC are the following:

$$MAC = \frac{2}{S} \int_0^{\frac{b}{2}} c^2 dy \quad (9.18)$$

$$x_{MAC} = \frac{2}{S} \int_0^{\frac{b}{2}} x_{le}(y) c(y) dy \quad (9.19)$$

$$y_{MAC} = \frac{2}{S} \int_0^{\frac{b}{2}} y_{le}(y) c(y) dy \quad (9.20)$$

6. Finally it's possible to evaluate the pitching moment about the point at a quarter of MAC with the product between the lift force and the arm.

Repeating the process to vary the angle of attack it's possible to estimate the slope of the pitching moment curve. In fact, the aerodynamic center, is that point on an aircraft, wing, or airfoil section about which the pitching moment is independent of angle of attack. If the slope is positive, the aerodynamic center is behind the quarter of the MAC, conversely if the slope is negative, the aerodynamic center is the quarter of the MAC is behind the aerodynamic center.

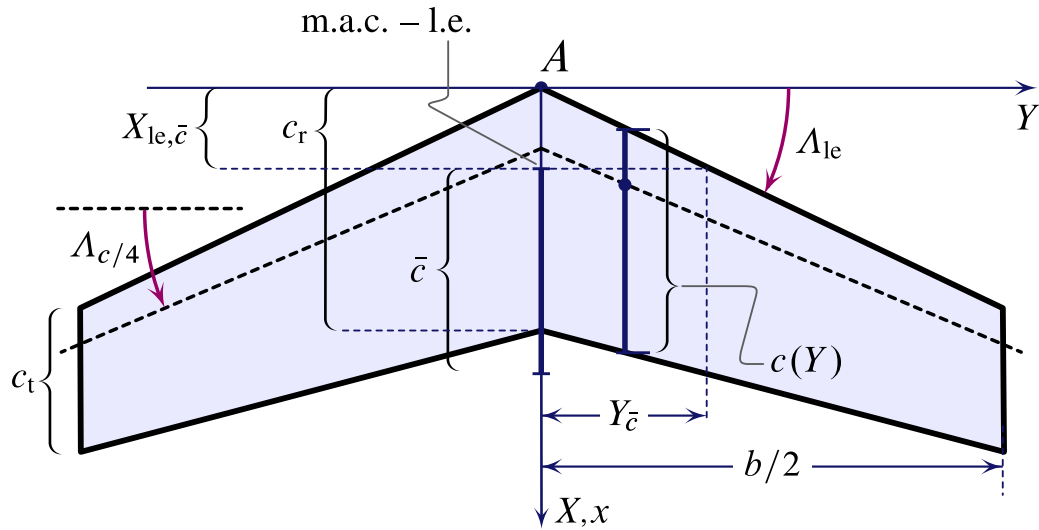


Figure 9.15: Wing topview definitions.

9.3.2 Additional moment due to elevator

The horizontal tail is usually a symmetric section so that and $M_{ac,t} = 0$ for $\delta_e = 0$. If there is a deflection of elevator it's necessary to consider a additional term. According to [49], the generalized expression, for airfoils, in (9.21) represents a useful starting point when experimental data are not available.

$$\Delta C_{m_{\frac{c}{4}}} = -\mu_1 \Delta C_{l_{\max}} \left(\frac{c'}{c} \right)^2 - \frac{C_l}{4} \frac{c'}{c} \left(\frac{c'}{c} - 1 \right) + \left(C_{m_{\frac{c}{4}}} \right)_{\delta_f=0} \left[\left(\frac{c'}{c} \right)^2 - 1 \right] \quad (9.21)$$

where extended chord c' allows for the effects of the backward movement of the flap while it is being extended. In this equation, the first contribution is due to the increased section camber and the factor μ_1 is defined as follows according to Glauert's linear theory for small flap deflections.

$$\mu_1 = \frac{1}{2} \left(1 - \frac{c_f}{c} \right) \frac{\sin \theta_f}{\pi - (\theta_f - \sin \theta_f)} \quad (9.22)$$

This theoretical value of μ_1 generally underpredicts the pitching moment coefficient; in fact it has been found that, for slotted flaps with, or without, Fowler movement, most data are on a single line, provided the second term of the equation (9.22), representing the theoretical rearward shift of the airfoil aerodynamic center, is halved. Furthermore, in the case of split and plain flaps, the flap angle is observed to exert a pronounced influence on μ_1 as shown in figure 9.16.

The last term of the (9.22) is generally of a low order and can be ignored. This, together with the halving of the second term of the previous equation, leads to the following practical expression of $\Delta C_{m_{\frac{c}{4}}}$.

$$\Delta C_{m_{\frac{c}{4}}} = -\mu_1 \Delta C_{l_{\max}} \left(\frac{c'}{c} \right) - \frac{C_l}{8} \frac{c'}{c} \left(\frac{c'}{c} - 1 \right) \quad (9.23)$$

The obtained two-dimensional equation can, then, be converted into a three-dimensional one,

which computes the pitching moment change on the entire wing, as follows.

$$\Delta C_{M_{\frac{c}{4}}} = \mu_2 \Delta C_{m_{\frac{c}{4}}} + 0.7 \frac{\mathcal{R}}{1 + \frac{2}{\mathcal{R}}} \mu_3 \Delta C_{l_{\max}} \tan A_{\frac{c}{4}} \quad (9.24)$$

where $\Delta C_{m_{\frac{c}{4}}}$ is the one from (9.23), provide that $C_l = C_L + \Delta C_{l_{\max}} \left(1 - \frac{S_{w,f}}{S}\right)$, and the correction factors μ_2 and μ_3 are the one shown in figures 9.17 and 9.18. Making the appropriate substitutions, the following operational formula is, finally, obtained.

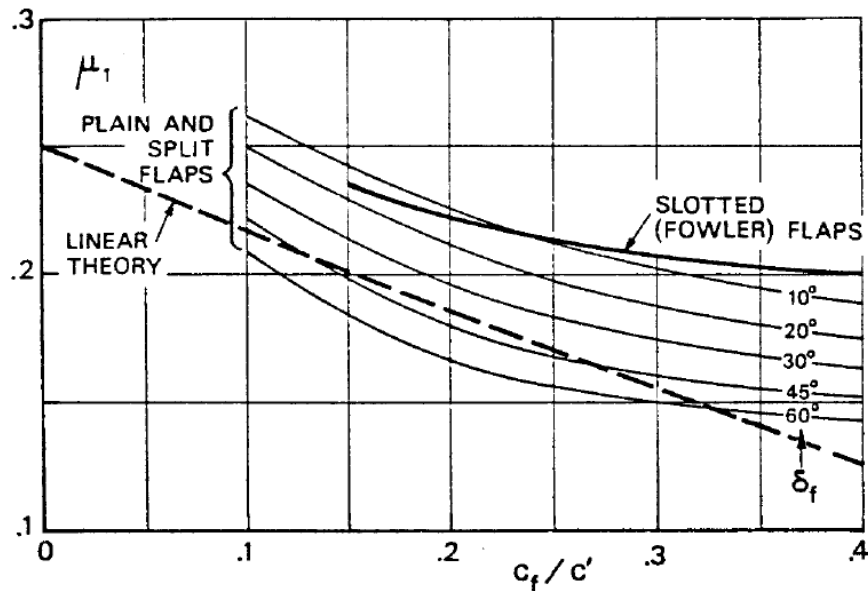


Figure 9.16: The pitching moment function μ_1

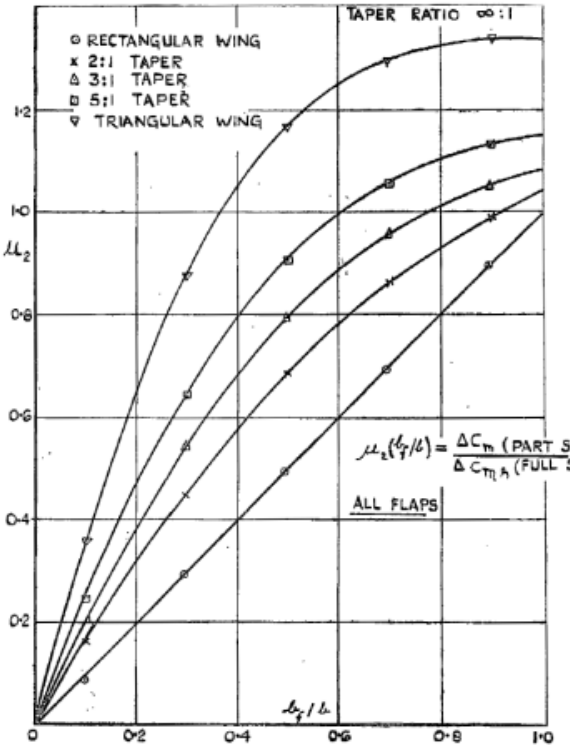


Figure 9.17: The pitching moment function μ_2

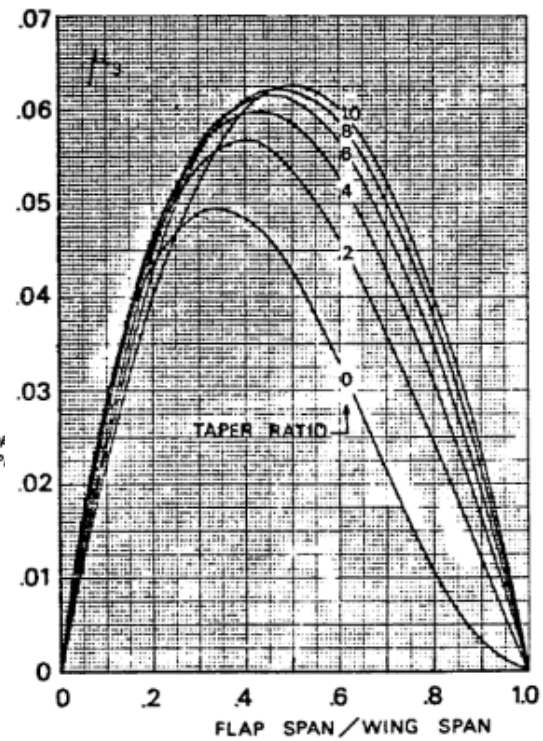


Figure 9.18: The pitching moment function μ_3

$$\begin{aligned}\Delta C_{M\frac{c}{4}} = & \mu_2 \left\{ -\mu_1 \Delta C_{L\max} \frac{c'}{c} - \left[C_L + \Delta C_{l\max} \left(1 - \frac{S_{w,f}}{S} \right) \right] \frac{1}{8} \frac{c'}{c} \left(\frac{c'}{c} - 1 \right) \right\} \\ & + 0.7 \frac{\mathcal{R}}{1 + \frac{\mathcal{R}}{2}} \mu_3 \Delta C_{l\max} \tan A_{\frac{c}{4}}\end{aligned}\quad (9.25)$$

9.3.3 Fuselage

The moment coefficient of the fuselage is a pure couple, so it is not necessary to specify the pole.

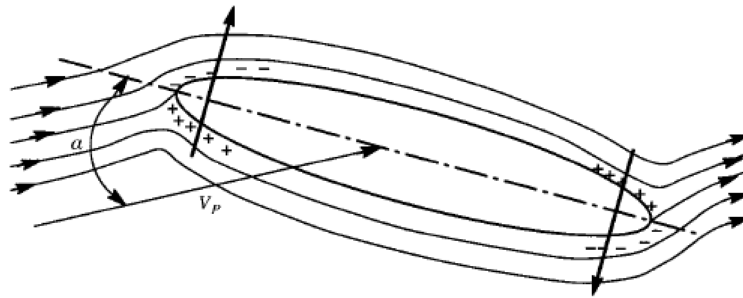


Figure 9.19: Fuselage in potential flow at angle of attack.

Assuming the linearity, is possible to represent the pitching moment coefficient by the following equation in function of the angle of attack.

$$C_{M_f} = C_{M_{0f}} + C_{M\alpha_f} \alpha_{body} \quad (9.26)$$

In JPAD it's possible to evaluate these two contributes using different methods.

Multhopp method

Each term in the equation 9.26 can be calculated by the Multhopp method. The fuselage is divided into strips, each of which gives a contribution to the pitching moment according to its distance from the wing.

The two coefficients $C_{M_{0f}}$ and $C_{M\alpha_f}$ in eq. 9.26 can be obtained from the following equations.

$$C_{M_{0f}} = \frac{K_2 - K_1}{36.5 \cdot S \cdot MAC} \cdot \int_0^{l_f} W_f^2 \cdot (\alpha_{0L_w} + i_w + i_{cl_f}) \, dx \quad (9.27)$$

$$C_{M\alpha_f} = \frac{1}{36.5 \cdot S \cdot MAC} \cdot \left\{ \int_0^{l_{f1}} W_f^2 \cdot \left[\left(\frac{\partial \epsilon_u}{\partial \alpha} \right)_1 + 1 \right] \, dx_1 + \int_0^{l_{f2}} W_f^2 \cdot \left[\left(\frac{\partial \epsilon_d}{\partial \alpha} \right)_2 + 1 \right] \, dx_2 \right\} \quad (9.28)$$

Instead of the integrals it's possible to substitute them with summations.

$$C_{M_{0f}} = \frac{K_2 - K_1}{36.5 \cdot S \cdot MAC} \cdot \sum_{j=1}^n W_{f_j}^2 \cdot (\alpha_{0L_w} + i_w + i_{cl_f}) \cdot \Delta x; \quad (9.29)$$

$$C_{M\alpha_f} = \frac{1}{36.5 \cdot S \cdot MAC} \cdot \left\{ \sum_{j=1}^{n_1} W_{f_j}^2 \cdot \left[\left(\frac{\partial \epsilon_u}{\partial \alpha} \right)_1 + 1 \right] \cdot \Delta x_1 + \sum_{j=1}^{n_2} W_{f_j}^2 \cdot \left[\left(\frac{\partial \epsilon_d}{\partial \alpha} \right)_2 + 1 \right] \cdot \Delta x_2 \right\} \quad (9.30)$$

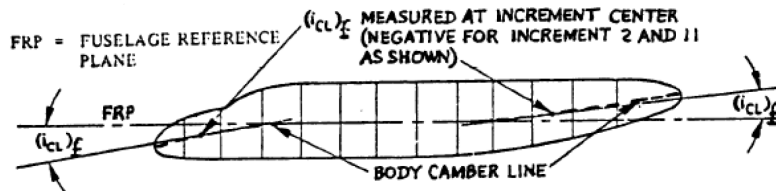


Figure 9.20: Strips definition for the determination of C_{M0_f} .

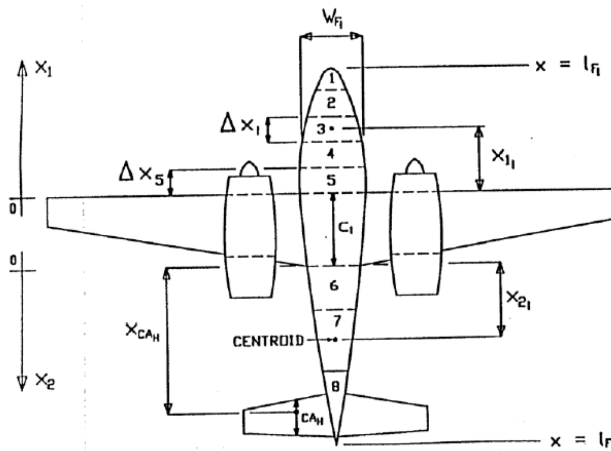


Figure 9.21: Strips definition for the determination of $C_{M\alpha_f}$.

The parameter $K_2 - K_1$ is a correction factor that is dependent on the value of the fineness ratio and is evaluated by the following figure.[16]

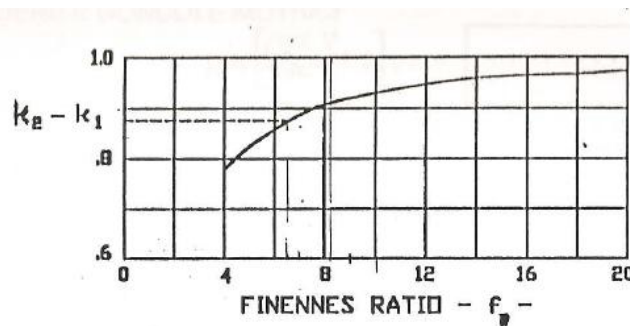


Figure 9.22: $K_2 - K_1$ correction factor in function of fineness ratio.

For stability it's necessary to evaluate the new aerodynamic center (wing-body) and the pitching moment coefficient respect to this point. In fact the fuselage introduces a shift of the aerodynamic center to the leading edge. It's possible to obtain the new aerodynamic center using the Eq. 9.31

$$\Delta X_{ac} = x_{ac_{wb}} - x_{ac_w} = -\frac{C_{M_{\alpha_f}}}{C_{L_{\alpha_f}}} \quad (9.31)$$

The wing-body pitching moment respect to the new aerodynamic center is :

$$C_{M_{ac_{wb}}} = C_{M_{ac_w}} + C_{M_{0f}} \quad (9.32)$$

Fuselage Pitching moment prediction method

This method has been developed in the Dept. of Industrial Engineering, University of Study of Naples Federico II, by numerical aerodynamic analyses performed with STAR-CCM+. From a reference fuselage layout the nose, cabin (constant fuselage diameter), and tailcone geometry have been parametrically changed. Then, the aerodynamic drag, the pitching moment at zero incidence, the longitudinal static stability derivative, and the yawing moment coefficients C_D , C_{M_0} , C_{M_α} , and C_{N_β} respectively, have been evaluated by numerical analysis. Aerodynamic effects of each component (nose, cabin, tailcone) have been directly obtained from the CFD aerodynamic solver, separating the forces and moments contributions of each fuselage part. [33]

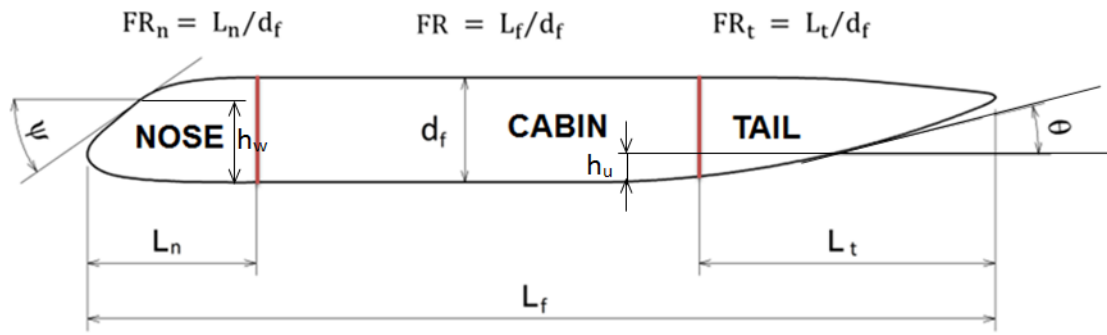


Figure 9.23: Main fuselage geometrical parameters.

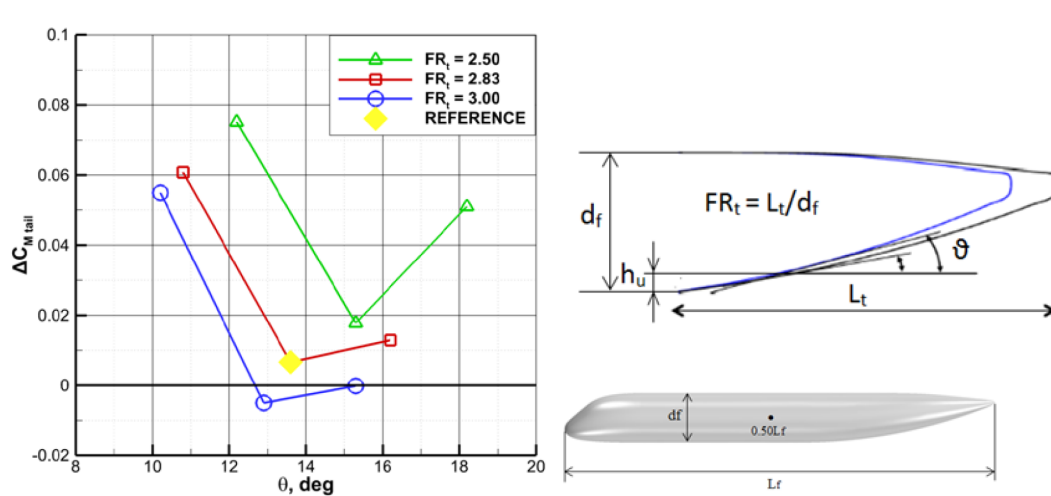
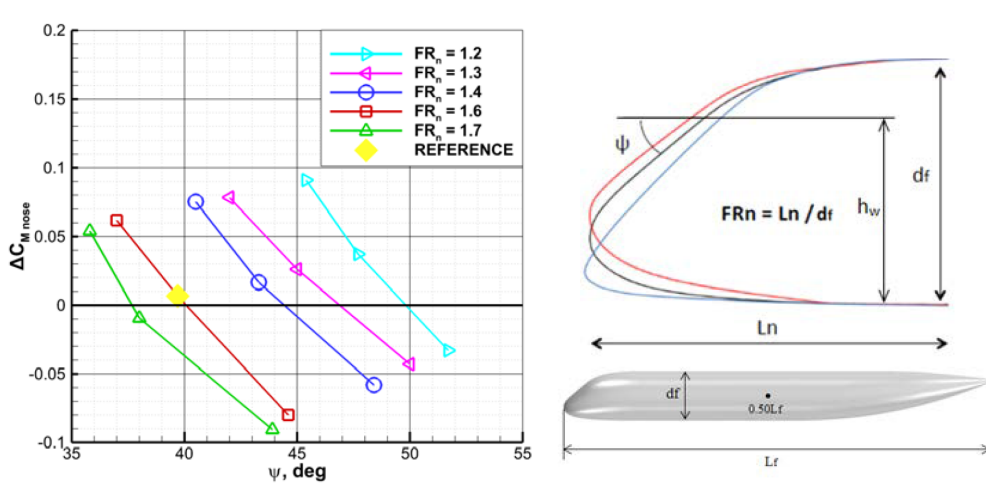
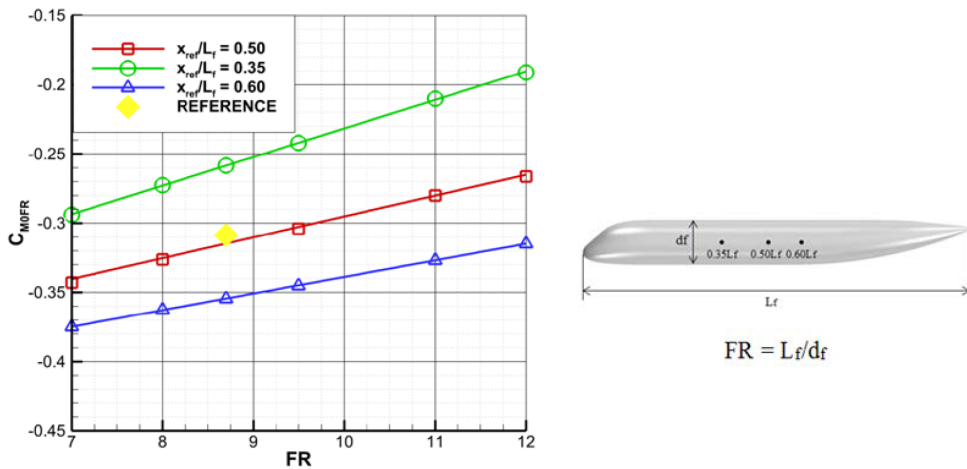
The fuselage pitching moment coefficient can be estimated according to the equation 9.26 where :

$$C_{M_0} = C_{M_{0FR}} + \Delta C_{M_{0NOSE}} + \Delta C_{M_{0TAIL}} \quad (9.33)$$

$$C_{M_\alpha} = C_{M_{\alpha FR}} + \Delta C_{M_{\alpha NOSE}} + \Delta C_{M_{\alpha TAIL}} \quad (9.34)$$

where the subscript FR refers to the pitching moment coefficient as function of fuselage fineness ratio. The subscript $NOSE$ the pitching moment nose correction factor. It depends on windshield angle Φ and on the nose fineness ratio FR_n . Finally the subscript $TAIL$ refers to the pitching moment tail correction factor. It depends on upsweep angle θ and on the tail fineness ratio FR_t .

The following figures show the variability of introduced parameters.



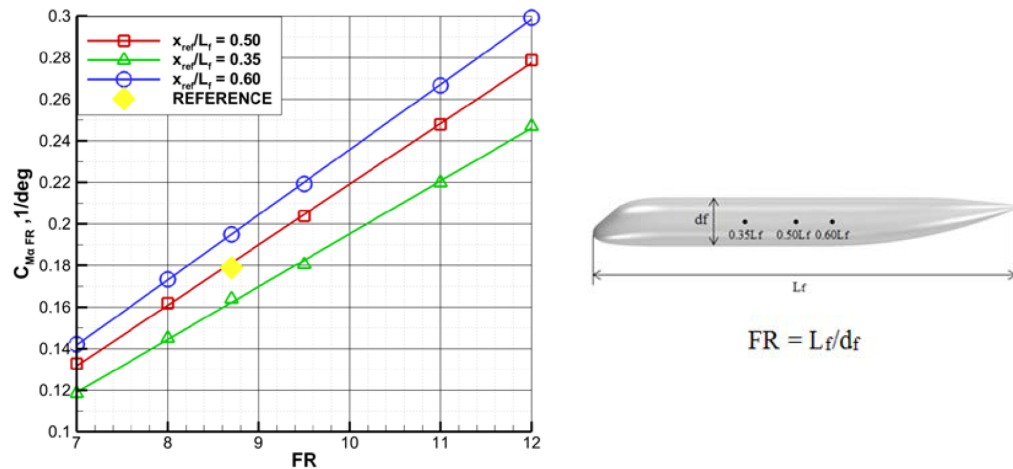


Figure 9.27: Pitching moment derivative with respect to FR.

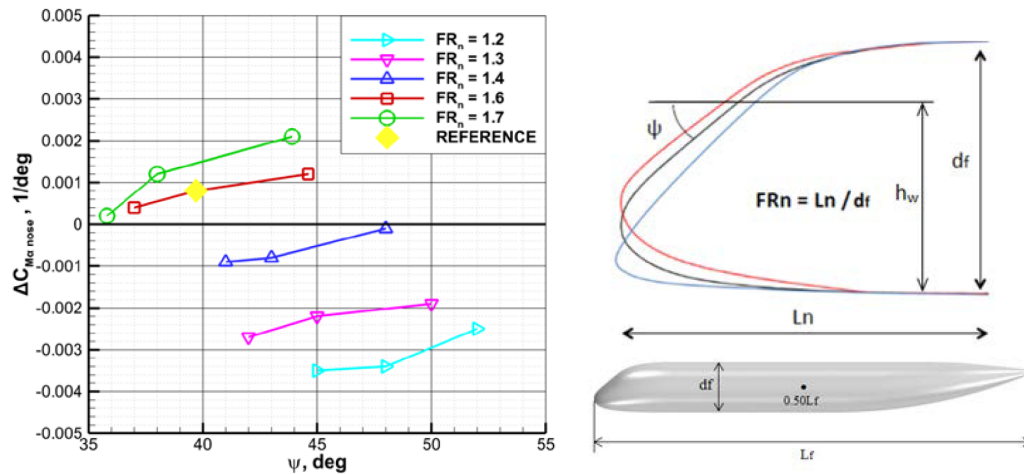


Figure 9.28: Pitching moment derivative nose correction factor.

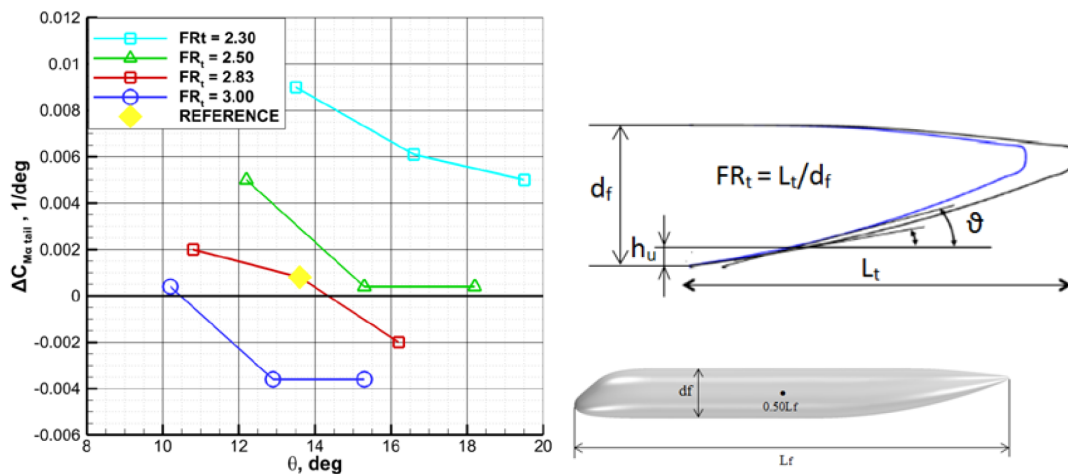


Figure 9.29: Pitching moment derivative tail correction factor.

9.4 Propulsors

The effects of propeller and slipstream on airplane static longitudinal stability may be significant. It is possible to divide the power effects on longitudinal static stability in two categories: direct effects and Indirect effects.

9.4.1 Direct Effects

These effects are principally the following:

- Effect due to the thrust and moments result from the line of action of force with respect to the CG.
- Pitching moment due to non axial flow.

Due to these effects, the airplane pitching curve must be accounted for a change in slope $\frac{dC_m}{dC_L}$. The equations differ between turboprop engine aircraft and turbojet.

In case of **turboprop** it is possible to express the power direct effects with the following equations:

Pitching moment due to thrust effect

Starting from the total lift acting on the aircraft it is possible to evaluate the dynamic pressure as follows

$$q = \frac{W}{SC_L} \quad (9.35)$$

Known the dynamic pressure, the total drag is calculated

$$D = qSC_D \quad (9.36)$$

Consequently it is possible to evaluate the thrust and the relative pitching moment.

$$C_{M_P} = \frac{Tz_T}{q_\infty S_{ref} \bar{c}} \quad (9.37)$$

This equation means that if the thrust acting under the cg ($h_p > 0$) with increasing alpha (and CL) the moment coefficient undergoes a positive change, ie the power effect has an unstable contributions.

Pitching moment due to non axial effect

$$\frac{dC_{M_P}}{dC_L} = \frac{dC_{N_P}}{d\alpha_p} \frac{S_p}{S} \frac{l_p}{\bar{c}} \frac{\left(1 + \frac{d\epsilon}{d\alpha}\right)}{C_{L_{\alpha w}}} N_{prop} \quad (9.38)$$

Whre $\frac{d\epsilon}{d\alpha}$ is the upwash effect forward wing, represented in fig. 9.30

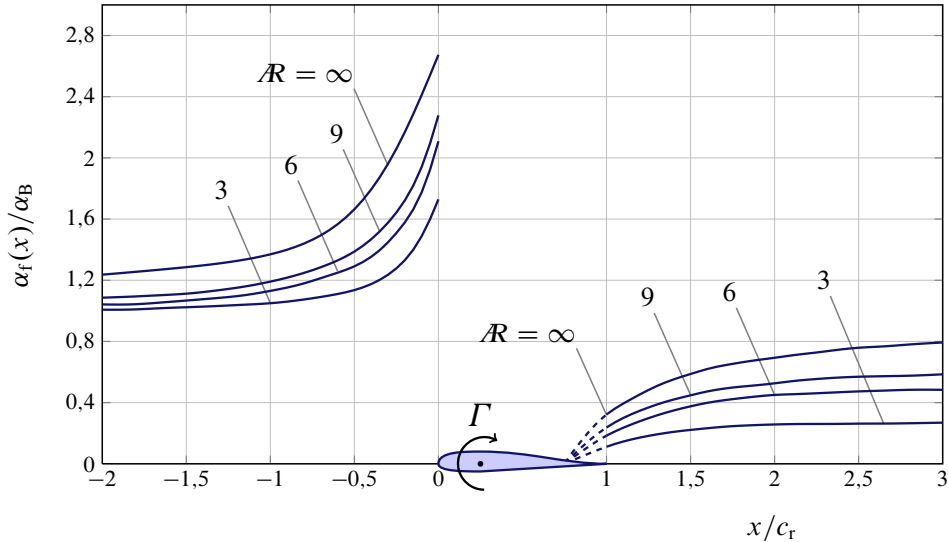


Figure 9.30: Wing upwash and downwash.

9.5 Stability Calculation

The forces and moments acting on an aircraft are introduced in the previous sections. In this section will be introduced the stability equation of the aircraft. Starting from the forces and the moment of single component it's possible to evaluate the moment of the aircraft. The moments are summed about the center of gravity for each aircraft. The moment or trim equations are usually placed in coefficient form by dividing through by $(q_\infty S_{ref} \bar{c})$, where (q_∞ is the dynamic pressure ($\frac{1}{2}\rho v^2$), S_{ref} is the wing reference area, and \bar{c} is the mean aerodynamic chord of the wing). Now, replace the wing by its mac and locate the lift, drag, and moment of the wing at the aerodynamic center a.c.

Trim equation for a conventional aircraft with horizontal tail aft of the wing is

$$C_{M_{c.g.}} = C_N \frac{x_w}{\bar{c}} + C_C \frac{z_w}{\bar{c}} + C_{M_{a.c.w}} + \frac{T z_T}{q_\infty S_{ref} \bar{c}} - C_{L_T} \bar{V}_H \eta_T + C_{D_T} \frac{S_H}{S_w} \frac{\bar{z}_h}{\bar{c}_w} \eta_T + C_{M_{a.c.T}} \eta_T \frac{S_H}{S_w} \frac{\bar{c}_h}{\bar{c}_w} \quad (9.39)$$

The term $\frac{q_\infty T}{q_\infty}$ is called the tail efficiency factor and comes about because of the influence of the wing on the free-stream velocity striking the tail. The tail efficiency η_H accounts for the possibility that the horizontal tail will see a somewhat reduced velocity due to the downwash generated by the lifting wing, particularly at higher angles of attack of the wing.[42]. The therm \bar{V}_H is the volumetric ratio and it's an important design parameter.

An aircraft must be able to stay in equilibrium for any attitude or flight condition and all thrust levels. This requires that there be no net force or moment acting on it. The equilibrium of forces in the vertical direction is

$$W = L_W + L_T \quad (9.40)$$

While to have equilibrium of moments the trim equation must be equal to zero.

$$C_{M_{c.g.}} = 0 \quad (9.41)$$

The aircraft can, in general, be trimmed, that is, put into an equilibrium state where the

combined lift of the wing and the tail balances the weight while the moment about the center of gravity is zero. The horizontal tail is movable, either all movable or a portion (called the elevator on an aft tail) is movable. In this way, the horizontal tail can cause the aircraft to rotate from one equilibrium (trimmed) condition to another.[32]

The aircraft is said to be statically stable if the response of the aircraft to a disturbance in angle of attack is to tend to return to the original equilibrium position. As mentioned the criterion for static stability in an aircraft is that the derivative of $C_{M_{c,g}}$ respect to α is negative. This means that if an aircraft with $C_{M_\alpha} < 0$ is in equilibrium (trimmed) at a positive α and suddenly α is increased the aircraft will generate a negative moment to push the nose down toward the original equilibrium.

9.5.1 Neutral Point and Static Margin

It is possible now to find the aerodynamic center of the aircraft, or, as it's usually called, the neutral point, by setting the derivative of the moment coefficient with respect to angle of attack in Eq. 9.39 equal to zero. In this case we assume the control stick is fixed so that the horizontal tail acts without any deflection of the control surface, that is, without deflecting the elevator.

The center of gravity location which satisfies this condition is called the neutral point. The difference between the position of the center of gravity and the neutral point is called the static margin. It expresses how far the center of gravity of the airplane is forward of the neutral point, expressed as a fraction of the mean aerodynamic chord. The larger this quantity is, the more stable the aircraft and the less maneuverable it is. However, with greater stability the pilot workload decreases because fewer control inputs are required to keep a particular course. The airplane is said to be stiffer as the static margin increases. Typical commercial aircraft has a static margin of around 5–10%. When the static margin is zero the airplane is neutrally stable, while if the static margin is negative the aircraft is statically unstable.

9.5.2 Pendular Stability

It is important to note that the horizontal component of the aerodynamic force introduces a contribute in stability equation. The arm of this force is z_a .

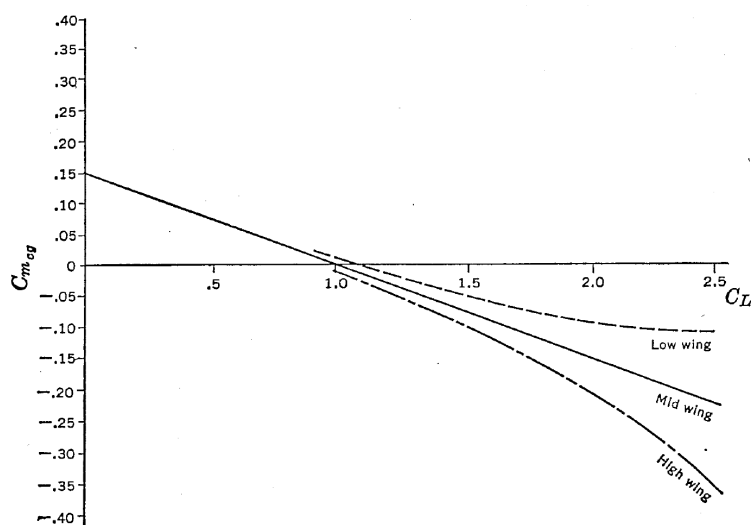


Figure 9.31: Effect of vertical location of c.g. on pitching moment.

If the c.g. position is under the wing aerodynamic center, z_a will be negative and the term will bestabilizing, whereas if the c.g. is over the wing aerodynamic center, the term will be unstable. This term is usually very small with respect to the first term except at high values of the lift coefficient. [36]

9.6 Java Class Architecture

In order to manage all required methods a manager stability class has been created, named `ACStabilityManager`. This is a complex class that defines and assigns all the useful data for the stability analysis having the operative condition as input. This class calls various method for the other class described in the previous chapter in order to evaluate the moment respect to the center of gravity of the aircraft. This moment, infact, is obtained starting from the forces acting on the aircraft's components.

Depending on the value of plot check the Class draws some chart useful for the knowledge of output data.

Table 9.1: `ACStabilityManager` input variables.

Input Variable	Description
<code>Aircraft</code> - the Aircraft	The object of analysis.
<code>MyAirfoil</code> - Mean Airfoil	In order to make computing faster the mean airfoil is calculated in the test class.
<code>ConditionEnum</code> - the Operative Condition	In JPAD is defined an enumeration of operating condition: TAKE-OFF, CRUISE and LAND-ING. Giving the condition as input, the builder of the stability manager automatically calculates all the parameters (such as Mach number or high-lift devices deflection).
<code>Amount<Angle></code> - alpha Min, alpha Max	These are the first and the last value of the α_b array for which will be made the analysis. They can be in degree or radian. These values may be null in order to execute analysis only for an angle of attack. In this case the values of alpha max and alpha min will be alpha body $\pm 1^\circ$. It's possible to set the number of values with a setter.
<code>Amount<Angle></code> - alpha Body	Is the angle of attack (alpha body) for the calculation of numerical value of CL, CD, CM. This value may be null. In this case the class calculates only all stability characteristics at an array of alpha body
<code>boolean</code> - plot Check	This is a check value in order to make charts or not.
<code>String</code> - subfolder Path	This is the folder path where the charts will be saved.
<code>String</code> - path XML HighLift	This is the path of the input file for high-lift data in take off condition or landing.

The class ACStabilityManager contains different methods in order to evaluate Lift, Drag and Moments contributes. All methods and related functionality are expressed in the following table.

Table 9.2: Methods of the class ACStabilityManager.

Method	Description
ACStabilityManager	It is the builder of the class. It initialize all useful data
calculateAll	This method call all the other methods of the class in order to calculate lift, drag and pitching moment characteristics of the component.
calculateLiftCharacteristics()	This method call the methods related to the lift calculation that fill the array and, eventually, produce charts.
calculateDragCharacteristics()	The same of previous for drag.
calculateMomentCharacteristics()	The same of previous for pitching moment.
calculateWingLiftCharacteristics()	This method uses methods of lift calculation classes in order to fill the lift arrays for wing both in cruise and in take off or landing.
calculateHTailLiftCharacteristics()	This method uses methods of lift calculation classes in order to fill the lift arrays for wing both in cruise and in take off or landing.
calculateFuselageLiftCharacteristics()	This method uses methods of lift calculation classes in order to correct the lift coefficient of an isolated wing.
calculateWingDragCharacteristics	This method uses methods of lift calculation classes in order to fill the lift arrays for wing both in cruise and in take off or landing.
calculateHTailDragCharacteristics	The same of previous for horizontal tail. This method consider also the elevator deflections.
calculateWingMomentCharacteristics()	This method call the methods related to the pitching moment calculation that fill the array and, eventually, produce charts.
calculateHTailMomentCharacteristics()	The same of previous for horizontal tail.
calculateFuselageMomentCharacteristics()	The same of previous for fuselage.
calculatePowerEffects	This method introduces power effect on the stability.
deltaEElevatorCalculator	This method calculates the deflection of the elevator at alpha.
calculateMoment()	This method calculates the pitching moment of the entire aircraft respect to the center of gravity.
calculatedeltaEEquilibrium()	This method calculates the angle of deflection of the horizontal tail for the trim..
neutralPointCalculator	This method calculates the neutral point and eventually draws the charts.

Table 9.3: Output charts for the class ACStabilityManager.

Clean	Cl vs α - airfoils.
	CL vs α_w - wing.
	Stall path - wing.
	CD parasite vs α_w - wing.
	CD induced vs α_w - wing.
	CD total vs α_w - wing.
	CL vs α_h - horizontal Tail. With elevator deflections.
	CD total vs α_h - horizontal Tail. With elevator deflections.
	Stall path - horizontal Tail.
	CL vs α_w - wing-body.
	CL vs α_w - Total. With elevator Deflection.
	Downwash gradient vs α_b - linear and non-linear.
	Downwash angle vs α_b - linear and non-linear.
	Cm vs α_b - respect to c/4 of MAC for wing.
	Cm vs α_b - respect to ac for wing.
	Cm vs α_b - respect to c/4 of MAC for horizontal Tail.
	Cm vs α_b - respect to ac for horizontal Tail.
	Cm vs α_b - for fuselage.
	Cm vs α_b - respect to cg for aircraft. With elevator deflections.
	Cm vs α_b - respect to ac for wing.
	δ_{ee} vs α_b
	Neutral Point vs $C_{L_{tot}}$
Take Off - Landing	The same for cruise
	CL vs α_w - wing. Whith High Lift devices effects.
	CD total vs α_w - wing. With high lift devices effects.

9.6.1 Focus on the class methods

The first method of the class is the builder. An important function is carried out by this method that assigns all the useful data. The main purposes of the builder are the following

1. An array of α_b is defined . This is an array of nValue in Deg. The number of elements is settable by the user.
2. According to the condition it sets the Mach number. The Cruise, take Off and Landing Mach numbers are defined in the aircraft aerodynamic manager ACAerodynamicManager. In this way it's possible to access to the value from the aircraft object.
3. The operating condition (such as altitude and Mach number) are defined according to the flight condition.
4. The center of gravity is defined starting from the correct weight of the aircraft. In particular:
 - Take Off → MTOW
 - Cruise → $\frac{(MTOW+MZFW)}{2}$
 - Landing → MZFW

All the other methods are structured in order to obtain the following results:

1. Array filling

2. Value at α_b

3. Charts

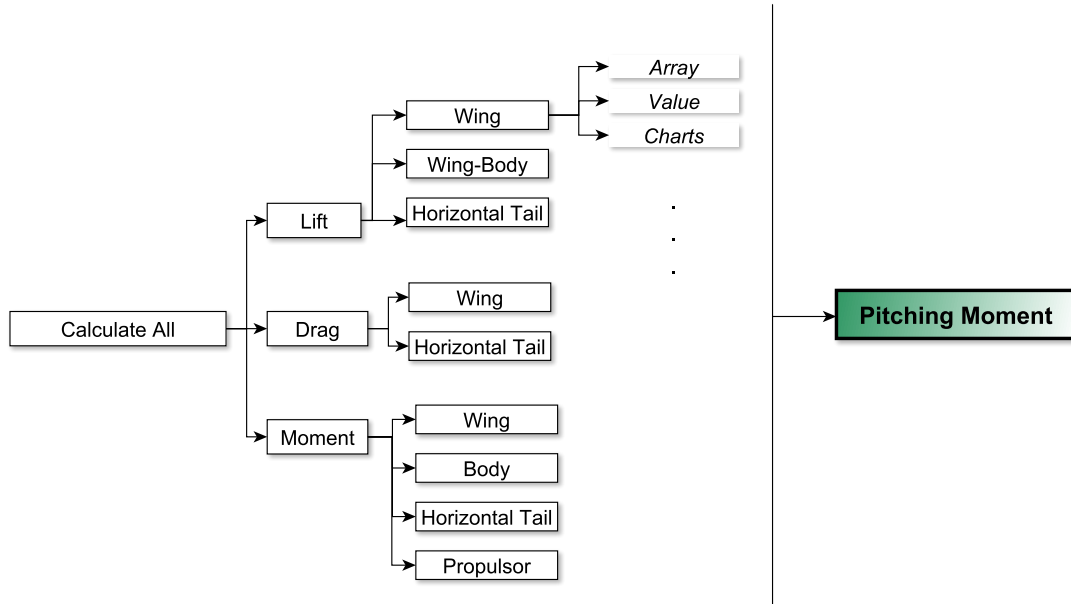


Figure 9.32: Methods in ACStabilityManager class.

The value for the α_b array are saved in array which can be read via getter methods.

Listing 9.1 Some of Output Array

```

//Output Arrays // Correspond to alpha body array

private double [] cLWingCleanArray;
private double [] cLWingTOArray;
private double [] cLWingLandingArray;
private double [] cLWingBodyArray;
private double [] cLAlphaArray;
private double [] cLHTailCleanArray;
private Double [] downwashAnglesArray;
private double [] tauIndexArray = new double [deltaEArray.length];
private double [] cLCompleteAircraftdeltaEArray = new double [deltaEArray.length];

private double [] parasiteCDWingCleanArray;
private double [] parasiteCDHTailCleanArray;
private double [] inducedCDWingArray;
private double [] inducedCDHTailArray;
private double [] cDWingCleanArray;
  
```

The results for the horizontal tail are obtained for an array of elevator deflections which value can be set by the user. Consequently the resultant values for the horizontal tail are organized in a Map.

9.7 Case Study

Several graphs used in this modulus are presented in previous chapter. So, following, there will be only the new results.

9.7.1 ATR 72

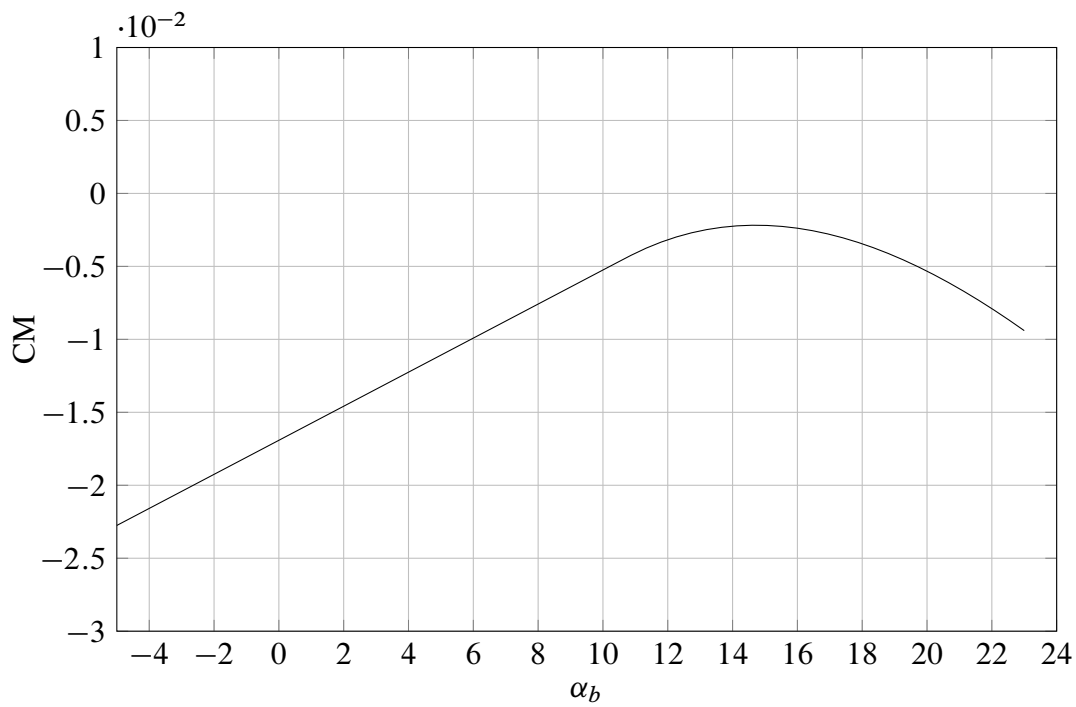


Figure 9.33: ATR 72 . Mach 0.45. Pitching Moment Coefficient of the Wing respect to a quarter of MAC.

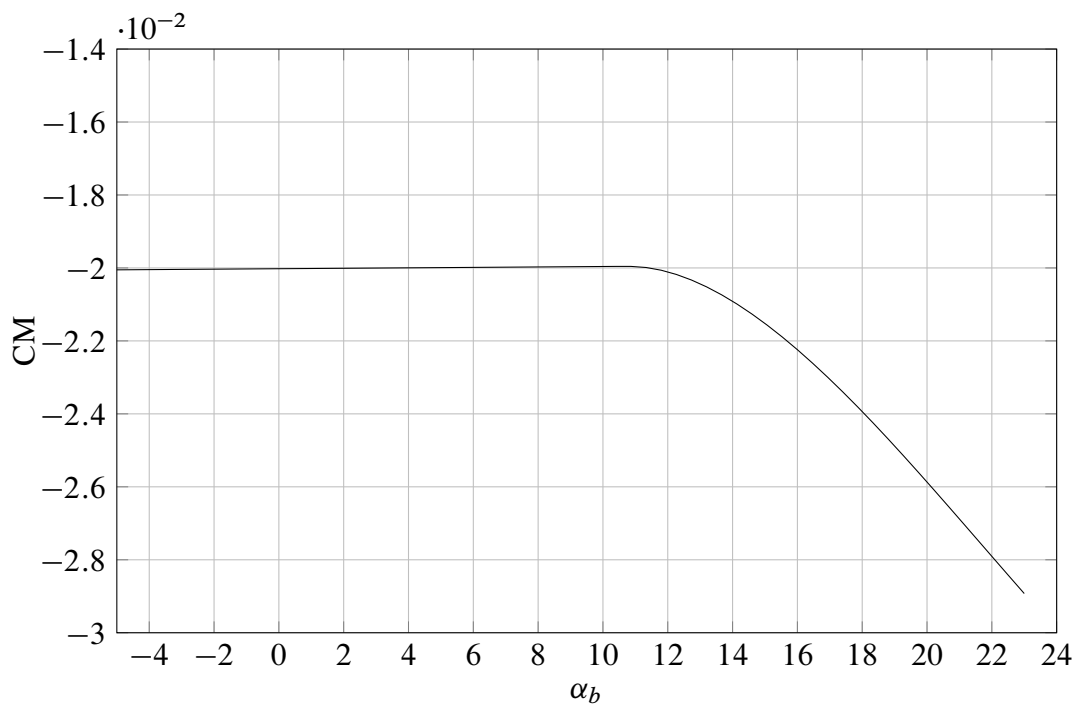


Figure 9.34: ATR 72 . Mach 0.45. Pitching Moment Coefficient of the Wing respect to AC. AC=0.2374 implemented method. AC= 0.24445 DeYoung Harper.

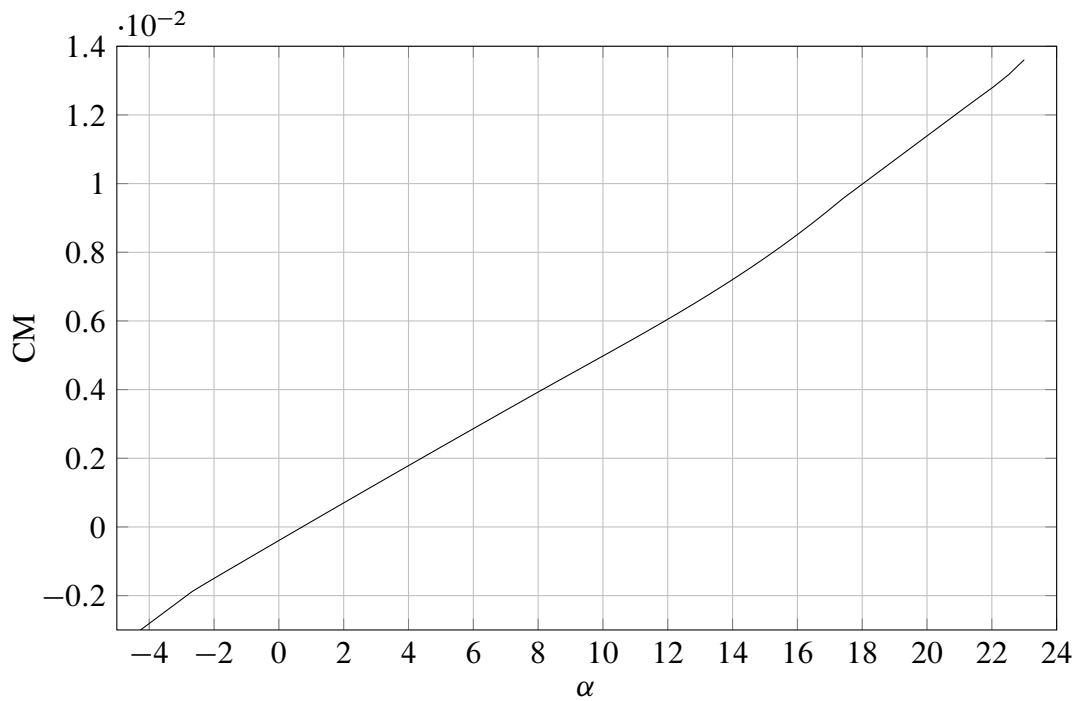


Figure 9.35: ATR 72 . Mach 0.45. Pitching Moment Coefficient of the Horizontal Tail respect to a quarter of MAC.

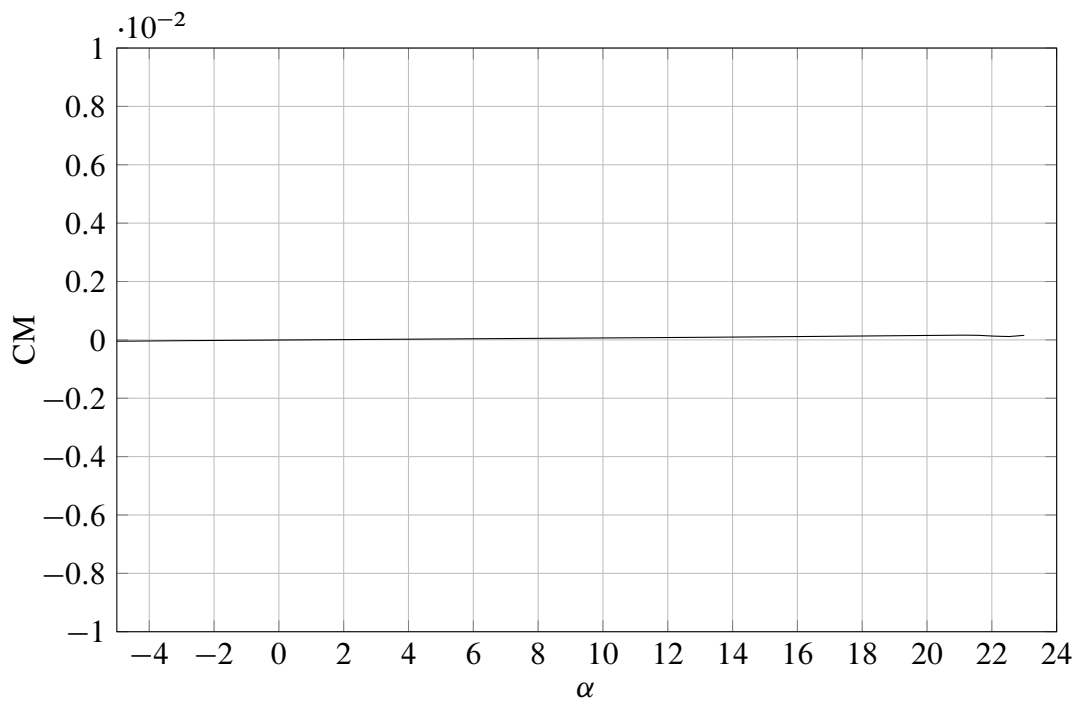


Figure 9.36: ATR 72 . Mach 0.45. Pitching Moment Coefficient of the Horizontal Tail respect to AC. AC=0.2396 implemented method. AC= 0.2352 DeYoung Harper.

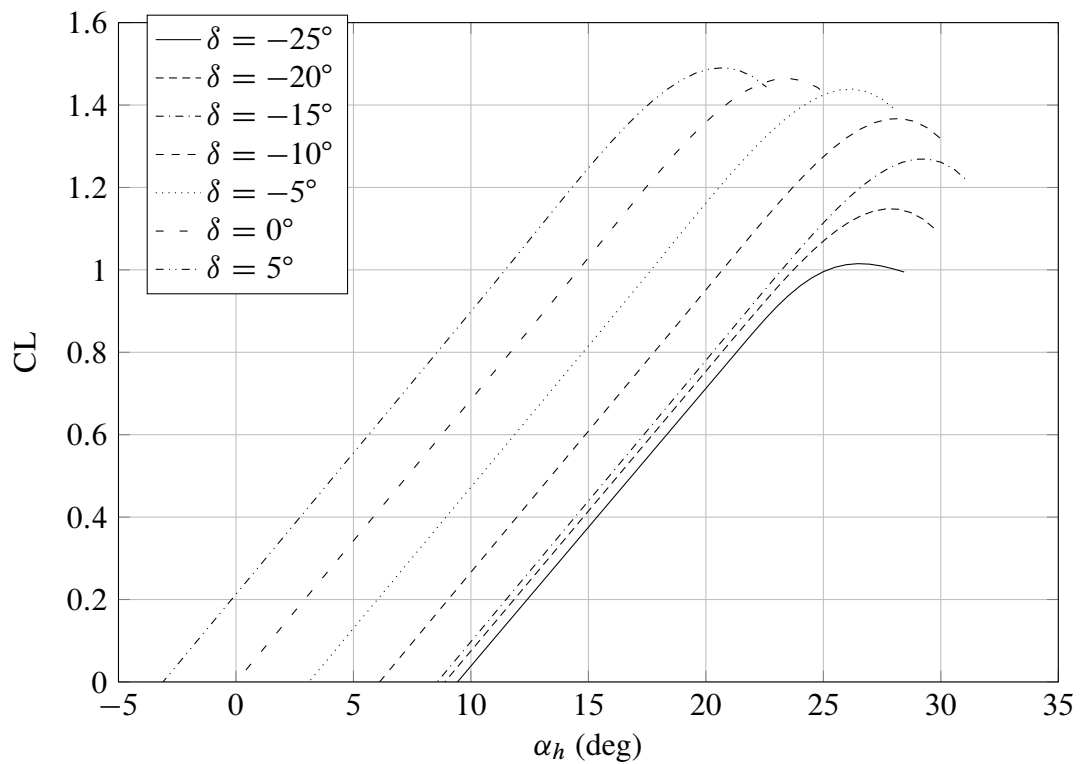


Figure 9.37: ATR 72 . Mach 0.45. CL vs α_h for the horizontal tail with elevator deflections.

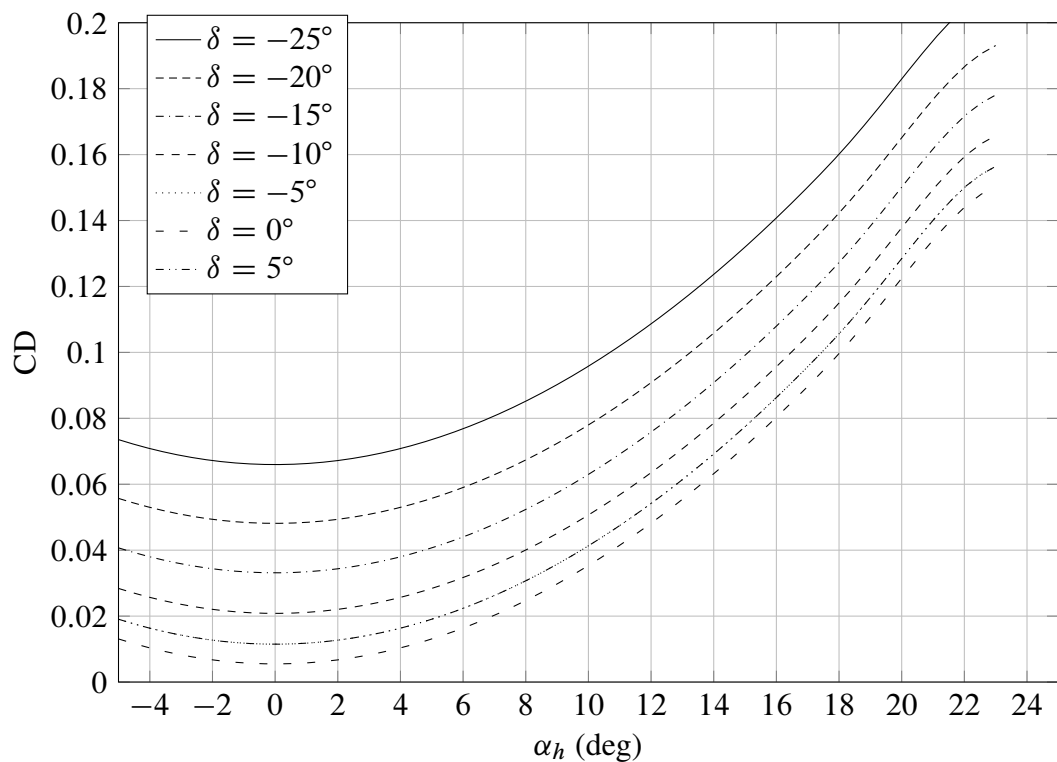


Figure 9.38: ATR 72 . Mach 0.45. CD vs α_h for the horizontal tail with elevator deflections.

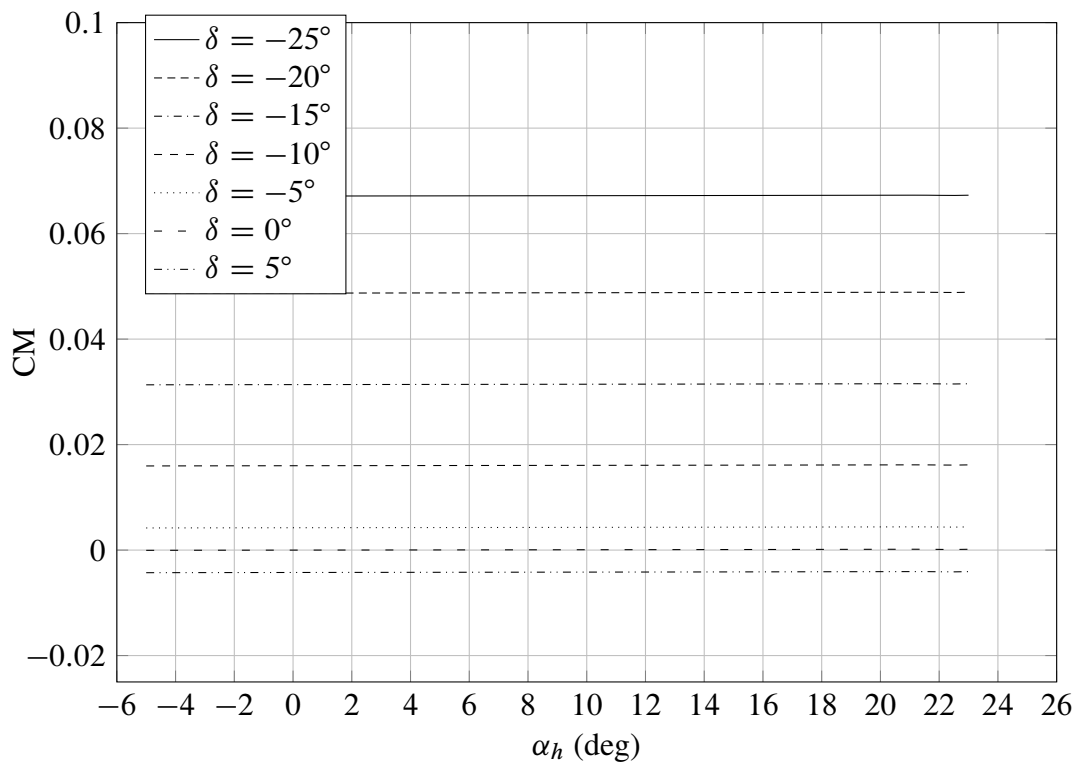


Figure 9.39: ATR 72 . Mach 0.45. CM_{ac} vs α_h for the horizontal tail with elevator deflections.

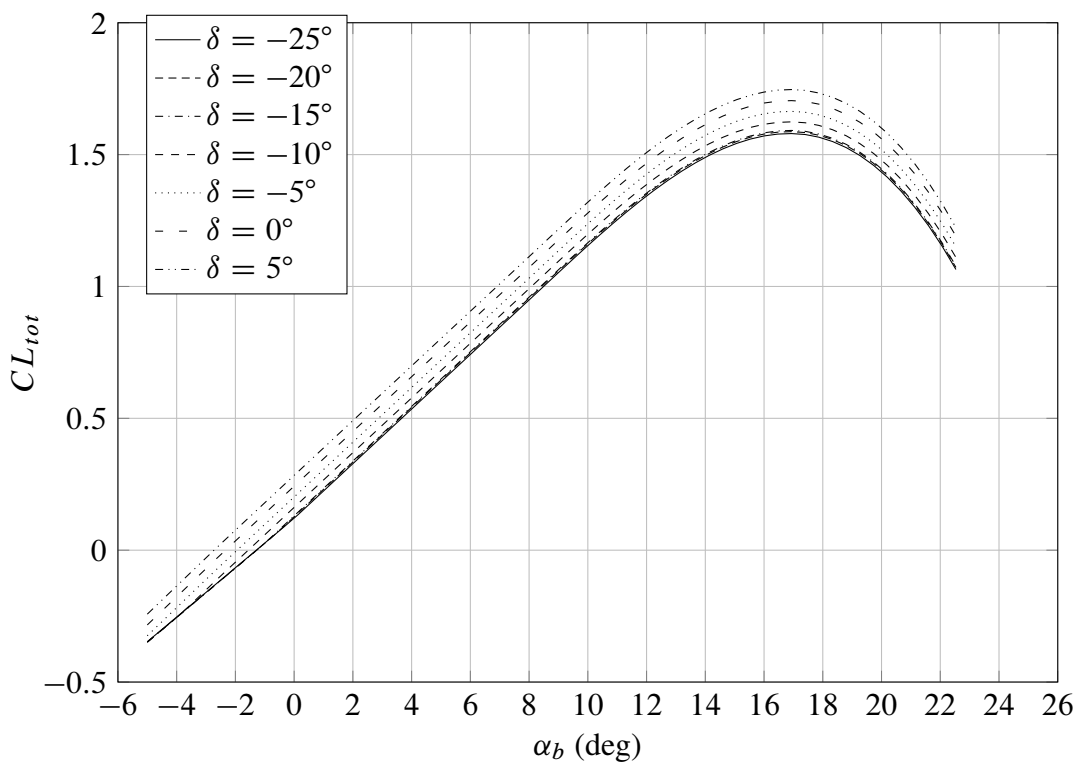


Figure 9.40: ATR 72 . Mach 0.45. CL_{tot} vs α_b with elevator deflections.

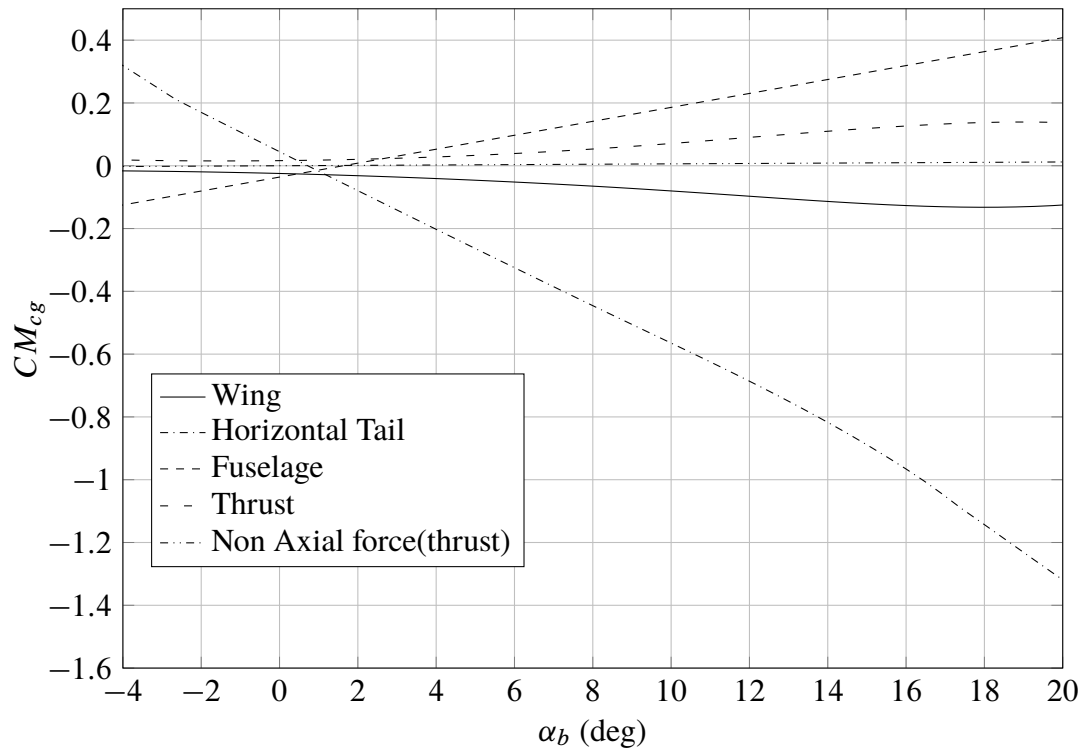


Figure 9.41: ATR 72 . Mach 0.45. CM respect to CG vs α_b of aircraft's components.

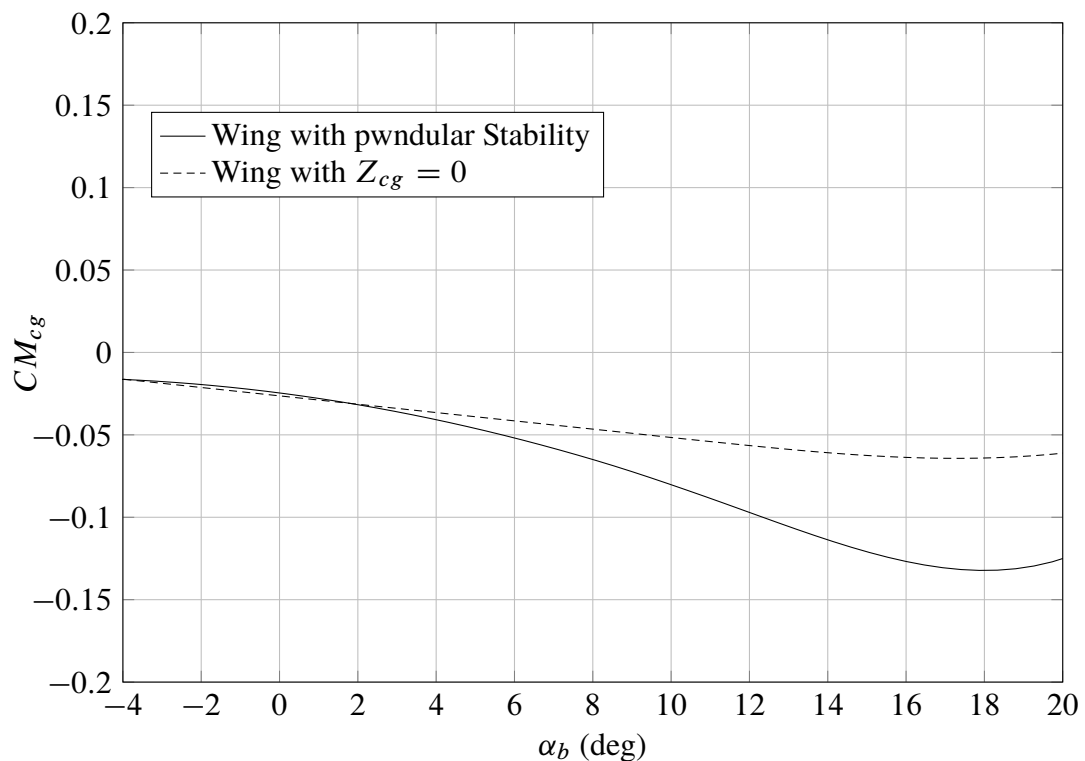
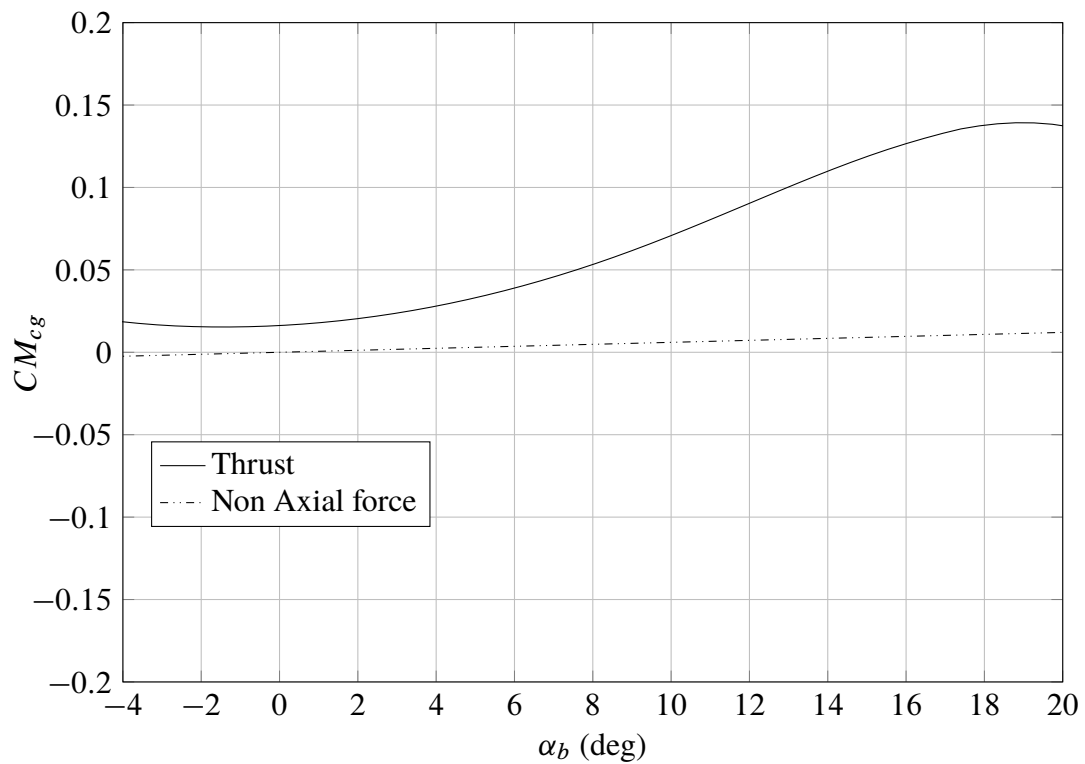
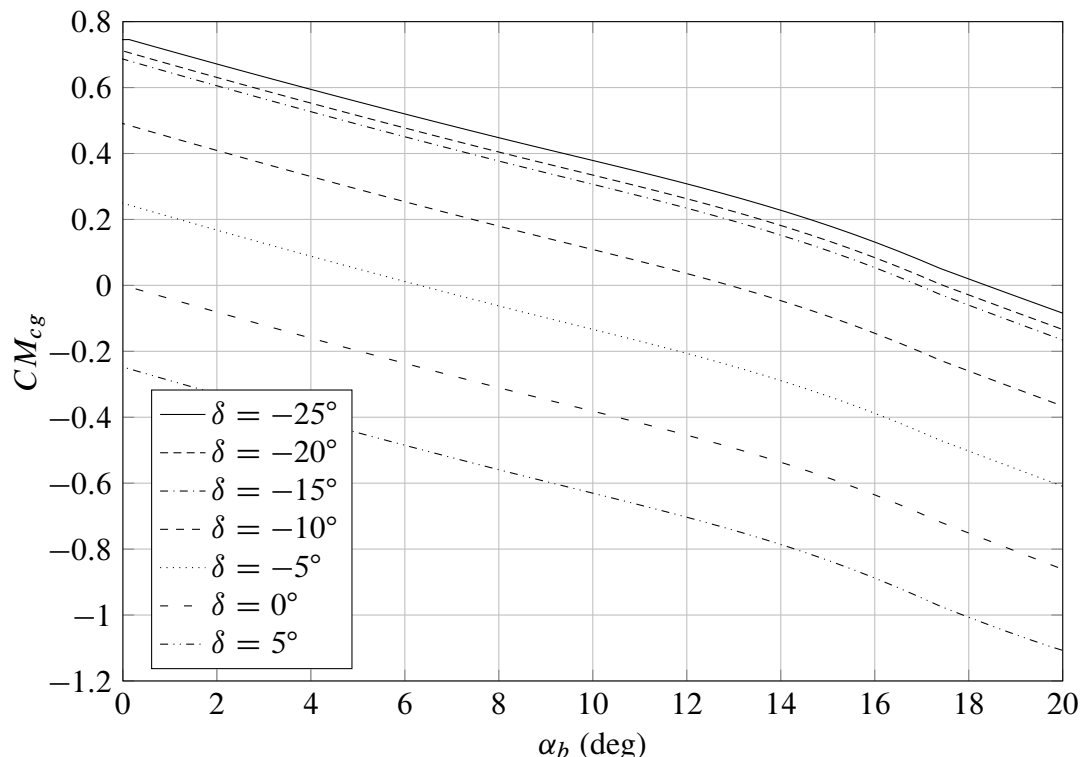


Figure 9.42: ATR 72 . Mach 0.45. Cm_{cg} vs α_b for the wing. Comparison with and without pendular stability.

Figure 9.43: ATR 72 . Mach 0.45. CM_{cg} vs α_b . Power effects.Figure 9.44: ATR 72 . Mach 0.45. Aircraft CM_{cg} vs α_b with elevator deflections.

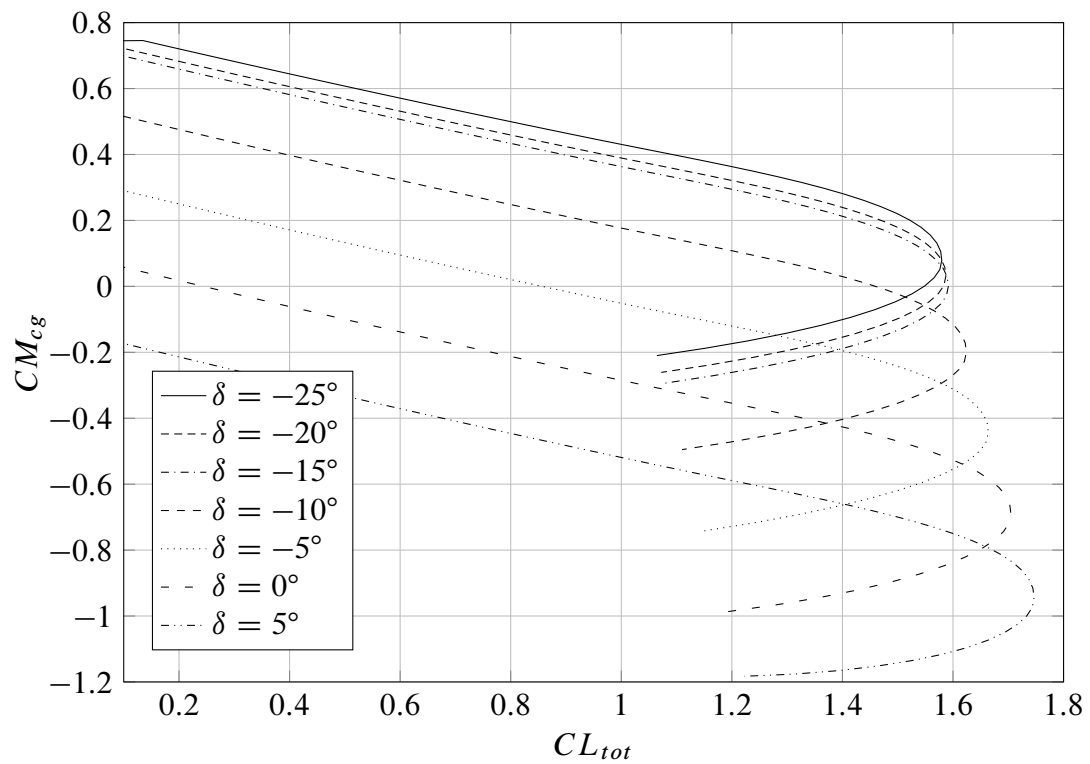


Figure 9.45: ATR 72 .Mach 0.45. Aircraft CM_{cg} vs CL_{tot} with elevator deflections.

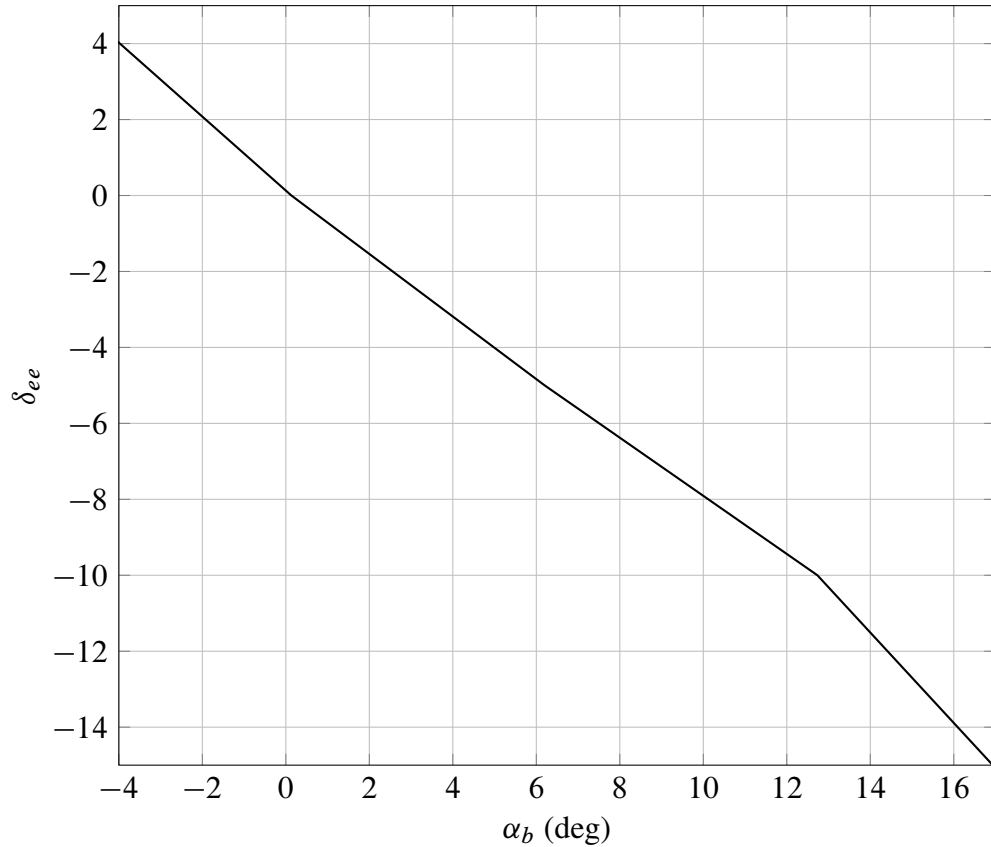


Figure 9.46: ATR 72 . Mach 0.45. δ_{ee} of elevator.

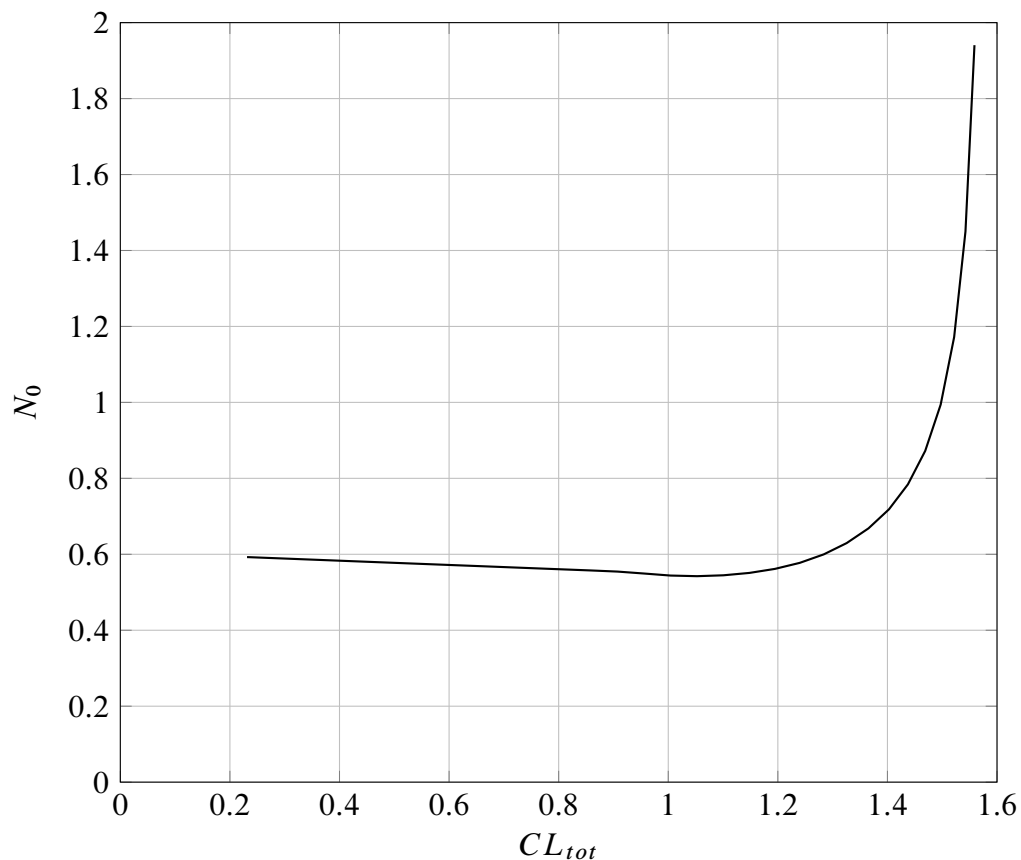


Figure 9.47: ATR 72 . Mach 0.45. Neutral Point, stick fixed, $\delta_e = 0$.

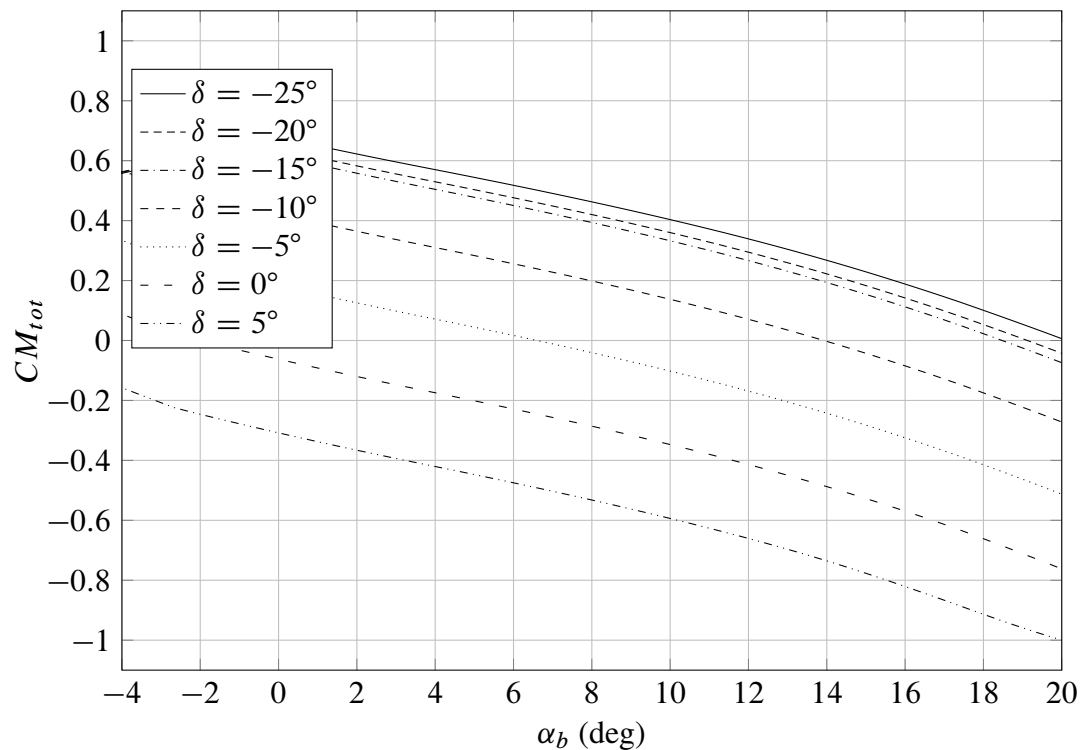


Figure 9.48: ATR 72 . Mach 0.2. TakeOff Conditions. CM_{tot} vs α_b with elevator deflection.

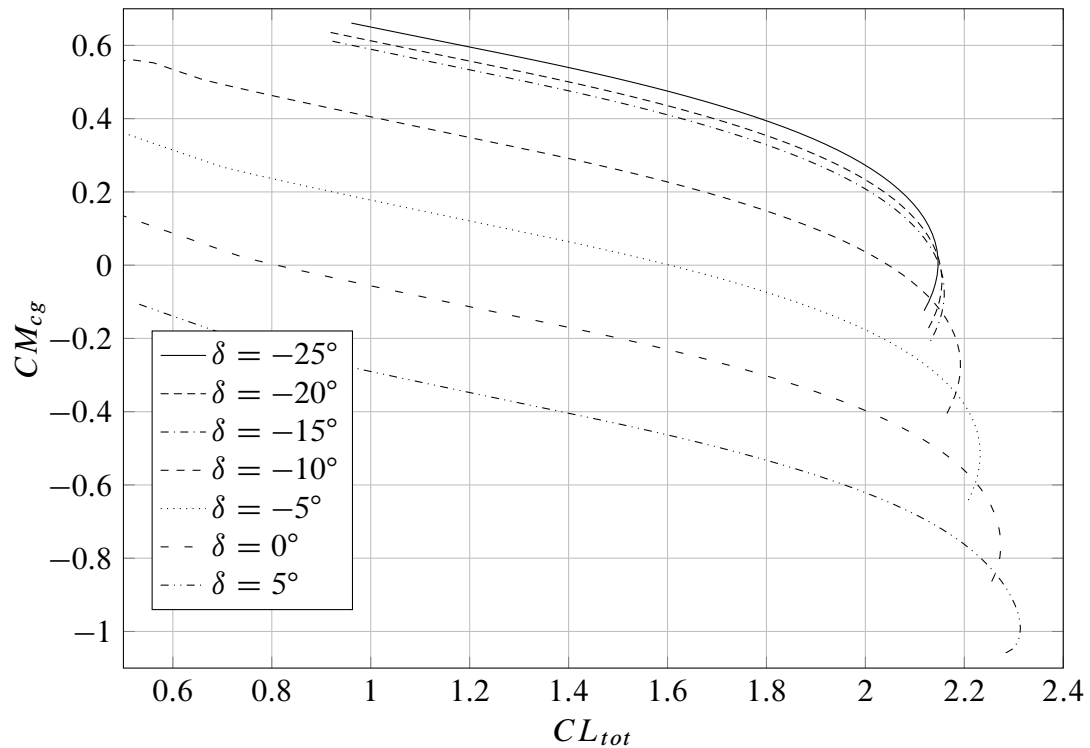


Figure 9.49: ATR 72 . Mach 0.2. TakeOff Conditions. CM_{tot} vs CL_{tot} with elevator deflection.

9.7.2 Boeing 747-100B

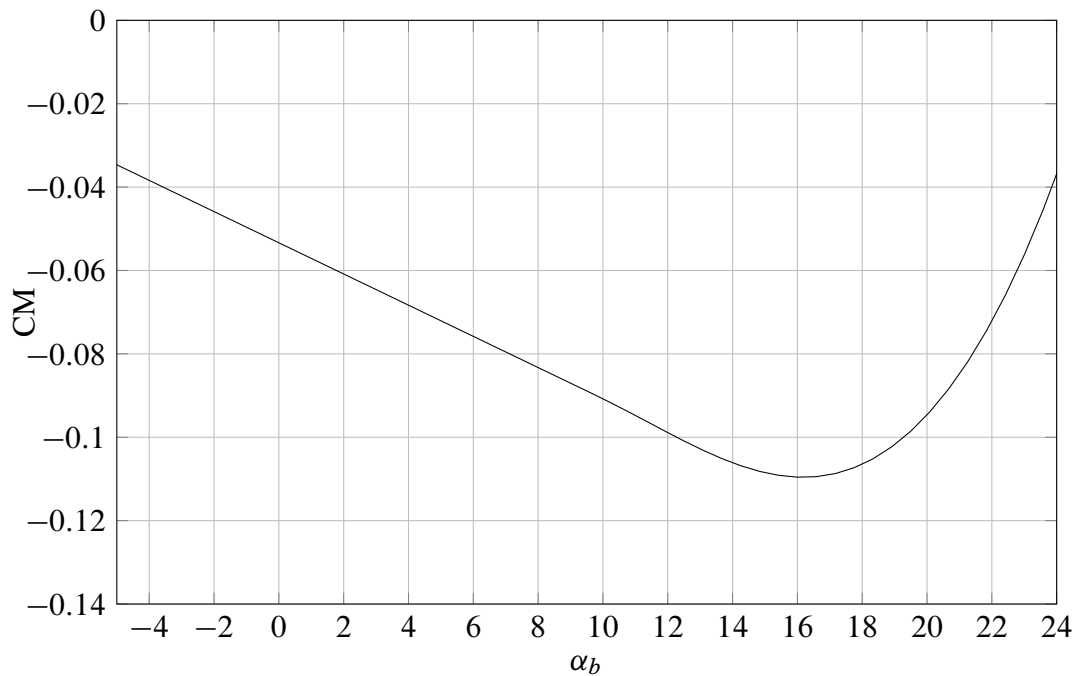


Figure 9.50: BOEING 747-100B . Mach 0.7. Pitching Moment Coefficient of the Wing respect to a quarter of MAC.

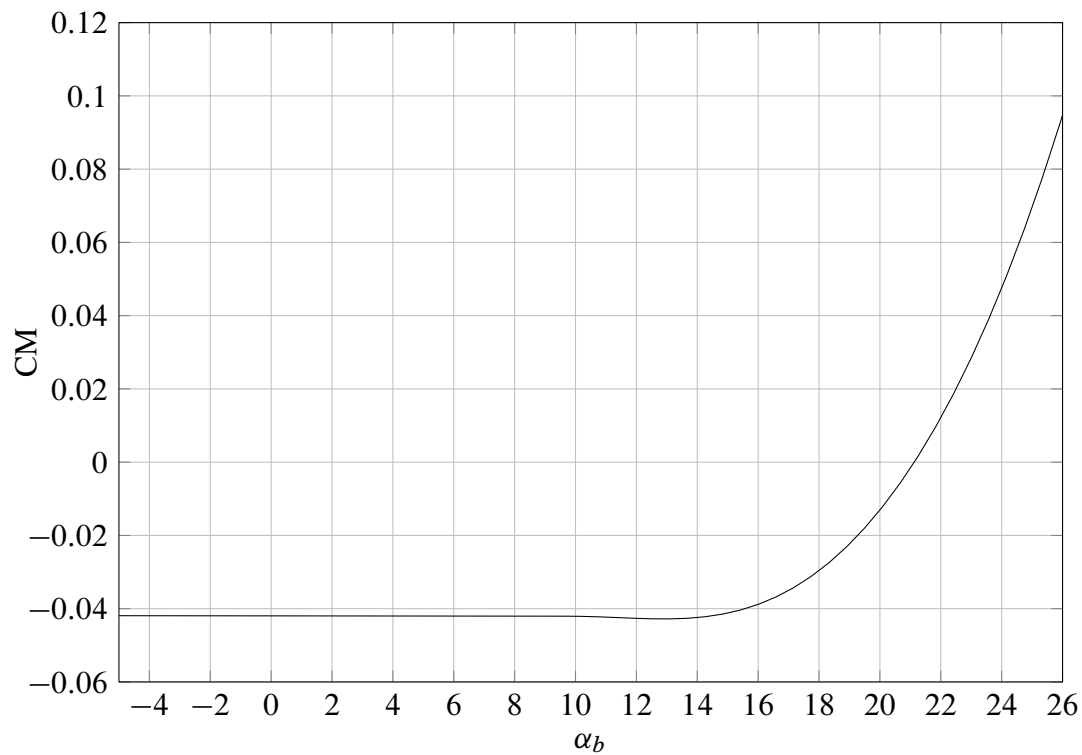


Figure 9.51: BOEING 747-100B . Mach 0.7.Pitching Moment Coefficient of the Wing respect to AC. AC=0.308 implemented method. AC= 0.29 DeYoung Harper.

Chapter 10

Induced Angle of Attack

*Once we accept our limits,
we go beyond them.*

– Albert Einstein

10.1 Induced Angle of Attack

When a wing passes through the air, it creates a perturbation, which leads to a vertical component on the relative motion on the air over the wing. Consequently the air flow past the wing is inclined in regard of the initial free stream. Then, the wing behaves as thought the flow were coming from a different direction: the local flow direction.

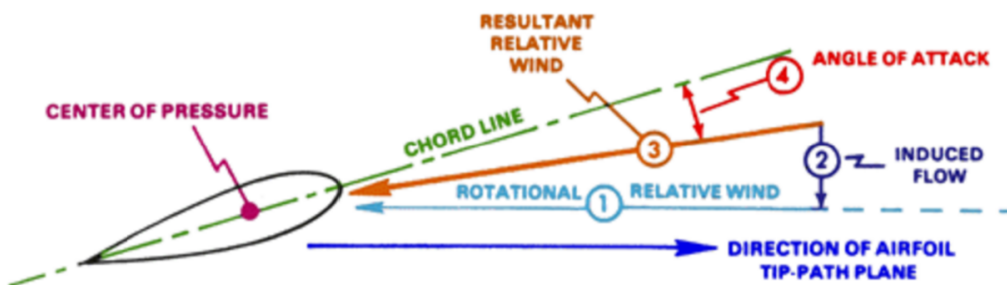


Figure 10.1: Definitions of induced end effective angles of attack.

In practice, these perturbations are generated by the wingtip vortices, which create downwash and deflect the local airflow in the vicinity of the wing downward. This angle is the induced angle of attack α_i . The airfoil section itself is then responding to an effective angle of attack equal to the geometric angle of attack minus the induced angle of attack: $\alpha_e = \alpha - \alpha_i$. In most cases, the absolute value of the angle of attack is decreased, and so as for the lift force. Then, in order to produce a given lift force, the AOA of the wing must be greater than the AOA that would be given by a theoretical study of the wing section (2D wing). Moreover, the resulting force exerted by the air on the wing, now perpendicular to the local flow direction, is tilted backwards by an angle equal to the induced angle of attack and then is no longer perpendicular to the free stream velocity. This important phenomenon is at the origin of the induced drag (i.e. the component of the resulting force parallel to the free stream velocity), and therefore for a given lift, a greater induced AOA implies a greater drag. One must bear

in mind that because this is a 3-dimensional effect.[6]

In order to evaluate the effective angle of attack for each spanwise station, it's possible to implement an iterative process in which at a load distribution it's evaluated the related induced angles that generates a new load distribution.

The induced angle of attack is in eq. 10.1, where w is the vertical downwash component:

$$\alpha = \arctan\left(\frac{w}{V}\right) \quad (10.1)$$

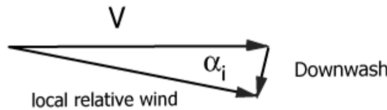


Figure 10.2: Geometrical representation of induced angle of attack.

The lifting surface is considered as divided in several rectangular horse-shoe vortices along the span; one horseshoe vortex along the chord is used, that is, the midpoints of the vortices are placed only at points along the quarter-chord lines. An equal number of control points are located along the three-quarter-chord lines. The velocity from the total vortex system is equated to the component of free-stream velocity normal to the lifting surface chord at each control point.

The downwash velocity at any of the control points P, which results from the $2N$ horseshoe vortices is:

$$w = \frac{1}{4\pi} \sum_{n=1}^N \Gamma_n F'_{w,v_n} \quad (10.2)$$

where Γ is circulation strength, F is the downwash influence function, N are the vortex point and v are the vortex points.

In JPAD this effect is calculated in the class `AlphaEffective`. This method has as output an array of value that indicates the effective angles of attack semi-spanwise using the equations introduced before. In order to evaluate these angles you must have as input the operating conditions.

Listing 10.1 Effective angle of attack Test Class

```
// -----
// Evaluate effective angle of attack
// -----
```

```
System.out.println("\n-----");
System.out.println("STARTING_EVALUATE_EFFECTIVE_ANGLE_OF_ATTACK_");
System.out.println("-----");

double[] alphaEffective;

AlphaEffective theAlphaCalculator = new AlphaEffective(
    theLSAnalysis, theWing, theOperatingConditions);
Amount<Angle> inputAngle =
    Amount.valueOf(toRadians(8.), SI.RADIAN);

alphaEffective = theAlphaCalculator.calculateAlphaEffective(inputAngle);

double [] alphaInduced = theAlphaCalculator.getAlphaInduced;
```

10.2 Case Study

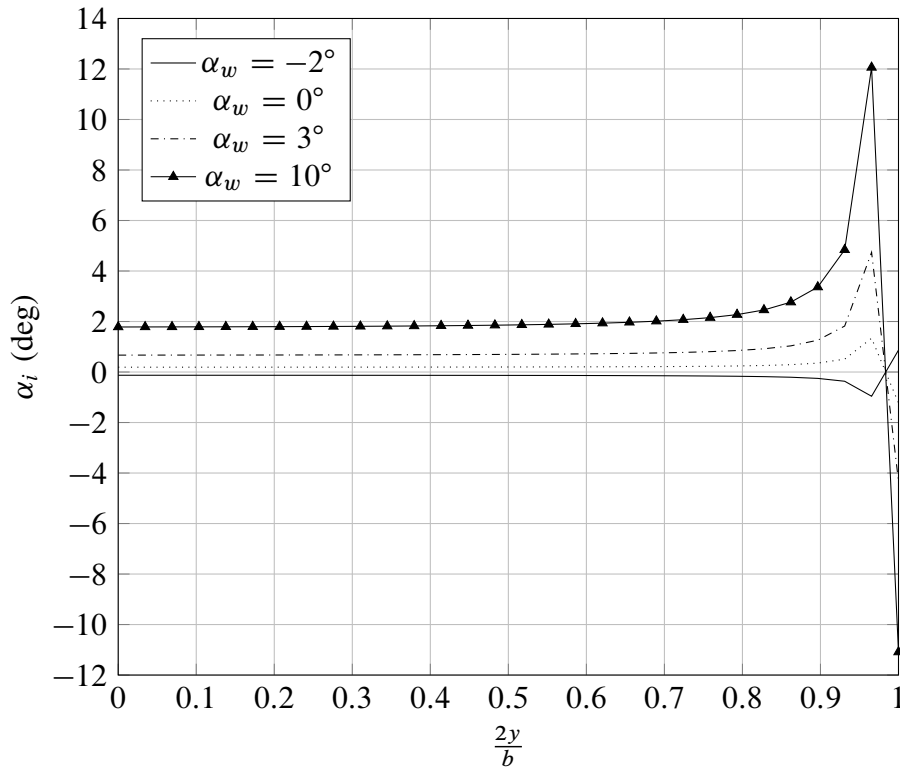


Figure 10.3: Distribution of induced angle of attack along semi-span. ATR 72. $M=0.43$

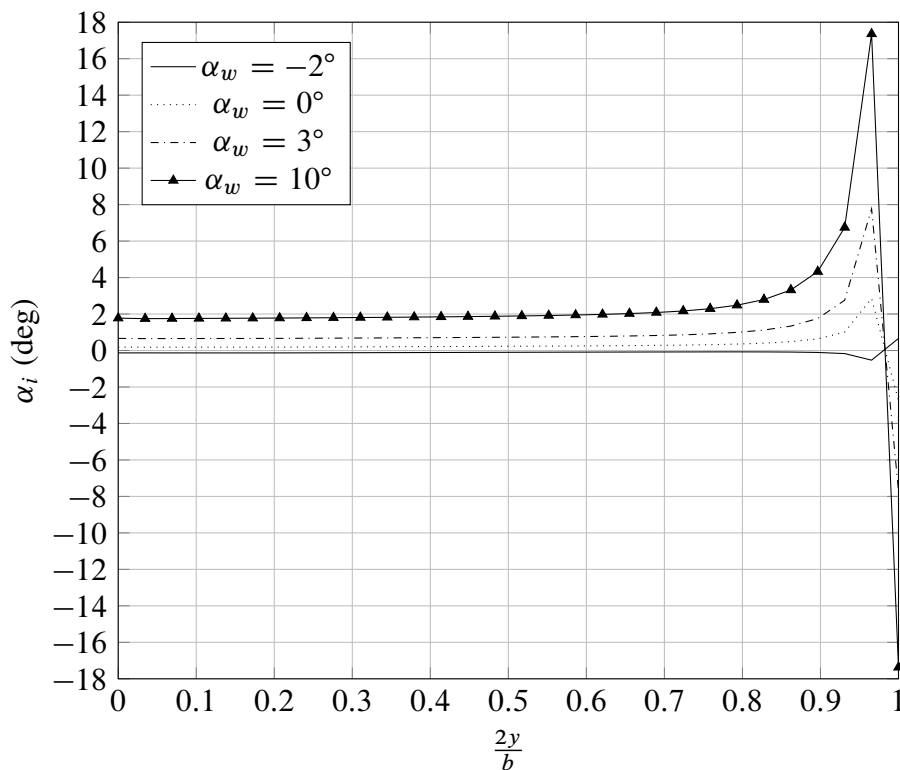


Figure 10.4: Distribution of induced angle of attack along semi-span. BOEING 747-100B. $M=0.75$

Conclusions

An aircraft design and optimization desktop application written in Java, and its functionality, has been introduced. The adoption of established software engineering practices, the use of advanced development tools, and concurrent development enabled the developer team to build a feature-rich application in a relatively short period of time. As of its design, the application is easily maintainable and extensible. The software is still growing and the choice of Java language was really helpful. Infact being Java a pure object oriented programming language, it greatly encourages and simplifies modularization. Each module (package) can be programmed quite independently so that it is relatively easy to divide the work among several programmers working simultaneously or one after the other.

The application, moreover, can be easily integrated into a comprehensive aircraft optimization cycle. As all analysis modules inside the JPADCORE package will be completed and tested, the final purpose of the code will be to allow users to define a certain numbers of macroscopical geometrical parameters, along with a given objective function, and to receive as output the best set of the previous parameters which suits the wanted objective. These future targets will make the software able to carry out an analysis of an aircraft during its preliminary design phase in a fast and flexible way.

Appendix A

HDF dataset and database reader creation

In a tool for preliminary design phase of an aircraft, it's very important to have available database. It's possible to create database starting from graphics using external software. In this appendix will be explained the step required in order to digitalize the graphics, create an HDF dataset and set up the database-reader class in Jpad.

A.1 Chart Digitization

The first step required for create a dataset is to digitalize a chart. Often data are presented in reports and references as functional X-Y type scatter or line plots. In order to use this data, it must somehow be digitized. This is made with an external software, such as *Plot Digitizer*. Plot Digitizer is a Java program used to digitize scanned plots of functional data. This program will allow you to take a scanned image of a plot (in GIF, JPEG, or PNG format) and quickly digitize values off the plot just by clicking the mouse on each data point.[8]

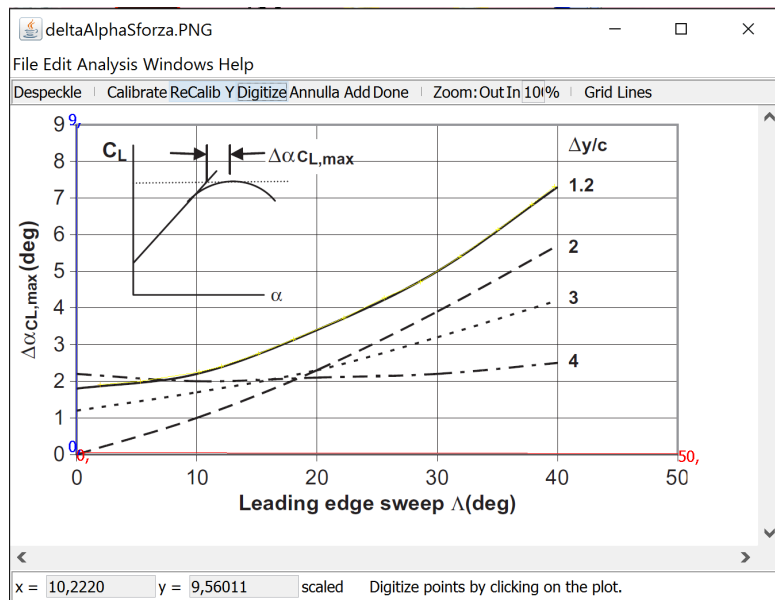


Figure A.1: Chart digitization using Plot Digitizer.

In order to digitize a chart, first of all it's necessary to calibrate the axis. Plot Digitizer works with both linear and logarithmic axis scales. After it's possible to digitize a curve

simply click on it. The values obtained can then be saved to a tex file or .csv file.

A.2 Creation of an HDF file with Matlab

Obtained the .csv file from digitization is necessary to create the HDF file. First of all it's necessary to import the file with couple of coordinates as matrix. After saving the imported files as .mat file, Matlab code comes in play to manage these data and to generate the digitalized curves and the HDF dataset. The code interpolates curves points with cubic splines in order to have more points to plot for each curve.

Listing A.1 MATLAB script for creating the HDF Database

```
clc; close all; clear all;

%% Import data
DeltaAlphaCLmax_vs_LambdaLE_dy1p2 = importdata('DeltaAlphaCLmax_vs_LambdaLE_dy1p2.mat');
DeltaAlphaCLmax_vs_LambdaLE_dy2p0 = importdata('DeltaAlphaCLmax_vs_LambdaLE_dy2p0.mat');
DeltaAlphaCLmax_vs_LambdaLE_dy3p0 = importdata('DeltaAlphaCLmax_vs_LambdaLE_dy3p0.mat');
DeltaAlphaCLmax_vs_LambdaLE_dy4p0 = importdata('DeltaAlphaCLmax_vs_LambdaLE_dy4p0.mat');

nPoints = 30;
lambdaLEVector_deg = transpose(linspace(0, 40, nPoints));

%% dy/c = 1.2
smoothingParameter = 0.999999;
DAlphaVsLambdaLESplineStatic_Dy1p2 = csaps( ...
    DeltaAlphaCLmax_vs_LambdaLE_dy1p2(:,1), ...
    DeltaAlphaCLmax_vs_LambdaLE_dy1p2(:,2), ...
    smoothingParameter ...
);

DAlphaVsLambdaLESplineStatic_Dy1p2 = ppval( ...
    DAlphaVsLambdaLESplineStatic_Dy1p2, ...
    lambdaLEVector_deg ...
);

%% dy/c = 2.0
smoothingParameter = 0.999999;
DAlphaVsLambdaLESplineStatic_Dy2p0 = csaps( ...
    DeltaAlphaCLmax_vs_LambdaLE_dy2p0(:,1), ...
    DeltaAlphaCLmax_vs_LambdaLE_dy2p0(:,2), ...
    smoothingParameter ...
);

DAlphaVsLambdaLESplineStatic_Dy2p0 = ppval( ...
    DAlphaVsLambdaLESplineStatic_Dy2p0, ...
    lambdaLEVector_deg ...
);

%% dy/c = 3.0
smoothingParameter = 0.999999;
DAlphaVsLambdaLESplineStatic_Dy3p0 = csaps( ...
    DeltaAlphaCLmax_vs_LambdaLE_dy3p0(:,1), ...
    DeltaAlphaCLmax_vs_LambdaLE_dy3p0(:,2), ...
    smoothingParameter ...
);

DAlphaVsLambdaLESplineStatic_Dy3p0 = ppval( ...
    DAlphaVsLambdaLESplineStatic_Dy3p0, ...
    lambdaLEVector_deg ...
);

%% dy/c = 4.0
smoothingParameter = 0.999999;
DAlphaVsLambdaLESplineStatic_Dy4p0 = csaps( ...
    DeltaAlphaCLmax_vs_LambdaLE_dy4p0(:,1), ...
    DeltaAlphaCLmax_vs_LambdaLE_dy4p0(:,2), ...

```

```

smoothingParameter ...  

);  
  

DAlphaVsLambdaLEStatic_Dy4p0 = ppval( ...  

    DAlphaVsLambdaLESplineStatic_Dy4p0, ...  

    lambdaLEVector_deg ...  

);  
  

%% Plots  

figure(1)  

plot ( ...  

    lambdaLEVector_deg, DAlphaVsLambdaLEStatic_Dy1p2, '-*b' ... , ...  

);  

hold on  
  

plot ( ...  

    lambdaLEVector_deg, DAlphaVsLambdaLEStatic_Dy2p0, '-b' ... , ...  

);  

hold on  
  

plot ( ...  

    lambdaLEVector_deg, DAlphaVsLambdaLEStatic_Dy3p0, '*b' ... , ...  

);  

hold on  
  

plot ( ...  

    lambdaLEVector_deg, DAlphaVsLambdaLEStatic_Dy4p0, 'b' ... , ...  

);  
  

xlabel('\Lambda_{le}_{(deg)}'); ylabel('Delta\alpha_{C_{L,max}}');  

title('Angle_of_attack_increment_for_wing_maximum_lift_in_subsonic_flight');  

legend('\Delta_y/c=1.2', '\Delta_y/c=2.0', '\Delta_y/c=3.0', '\Delta_y/c=4.0');  

axis([0 50 0 9]);  

grid on;  
  

%% preparing output to HDF  
  

% dy/c  

dyVector = [ ...  

    1.2; 2.0; 3.0; 4.0 ...  

];  
  

%columns --> curves  

myData = [ ...  

    DAlphaVsLambdaLEStatic_Dy1p2, ...  

    DAlphaVsLambdaLEStatic_Dy2p0, ... % -> 2  

    DAlphaVsLambdaLEStatic_Dy3p0, ... % -> 3  

    DAlphaVsLambdaLEStatic_Dy4p0]; % -> 4  
  

hdfFileName = 'DAlphaVsLambdaLEVsDy.h5';  
  

if ( exist(hdfFileName, 'file') )  

    fprintf('file %s exists, deleting and creating a new one\n', hdfFileName);  

    delete(hdfFileName)  

else  

    fprintf('Creating new file %s\n', hdfFileName);  

end  
  

% Dataset: data  

h5create(hdfFileName, '/DAlphaVsLambdaLEVsDy/data', size(myData));  

h5write(hdfFileName, '/DAlphaVsLambdaLEVsDy/data', myData);  
  

% Dataset: var_0  

h5create(hdfFileName, '/DAlphaVsLambdaLEVsDy/var_0', size(dyVector));  

h5write(hdfFileName, '/DAlphaVsLambdaLEVsDy/var_0', dyVector);  
  

% Dataset: var_1  

h5create(hdfFileName, '/DAlphaVsLambdaLEVsDy/var_1', size(lambdaLEVector_deg));  

h5write(hdfFileName, '/DAlphaVsLambdaLEVsDy/var_1', lambdaLEVector_deg);

```

This script draws the graph after digitization. In this way it's possible to compare the initial graph and the digitized one.

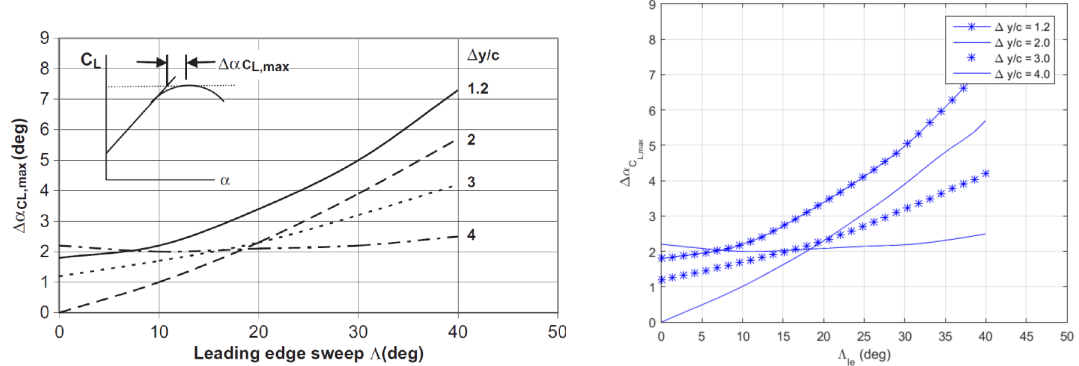


Figure A.2: Chart and its digitization.

Appendix B

Java Reference

B.1 Object and Class in Java

Object oriented programming scales very well, from the most trivial of problems to the most complex tasks. It provides a form of abstraction that resonates with techniques people use to solve problems in their everyday life. And for most of the dominant object-oriented languages there are an increasingly large number of libraries that assist in the development of applications for many domains.[13]

An entity that has state and behavior is known as an object. It can be physical or logical (tangible and intangible). The example of tangible object is banking system.

An object has three characteristics:

- **State:** represents data (value) of an object.
- **Behavior:** represents the behavior (functionality) of an object such as deposit, withdraw etc.
- **Identity:** Object identity is typically implemented via a unique ID. The value of the ID is not visible to the external user. But, it is used internally by the JVM to identify each object uniquely.

Object is an instance of a class. Class is a template or blueprint from which objects are created. So object is the instance (result) of a class.

B.2 Packages

A Java package is a mechanism for organizing Java classes into namespaces, providing modular programming. Java packages can be stored in compressed files called JAR files, allowing classes to be downloaded faster as groups rather than individually. Programmers also typically use packages to organize classes belonging to the same category or providing similar functionality.

A package provides a unique namespace for the types it contains. In general, a namespace is a container for a set of identifiers (also known as symbols, names). Namespaces provide a level of direction to specific identifiers, thus making it possible to distinguish between identifiers with the same exact name. For example, a surname could be thought of as a

namespace that makes it possible to distinguish people who have the same given name. In computer programming, namespaces are typically employed for the purpose of grouping symbols and identifiers around a particular functionality.

B.3 Documentation

The doc comments, which are a particular type of comments provided by Java, are automatically recognized by the most popular IDE programs; this helps the developer to quickly get an idea of the actions performed by each method, the parameter which has to be passed to it and the what it returns to the user.

Glossary

Aircraft Construction Reference Frame The reference frame which has its origin in the fuselage forwardmost point, the x-axis pointing from the nose to the tail, the y-axis from fuselage plane of symmetry to the right wing (from the pilot's point of view) and the z-axis from pilot's feet to pilot's head.

DATCOM Digital Datcom is a computer program which calculates static stability, high lift and control, and dynamic derivative characteristics using the methods contained in the USAF Stability and Control Datcom (Data Compendium). Configuration geometry, attitude, and Mach range capabilities are consistent with those accommodated by the Datcom. The program contains a trim option that computes control deflections and aerodynamic increments for vehicle trim at subsonic Mach numbers.

Enumeration The `java.util Enumeration` interface represents a special data type that enables for a variable to be a set of predefined constants. The variable must be equal to one of the values that have been predefined for it. Because they are constants, the names of an enum type's fields are in uppercase letters..

Graphical User Interface In computing, a Graphical User Interface is a type of interface that allows users to interact with electronic devices through graphical icons and visual indicators such as secondary notation, as opposed to text-based interfaces, typed command labels or text navigation.

Integrated Development Environment An integrated development environment (IDE) is a software application that provides comprehensive facilities to computer programmers for software development. An IDE normally consists of a source code editor, build automation tools and a debugger. Most modern IDEs have an intelligent code completion. Some IDEs contain a compiler, interpreter, or both, such as NetBeans and Eclipse; others do not, such as SharpDevelop and Lazarus. The boundary between an integrated development environment and other parts of the broader software development environment is not well-defined. Sometimes a version control system, or various tools to simplify the construction of a Graphical User Interface (GUI), are integrated. Many modern IDEs also have a class browser, an object browser, and a class hierarchy diagram, for use in object-oriented software development.

Interface In the Java programming language, an interface is a reference type, similar to a class, that can contain only constants, method signatures, default methods, static methods, and nested types. Method bodies exist only for default methods and static methods. Interfaces cannot be instantiated—they can only be implemented by classes or extended by other interfaces..

Knowledge-Based Engineering KBE is essentially engineering on the basis of knowledge models. A knowledge model uses knowledge representation to represent the artifacts of the design process (as well as the process itself) rather than, or in addition to, conventional programming and database techniques. KBE can have a wide scope that covers the full range of activities related to Product Lifecycle Management and Multidisciplinary Design Optimization. KBE's scope includes design, analysis, manufacturing, and support.

List The `java.util.List` interface is a subtype of the `java.util.Collection` interface. It represents an ordered list of objects, meaning you can access the elements of a List in a specific order, and by an index too. You can also add the same element more than once to a List.

Map The `java.util.Map` interface represents a mapping between a key and a value. The Map interface is not a subtype of the Collection interface. Therefore it behaves a bit different from the rest of the collection types.

Multi-disciplinary Design Optimization Multi-disciplinary design optimization (MDO) is a field of engineering that uses optimization methods to solve design problems incorporating a number of disciplines. MDO allows designers to incorporate all relevant disciplines simultaneously. The optimum of the simultaneous problem is superior to the design found by optimizing each discipline sequentially, since it can exploit the interactions between the disciplines. However, including all disciplines simultaneously significantly increases the complexity of the problem.

static method The term static means that the method is available at the Class level, and so does not require that an object is instantiated before it's called.

user developer The term refers to the developer which will use a method without being interested in how the method performs the required action. This is the case of a utility method: the developer is the one who writes the method, while the user developer is who uses that method to accomplish some action which requires the functionality provided by the utility method. It has to be noticed that the user developer and the developer can be the same person.

Acronyms

ACRF Aircraft Construction Reference Frame.

ADOpt Aircraft Design and Optimization Tool.

AIAA American Institute of Aeronautics and Astronautics.

BRF Body Reference Frame.

CAD Computer-Aided Design.

FAA Federal Aviation Administration.

GC Gravity Center.

GNC Guidance Navigation and Control.

GUI Graphical User Interface.

GUI Graphical User Interface.

IDE Integrated Development Environment.

IDE Integrated Development Environment.

JPAD Java Program toolchain for Aircraft Design.

KBE Knowledge-Based Engineering.

LRF Local Reference Frame.

MAC Mean Aerodynamic Chord.

MAPE Mean Absolute Percentage Error.

MDO Multi-disciplinary Design Optimization.

MLW Maximum Landing Weight.

MSL Mean Sea Level.

MTOW Maximum Take Off Weight.

MZFW Maximum Zero Fuel Weight.

List of symbols

()_H quantity related to the horizontal tail.

()_{LG} quantity related to the landing gear.

()_N quantity related to the nacelle.

()_S quantity related to systems.

()_V quantity related to the vertical tail.

()_F quantity related to the fuselage.

()_{WF} quantity related to the wing-fuselage configuration.

D aerodynamic drag.

CG Center of Gravity.

i_H the angle between the horizontal tail root chord and the ACRF x-axis.

i_W the angle between the wing root chord and the ACRF x-axis.

L aerodynamic lift.

T Thrust.

M Mach number.

A_R aspect ratio.

c chord.

d diameter.

l length.

m mass, in kg or lb.

b span.

S surface.

A sweep.

λ taper ratio.

t thickness.

V scalar velocity.

W weight, in Newtons.

m_w wing mass.

q dynamic pressure.

Re Reynolds number (evaluated with respect to \bar{c}).

α_w angolo d'attacco riferito alla corda di radice dell'ala.

β sideslip angle.

ρ air density.

Bibliography

- [1] I. H. Abbott and A. E. von Doenhoff. *Theory of Airfoil Sections*. Dover, 1959.
- [2] L. Attanasio. «Development of a Java Application for Parametric Aircraft Design». Master thesis. University of Naples "Federico II", 2014.
- [3] Various Authors. *ATR 72. Aircraft description*. URL: https://en.wikipedia.org/wiki/ATR_72.
- [4] Various Authors. *Boeing 747. Aircraft description*. URL: https://en.wikipedia.org/wiki/Boeing_747.
- [5] Various Authors. *eXtensible Markup Language (XML)*. URL: <https://en.wikipedia.org/wiki/XML>.
- [6] Various Authors. *Induced and Effective AOA for a Wing*. URL: http://gtae6343.wikia.com/wiki/Angle_of_Attack#cite_ref-1.
- [7] Various Authors. *Java (programming language)*. URL: [https://en.wikipedia.org/wiki/Java_\(programming_language\)](https://en.wikipedia.org/wiki/Java_(programming_language)).
- [8] Various Authors. *Plot Digitizer, description*. URL: <http://plotdigitizer.sourceforge.net/>.
- [9] Various Authors. *SUAVE: AN AEROSPACE VEHICLE ENVIRONMENT FOR DESIGNING FUTURE AIRCRAFT*. URL: <http://suave.stanford.edu/>.
- [10] Various Authors. *The Lift Coefficient*. 2006. URL: <https://www.grc.nasa.gov/www/K-12/airplane/liftco.html>.
- [11] Various Authors. *What is CFD?* URL: <http://www.cd-adapco.com/>.
- [12] J. A. Jr Blackwell. *A Finite-Step Method for Calculation of Theoretical Load Distributions for Arbitrary Lifting-Surface Arrangements at Subsonic Speeds*. Washington, D.C., 1969.
- [13] Timothy Budd. *An Introduction to Object-Oriented Programming*. Addison-Wesley, 2002. ISBN: 0201760312. URL: <http://web.engr.oregonstate.edu/~budd/Books/oopintro3e/>.
- [14] AIR FORCE TEST PILOT SCHOOL EDWARDS AFB CA. *Volume II. Flying Qualities Phase. Chapter 5: Longitudinal Static Stability*. published by the author, OCT 1990.
- [15] M. Drela and H. Youngren. *XFOil, Subsonic Airfoil Development System*. 2008. URL: <http://web.mit.edu/drela/Public/web/xfoil/>.
- [16] Giuseppe Paduano Fabrizio Nicolosi. *BEHIND ADAS 1.0*. Napoli, 2011.
- [17] D. Gambardella. «Development of a Java-Based Framework for Aircraft Preliminary Design». Master thesis. University of Naples "Federico II", 2014.

- [18] D. et al Gilbert. *JFreeChart*. URL: <http://www.jfree.org/jfreechart/>.
- [19] Vincenzo Giordano. *Alcune considerazioni sul downwash dell'ala*. 1966.
- [20] The HDF Group. *HDF*. URL: <http://www.hdfgroup.org/HDF5/>.
- [21] M. Hepperle. *Applet JavaFoil*. 2006. URL: <http://www.mh-aerotools.de/airfoils/javafoil.htm>.
- [22] D. Howe. *Aircraft conceptual design synthesis*. Aerospace Series. Professional Engineering Publishing, 2000. ISBN: 9781860583018. URL: <https://books.google.it/books?id=QJZTAAAAMAAJ>.
- [23] D. Howe. *Aircraft Loading and Structural Layout*. AIAA Education Series, 2004.
- [24] L.R. Jenkinson, D. Rhodes, and P. Simpkin. *Civil jet aircraft design*. AIAA education series. Arnold, 1999. ISBN: 9780340741528. URL: <https://books.google.it/books?id=6tMeAQAAIAAJ>.
- [25] Erik K. Antonsson Karl-Heinrich Grote. *Springer Handbook of Mechanical Engineering*. Grote Antonsson.
- [26] K. Kawaguchi. *Args4j*. URL: <http://args4j.kohsuke.org/>.
- [27] Ajoy Kumar Kundu. *Aircraft Design*. Cambridge University Press, 2010.
- [28] A. De Marco et al. *A Java desktop application for Aircraft Preliminary Design*. Naples, 2015.
- [29] B. W. McCormick. *Aerodynamics, Aeronautics, and Flight Mechanics*. John Wiley & Sons, 1979.
- [30] Daniel Webster College Mohammad Sadraey. *Aircraft conceptual design*. 2012.
- [31] Marcello R. Napolitano. *Aircraft Dynamics: From Modeling to Simulation*. John Wiley, 2012. ISBN: 9780470626672. URL: <http://www.amazon.com/Aircraft-Dynamics-From-Modeling-Simulation/dp/0470626674>.
- [32] L.M. Nicolai and G. Carichner. *Fundamentals of Aircraft and Airship Design*. AIAA education series v. 1. American Institute of Aeronautics and Astronautics, 2010. ISBN: 9781600867514. URL: <https://books.google.it/books?id=qA0oAQAAIAAJ>.
- [33] F. Nicolosi et al. *Fuselage aerodynamic prediction methods*. Naples, 2015.
- [34] E. Obert. *Aerodynamic Design of Transport Aircraft*. IOS Press, 2009. ISBN: 9781607504078. URL: <https://books.google.it/books?id=axPvAgAAQBAJ>.
- [35] Oracle. *1.2 Design Goals of the Java Programming Language*. 2013.
- [36] C. D. Perkins and R. E. Hage. *Airplane Performance Stability and Control*. New York: John Wiley & Sons, 1949. ISBN: 9780471680468. URL: <http://books.google.it/books?id=DHxTAAAAMAAJ>.
- [37] Warren F. Phillips. *Mechanics of Flight*. John Wiley and Sons, 2004. URL: https://books.google.it/books/about/Mechanics_of_Flight.html?id=6-_iGbJHM-8C&redir_esc=y.
- [38] J. Roskam. *Airplane Design*. Airplane Design pt. 5. DARcorporation, 1999. ISBN: 9781884885501. URL: <https://books.google.it/books?id=mMU47Ld7yQkC>.
- [39] J. Roskam. *Airplane Design*. Airplane Design pt. 8. DARcorporation, 2002. ISBN: 9781884885556. URL: <https://books.google.it/books?id=GIHHFkd829cc>.

-
- [40] J. Roskam. *Methods for Estimating Stability and Control Derivatives of Conventional Subsonic Airplanes*. published by the author, 1971.
 - [41] David Schmidt. *Modern Flight Dynamics*. McGraw-Hill, 2012. ISBN: 97800711339811.
 - [42] P.M. Sforza. *Commercial Airplane Design Principles*. Elsevier Science, 2014. ISBN: 9780124199774. URL: <https://books.google.it/books?id=knhHAgAAQBAJ>.
 - [43] Abe Silverstein and S. Katzoff. *Design Charts for Predicting Downwash Angles and Wake Characteristics behind Plain and Flapped Wings*. Tech. rep. 1939.
 - [44] R. Slingerland. *Prediction of Tail Downwash, Ground Effect and Minimum Unstick Speed of Jet Transport Aircraft*. 2015.
 - [45] *The Java Language Specification*. 2015.
 - [46] *Theoretical Calculation of the Effect of The Fuselage on the Spanwise Lift Distribution on a Wing*. Washington, D.C., 1952.
 - [47] E. Torenbeek. *Advanced Aircraft Design: Conceptual Design, Technology and Optimization of Subsonic Civil Airplanes*. Aerospace Series. Wiley, 2013. ISBN: 9781118568095. URL: <https://books.google.it/books?id=C0gUyoYewhoC>.
 - [48] E. Torenbeek. *Synthesis of Subsonic Aircraft Design*. 1976.
 - [49] E. Torenbeek. *Synthesis of Subsonic Airplane Design: An Introduction to the Preliminary Design of Subsonic General Aviation and Transport Aircraft, with Emphasis on Layout, Aerodynamic Design, Propulsion and Performance*. Springer, 1982. ISBN: 9789024727247. URL: https://books.google.it/books?id=NG2%5C_qiSjmMEC.
 - [50] Dimitri Van Heesch. *Doxxygen*. 1997-2014. URL: www.doxxygen.org.
 - [51] A.D. Young. *The Aerodynamic Characteristics of Flaps*. Technical Report. 1947.